



Universitat Ramon Llull

TESI DOCTORAL

**Títol : KINETIC STUDIES OF A XYLOGLUCAN ENDOTRANSGLYCOSYLASE,
A KEY ENZYME IN PLANT CELL MORPHOGENESIS**

Realitzada per Marc Saura Valls

el Centre Escola Tècnica Superior IQS

i en el Departament de Bioenginyeria

Dirigida per el Dr. Antoni Planas Sauter

Barcelona, setembre del 2007

*C. Claravall, 1-3
08022 Barcelona
Tel. 936 022 200
Fax 936 022 249
E-mail: urisc@sec.url.es
www.url.es*

**Als meus pares,
al meu germà
i a la Rita**

“Millor saber alguna cosa de tot, que tot d’una sola cosa”
Adaptació de Blaise Pascal

Agraïments:

Aquest treball ha estat realitzat en el laboratori de bioquímica de l'Institut Químic de Sarrià, emmarcat en un projecte europeu anomenat EDEN.

Primer de tot agrair al director de la meua tesis, al doctor Toni Planas, l'oportunitat de formar part del seu equip de recerca inicialment com a estudiant de TFC i posteriorment donant-me l'oportunitat de participar en un projecte de recerca a nivell Europeu, que ha estat un dels puntals de la meua formació com a investigador i també en altres àmbits de la meua vida. Agrair-te el suport donat durant tot aquest temps que em compartit i patit des de el trasllat del laboratori fins gairebé al seu nou trasllat.

Seguidament un menció especial a tots els companys amb els que he compartit la meua llarga estada al laboratori de bioquímica: A les doctorants inicials, la Mireia, la Magda, l'Ana i en Carlos que em van fer apassionar per la recerca i també adonar-me de la seva duresa; als companys de promoció: Toni, Montse, Odette; als doctorants/amics amb els que he treballat i sofert durant tota la tesi i sense els quals la meua tesi no hagués estat el que ha estat: Joan gràcies per escoltar, per discutir i criticar; Xavi company de pis, de trifulgues i de preocupacions pel que ens espera en el futur; Trevor the new Catalan, thank you for your friendship, all the discussion and English classes, hopping your good luck starts now; Javier i Edu per les vostres aportacions a la curiosa vida "bioch" i Núria pel canvi d'aires que has donat a la casa bioch, et dono tots els ànims que puc perquè segueixis endavant amb aquesta il·lusió. No voldria pas oblidar-me de tots els TFC i estudiants que han passat per bioquímica durant aquests 8 anys i sobretot al Sergi per la seva col·laboració en la realització d'aquesta tesi.

També agrair a tots els professors del IQS que sempre han tingut un porta oberta per ajudar-me en diferents punts d'aquest llarg treball, sobretot de la secció de cromatografia (gairebé el meu segon laboratori), la secció de fotoquímica i la d'esteroides (font inesgotable de saviesa).

Je veux aussi remercier a tout le group du CERMAV-CNRS pour votre accueil et votre aide pendant les quatre amusants mois que j'ai passé a Grenoble. Toute ma gratitude à Hugues Driguez, pour m'avoir donné la possibilité de faire un stage dans votre group, et d' améliorer mon niveau de chimie.

Aussi a touts les amis françaises pour votre aide avec mon français et pour faire que je me sent comme un autre dans votre group (Sami, Marie, Jean Pierre, LEMONIA, Emilie (mes félicitation pour ton petit enfant), Laurence, Sylvain, Sébastien et très spécialement à la toujours positive :) Marie-Pierre pour être ma guide dans Grenoble et dans le laboratoire). Merci a touts.

I would like to thank members of EDEN team for all the meetings spent together with a lot of work done and also very good moments. Specially I would like to thank Harry, Kathleen and Tuula for your collaboration and help. And of course mon ami Régis, it is long time ago from our last contact, but our conversations and your help is still in my memory. Good luck in you scientific career.

No em voldria pas oblidar a tots els meus amics, que amb la seva confiança en el científic boig de la colla, sense saber-ho m'han estat donant ànims per acabar aquest llarg camí. Als de sempre: Saldí, Gerard, Jack, Dani i Petri i als de la universitat: Marc i Dolors, Marçal i Olga, Quico i Maca, Dari i Sabi i Jaume i Mireia. Sort n'hi ha hagut dels caps de setmanes amb uns o altres per desconnectar i recarregar les piles per emprendre una nova setmana.

Però a qui cal que agraeixi més la finalització de la tesi és a la meva família: pare, mare i David, per tot el suport que m'heu donat sobretot en els moments que més ho necessitava, quan l'humor estava sota mínims. A més durant aquest temps una persona molt especial m'ha fet sempre costat tot i que potser sense entendre-ho gaire. Rita, si hem superat aquesta etapa tant dura per tots dos, el futur junts serà genial. Moltes gràcies.

Aquest treball ha estat finançat pel contracte EU (QLK5-CT-2001-00443) i també per la "Marie Curie fellowship for early stage research training" concedida per l'estada a Grenoble.

CONTENTS

LIST OF ABBREVIATIONS.....	i
STRUCTURES.....	iii
SUMMARY:	vii
INTRODUCTION:	1
1.- Plant cell wall related products.....	1
2.- Plant cell wall functions.....	2
3.- Plant cell wall composition.....	3
4.- Plant cell wall architecture.....	7
5.- Plant cell wall biosynthesis.....	9
6.- Xyloglucan nomenclature and biosynthesis.....	11
6.1.- Xyloglucan nomenclature.....	11
6.2.- Xyloglucan biosynthesis.....	13
7.- Plant cell wall dynamics.....	15
8.- EDEN project.....	18
9.- Xyloglucan endotransglycosylases.....	19
9.1.- Enzymatic assays for XET activity <i>in vitro</i>	22
9.1.1.- Assays based on physico-chemical changes.....	22
9.1.2.- Assays that measure XG molecular weight distributions:.....	22
9.1.3.- Assays using labeled acceptors:	23
9.2.- Classification (Enzyme Commission (E.C.), CAZY).....	24
9.3.- Nomenclature.....	25
9.4.- Occurrence of <i>XTH</i> in plants (genomic information).....	25
9.5.- Mechanism of action.....	27
9.6.- Biochemical properties.....	30
9.7.- Substrate specificity.....	32
9.7.1.- Donor substrates.....	32
9.7.2.- Acceptor substrates.....	33
9.8.- Subsite mapping.....	35
9.9.- <i>XTH</i> studies <i>in vivo</i>	37
9.9.1.- <i>XTH</i> expression.....	37
9.9.2.- XET activity.....	38
OBJECTIVES.....	39
CHAPTER 1: attempts of <i>Ptt</i> -XET16A expression in <i>Escherichia coli</i>	41
1.- Background:.....	41
2.- pD62XET16A construct.....	43
2.1.- pD62XET16A design and construction.....	43
2.2.- Expression attempts with the pD62-XET16A construct.....	51
3.- pET15XET16A construct.....	52
3.1.- pET15XET16A design and construction.....	52
3.2.- Expression attempts with pET15b-XET16A construct:	56
3.3.- Purification by affinity chromatography:.....	56
CHAPTER 2: development of XET-activity assay.....	57
1.- Introduction.....	57
2.- HPCE method development: separation of XGOs-ANTS.....	59
2.1.- Synthesis of XGOs-ANTS.....	59
2.1.1.- Synthesis of XGOs.....	59
2.1.2.- XGOs ANTS-labeling.....	59
2.2.- HPCE conditions.....	60
3.- Monitoring XET activity: Xyloglucan as donor and XGOs-ANTS as acceptor.....	66
4.- Search of a minimal donor for <i>Ptt</i> -XET16A.....	68
4.1.- Hypothesis 1: β -xylogluco-oligosaccharidyl fluorides as donors.....	68
4.1.1.- Synthesis of GG β F(1), XG β F(2), and XXXG β F(14).....	69
4.1.2.- Evaluation of β -glycosyl fluorides as donors of <i>Ptt</i> -XET16A.....	72

4.2.- Hypothesis 2: XGOs with at least one glucosyl unit at the positive subsites.	74
4.2.1.- (XG) _n GG synthesis.	76
4.2.2.- (XXXG) _n and (XXXG) _n GG synthesis.	76
4.2.3.- Evaluation of (XG) _n GG and (XXXG) _n (GG) _m as putative donors for Ptt-XET16A.	76
5.- HPCE assay for kinetic characterization of Ptt-XET16A.	79
5.1.- XXXGXXXG (23) synthesis.	79
5.2.- XXXG-ANTS(25) synthesis.	82
5.3.- HPCE method validation.	83
5.4.- Ptt-XET16A reaction monitoring and product identification.	85
 CHAPTER 3: Ptt-XET16A enzyme characterization.	 89
1.- Introduction.	89
2.- Specific activity.	90
3.- pH profile.	91
4.- Temperature profile.	93
5.- Kinetic mechanism of Ptt-XET16A.	94
5.1.- Background.	94
5.2.- Steady state kinetics.	96
5.3.- Steady state kinetic parameters using a blocked donor.	102
5.3.1.- Background.	102
5.3.2.- GalGXXXGXXXG (38) synthesis.	103
5.3.3.- Ptt-XET16A reaction monitoring and product identification with GalGXXXGXXXG (38) as blocked donor.	104
5.3.4.- Steady state kinetic parameters of Ptt-XET16A using the blocked donor GalGXXXGXXXG (38).	106
 CHAPTER 4: Donor screening and subsite mapping.	 111
1.- Background.	111
2.- Donor library design.	114
3.- Donor library synthesis.	116
4.- Donor concentration determination.	122
5.- Synthesis of standard XGOs-ANTS compounds.	123
6.- Donor screening.	124
6.1.- Product identification.	124
6.1.1.- Family 1. Single transglycosylation product.	125
6.1.2.- Family 1. Multiple transglycosylation products.	126
6.1.3.- Family 2. Donors with non branched Glc in negative subsites.	127
6.1.4.- Family 2. Donors with a terminal Gal group.	131
6.1.5.- Family 2. Donors with branched chain in the non reducing end fragment.	134
6.2.- Relative reactivity after 24 hours reaction.	139
7.- Subsite mapping.	144
7.1.- Background.	144
7.2.- k_{cat}/K_M determination.	145
7.3.- Subsite mapping.	147
7.3.1.- Positive subsites mapping.	147
7.3.2.- Negative subsites mapping.	149

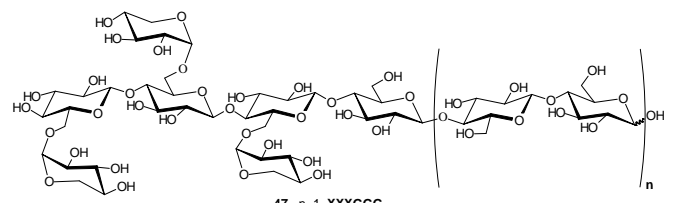
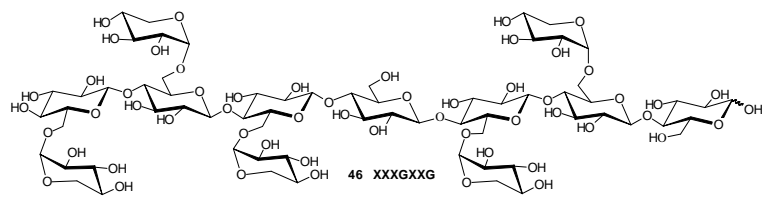
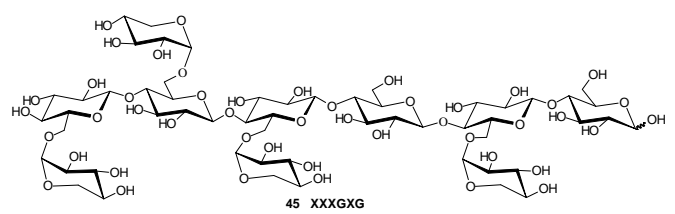
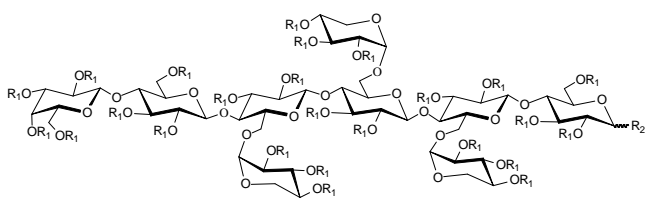
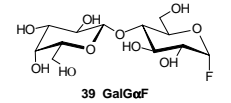
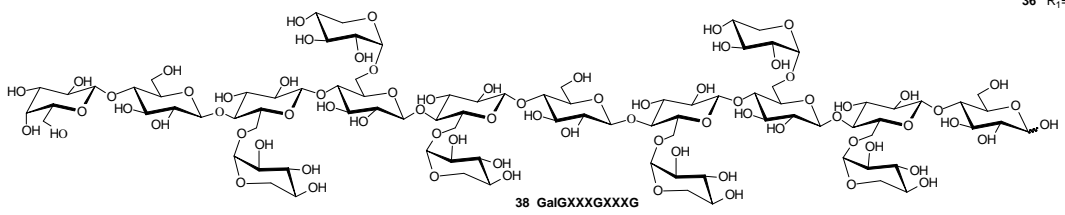
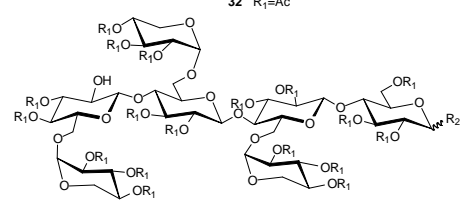
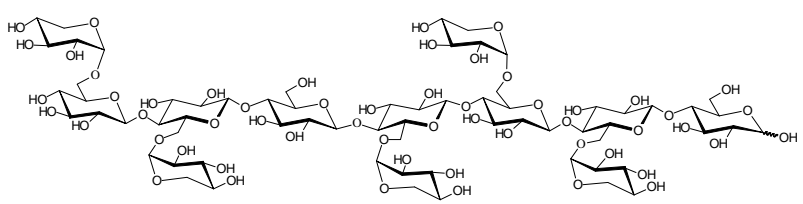
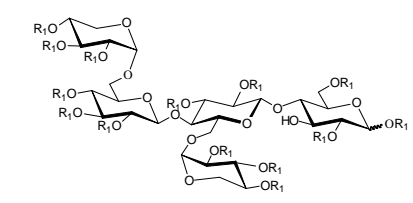
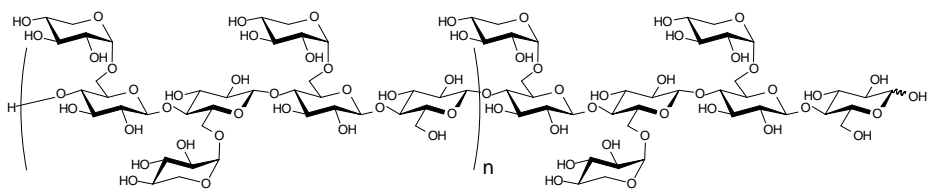
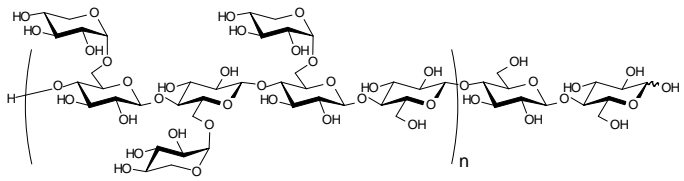
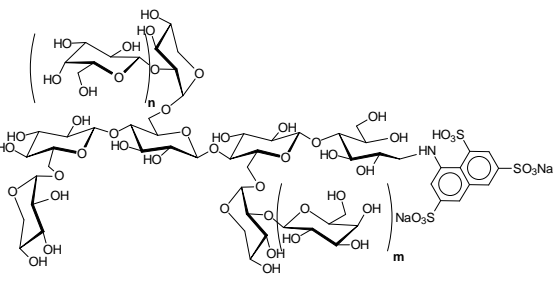
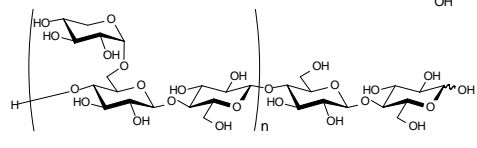
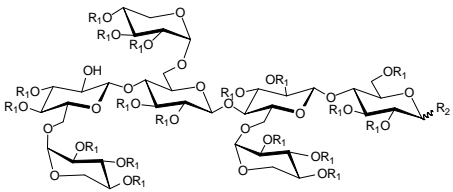
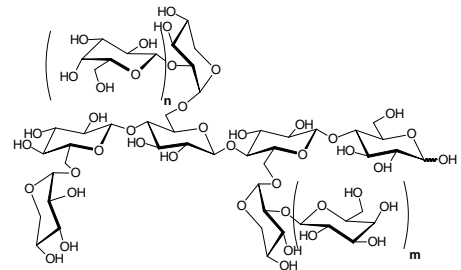
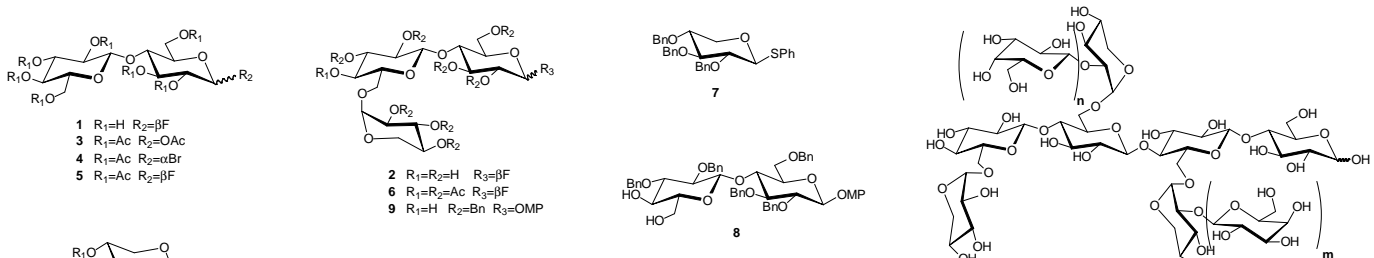
CHAPTER 5: Design of an assay for transglycosylase /hydrolase activity measurements for <i>XTHs</i> .	153
1.- Background.....	153
2.- FRET substrate design.	157
3.- FRET substrate design II.	160
4.- Synthesis of FRET substrates.....	164
4.1.- Synthesis of 4-azido-4-deoxy-cellobiosyl fluoride (74).	164
4.2.- Synthesis of XXXGXXXG-EDANS (70)	167
4.2.1.- Synthesis of XXXGXXXG (23).....	167
4.2.2.- EDANS labeling.	169
4.3.- Coupling of 74 with 70 and final labeling.	171
5.- <i>Ptt</i> -XET16A FRET assays.....	174
5.1.- Preliminary fluorescence assays with 76	174
5.2.- Fluorescence characterization of FRET substrate 76	175
5.3.- Kinetic assays using DAB-GGXXXGXXXG-EDANS (76).....	176
CONCLUSIONS:.....	179
EXPERIMENTAL PART.....	183
BIBLIOGRAPHY.	247

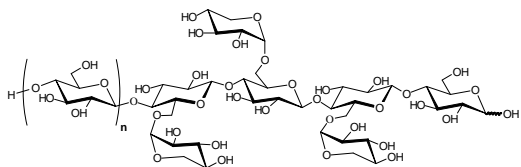
List of abbreviations.

3D: tridimensional
ABEE: aminobenzoic acid ethyl ester
Ac₂O: acetic anhydride
ACN: acetonitrile
AcOEt: ethyl acetate
AcOH or HAcO: acetic acid
AcONa: sodium acetate
ANTS: 8-aminonaphtalene-1,3,6-trisulfonic acid sodium salt
aq: aqueous
Ara: arabinose
At. Arabidopsis thaliana
bp: base pairs
BSA: bovine serum albumine
CAZY: carbohydrate active enzymes
Conc: concentration
CV: variance coefficient
Cy: cyclohexane
DAB: 4-dimethylaminoazobenzene
DABITC: 4-dimethylaminoazobenzene-4'-isothiocyanate
DAST: diethylaminosulfur trifluoride
DCI: chemical desorption ionization
ddNTP: dideoxynucleotide triphosphate
DEAE: diethylamino ethanol
DMAP: dimethylaminopyridine
DMF: dimethylformamide
DMSO: dimethylsulfoxide
DNA: deoxyribonucleic acid
dNTP: deoxynucleotide triphosphate
DP: degree of polymerization
dsDNA: double strand DNA
E. coli: Escherichia coli
E: enzyme
EC: enzyme commission
EDANS: 5-((2-aminoethyl)-amino)-naphtalene-1-sulfonic acid
EDEN: enzyme discovery in hybrid aspen for fiber engineering
EDTA: ethylenediamine tetraacetic acid
EET: excitation energy transfer or electronic energy transfer
Em: emission
Endo H: endoglycosidase H
EOF: electro osmotic flow
Eq.: equation
ESI-TOF: electrospray ionization-time of flight
EST: expressed sequence tags
et al.: et alii/alia
EtOH: ethanol
Exc: excitation
FAB: fast atom bombardment
FITC: fluorescein isothiocyanate
FRET: fluorescence or förster resonance energy transfer
FSE: fluoride selective electrode
Fuc: fucose
Gal: galactose
GalA: galacturonic acid

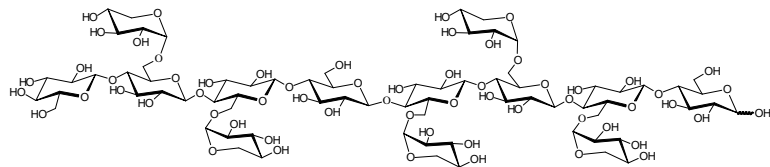
GalAMe: methyl galacturonate
Glc: glucose
GPC: gel permeation chromatography
H. insolens: *Humicola insolens*
HGA: homogalacturonan
HMPA: hexamethylphosphoramide
HPCE: high performance capillary electrophoresis
ID: internal diameter
IPTG: isopropyl-beta-D-thiogalactopyranoside
IUBMB: international union of biochemistry and molecular biology
kbp: kilo base pairs
LC/MS: liquid chromatography / mass spectrometry
MALDI: matrix assisted laser desorption ionization
Man: manose
MeOH: methanol
MeONa: sodium metoxide
mRNA: messenger ribonucleic acid
MS: mass spectrometry
MW: molecular weight
N: efficacy
NMR: nuclear magnetic resonance
p.: page
PCR: polymerase chain reaction
PNGase F: peptide:N-glycosidase F
Ptt: *Populus tremula x temuloides*
Py: pyridine
R.T. or RT: room temperature
 R_0 : Förster radius
Rel: relative
RET: resonance energy transfer
RF: response factor
Rf: retention factor
RG-I: rhamnogalacturonan I
RG-II: rhamnogalacturonan II
Rha: rhamnose
Rs: resolution
SDM: site directed mutagenesis
SDS-PAGE: sodium dodecyl sulphate polyacrylamide gel electrophoresis
St. dev.: standard deviation
TEA: triethylamine
THF: tetrahydrofurane
TLC: thin layer chromatography
 t_m : migration time
TMS: tetramethylsilane
Tol: toluene
TS: transition state
UDP:
UV-Vis: ultraviolet-visible
 v_0 : initial rate
vs: versus
XEH: xyloglucan endotranshydrolase
XET: xyloglucan endotransglycosylase
XG: xyloglucan polymer or xyloglucan
XGO: xyloglucan oligosaccharide
XGOs: Xyloglucan oligosaccharides

XGOs-ANTS: mixture of ANTS labeled xyloglucan oligosaccharides
XTH: xyloglucan endo-tranglycosylase / endo-hydrolase
Xyl: xylose
 λ : wave length

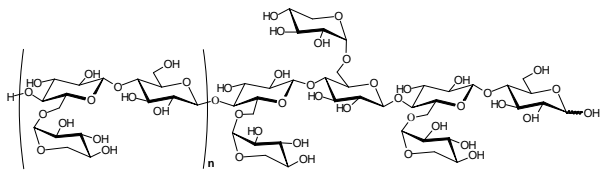




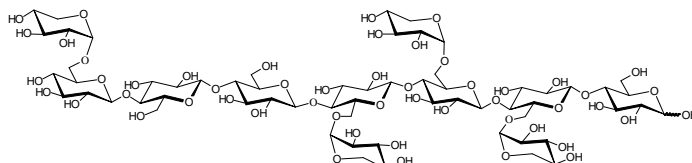
49 n=1 GXXXG
50 n=2 GGXXXG
51 n=3 GGGXXXG
52 n=4 GGGGXXXG



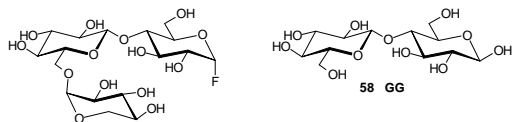
53 GXXXGXXXG



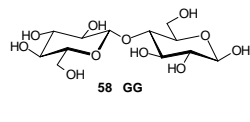
54 n=1 XGXXXG
56 n=2 XGXGXXXG



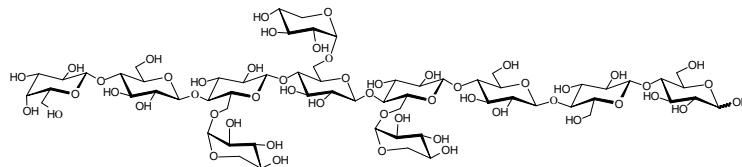
55 XGXXXG



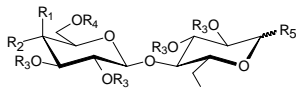
57 XG α F



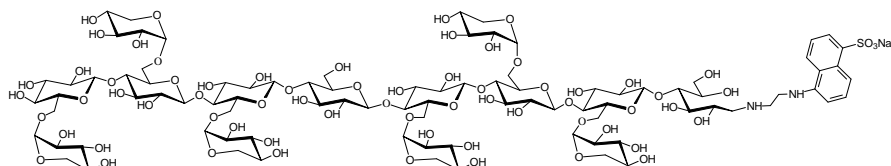
58 GG



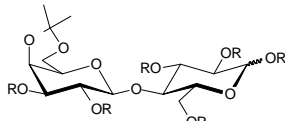
59 GalGXXXGGG



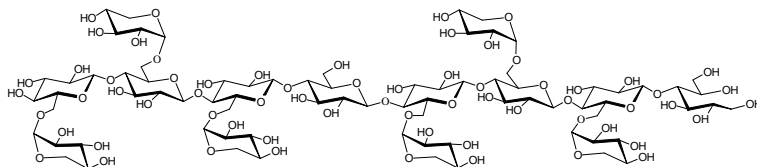
62 R₁=OH, R₂=R₄=H, R₃=Ac, R₅=OAc
63 R₁=OH, R₂=H, R₃=Ac, R₄=Bz, R₅=OAc
64 R₁=OBz, R₂=H, R₃=Ac, R₄=H, R₅=OAc
65 R₁=OTf, R₂=H, R₃=Ac, R₄=Bz, R₅=OAc
66 R₁=H, R₂=N₃, R₃=Ac, R₄=Bz, R₅=OAc
67 R₁=H, R₂=N₃, R₃=Ac, R₄=Bz, R₅=OH
68 R₁=H, R₂=N₃, R₃=Ac, R₄=Bz, R₅= α / β F
69 R₁=H, R₂=N₃, R₃=Ac, R₄=Bz, R₅= α F
74 R₁=H, R₂=N₃, R₃=H, R₄=H, R₅= α F



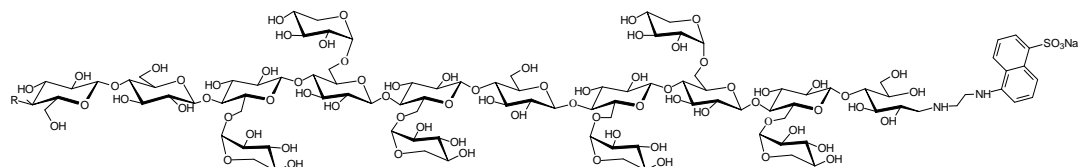
70 XXXGXXXG-EDANS



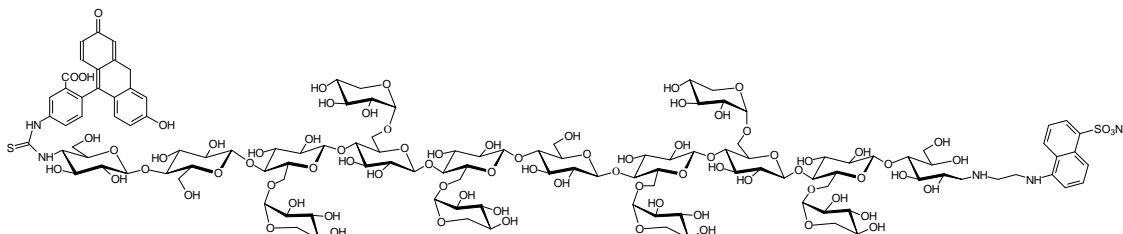
60 R=H
61 R=Ac



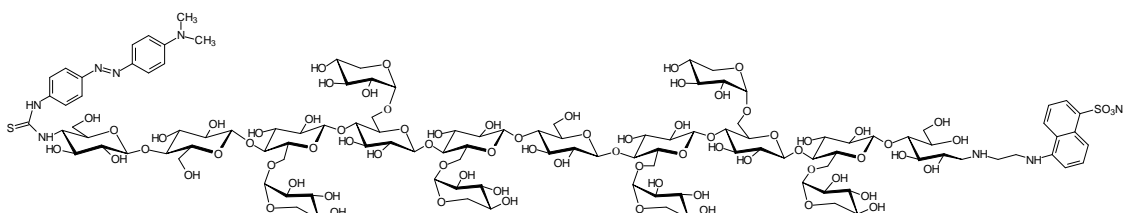
71 XXXGXXXGal



72 R=N₃ N₃-GGXXXGXXXG-EDANS
73 R=NH₂ NH₂-GGXXXGXXXG-EDANS



74 FI-GGXXXGXXXG-EDANS



75 DAB-GGXXXGXXXG-EDANS

SUMMARY

SUMMARY:

The present work is part of an European project named E.D.E.N. (Enzyme Discovery in hybrid aspen for fiber ENgineering). The general objective of the project is to identify novel plant enzymes for deeper understanding of the process of fiber formation and modification for future improvement of the quality parameters of wood fibers.

The present project pretends to increase the knowledge about xyloglucan endotransglycosylases (XET), which are thought to be key enzymes in the construction and controlled modification of the xyloglucan-cellulose network. It is pretended to study the mechanism of action and the substrate specificity of a XET from *Populus tremula x tremuloides*, concretely XET16A (*Ptt*-XET16A).

A new enzymatic assay based on capillary electrophoresis is designed and validated. This assay allows the kinetic study of XETs using as substrates, low molecular mass xyloglucan oligosaccharides with defined structures. These substrates have been synthesized in the present work and also in collaboration with Dr. Driguez team from CERMAV-CNRS.

It is concluded that the maximum of activity of *Ptt*-XET16A is between pH 5 and 5.5 and 30 and 40 °C. It is demonstrated that *Ptt*-XET16A follows a *bi-bi* ping-pong kinetic mechanism, in which the acceptor acts as competitive inhibitor of the donor binding to the free enzyme and depending on the donor used, this one can act also as competitive inhibitor of the acceptor binding to the acceptor subsites of the glycosyl-enzyme intermediate giving rise to side reaction such as donor polymerization and product elongation only in case that the donor shows a glucosyl residue in the non reducing end.

A library of xylogluco-oligosaccharides, synthesized in CERMAV-CNRS by Dr. Driguez team, is evaluated as *Ptt*-XET16A donors. With this studies we are able to deeper understand the activity of XETs, their substrate specificity and a subsite mapping of the binding cleft is done, obtaining the contribution of different subsites of *Ptt*-XET16A to the stabilization of the transition state of the transglycosylation reaction catalyzed by the studied enzyme.

Finally, a bifluorogenic substrate derived from the tetradecasaccharide used as standard substrate in this project has been designed to measure hydrolase and transferase activities of XET enzymes by fluorescence resonance energy transfer (FRET). The bifluorogenic substrate was obtained, however, it could not be demonstrated if it is an adequate substrate to measure hydrolase and transferase activities because the fluorescent properties of the label were lost during substrate synthesis.

INTRODUCTION

INTRODUCTION:

1.- Plant cell wall related products.

Humans have been using plants since the beginning of history for a variety of purposes: feeding, fuels, material for construction, for tools, for furniture, for paper, etc. each product obtained from selected plant species.

With the agriculture invention, humans started to genetically modify plant species. Initially, humans selected more adequate variants for agriculture, and nowadays we are able to genetically modify plants for the desired purposes. Classical genetic techniques have the objective of generating variability in the studied specie followed by selection of plants with better characteristics. With molecular biology, the target is the specific addition, suppression or modification of some genes previously chosen. For that reason, it is necessary to have a profound knowledge on the genetic and biochemical mechanisms which control plant development to choose the target genes or processes to be modified.

The general objective of this work and the project in which it is included is the study of the molecular mechanisms and genes involved in plant cell wall biosynthesis and modification.

The most relevant characteristic feature of plant cells is the wall that envelops the cell. This cell wall has a number of roles, as it will be presented later, including: structural and protective functions, source of signaling, growth regulation, etc.^{1,2}.

Our knowledge on plant cell wall structure has evolved significantly since the first observation in the early 18th century when microscope was invented. Initially it was considered a rigid housing for plant cells, and nowadays it is described as a dynamic and highly regulated organelle located outside the plasma membrane³.

2.- Plant cell wall functions.

Plant cell wall has different functions for plant growth and development:

a) Mechanical support: cell wall dictates plant cell morphology and as a consequence it is the final responsible of the plant shape. Plant cells treated with cell-wall degrading enzymes, which remove the cell wall, are invariably spherical, contrasting with the different cell shapes observed in plants with walled-cells. Therefore the rigidity that defines cell morphology and as a result plant morphology and structure is given by the cell wall².

b) Defense: cell wall functions as the frontier defense system against various types of microbial pathogens and stress from the surrounding environment³.

c) Signaling: cell wall has an important role in cell-to-cell communication with other cells or microbes, particularly in symbiotic interactions³⁻⁶. Fragments of cell wall polysaccharides could provoke the secretion of defense molecules and induce the impregnation of walls with protein and lignin to armor it against invading fungal and bacterial pathogens².

d) Expansion regulation: cell wall governs the rate and direction of expansion, and the ultimate size and shape of the cell⁴.

e) Cell differentiation: cell wall contributes to the functional specialization of cell types. For example in *Zinnia* leaves, the shape of spongy parenchyma cells maximizes both the volume of intercellular spaces and the surface area available for gas exchange, etc.²...

3.- Plant cell wall composition.

Physiologically, cell walls can be classified as primary and secondary cell walls. The primary cell wall is present in young cells or cells able to expand. The secondary one, on the other hand, is normally more thick, rigid and inextensible and it is formed in the inner part of the primary cell wall in cells that have finished its expansion³ (Figure 1). Sometimes, differences between these cell types are no so clear and the borderline is vague.

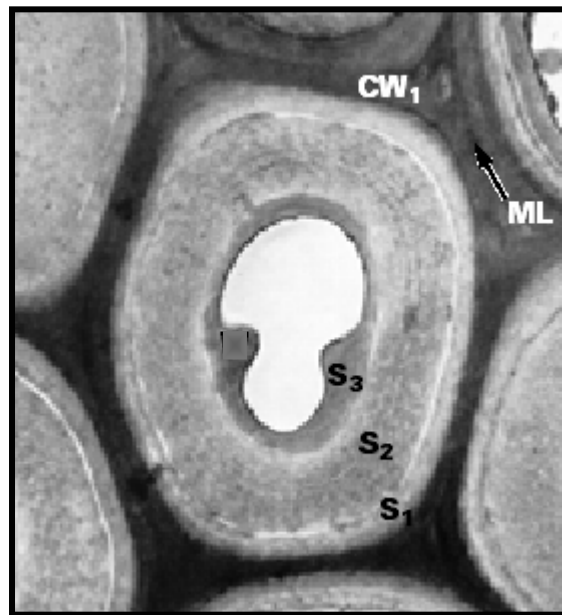


Figure 1: Schematic representation of cells, showing middle lamella (ML), original primary cell wall (CW₁) and secondary cell wall layers (S₁, S₂ and S₃ in deposition order), from Carpita *et al.* (2000)²

Due to the great diversity of plants and differentiated cells in the same plant, it is difficult to make a precise and consensus description of cell wall structure. However, there are some general characteristics:

The principal constituents of the cell wall are polysaccharides: Cellulose, hemicelluloses, pectins, but also non-carbohydrate components are present such as lignin, proteins, minerals, etc².

Cellulose is the most abundant plant polysaccharide; it is a homopolysaccharide of β -(1→4)-D-glucopyranosyl units, where two adjacent units are oriented with 180° of rotation. Cellulose polymers are organized by inter and intra hydrogen bonds forming semi crystalline structures named microfibrills (Figure 2).

Callose consists of a β -(1 \rightarrow 3)-D-glucopyranosyl polymer chain grouped in helical duplexes and triplexes. Callose is produced in few cell types at specific stages of wall development, such as in growing pollen tubes, in cell plates of dividing cells, etc².

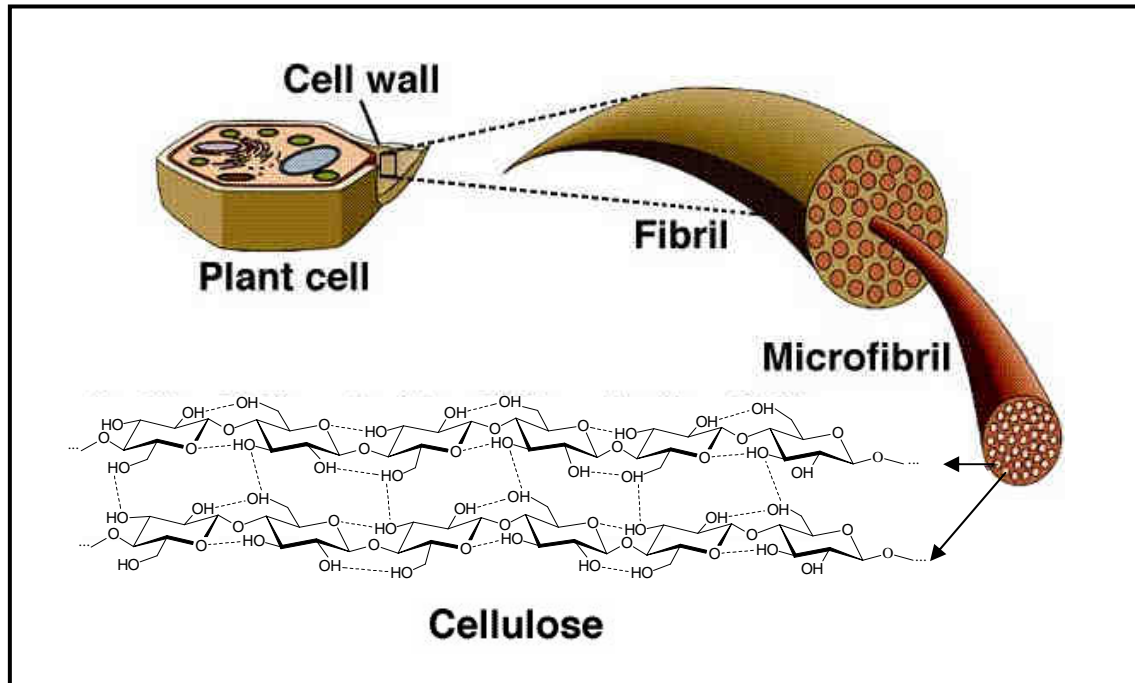


Figure 2: Schematic representation of fibrils, microfibrils and structure of cellulose polysaccharides showing inter and intramolecular hydrogen bonds (dotted line).

Hemicellulose is a general name given to polysaccharides that have a backbone which can be substituted at different positions with other oligosaccharides. They can hydrogen-bond cellulose microfibrils forming crosslinks between microfibrils. For that reason, more recently they are named as cross-linking glycans. There are different hemicelluloses: xyloglucans (XG), glucuronoarabinoxylans and the less abundant galactomannans, glucomannans, galactoglucomannans, etc. (Figure 3).

Pectin is a broad group of branched and ionic polysaccharides rich in D-galacturonic acid. It modulates cell wall porosity, pH and ion balance, also seems to regulate cell-cell adhesion, and it is proposed to contain recognition molecules that alert plant cells of the presence of symbiotic organisms, pathogens and insects⁷. It is composed of three main polymers (Figure 3): the homogalacturonan (HGA) composed of highly methyl sterified α -(1 \rightarrow 4)-D-galacturonic acid, the rhamnogalacturonan I (RG-I) composed of a repeating disaccharide α -(1 \rightarrow 2)-D-rhamnose- α -(1 \rightarrow 4)-D-galacturonic

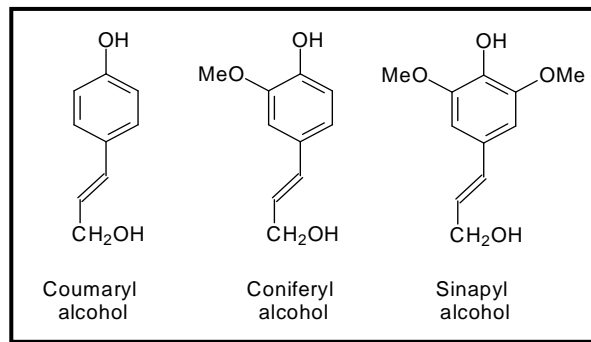


Figure 4: Structure of different monomers that form lignin.

Structural proteins are classified in four major classes: hydroxyproline-rich glycoproteins, proline-rich proteins, glycine-rich proteins and proteoglycans^{2,9}. All these related proteins are located in different parts of cells interacting with different polymers such as pectins, lignins, etc. Different functions were proposed for them although clear evidences are still lacking such as functions in development, wound healing, plant defense, plant vascular tissues, initial lignification nucleus, control cell division, cell adhesion, XG-cellulose matrix locking, etc^{1,2}.

Primary cell walls are classified in types I and II depending on the cross-linking glycans (hemicelluloses) that they contain: Type I is present in dicots and almost one half of the monocots in which xyloglucan is the most abundant hemicellulosic material. Type II is present in the “commelinoid” line of monocots and the glucuroarabinoxylans are the major cross-linking glycans. In this study we will focus on type I primary cell walls.

4.- Plant cell wall architecture.

The primary cell wall type I is made of two or sometimes three different but interacting networks: The XG-cellulose one, the pectin one and the structural protein one.

The **XG-cellulose network** is, in dry weight, the most abundant constituent of cells. The XG matrix interacts with cellulose microfibrils positioning them (Figure 5). Both together have been proposed to have the most important function in controlling cell expansion^{1,2,10-12}.

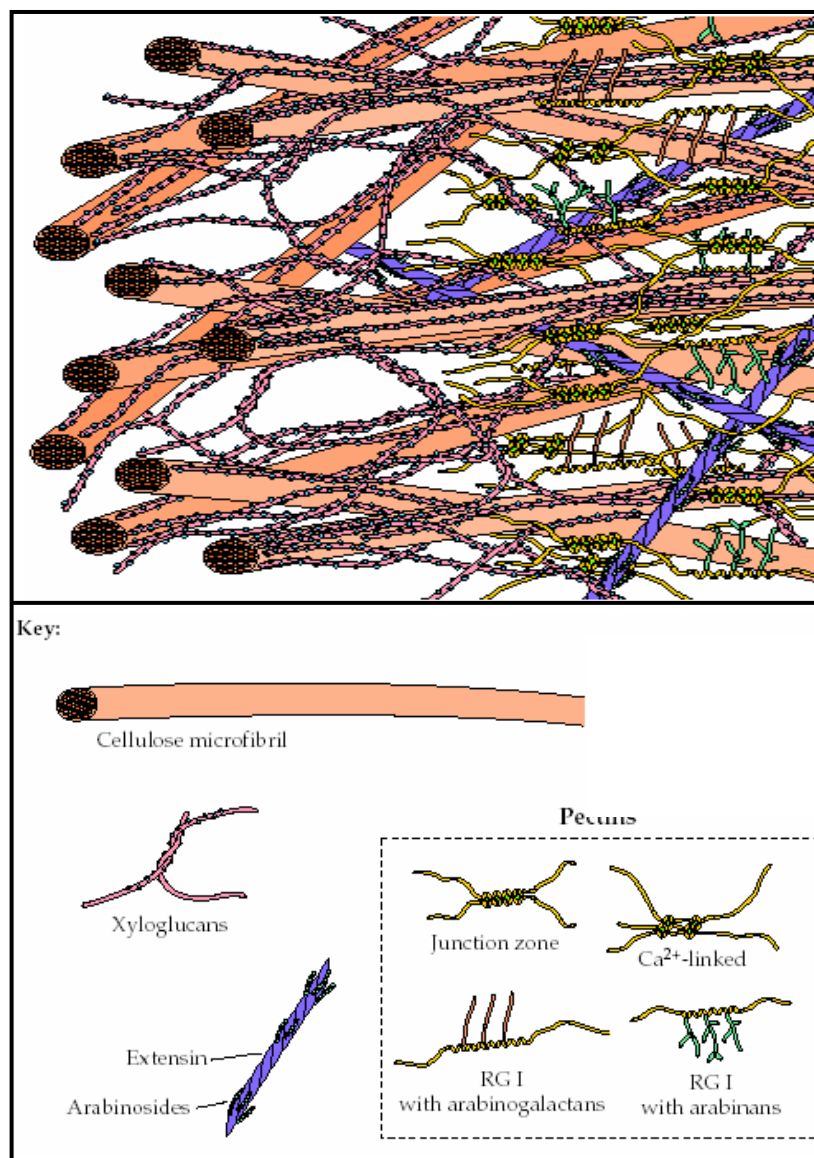


Figure 5: Schematic representation of structural model of dicot cell walls, adapte from Carpita *et al.* (2000)²:

XG-cellulose interactions were studied determining the quantity of XG recovered from cell walls using different extraction protocols. In this way different XG domains could be defined depending on the strength of the extraction protocol used which may indicate the cellulose interaction strength^{11,13-15}.

The first XG domain is extracted from cell walls only by treatment with specific XG-endoglucanases; This XG domain forms cross-links between different cellulose microfibrils, locking them in the correct spatial arrangement; for that reason it is accessible to XG-endoglucanases. These connecting fragments were observed by electron microscopy¹.

The second XG domain is extractable with basic solutions and it was proposed to bind the exposed faces of cellulose microfibrils by hydrogen bonding and it is covalently linked with the first XG domain.

The third XG domain seems to be entrapped in cellulose microfibrils because it is only extractable by cellulase digestion of cell wall material once the two first XG domains were extracted before from cell walls. These cellulases break the cellulose structure liberating the third XG domain. This entrapped XG could also be covalently connected with the first domain, but in less extension and it seems to give some extensibility to microfibrils, compared with pure cellulose microfibrils¹⁶.

This XG-cellulose matrix is the major responsible of the final structure of cell wall and seems to have a major role on cell-wall structural modifications.

The XG-cellulose network is embedded in a **pectin matrix** (Figure 5) which controls different physiological properties (pH, porosity, etc.). The pectin matrix is cross-linked by Ca^{2+} junction zones, interacting with the non-methylated carboxylates of pectin polysaccharides. The spacing of these junction zones defines the pore size in the cell wall. Modification of this pore size could modify diffusion of enzymes and molecules involved in cell wall modification^{1,2,7}.

The third network that can be present is a **structural protein network**. It is able to interact with the pectin network or form intermolecular bridges without necessarily binding to the polysaccharide components, although in some cases covalent links between polysaccharides and structural proteins were described^{2,9} (Figure 5). Its function is still unknown although it seems to have some role in plant defense, cell expansion, initial lignification nuclei, control cell division, and XG-cellulose matrix locking when cell wall extension stops, etc^{1,2}.

5.- Plant cell wall biosynthesis.

Primary cell wall polysaccharides are synthesized by various membranes of protoplasts. Cellulose (β -(1 \rightarrow 4)-glucan) and callose (β -(1 \rightarrow 3)-glucan) are synthesized in the plasma membrane, using donor substrates, probably UDP-glucose¹⁷. Terminal complexes, visible by electron microscopy (Figure 6) are the enzyme complexes which produce cellulose; in the angiosperms they present a Rosette-like organization with 6 Rosette subunits (Figure 6). Each rosette subunit is proposed to be the association of six identical cellulose synthase proteins (CeS), each one producing simultaneously one β -(1 \rightarrow 4)-glucan chain¹⁸. Therefore, terminal complexes produce several dozens of cellulose chains that immediately form cellulose microfibrils by hydrogen bonding¹⁹. These microfibrils are fixed immediately by xyloglucan polymers into the cell wall provoking the displacement of terminal complexes in the plasma membrane⁴.

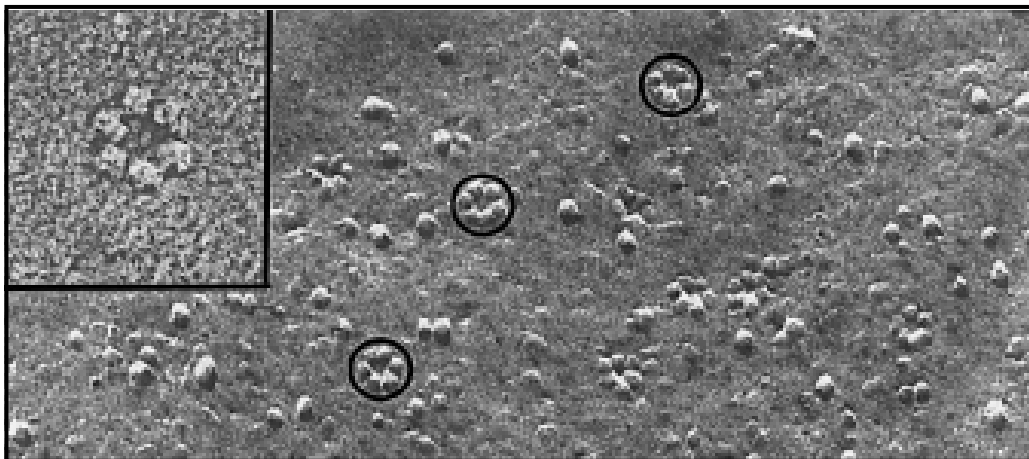


Figure 6: Electron microscopy of freeze fracture plant cells, showing (circle surrounded) different terminal complexes with a Rosette shape. A magnification of one of these Rosettes is also presented, from Delmer (1999)¹⁹.

Callose is synthesized in the plasma membrane when cells are damaged; the inverse association of the activation of callose synthesis with the lost of cellulose synthesis seems to support the concept that callose synthase is an altered cellulose synthase¹⁷.

Other cell wall polysaccharides are synthesized in the Golgi apparatus by different polysaccharide synthase enzymes (pectin synthase, xylan synthase...) using nucleotide sugars as donors²⁰. These polysaccharides are exported to the cell wall by Golgi-derived vesicles which are fused with the plasma membrane. Polysaccharides are liberated in the cell wall and incorporated as new material on it.

Different studies have shown synthase activities in different parts of the Golgi apparatus, for example incorporation of ³H labeled xylose in xyloglucan or xylans². This studies proved the location where the synthesis of these polysaccharides takes place. Normally these synthase activities can not be isolated because they are often lost after detergent solubilization of the Golgi apparatus.

It seems that these polysaccharides are synthesized by sequential action of cooperating synthases. For example, for xyloglucans synthesis, first a β -(1→4)-D-glucopyranose backbone is synthesized, immediately α -xylosyltransferases incorporate xylosyl residues at 75% of the glucoses and after that galactosyl and fucosyl residues can be incorporated²¹.

6.- Xyloglucan nomenclature and biosynthesis.

6.1.- Xyloglucan nomenclature.

An unifying nomenclature was proposed as an attempt to rationalize the nomenclature of XG related structures and to facilitate its description. This system is based on chemically consistent rules. All xyloglucan oligosaccharides have a β -(1 \rightarrow 4)-glucopyranosyl backbone, some of them substituted with one or more additional residues. In the proposed nomenclature, a code letter is defined for each glucosyl residue in the backbone depending on the pattern of side-chain substitution as it is described in the following list²² (Table 1):

Code letter	Structure represented
G	β -D-Glcp
X	α -D-Xylp-(1 \rightarrow 6)- β -D-Glcp
L	β -D-Galp-(1 \rightarrow 2)- α -D-Xylp-(1 \rightarrow 6)- β -D-Glcp
F	α -L-Fucp-(1 \rightarrow 2)- β -D-Galp-(1 \rightarrow 2)- α -D-Xylp-(1 \rightarrow 6)- β -D-Glcp
A	$\left. \begin{array}{l} \alpha\text{-L-Araf(1}\rightarrow\text{2)-} \\ \alpha\text{-D-Xylp(1}\rightarrow\text{6)-} \end{array} \right\} \text{-}\beta\text{-D-Glcp}$
B	$\left. \begin{array}{l} \beta\text{-D-Xylp(1}\rightarrow\text{2)-} \\ \alpha\text{-D-Xylp(1}\rightarrow\text{6)-} \end{array} \right\} \text{-}\beta\text{-D-Glcp}$
C	$\left. \begin{array}{l} \alpha\text{-L-Araf(1}\rightarrow\text{3)-}\beta\text{-D-Xylp(1}\rightarrow\text{2)-} \\ \alpha\text{-D-Xylp(1}\rightarrow\text{6)-} \end{array} \right\} \text{-}\beta\text{-D-Glcp}$
S	α -L-Araf-(1 \rightarrow 2)- α -D-Xylp-(1 \rightarrow 6)- β -D-Glcp

Table 1: Codification for XG related structures. The code names each glucose in the backbone and the side chain substitution it presents.

One code-letter is assigned to each glucose on the backbone with its branching groups starting from the non reducing end to the reducing end.

As example, the given names of the following xyloglucan oligosaccharides are:

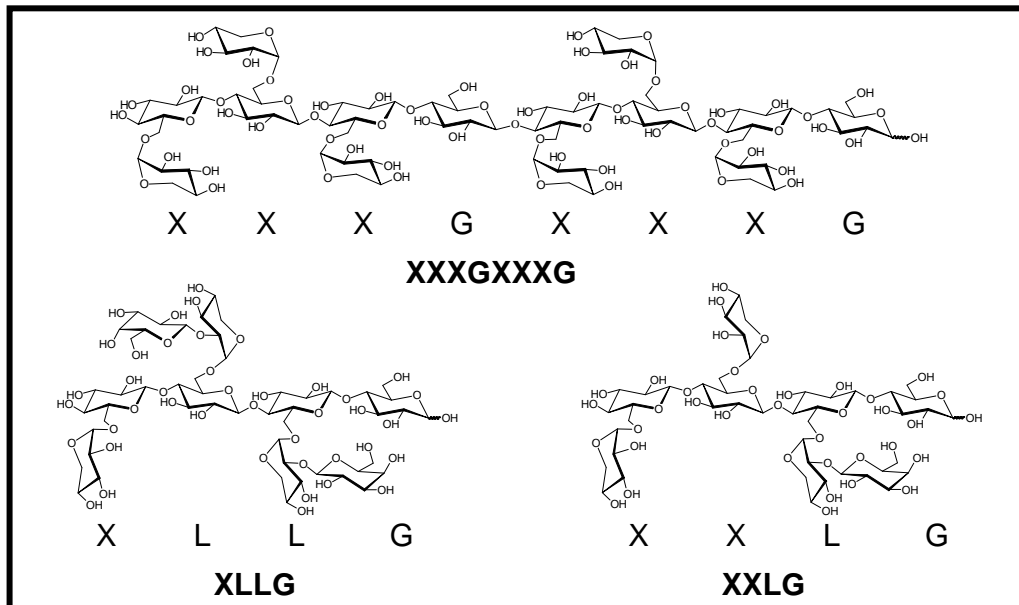


Figure 7: Examples of specific nomenclature of some xyloglucan oligosaccharides.

6.2.- Xyloglucan biosynthesis.

Xyloglucan (XG) is synthesized in the Golgi apparatus by different glycosyl transferases and later it is exported by the Golgi derived vesicles to the plasma membrane. Enzymes responsible of XG synthesis are not still unequivocally identified due to the inactivation they suffer due to cell extraction processes.

Different research groups have started to obtain some conclusions on XG biosynthesis: XG biosynthesis can be observed in membranes preparations, when both UDP-glucose and UDP-xylose were added^{21,23,24}, demonstrating the existence of XG-glucosyl and XG-xylosyl transferases involved in XG biosynthesis. These studies showed that the incorporation of xylose into XG is dependent on the presence of UDP-Glc in the incubation mixture, since in absence of it, only a restricted amount of Xyl was incorporated. On the other hand, incorporation of Glc was dependent of UDP-Xyl concentration, but it was inhibited at high UDP-Xyl concentrations. These results suggested that XG glucosyltransferase is regulated by UDP-Xyl and that the glucosyltransferase acts cooperatively with the xylosyltransferase^{21,25}. It was also described that the degree of xylosylation of the β -glucan backbone of xyloglucan depends on the UDP-Xyl:UDP-Glc concentration ratio²⁶.

Other monosaccharides such as D-galactose and L-fucose seem to be added to XG in later stages of XG synthesis. XG galactosyl and fucosyl transferase activities were detected in pea epicotyl microsomes preparations. It was observed that XG galactosyltransferase preferentially transfer the galactose unit to $-XX\underline{X}G-$ to form $-XX\underline{L}G-$, observed by measuring radioactive labeling incorporation in newly synthesized XG (the same reaction was detected with $-XL\underline{X}G-$ to produce $-XL\underline{L}G-$)²⁵. It was also concluded that this galactosyltransferase complex should recognize three XG subunits to explain normal pea XG galactosylation/fucosylation pattern $-XXLGXXXG-$ (Figure 8).

Fucosyltransferase activity occurs separately from galactosyltransferase²⁵. This enzyme is more studied, it has been purified and characterized and its encoding genes were identified^{20,27,28}. Again this fucosyltransferase show higher affinity for XG trimmers than for monomers, rendering the repeating hepta:nonasaccharide subunits ($-XXXGXXFG-$) (Figure 8). Fucosylation always occurs on the galactosyl group nearer to the reducing end (only XXFG and XLFG were detected but neither XFXG nor XFLG were detected)²⁷.

A clarifying schematic representation of XG biosynthesis was proposed by Faik *et al.*²⁵ and it is adapted below:

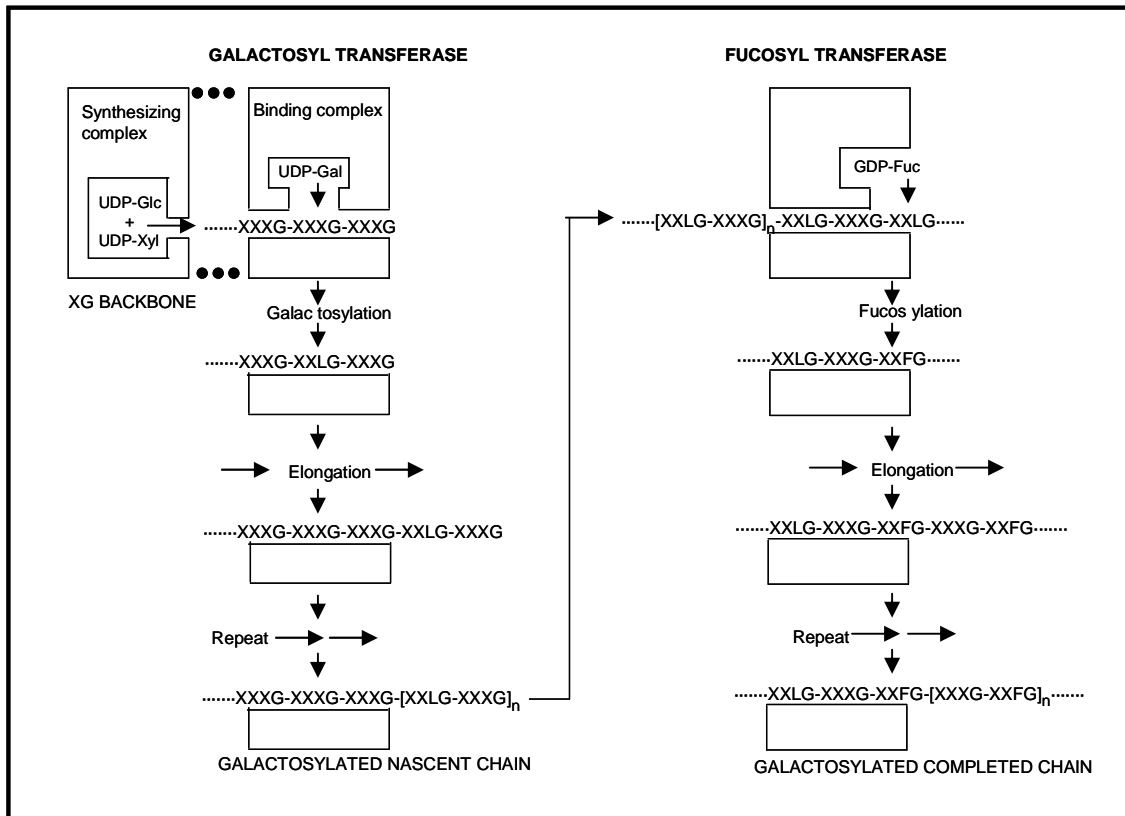


Figure 8: Xyloglucan biosynthesis proposed model. A synthetic complex was proposed for the synthesis of XG backbone ($-\text{XXXG-XXXG}-$). The binding complex recognizes three units of XG and transfer a galactose unit from UDP-Gal. Fucosylation to previously added galactose was proposed, adapted from Faik *et al.* (1997)²⁵.

7.- Plant cell wall dynamics.

Although cell wall is the unique structure responsible of plant cell strength and rigidity, it also has to be an extremely flexible and dynamic structure to allow the huge changes experienced by a plant cell during its life. Cells could extend to ten, hundred or thousand fold their original length, normally maintaining cell wall thickness² indicating the existence of a coordinate action of different cell wall loosening enzymes and deposition of nascent material.

There is a general agreement that cellulose-XG network serves to hold the primary cell wall together and it is the key determinant of wall extensibility^{1,2,4,29-31}. Current hypothesis propose that modification of the cellulose-XG network is the key process that controls cell wall extensibility. Clearly, the deposition of new wall material is necessary to maintain wall strength and wall thickness during extension. Some studies seem to indicate that wall deposition might induce somehow wall extension, but some controversy exist on this because cell wall extension was observed *in vitro*, without the direct need for wall synthesis³². More recent studies on wall loosening focus on the enzymatic basis for cell wall extension despite of some proposals on non-enzymatic cell wall modification that produce loosening.

In the present work the basic enzymatic models will be presented. In these models different wall-modifying enzymes seem to have important roles on cell wall modification that results in cell extension:

a) **Expansins** were identified as mediators of acid-induced wall extension^{33,34}, and is one of the only enzyme classes that directly modulate wall mechanical properties. Current hypotheses propose that expansins disrupt non-covalent bonds between wall polysaccharides, acting as a kind of “molecular grease” allowing polymers to slide between them^{12,32}.

b) **Yieldins** are characterized by their ability to lower the threshold for extension (minimum force or pressure necessary to drive the extension of cell wall)^{35,36} although their mode of action was still unrevealed.

c) **Polysaccharide hydrolases** are present in cell walls and they are able to hydrolyze the major components of the cell matrix. Then, it is easy to think of these enzymes as possible responsible actors of cell wall loosening due to hydrolysis of load-bearing links between cellulose microfibrils. In contrast, no definitive experimental proof has demonstrated the ability of hydrolase preparations to provoke cell loosening in *in vitro* assays³⁷, so a direct role in wall loosening awaits confirmation. Only in one

case it was found that an endoglucanase exhibits extension activity on heat-inactivated hypocotyls similar to expansin activity, although it is a fungal endoglucanase³⁸.

d) **Xyloglucan endotransglycosylases / hydrolases (XTHs)** are proposed to have a key role in all changes that xyloglucan polymers experience during cell expansion. They cut a xyloglucan polymer forming a relative stable glycosyl-enzyme intermediate and can reconnect the newly-formed reducing end to another xyloglucan molecule^{3,31}. This activity makes xyloglucan endotransglycosylases (XETs) good candidates for **controlled** XG modification, because they cut the XG polymer allowing reorganization of cellulose microfibrils and then recover the strength of cell wall by transglycosylation with another XG polymer (Figure 9).

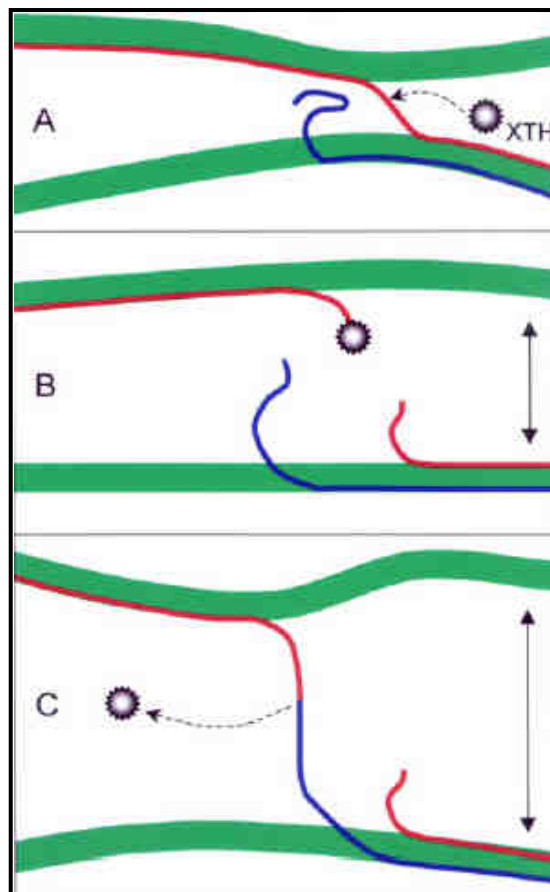


Figure 9: XET catalyzed transglycosylation causing cell wall restructuring. First XET binds to a XG polymer (A) which acts as tether between two microfibrils, after that, XET cuts the XG molecule forming a stable intermediate and allows movement between microfibrils (B). Finally, another XG molecule acting as acceptor liberates the XG-XET intermediate reforming a tether between microfibrils. Picture from Rose *et al.* (2002)³¹.

Surprisingly, in contrast with expansins or yieldins, *XTHs* do not induce unilateral cell wall extension *in vitro*³⁷. Despite of these results it has to be taken into account that boiled plant tissues were used as substrates in these experiments and this treatment would have eliminated cellular turgor and any active process, including secretion of xyloglucan into cell wall. Despite of this controversy, different roles in cell wall expansion have been demonstrated for *XTHs*: wall biogenesis, rearrangement of xyloglucan-cellulose network during wall assembly and growth, modification of XG size, etc.^{3,10,31,39}.

A summary model for wall extension could divide these enzymes in two subgroups: Primary wall-loosening agents, known as agents that are able to induce extension of walls *in vitro*, without any other process involved on it. And secondary wall-loosening agents, defined as those substances and processes that modify wall structure to enhance the action of primary agents, or that stabilize the new extended conformation of cell wall³², or that need a cooperating action of different processes (XET action plus cellulose and xyloglucan biosynthesis).

8.- EDEN project.

This work is part of an European project called EDEN (Enzyme Discovery in hybrid aspen for fiber ENgineering) which include 9 different laboratories. The main objective of the project was to identify novel plant enzymes for deeper understanding of the process of fiber formation/modification for future improvement of the quality parameters of wood fibers (<http://afmb.cnrs-mrs.fr/EDEN/home2.html>).

Concretely, the different objectives to be achieved were:

a) Global expression profiling of the entire EST (expressed sequence tags) library of the wood-forming tissues of hybrid aspen in order to identify genes that are highly expressed during cambial derivatives differentiating into wood cells.

b) Sensitive sequencing and domain organizational analysis of selected enzymes using novel software and sequence comparison tools available within the consortium.

c) Heterologous expression, assay development and enzymatic characterization of selected enzymes to establish new details of the metabolic routes of wood fiber formation.

d) Analysis of the xylem fiber structure and chemistry of *Arabidopsis* knock-out mutants in genes homologous to the wood-specific transcripts in hybrid aspen.

e) Protein localization analyses and fiber characterization of transgenic lines of hybrid aspen with up/down regulated expression of the selected genes.

f) Micropulping experiments using engineered fibers from a few most interesting transgenic lines of hybrid aspen to correlate product characteristics with the novel enzymatic activities.

In the framework of the EDEN project, the present work focuses on the biochemical characterization of a new xyloglucan endotransglycosylase from *Populus tremula x tremuloides*, cloned and expressed within the EDEN consortium.

9.- Xyloglucan endotransglycosylases.

The xyloglucan-cellulose matrix is the scaffold in which all the cell wall is built. Actually one enzyme family was thought to have the most important role on building and modifying this matrix. These enzymes named xyloglucan endotransglycosylases (XETs) are able to cut a xyloglucan molecule and reconnect the newly generated reducing end with another xyloglucan molecule (Figure 10).

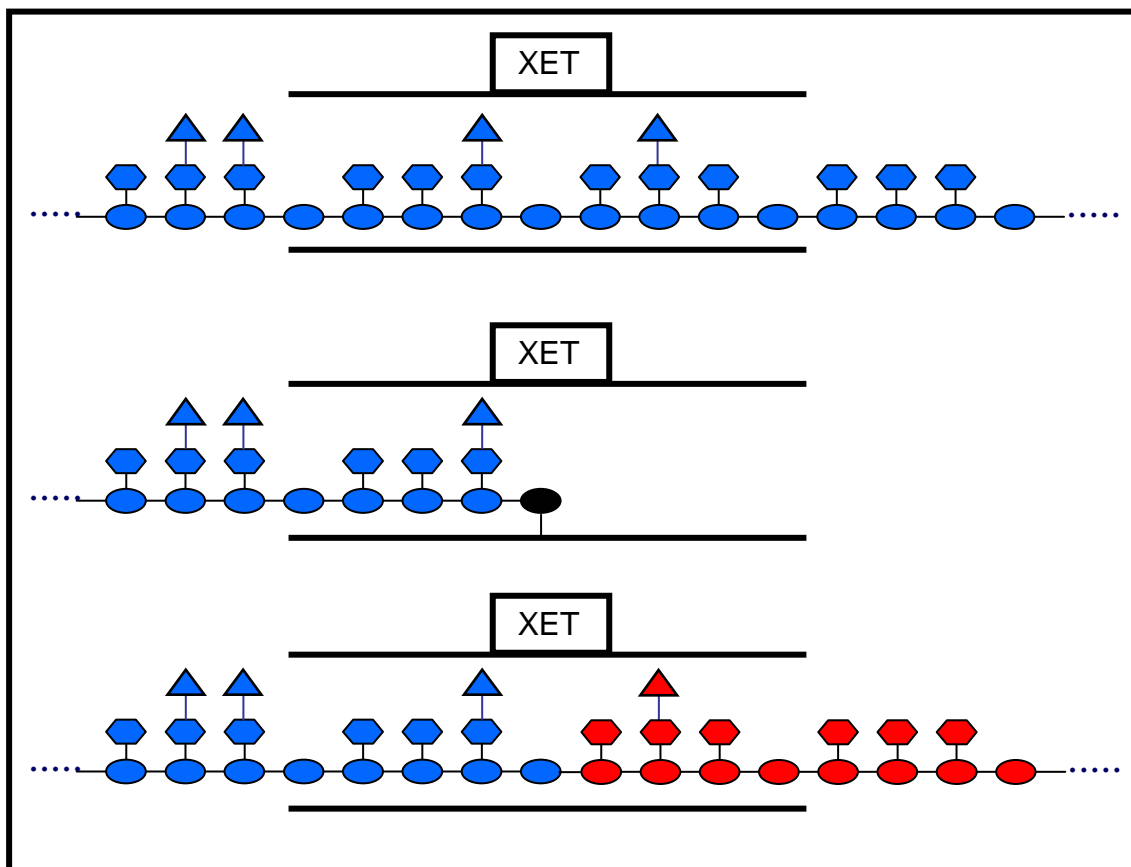


Figure 10: Schematic representation of XET catalyzed reaction where a xyloglucan molecule is splitted (blue) and newly generated reducing end (black) is reconnected to another xyloglucan molecule (red).

At the beginning of XET history, three independent groups detected a new activity on plant cell extracts⁴⁰⁻⁴². They observed XG depolymerization using different enzyme preparations when low molecular weight XG oligosaccharides were present in the media.

Nishitani and coworkers⁴⁰ purified an enzyme from the extracellular space of epycotyls of *Vigna angularis* which, when assayed with high molecular weight xyloglucan (230 kDa) and low molecular weight pyridylamino xyloglucan (15 kDa) as substrates, produced high molecular weight pyridylamino xyloglucan products (149 kDa). This experiment clearly indicates transglycosylation of a large xyloglucan oligomer (134 kDa) from the initial 230 kDa xyloglucan molecule to the 15 kDa pyridylamino sugars. When this enzyme was assayed with xyloglucan with a defined molecular weight distribution it caused only broadening of the elution peak profile on gel permeation chromatography (GPC), indicating the transfer of a segment from one XG molecule to another XG molecule giving higher and lower molecular weight xyloglucan species. No oligomers were detected in this experiment rejecting hydrolytic activities.

Fry and coworkers⁴¹ detected transglycosylase activity on pea stem homogenates, where transfer of a part of a large (200 kDa) non-radioactive xyloglucan molecule to a ³H-xyloglucan nonasaccharide was detected. The radioactive product was distinguished from the nonasaccharide by affinity binding to cellulose, by precipitation with ethanol or by paper chromatography. In these experiments, they demonstrated that the low molecular weight substrate acts as an acceptor.

Finally, Farkas and coworkers⁴² found transglycosylase activity on nasturtium (*Tropaeolum majus*) seeds extracts by measuring the reduction on viscosity of a solution of tamarind (*Tamarindus indica*) xyloglucan. They demonstrated that this enzyme preparation showed some hydrolytic activity on xyloglucan by reducing power measures. But the activity (by viscometric methods) of these enzyme preparations was enhanced (10-20 fold) by addition of XG oligosaccharides without the correspondent increase on reducing power. Finally they clearly demonstrated transglycosylation observing the gel permeation elution patterns and radioactive incorporation on high molecular weight oligomers using a non labeled xyloglucan oligosaccharide (XGO) solution and fucose-labeled XG nonasaccharide²⁶.

A hypothetical scheme of xyloglucan endotransglycosylase action on cell wall construction and modification was proposed¹⁰:

XG is synthesized in the Golgi apparatus and secreted into the cell wall space whereas cellulose microfibrils are synthesized in the plasma membrane. During cellulose microfibril synthesis XG interacts with nascent cellulose chains and it is incorporated in the semi crystalline structure of cellulose microfibrils. Other XG

molecules may interact with finalized microfibrils being adsorbed on the surface of them. This cellulose microfibrils with two different XG domains may anchor to the pre-existing XG-cellulose matrix. This phenomenon is proposed to occur via XET-mediated processing where transglycosylation between XG on newly synthesized cellulose microfibril and XG on the XG-cellulose matrix may create new covalent linkages between XG-cellulose matrix and new cellulose microfibril. In this way, incorporation of nascent polysaccharides into preexisting XG-cellulose matrix can be explained.

Plant cell experiences huge changes in cell wall structure during its life, then, XG-cellulose matrix may suffer continuous and controlled modification of its structure. These modifications can be produced via XET mediated processes. XETs are able to cut a XG bridge between two microfibrils allowing net movement between them rendering restructuring of XG-cellulose matrix and finally fixing again XG-cellulose matrix by transglycosylation (Figure 9).

Other enzymes such as endoglucanases and others can have co-adjutant roles in this XG network modification by XG hydrolysis, although these enzymes are not able to reform a XG bridge. XETs also can “cut” XG bridges via direct hydrolysis of them or transglycosylation to a low molecular weight XG oligomer.

During the last decade different studies on XETs were done, demonstrating their important role and the increasing knowledge in their mode of action, regulation, etc.

For the biochemical characterization and study of an enzyme, an activity assay is needed. To measure xyloglucan endotransglycosylase activity the commonly used assays for hydrolytic enzymes were not appropriate, because no increase on reducing ends is obtained.

9.1.- Enzymatic assays for XET activity *in vitro*.

Different assays have been designed to detect xyloglucan endotransglycosylase activity and they can be classified in three different groups:

9.1.1.- Assays based on physico-chemical changes.

Viscometric: High molecular weight XG solutions present high viscosity. Depolymerization of this high molecular weight XG, due to hydrolysis or transglycosylation to a low molecular weight acceptor renders a decrease in the solution viscosity⁴²⁻⁴⁴. This is not a specific assay for xyloglucan endotransglycosylases nor transglycosylation activity. It monitors a parallel effect, but it could render an indirect measure of transglycosylase activity with the correct controls to measure possible hydrolytic activity without low molecular weight acceptors.

Absorbance of the iodine-XG complex: As it is commonly known for starch, XG forms with iodine/iodide a colored complex with an absorbance maximum at 620 nm. This stainability is limited to XG molecules with a molecular weight higher than 10 kDa⁴⁵. Again an indirect measure of depolymerization of XG can be obtained measuring the decrease on absorbance at this wavelength with the adequate controls to correct possible hydrolytic activities^{42,45-47}.

9.1.2.- Assays that measure XG molecular weight distributions:

Incubation of a defined molecular weight XG with XETs gives an increase in peak width in the elution pattern of this XG by gel permeation chromatography (GPC) without any change in the elution volume. This increase in the peak width was proportional to the dose of enzyme^{40,48}. In contrast, when some hydrolytic activity was present in the enzyme crude assayed, some low molecular weight oligosaccharides appear, in parallel to the increase in peak width, giving a prove of hydrolytic activity contamination.

9.1.3.- Assays using labeled acceptors:

Different enzymatic methods were developed to monitor XET activity using low molecular weight labeled acceptors, the differences between them depend on the label (radiometric, fluorescent) and on the method used to separate the labeled acceptors from the labeled products (chromatography, cellulose binding, precipitation, etc.).

Nishitani and coworkers^{40,48} used pyridylamino XG oligosaccharides (fluorescent label) as acceptors and monitored the incorporation of the label to a XG having a defined molecular weight by GPC. With this method a clear proof of transglycosylation was obtained although it was very difficult to obtain quantitative results.

Farkas *et al.*⁴² used ¹⁴C-fucosylated XG nonasaccharides as acceptors (obtained by ¹⁴C-fucosylation of a XG octasaccharide by pea fucosyltransferase) and transglycosylation products were isolated from labeled acceptors by precipitation in 50% ethanol. Molecular weight profiles of labeled and isolated transglycosylation products were analyzed by GPC.

Fry and coworkers⁴¹ used radiometrically labeled xyloglucan acceptors (XGOs were reduced with ³H₂ and a catalyst to obtain labeled XGOs) and they measured transglycosylation between high molecular weight non labeled XG donor and labeled XG oligosaccharides by separating different labeled species taking advantage of the high affinity that high molecular weight XG have for cellulose in contrast to the low affinity of the labeled low molecular weight acceptors.

The last separation method between labeled products and labeled acceptor is the most widely used on XET studies, because it allows accurate measure of reaction progress and permits obtaining quantitative data. Different authors have used this method with different labeled acceptors (¹⁴C-fucosylated⁴⁴, ³H-labelled^{46,49-52}, and fluorescently labeled acceptors⁵³).

All the above described enzymatic methods have important drawbacks; the most important one is the use of polymeric XG as donor substrate which is a polydisperse mixture of molecules, so that multiple turnovers render complex behavior preventing detailed kinetic evaluation. For that reason, in the present work one objective is **to design a new activity assay to study xyloglucan endotransglycosylases using low molecular weight substrates, with defined structures.**

9.2.- Classification (Enzyme Commission (E.C.), CAZY).

Each enzyme is named by the International Union of Biochemistry and Molecular Biology (IUBMB) which assigns an EC number based on the reaction catalyzed and its substrate specificity (<http://www.chem.qmul.ac.uk/iubmb/>). Xyloglucan endotransglycosylases have the E.C. 2.4.1.207.

This classification is useful to indicate the activity of an enzyme, but it doesn't give any information about mechanism, neither sequence homologies nor 3D structure. And also it is limited because the same enzyme could have activity on different substrates or catalyze different reactions, having different EC numbers.

For that reason, in 1991 B. Henrissat⁵⁴ proposed a new classification for glycosyl hydrolases based on sequence similarity. Initially they started with 291 sequences of glycosyl hydrolases classified in 35 families. After some years, the classification was extended to other carbohydrate acting enzymes such as lyases, glycosyltransferases, and carbohydrate binding modules⁵⁵⁻⁶⁰.

This classification based on sequence similarities is related with the 3D structure of the proteins, thus within the same family there are enzymes with different specificities, but they have similar 3D structures and mechanism of action. It was also observed that there are 3D structural similarities between members of different families indicating that probably they have a common evolutionary ancestor. It allows grouping families in clans. Within one clan, different enzymes present similarities in tertiary structure together with conservation of the catalytic residues and the catalytic mechanism⁶¹⁻⁶³.

This classification is actualized and maintained by Henrissat and coworkers and it is available on the internet: www.cazy.org/CAZY/. Currently, more than 100 glycosyl hydrolase families, 78 glycosyl transferase families, 18 polysaccharide lyases families and 43 carbohydrate binding module families are found.

XTH belongs to family 16 glycosyl hydrolases and up to now, it is the unique transferase in this family.

9.3.- Nomenclature.

Recently an unifying nomenclature for xyloglucan endotransglycosylases has been proposed which pretends to describe the biochemical activities of these enzymes³¹. These authors propose to name all xyloglucan endotransglycosylases as *XTH* (xyloglucan endotransglycosylase / hydrolase), because in some cases some hydrolase activity was detected for different xyloglucan endotransglycosylases^{42,49,64}.

Each *XTH* enzyme should be named with a two letter prefix being the initials of the genus and the specie followed by *XTH* and finally, a number indicating the number of *XTH* gene in the specie. For example *XTH* genes from *Arabidopsis thaliana* should be named as *At-XTHx* (x is a number). They propose to use XET and XEH only to refer to enzyme activities: XET (xyloglucan endotransglycosylase) and XEH (xyloglucan endohydrolase).

In EDEN consortium, it is thought that this new nomenclature is not adequate, while *XTH* may be an appropriate designation for genes with undetermined activity, it could provoke some confusions when applied to enzymes and moreover with enzymes with extremely little (immeasurable) hydrolytic activity.

In this work, this new unifying nomenclature will be used for genes with undetermined activity, to describe the gene or enzyme family in a non specific way and also to name specific enzymes described in bibliography as *XTHs*.

9.4.- Occurrence of *XTH* in plants (genomic information).

Nowadays, by sequencing comparison of the emerging genomic information from sequencing projects, different putative *XTH* sequences can be identified in different organisms. For example: In the *Arabidopsis* genome 33 *XTHs* were found, in the tomato genome 25 *XTHs*, in the rice genome 29 *XTHs* <http://labs.plantbio.cornell.edu/XTH/> and in Poplar genome 37 *XTHs* were identified. XET activity has been detected in all plant species analyzed.

In *Arabidopsis*, *XTHs* are classified into three major phylogenetic groups (Figure 11), or subfamilies³¹ in agreement with other phylogenetic studies of *XTH* genes from a broad range of plant species^{3,65-67}. In our project, a phylogenetic tree of *XTH* genes from *Populus trichocarpa* has been obtained (Figure 12), although the traditional 1-3 grouping has been presented (Figure 12) more recent studies propose that the division

between subgroups I and II it is not clearly observed and that traditional group III can be divided in Group III-A and B⁶⁸.

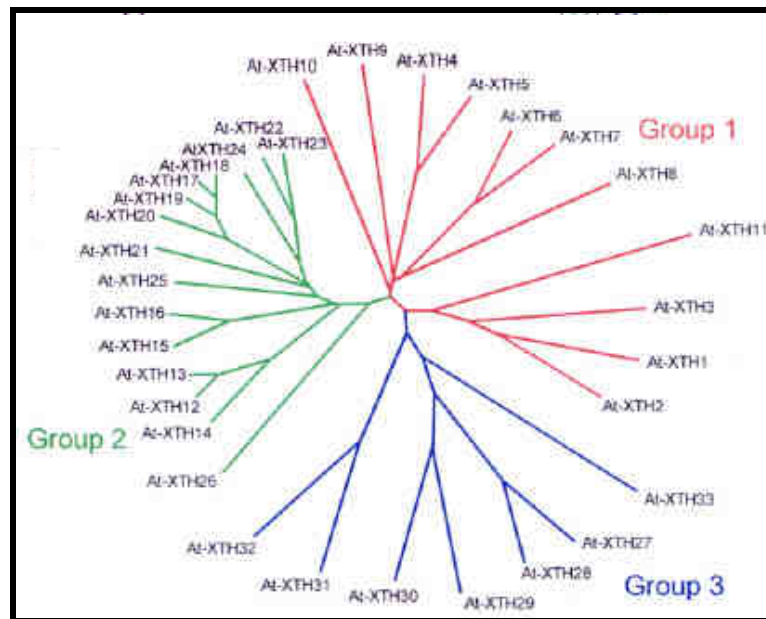


Figure 11: Dendrogram representing phylogenetic relationship between the members of the *Arabidopsis XTH* gene family, from Rose *et al.* (2002)³¹.

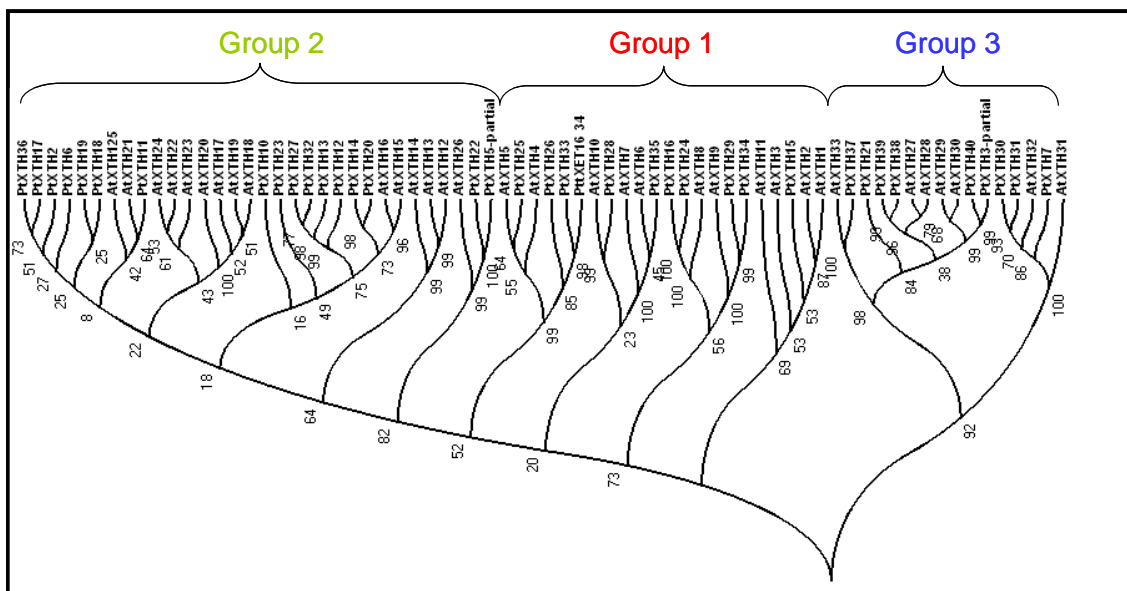


Figure 12: Phylogenetic tree of *Arabidopsis XTH* gene family and Poplar gene family including *Ptt-XET16A*. (Provided by Jens Eklöf from KTH (EDEN partner)).

It is quite surprising that there are so much *XTH* genes in one organism; that raises the question of whether these genes are redundant in terms of their physiological role. To answer this question, it has been shown that different genes have distinct organ or tissue expression profiles, and sometimes in the same tissue different *XTH* genes are differently regulated by auxin, gibberellins, brassinolide and abscisic acid, or differentially expressed in response to environmental stimuli³¹.

Therefore it seems that every *XTH* gene has a unique expression and regulation profile, reflecting a unique biological role for each *XTH* enzyme in a specific organ or tissue and as response to a regulation process³¹.

9.5.- Mechanism of action.

Since 1992 when first xyloglucan transglycosylase/hydrolase (*XTH*) were identified^{41,42,48}, a number of biochemical studies on these enzymes have been done. In this section different proves of the mechanism of action of these enzymes will be presented and discussed.

Two activities were observed in different purified *XTH*. A group of enzymes were exclusively transglycosylases without any hydrolase activity^{46,47}. Others had transglycosylase activity when a relative high concentration of XGOs acceptors were present, but they have hydrolase activity when no acceptors were present^{42,49,64}.

Initially, these different activities were proposed to correlate with the phylogenetic groups presented before (Figure 11 and Figure 12). For example in Group 1 and 2 only pure transglycosylases have been found^{40,69,70}; in contrast, xyloglucan endohydrolases have been found only in Group 3⁷¹⁻⁷³, although some exceptions have been reported⁴⁹. Recent studies seems to indicate that this phylogenetic subgroups in *Arabidopsis XTH* gene family seem not to correlate with hydrolytic or transglycosylase activities⁷⁴, and it is proposed that all *XTH* should have both activities with different hydrolase/transglycosylase ratio depending on the *XTH*. Another study propose the structural requirements for a *XTH* to have xyloglucan endohydrolase activity (always present in enzymes classified in the new subgroup A of Group 3 of newly published phylogenetic tree)⁶⁸.

First studies have demonstrated that when reaction between high molecular weight xyloglucan polymers and ³H-labeled xyloglucan oligosaccharides occurs, the label was present in the reducing end of the product, as seen by oxidation in warm

NaOH of the terminal glucose to yield $^3\text{H}_2\text{O}$; therefore **the labeled xyloglucan oligosaccharide acts as acceptor**^{41,75}.

In parallel, it was demonstrated by $^1\text{H-NMR}$ that there is no change in the ratio of anomeric protons during enzyme reaction, therefore a single type of glycosidic linkage was involved in both the splitting and reconnection steps of the XET reaction⁴⁰, that means that **XTHs act with retention of configuration**. The same conclusion was obtained by degradation of ^3H -labeled XG products by *Trichoderma* cellulose (endo- β -(1 \rightarrow 4)-D-glucanase) when the ^3H -labeled acceptor was recovered⁴¹ demonstrating that a β -(1 \rightarrow 4) linkage is hydrolyzed.

XTHs belong to family 16 of glycosyl hydrolases and this classification could lead to propose that **XTHs work via a double displacement mechanism** with retention of configuration, forming a glycosyl-enzyme intermediate (Figure 13) by analogy with the demonstrated mechanism of action of glycosyl hydrolases in family 16⁷⁶⁻⁷⁸.

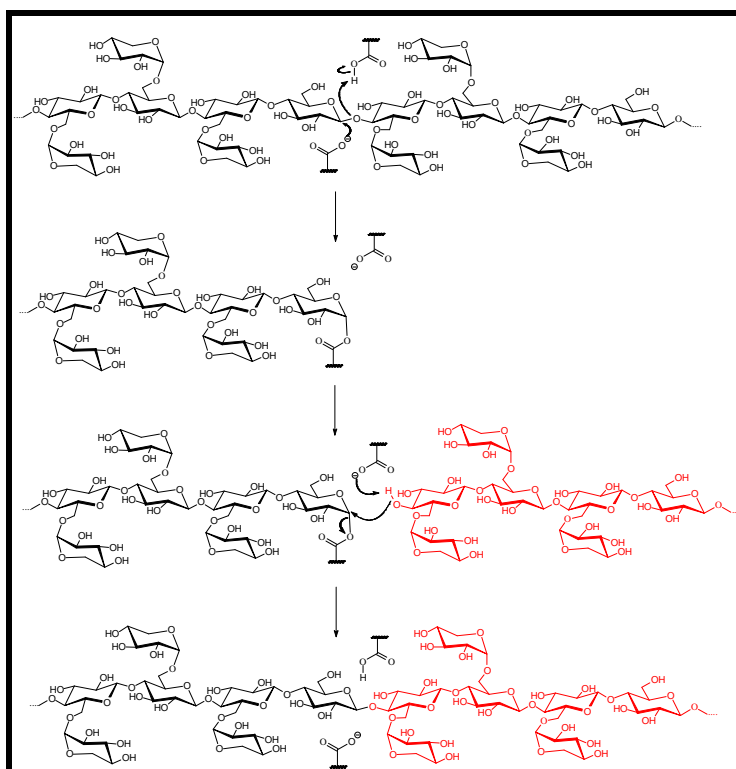


Figure 13: Mechanism of action of XET. First step: The nucleophile residue attacks the anomeric carbon, forming a glycosyl-enzyme intermediate and a fragment of the donor (black) is liberated. Second step: An acceptor molecule (red) enters the catalytic site and by basic catalysis, it attacks the glycosyl-enzyme intermediate rendering the transglycosylation product with retention of configuration.

Taking into account the mechanism of action of XETs presented above (Figure 13), it could be clearly explained the existence of some enzymes presenting xyloglucan endohydrolase activity (XEH). The only difference between XET and XEH activities is the acceptor involved in the second step if a water molecule acts as acceptor hydrolysis of the XG molecule occurs, in contrast if a XGO molecule acts as acceptor, transglycosylation occurs.

Existence of the **stable intermediate** proposed in Figure 13 was supported by different experiments:

a) When a XET was incubated with XG polymer, substrate depolymerization is initially observed, but the reaction stops. The magnitude of depolymerization is proportional to enzyme concentration. The entire enzyme was probably bound as an intermediate complex with XG, relatively stable against water, so that, this enzyme complex becomes temporarily inactive. This stage could be disbalanced by the addition of more XET or xyloglucan oligosaccharides (XGOs). A new equilibrium was formed at a higher level of conversion when all the enzyme was trapped again as XG intermediate complex or XGOs concentration was zero⁷⁹.

b) This intermediate was used to purify XETs by affinity absorption of the XG molecule, carrying XET as its covalent stable intermediate, to cellulose. The XET was liberated using XGOs as acceptors^{80,81}.

c) It was demonstrated that this intermediate was present also in cell walls: Isolated cell walls were washed with 1M NaCl to remove loosely bound proteins (82-86% XET activity was removed). After that, cell walls were incubated with ³H-XGOs and a time dependant release of XET activity in the supernatant was observed in parallel to the incorporation of radioactive acceptors into the insoluble fraction⁸².

By sequence similarity analysis between *XTH* gene products and by comparison with glycosyl hydrolases in family 16, the amino acid sequence of the active site of *XTHs* was proposed to be DEIDFEFLG or DEIDIEFLG⁸³. **The glutamate residues were proposed to be essential** by analogy to β -(1→3)(1→4)-glucanases, **the first acting as nucleophile and the second as general acid base**⁸⁴. This was demonstrated by Braam and coworkers for the first glutamate by site directed mutagenesis⁷⁰.

Another question is **the site of donor cleavage**. To answer this question, different studies were done obtaining different conclusions. First of all, it was demonstrated that *XTHs* split the donor molecule by a non branched glucose of XG^{41,71,85}.

Another open question is whether *XTHs* act by **random or specific cleavage**. In different studies it was demonstrated that *XTHs* could split XG molecule randomly^{40,86} where ten *XTH* enzymes were evaluated and all of them act in a random mode. In contrast, there are other studies that seem to demonstrate that some *XTHs* split XG molecule at a fixed distance of the reducing end or the non reducing end:

a) An enzyme from azuki bean epicotyls hydrolyses XG from 1500 to 400 kDa to fragments of 50 kDa without formation of smaller oligosaccharides. This enzyme had no hydrolytic activity towards 64 kDa XG donors. But again, it transferred a fragment of 50 kDa when activity was evaluated with pyridylamino-labeled xyloglucan oligosaccharides⁶⁴. Therefore it seems that this enzyme recognize XG donor by the way of transferring a 50 kDa from the non reducing end.

b) *Tropaelum majus XTH* gene product from epicotyls seems to act transferring low molecular weight xyloglucan fragments, thus it cleaves XG very near to the reducing end⁸⁷.

9.6.- Biochemical properties.

Other biochemical characteristics of *XTHs* were studied such as enzyme activities at different experimental conditions (pH, temperature, cations), inhibitors, inactivation, stability, effect of protein glycosylation, etc. In the following paragraphs these biochemical studies will be summarized and discussed.

Comparison of different *XTH* sequences indicate that there are some consensus regions in their genes (signal peptide, DEIDXEFGL catalytic sequence, putative N-glycosylation site, and different pairs of cysteines on the carboxy-terminal region that could form disulfide bridges, etc.)⁶⁵.

Presence of at least one **disulfide bond** was observed in different *XTHs* such as a *XTH* from pea internodes⁴¹ or the *At-XTH22* recombinantly expressed in baculovirus infected insect cells⁸⁸ or *E. coli*⁵⁰. *Ptt-XET16A* presents two disulfide bonds^{68,89}.

Another possible common feature of *XTH* enzymes is the **putative N-glycosylation site**: most *XTHs* studied are glycosylated^{46,68,88}. In general, a glycoprotein could be treated with Endoglycosidase H (Endo H), which leaves a N-acetylglucosamine residue attached to the amino acid residue, and with peptide:N-glycosidase F (PNGase F), which removes all sugar units and convert the asparagine residue to an aspartic acid. Implication of the N-glycosylation in *XTH* activity was evaluated in different studies:

For example, treatment of *At-XTH22* heterologously expressed with baculovirus infected insect cells with PNGase F eliminated 98% of the activity and treatment with Endo H removed 48% of activity⁸⁸. This lost of activity was not a general behavior as it is exemplified by some authors⁷⁰ with other *Arabidopsis XTHs*: *At-XTH4*, *At-XTH14* and *At-XTH24* were treated with PNGase F and only *At-XTH24* showed a significant decrease in activity.

A profound study on XET N-linked glycosylation was done within this project (by T. Teeri group (EDEN partner) in a XET from cauliflower (*Brassica oleracea* var *botrytis*) florets, purified from plant extracts or recombinantly expressed in *Pichia pastoris*. This enzyme was nearly identical, by sequence alignment of known *At-XTH4*. The authors firstly demonstrated that the putative N-linked glycosylation site found in the majority of *XTH*-related protein sequences is the site of glycan attachment, by MS analysis. They observed that totally deglycosylation of this XET provoked a reduction of 40% of activity, but no totally elimination of activity. That could indicate that the glycosylation did not affect strictly the catalytic mechanism, and it is proposed that it could have some stabilization role⁴⁶.

The same group⁴⁷, have studied N-glycosylation in *Ptt-XET16A* expressed in *Pichia pastoris*. *Ptt-XET16A* and side directed deglycosylated *Ptt-XET16A* N93S were kinetically characterized obtaining similar apparent kinetic parameters and similar thermal stability, however, *Ptt-XET16A* N93A showed impaired secretion in *P. pastoris* and high susceptibility to precipitation and moreover any effect to intrinsic enzyme activity was detected due to endo H catalysed deglycosylation. They finally proposed the possibility that for other *XTH* enzymes, N-glycan can play a more crucial role in the positioning of the acceptor loop for catalysis than for *Ptt-XET16A*, although they discard this possibility for Group 3 *XTHs* taking into account that N-glycosylation position is shifted 15 residues towards C-terminus.

Different authors have evaluated the effect on XET activity of addition of different species to evaluate the inactivation or activation effects. No clear tendencies are reported, but it can be affirmed that Ag^+ , Zn^{2+} , La^{2+} and Hg^{2+} have some inhibition effect, and BSA and urea some activation effect.^{41,49,50,88}

Temperature and pH dependence of XET activity was evaluated for a quite high number of XETs. These enzymes act in the cell wall of plants, and normally it is thought that pH in cell walls is between 5 and 6, so a pH optimum near this range is expected, and in general, most of XETs show maximum activity between 5 and 6.5, some of them with a sharp and some with broad pH profiles^{41,46,49,50,70,87,90}.

Another fact to take into account is that plants can grow in a wide temperature range, then, enzymes should have a wide temperature margin of activity. Most XETs studied showed a relatively high activity in a wide temperature range, more than 50% of the maximum activity at least in a 25°C temperature range. Temperatures of maximum activity are described between 18 and 30 °C and some enzymes showed 50% of activity at extreme temperatures such as 5 °C and 45 °C^{46,50,70,90}.

9.7.- Substrate specificity.

A number of studies have evaluated different oligosaccharides as substrates for XETs, but always limited to natural oligosaccharides or oligosaccharides derived from them. This limitation is a drawback to obtain XET specificity information. In the following paragraphs current knowledge about substrate specificity is discussed:

9.7.1.- Donor substrates.

Different polysaccharides were tested as possible donor substrates for XETs (xyloglucan, pectin, dextran, cellulose, xanthan gum, laminarin methylcellulose, alginate, β -(1→3)(1→4)-glucan, nigeran, starch, xylan, arabinoxylan, guar, manan, inulin, chitosan, rhamnogalacturonan-I and -II, α -(1→5)(1→3)-L-arabinan, β -(1→4)-galactan, 4-O-Me-glucoronoxylan, arabinogalactan, carboxymethylcellulose) but only with XG, some activity was detected^{40,41,50}.

Some XETs prefer certain XG substructures in the donor molecule, for example some XETs prefer fucosylated XG donors^{40,70,91} others prefer non-fucosylated XG donors^{41,51,70}, others act similarly on Fuc or non-Fuc XG^{50,51,70}, and some XETs have higher activity on less branched XG substrate, i.e. XET from tomato (*Lycopersicon esculentum*) have 4 fold more activity against Tomato XG than against Fuc or non-Fuc XG⁹¹.

Although it is a surprising result, some XETs seem to prefer XG of relatively high molecular weight. For example, XET from *Vigna angularis* seems to prefer at least XG donors of 10 kDa molecular weight showing higher activities as larger the donor is⁴⁰; One XET from azuki bean is only active against XG of MW > 60 kDa⁶⁴. Other XETs seem to prefer relatively low molecular weight XG donors, for example a XET from kiwi fruit shows higher activity on XG with MW below 20 kDa⁴⁹, and at least some XET tolerate donors as small as XXXGXXXG and GXXGXXXG^{71,85}.

It is quite surprising that enzymes that are relatively small molecules in comparison to XG could “sense” if the XG substrate has the correct length. It is reasonable to assume that XET recognizes, at most, a specific pattern of substitution of small molecules as the mentioned XXXGXXXG. However, taking into account that XETs act on polymeric substrates, it is possible to hypothesize that some secondary interactions (superficial) can be produced between polymeric substrates and XETH which can revert higher efficiencies on larger substrates.

In some papers, it is proposed that most XETs do not use such small donors, but the problem could be that there are no enzymatic assays to verify if such small donors could be donors of different XETs. For that reason, the **design a new enzymatic assay to evaluate possible low molecular weigh donors** will be one of the objectives of the present work.

9.7.2.- Acceptor substrates.

Specificity for acceptor substrates was further more studied than for donors:

a) All XETs studied can use XGOs derived from cellotetraose (more or less substituted) as acceptors and also higher oligomers.

b) **Reducing terminus is not required:** It was proved by using NaBH₄ reduced XGOs acting as acceptors^{46,49,50,52,70,86-88,90,92-97} or reducing end labeled XGOs

acceptors e^{40,53,64,91,98-101} that the reducing end of the acceptor is not required for activity.

c) **Lineal oligosaccharides are not acceptors, therefore some branching is required:** only xyloglucan oligosaccharides can be used as acceptors for XET, neither cellotetraose (GGGG) nor cellohexaose (GGGGGG) are acceptors for XETs. Some xylosyl substitution should be a requirement for a substrate to act as acceptor^{40,41,71,95}. Recently, however a nasturtium xyloglucan endotransglycosylase / hydrolase have shown some transglycosylase activity on cellobiose (GG), celotriose (GGG), and cellotetraose (GGGG)⁶⁸.

d) **Acceptor specificities (XXG is the minimum acceptor):** most abundant XGOs (XXXG, XLXG, XLXG, XLLG, XXFG, XLFG, etc.) have been widely used in XET studies but only some authors have analyzed shorter acceptors: Fry and coworkers⁴¹ have evaluated different labeled XGOs using a competing assay to obtain relative measures of acceptor affinities, showing the following relative sequence XLFG \approx XFG \gg FG \approx X = 0. By these competing assays, estimated I₅₀ values were obtained: 19 μ M for XLLG, 33 μ M for XXXG and proposing XXG as the simplest structural unit for an acceptor⁴¹. The same minimal acceptor (XXG) was proposed by Steel *et al.* with cauliflower and mung bean XET, although for one isoenzyme minimal activity was detected using the trisaccharide XG as acceptor⁹⁰. In this study a pronounced preference for higher degree of polymerization (DP) oligosaccharides was detected showing higher activities for larger acceptors XLLG > XXXG > XXG > XG.

e) Fry and coworkers⁹⁵ tried to determine which of the xylosyl residues of XXG are needed to act as acceptor. They evaluated GXG and XGG as possible acceptor but neither of them showed activity, concluding that **both xylosyl substitutions of XXG are required**. This result were somehow limited due to the relatively lack of mono-xylosyl-substituted oligosaccharides and seems to be contradicted by qualitative results from Fanutti *et al.*⁸⁵ which indicate that xylosyl substitution at +1 was not required.

In summary, this studies shown that acceptor specificities is enzyme dependent where both the preferred length and the degree of branching can vary between XETs^{40-42,85,90,95}. This could explain the high diversity of activities proposed for XETs in cell walls. But we think it is necessary to have a substrate library to analyze XET specificity. For that reason, **one of the objectives of the present work is to design, synthesize and evaluate a XG-like oligosaccharide library to study donor specificity of XETs.**

9.8.- Subsite mapping.

Enzymes that bind oligomeric substrates have an extended binding site composed of subsites. One subsite is defined as the set of amino acid residues in the binding site that interact with one unit of the substrate.

Subsites are named using negative numbers starting from the catalytic machinery (the scissile glycosidic bond) to the non-reducing end, and with positive numbers starting from the scissile glycosidic bond to the reducing end^{102,103}. In our case, for XET, we use roman numbering for the glucosyl backbone and each xylosyl substitution is named with the same roman number assigned to the branched glucosyl unit with a prime superindex (Figure 14).

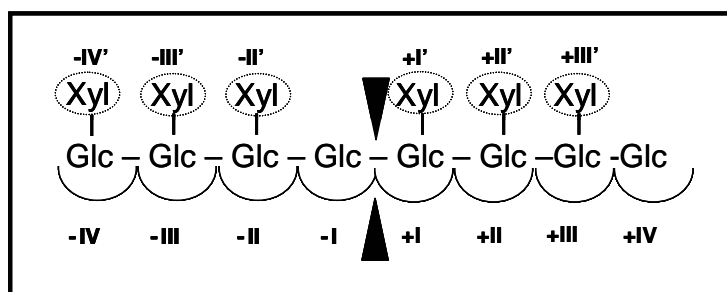


Figure 14: Subsite numbering in a XET bound to a xyloglucan oligosaccharide.

For XETs, only some research groups have tried to obtain information about subsite mapping, their hypotheses and conclusion will be discussed in the following paragraphs.

Fanutti *et al.* have studied qualitatively the transglycosylation and hydrolytic activity of a *XTH* from germinated nasturtium seeds with different isolated oligosaccharides (XXXGXXXG, XXXGXXLG + isomers, XXLGXXLG + isomers, XLLGXXLG + isomers, XLLGXLLG, GXXGXXXG and GLLGXLLG) and have proposed the substitution requirements at different positions of the donor molecule^{71,85}. Their conclusions are summarized as follows:

- a) **At -I subsite it has been shown that a non-substituted Glc has to be present.**
- b) GXXGXXXG underwent transglycosylation acting as donor and acceptor at the same time, the same is observed with GLLGXLLG. Therefore **xylosyl substitution was not necessary at -IV' subsite (when acting as donor) and +I subsite (when acting as acceptor).**

c) With the donor GXXGG-XXGXXXG a hydrolytic cleavage of “-“ glycosydic bond to give GXXGG and XXGXXXG was observed, indicating that **xylosyl substitution at -II’ subsite was not a requirement**. In contrast, no hydrolytical cleavage of GLLGG-LLGXLLG was observed, that was proposed as a clear indication that galactosyl-xylosyl substitution at +II prevent chain cleavage.

d) For subsites -III, +II and +III the conclusions they obtained were less clear. Taking into account the observation of transglycosylation with GXXG as acceptor, it could be concluded that **xylosyl substitution at +II’ subsite and/or +III’ subsite** are required. They had not obtained any direct evidence on which xylosyl substitution at +II and/or +III subsite is required, but taking into account molecular modeling studies which propose that XG polymer have an alternating conformation¹⁰⁴ (similar to the alternative flat “cellulosic” conformation), and the substitution requirements proposed before; Fanutti *et al.* hypothesized that **xylosyl substitution requirement at +III subsite seemed unlikely** (because xylosyl group at +III subsite would lie on the same side of the backbone as non-required xylosyl groups at -IV’, -II’, and +I’ subsites), but xylosyl substitution at -III and +II subsites were proposed to be required (because they would lie on the same side of the backbone) (Figure 64).

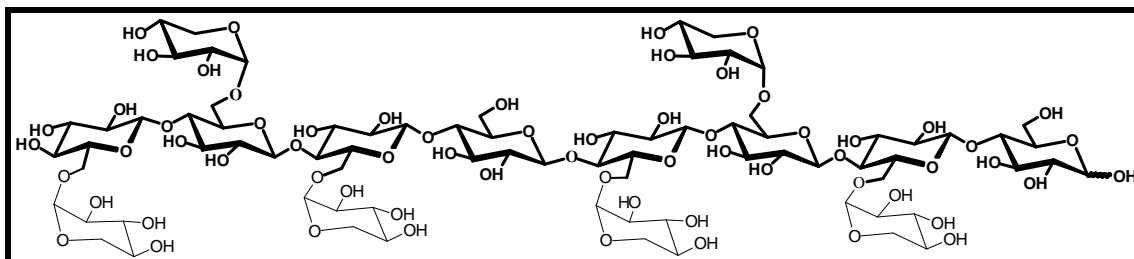


Figure 15: Schematic representation of structural requirements proposed by Fanutti and coworkers^{71,85}: In bold the glycosyl units proposed to be essential.

In the recently published tridimensional structures of *XTH* gene products^{68,89,105}, three positives and four negative subsites are proposed to exist.

9.9.- *XTH* studies in vivo.

Two main physiological roles for *XTHs* have been proposed by different research groups: **Incorporation of nascent XG in the cell walls**^{3,10,40,69,106}, and **XG matrix restructuring**^{3,10,40,41}.

XTH expression, function and activity *in vivo* have been evaluated in different studies:

9.9.1.- *XTH* expression.

Protein expression was assessed in different studies using different methodologies:

a) **Cell wall extractable XET activity:** different studies have correlated extractable XET activity with growth rate and have demonstrated the presence of active XETs in different plant extracts^{41,93,94,96,107-109}.

b) **In vivo detection by immunolocalization:** antibodies against *XTHs* have been used to detect *XTH* expression in different cellular localizations and/or in response to different stimuli or regulators/inductors^{100,107}.

c) **Northern analysis:** In situ mRNA hybridation or mRNA extraction and northern analysis have rendered similar results as *in vivo* detection by immunolocalization^{49,51,66,69,101,110,111}.

All these methods were useful to study *XTH* expression in different plant tissues and/or under different conditions. Despite of the useful information that these methods supply they are not direct proves of *in vivo* activity of *XTHs*, because maybe *XTHs* are expressed but there are no substrates available, or some natural inhibitors are present, etc.

For that reason some studies have tried to demonstrate that localized (and/or extracted) *XTHs* in plant are active in the plant tissues.

9.9.2.- XET activity

a) Exogenous substrates.

This kind of studies use endogenous or exogenous XG as donor substrate and then, exogenous labeled XGOs are provided to studied tissues. If XETs or XETs together with XG are present in the tissues the labeled acceptor is incorporated into these tissues and the excess of labeled acceptor could be removed by washing. Consequently XET action (maybe not activity) could be localized were the label was covalently linked to not extractable material (cell wall material).

The most extensively used label for this XET activity demonstration and localization is a fluorescent label (fluorescein, rhodamine, sulforhodamine)^{53,98-101}. These studies render important results in active XETs localization proposing new possible roles of XET activity. However these studies only detect XET action, they do not directly demonstrate XET activity *in vivo*.

b) Pulse chases experiment.

There are one study that demonstrated elegantly by pulse chase experiments using labeled XG precursors (¹³C]glucose, [¹³C, ²H]glucose, [¹²C, ¹H]glucose [¹H]arabinose) that XETs have, *in vivo*, the previously proposed roles (incorporation of nascent XG in the cell walls and restructuring of existing XG)^{4,106,112}.

OBJECTIVES

OBJECTIVES.

The present work is part of an European project named E.D.E.N. (Enzyme Discovery in hybrid aspen for fiber ENgineering), whose general objective is to identify novel plant enzymes for deeper understanding of the process of fiber formation/modification for future improvement of the quality parameters of wood fibers.

Within this project, the general objective of the present work is to develop enzymatic assays to characterize a XET from *Populus tremula x tremuloides* and study its substrate specificity. More concretely, the specific objectives of the present work are:

1) To attempt expression of recombinant and active *Ptt*-XET16A in *Escherichia coli*.

2) To design, develop, and validate an activity assay to characterize kinetically *Ptt*-XET16A using low molecular weight substrates. To achieve that, it is necessary to design and synthesize the adequate low molecular donor and acceptor substrates.

3) To characterize *Ptt*-XET16A kinetically, with the aim of determining the dependence of activity with pH and temperature and the enzyme kinetic mechanism.

4) To design and synthesize a low molecular weigh xylogluco-oligosaccharide library to study *Ptt*-XET16A donor specificity and to obtain a subsite mapping of its binding cleft.

4) To design and synthesize FRET (fluorescence resonance energy transfer) substrates to monitor hydrolytic and transglycosylase activities of *XTHs*.

RESULTS AND DISCUSSION

CHAPTER 1:
Attempts of Ptt-XET16A expression in E.coli

CHAPTER 1: attempts of *Ptt*-XET16A expression in *Escherichia coli*.

1.- Background:

The objective of this work is the study and characterization of the XET16A from *Populus tremula x tremuloides*. (*Ptt*-XET16A). For that reason, first of all, we have embarked the cloning of *Ptt*-XET16 in an *E. coli* expression system to obtain recombinant protein in an easy working system. *E. coli* expression systems are widely used and abundant commercial systems are available. In parallel to this work, the T. Teeri team at KTH, an EDEN partner, was developing a *Pichia pastoris* expression system.

It was known that *Ptt*-XET16A could be glycosylated *in vivo*, since a putative glycosylation site is predicted from sequence by standard bioinformatics tools, and for other *XTH* this glycosylation was demonstrated^{46,47,65,70,88}.

Using a procariotic system no glycosylation could be obtained, but previously reported results with *Sl-XTH10*, *Sl-XTH11* from tomato *Ad-XTH5* from kiwifruit, and *At-XTH22* from *Arabidopsis* expressed in *E. coli*, demonstrated the obtaining of non glycosylated but active enzyme production^{49,50,113} using a denaturing purification protocol.

The *Pichia pastoris* expression plasmid pPIC9-XET16A (Figure 16) was provided by KTH (EDEN partner). This plasmid contains an α -factor secretion signal followed by the wild-type *Ptt*-XET16A gene under the control of the 5'-AOX1 promoter. In the present work, two new plasmids for *E. coli* expression were designed: pET15XET16A based on the pET system from Novagen, and pD62XET16A based on the pD6-2- β -gluc^{114,115}, home made plasmid for expression of 1,3-1,4- β -glucanase from *Bacillus licheniformis*.

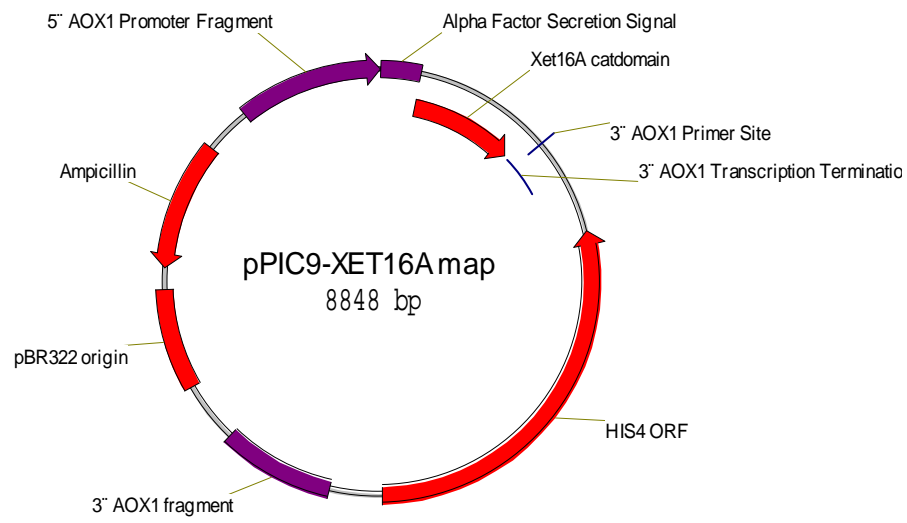


Figure 16: Representation of pPIC9-XET16A plasmid.

2.- pD62XET16A construct.

2.1.- pD62XET16A design and construction.

The pD6-2 plasmid was designed and obtained in our group^{114,115} to express 1,3-1,4- β -glucanase from *Bacillus licheniformis*. The pD6-2 vector contains a *Bacillus licheniformis* signal peptide and a promoter for constitutive expression and extracellular secretion, which are functional in *E. coli*. Moderate yields of soluble and extracellular enzyme were obtained in the group for several different mutants^{84,114-119}, due to the presence of a *Bacillus* signal peptide (Figure 17).

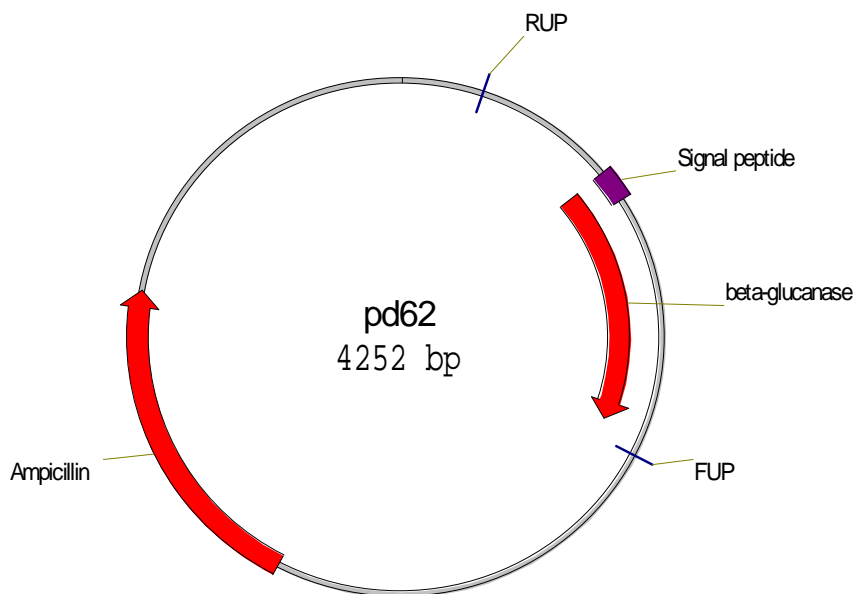


Figure 17: Representation of pD6-2 plasmid for heterologous expression of 1,3-1,4- β -glucanase from *Bacillus licheniformis*.

The new designed construct (pD62XET16A) is based on the use of the *Bacillus* signal peptide to obtain soluble and extracellular *Ptt*-XET16A. For that reason, the *Ptt*-XET16A catalytic domain gene has to be cloned just after the signal peptide keeping the reading frame, and before the terminator sequence of the pD6-2 plasmid. First of all, two new restriction sites have to be added in the original pD6-2 construct, to use them for *Ptt*-XET16A cloning conserving the amino acid sequence at least on the signal peptide. New restriction sites will be introduced by two site directed mutagenesis rounds: *Pst*I in the N-terminal part and *Bam*HI in the C-terminal part.

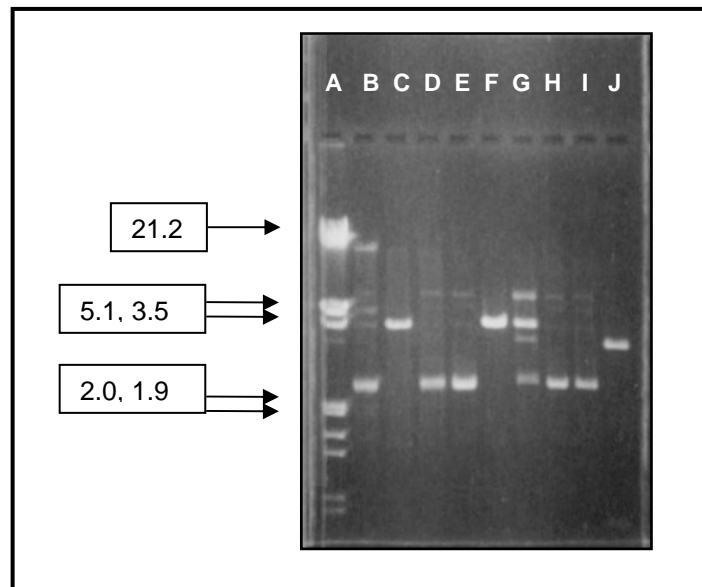


Figure 19: Scan of restriction analysis of pD62(*Pst*I) construct, in lane A the molecular weight marker III was observed; not digested pD6-2 in lane B; pD6-2 digested with *Eco*RI in lane C; pD6-2 digested with *Pst*I in lane D; pD62(*Pst*I) colony 1 not digested in lane E; pD62(*Pst*I) colony 1 digested with *Pst*I in lane F; pD62(*Pst*I) colony 1 digested *Pst*I and *Eco*RI in lane G; pD62(*Pst*I) colony 2 not digested in lane H; pD62(*Pst*I) colony 2 digested with *Pst*I in lane I; pD62(*Pst*I) colony 2 digested *Pst*I and *Eco*RI in lane J.

For the C terminal part of the gene, primer design was easier because a new restriction site could be added after the stop codon, and then amino acid changes would not affect the final *Ptt*-XET16A amino acid sequence. Finally, *Bam*HI restriction site was chosen, because it will be a unique restriction site for pD62(*Pst*I/*Bam*HI) and it does not exist in *Ptt*-XET16A gene. To obtain the *Bam*HI recognition sequence, three nucleotides have to be mutated, but all of them are located after the stop codon (Figure 20).

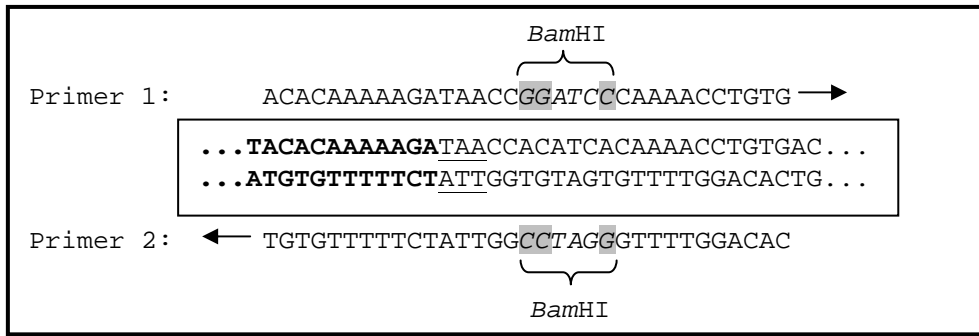


Figure 20: Hybridizing zone of complementary mutagenic primers, both primers contain the mutagenic nucleotides (highlighted). 1,3-1,4-β-glucanase sequence in bold and the stop codon is underlined, the *Bam*HI restriction site in italics.

Site directed mutagenesis on the pD62(*Pst*I) plasmid was done using the Quick change site directed mutagenesis kit from Novagen, screening of transformant DH5α colonies was done by restriction analysis on agarose gel (Figure 21).

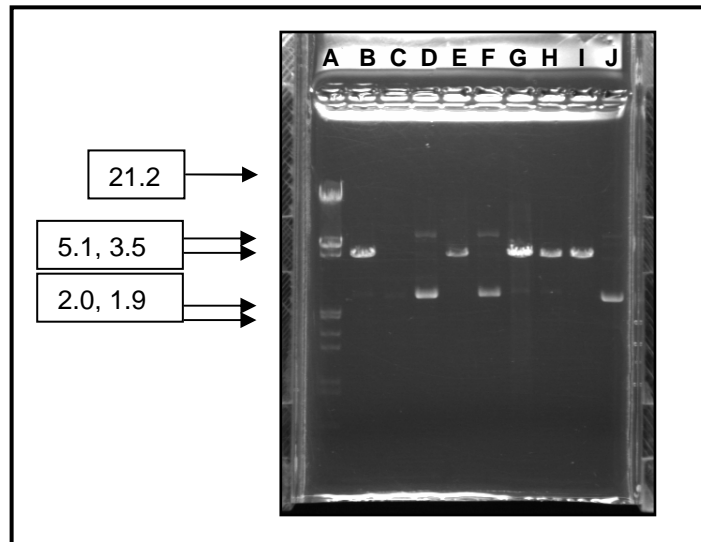


Figure 21: Restriction analysis of pD62(*Pst*I/*Bam*HI) transformant colonies, DNA molecular weight marker III is observed in lane A; colonies 1-6 of pD62(*Pst*I/*Bam*HI) digested with *Bam*HI in lanes B, C, D, E, G, and H; pD62(*Pst*I) digested with *Bam*HI in lane F; pD62(*Pst*I) digested with *Pst*I in lane I; and pD62(*Pst*I) not digested I lane J.

In Figure 21 it could be observed that colonies 1, 4, 5, 6 (lanes B, E, G and H) have the pD62(*Pst*/*Bam*HI) plasmid, because they were digested with *Bam*HI, obtaining the same band obtained with linearized pD62(*Pst*) (lane I). Therefore, all these colonies have the objective construct. In contrast, colony 3 (lane D) have wt pD62(*Pst*) plasmid, because it is not digested with *Bam*HI showing the typical double band of circular plasmid, comparing with circular pD62(*Pst*) (lane J).

Once the double mutated plasmid pD62(*Pst*/*Bam*HI) was obtained, the next step was cloning of *Ptt*-XET16A catalytic domain in the modified plasmid using the newly introduced restriction sites. First of all, the *Ptt*-XET16A catalytic domain gene fragment was amplified by PCR from pPIC9-XET16A using flanking primers. These primers were designed to add the restriction sites *Pst*I and *Bam*HI flanking the *Ptt*-XET16A gene (Figure 22) necessary to clone this gene in the pD62(*Pst*/*Bam*HI) plasmid.

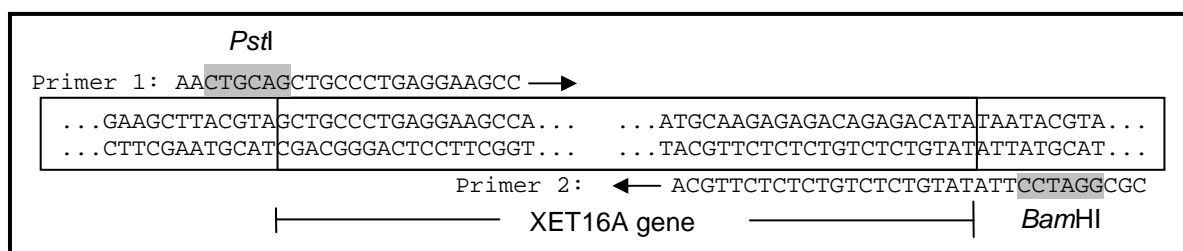


Figure 22: Representation of pPIC9-XET16A plasmid hybridization zones for flanking primers which add necessary restriction sites for cloning (*Pst*I & *Bam*HI). Restriction site recognized sequences were highlighted.

The amplified *Ptt*-XET16A catalytic domain and the pD62(*Pst*/*Bam*HI) plasmid were sequentially digested with *Bam*HI and *Pst*I restriction enzymes and purified by preparative agarose gel electrophoresis. Both linearized fragments, the double digested plasmid and the *Ptt*-XET16A gene, were ligated in 1:3 molar ratio using T4 ligase. DH5 α cells were transformed with the ligation product and were screened for insertion by PCR amplification of XET16A gene using FUP and RUP primers (Figure 22).

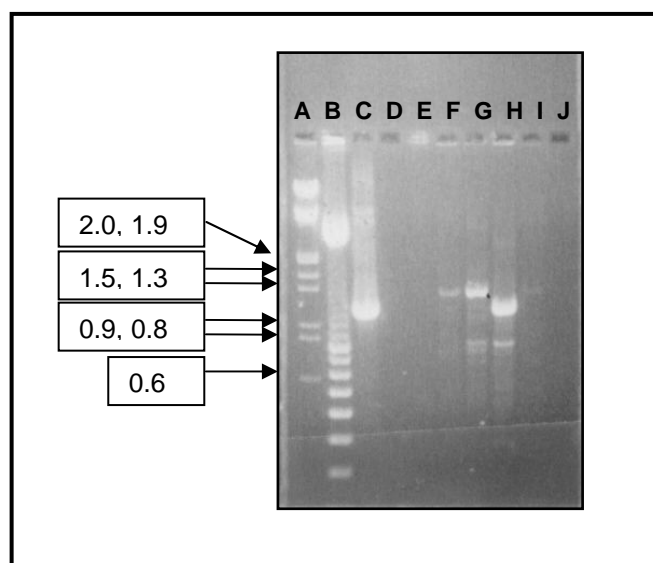


Figure 23: Agarose gel of the PCR amplification products of different transformant colonies of ligated product pD62XET using FUP & RUP primers. Molecular weight marker III is observed in lane A; DNA ladder 100 bp in lane B; amplification product of pD6-2 plasmid (1.2 kbp) in lane C; colony 1-5 amplification products (1.4 kbp) in lanes E-H.

The agarose gel showed the correct amplification product (pD62XET16A plasmid) in colonies 2,3 and 5 (lanes F,G and I), the initial plasmid (pD62) in colony 4 (lane H), and no amplification in colony 1 (lane E) probably due to recircularization of the plasmid.

Restriction analysis of colony 3 construct was done to show insertion of a new restriction site only present in the *Ptt*-XET16A sequence (*Stul*). (Figure 24)

A slightly higher molecular weight was observed comparing pD6-2 and pD62XET amplified fragments (lanes B, E). Double digestion of pD62XET plasmid (1.0 and 3.4 kbp fragments) was observed using *Hind*III and *Stul* in contrast to linearization observed in pD6-2plasmid with the same restriction enzymes, due to the presence of *Stul* restriction site in the XET16A sequence. Double digestion using *Hind*III and *Sac*I restriction enzymes showed a slight increase in molecular weight of the short fragments of pD62XET (lane G) comparing with pD6-2(lane D) that correlates with gene length (XET16A longer than 1,3-1,4- β -glucanase).

For these reasons it could be concluded that colony 3 have the *Ptt*-XET16A catalytic domain inserted.

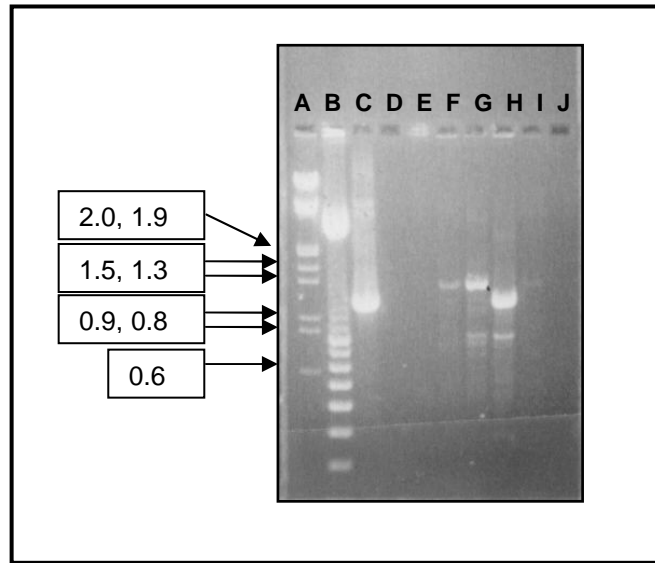


Figure 24: Agarose gel showing restriction analysis of final pD62XET16A construct comparing with pD6-2 initial construct. DNA molecular weight marker III is observed in lane A; pD6-2 linearized with *Hind*III (4.3kbp) in lane B; pD6-2 double digested with *Hind*III and *Stu*I (4.3 kbp) in lane C; pD6-2 double digested with *Hind*III and *Sac*I (1.2, 3.1 kbp) in lane D; pD62XET16A linearized with *Hind*III (4.4 kbp) in lane E; pD62XET16A double digested with *Hind*III and *Stu*I (1.0, 3.4 kbp) in lane F; and pD62XET16A double digested with *Hind*III and *Sac*I (1.3, 3.1 kbp) in line G.

Verification of final construct obtained in colony 3 was done by sequencing using FUP and RUP primers, as it is shown in Figure 25.

```

THEO ATCATTATTTAGACCGATTTTCCATTTTGAGAGAATCATGTATGATCAAA
FUP  ATCATTATTTAGACCGATTTTCCATTTTGAGAGAATCATGTATGATCAAA

THEO AAGAAAACGCTTTCAAAAAGAGAGGGGAATGCCTACATGTCCTTACCGTG
FUP  AAGAAAACGCTTTCAAAAAGAGAGGGGAATGCCTACATGTCCTTACCGTG

THEO TAAAACGAATGTTGATGCTGCTTGTCACTGGATTATTCTTAAGTTTGTCC
FUP  TAAAACGAATGTTGATGCTGCTTGTCACTGGATTATTCTTAAGTTTGTCC

THEO ACATTTGCTGCAAGTGCCTCTGCAGCTGCCCTGAGGAAGCCAGTGGATGT
FUP  ACATTTGCTGCAAGTGCCTCTGCAGCTGCCCTGAGGAAGCCAGTGGATGT

THEO GCGGTTTCGGTAGGAACATGTTTCTACATGGGCTTTTGACCACATTAAGT
FUP  GCGGTTTCGGTAGGAACATGTTTCTACATGGGCTTTTGACCACATTAAGT

THEO ACTTCAATGGAGGCAATGAGATTCAGCTGCACCTTGGATAAATACACAGGT
FUP  ACTTCAATGGAGGCAATGAGATTCAGCTGCACCTTGGATAAATACACAGGT

THEO ACTGGTTTCCAATCAAAGGTTTCATACTTATTTGGCCATTTTCAGTATGCA
FUP  ACTGGTTTCCAATCAAAGGTTTCATACTTATTTGGCCATTTTCAGTATGCA

THEO AATGAAGTTGGTTCCTGGTGACTCAGCTGGAACAGTCACTGCTTCTATC
FUP  AATGAAGTTGGTTCCTGGTGACTCAGCTGGAACAGTCACTGCTTCTATC

THEO TATCCTCACAAAACCTCGGAGCATGACGAGATAGACTTTGAGTTCTTAGGA
FUP  TATCCTCACAAAACCTCGGAGCATGACGAGATAGACTTTGAGTTCTTAGGA

THEO AACAGGACTGGCCAGCCCTACATTTTGCAGACAAATGTTTTCACAGGAGG
FUP  AACAGGACTGGCCAGCCCTACATTTTGCAGACAAATGTTTTCACAGGAGG

THEO CAAGGGGGATAGAGAACAGAGGATTTACCTCTGGTTTGACCCAACCAAGG
FUP  CAAGGGGGATAGAGAACAGAGGATTTACCTCTGGTTTGACCCAACCAAGG

THEO AATTCCTACTATTCTGTCTCTGGAACATGTACATGATAGTGTTCCTC
FUP  AATTCCTACTATTCTGTCTCTGGAACATGTACATGATAGTGTTCCTC

THEO GTGGATGACGTGCCAATCAGAGTGTTCAGAAGTCAAGATTGGGAGT
FUP  GTGGATGACGTGCCAATCAGAGTGTTCAGAAGTCAAGATTGGGAGT

THEO TAAGTTTCCATTCAACCAGCCAATGAAGATCTACTCAAGCCTATGGAATG
FUP  TAAGTTTCCATTCAACCAGCCAATGAAGATCTACTCAAGCCTATGGAATG

THEO CCGATGATTGGGCTACCAGGGTGGACTCGAGAAGACAGACTGGTCCAAG
FUP  CCGATGATTGGGCTACCAGGGTGGACTCGAGAAGACAGACTGGTCCAAG

THEO GCACCGTTCATTGCCTCCTACAGGAGCTTCCACATAGATGGGTGCGAGGC
FUP  GCACCGTTCATTGCCTCCTACAGGAGCTTCCACATAGATGGGTGCGAGGC

THEO CTCCTGGAAGCCAAGTTCTGCGCCACACAGGGTGCTAGATGGTGGGACC
FUP  CTCCTGGAAGCCAAGTTCTGCGCCACACAGGGTGCTAGATGGTGGGACC

THEO AGAAGGAGTTCCAAGATCTGGATGCCTTCCAGTACAGGAGGCTCAGCTGG
FUP  AGAAGGAGTTCCAAGATCTGGATGCCTTCCAGTACAGGAGGCTCAGCTGG

THEO GTCCGCCAGAAATATACCATCTACAATTACTGCACTGATAGATCAAGATA
FUP  GTCCGCCAGAAATATACCATCTACAATTACTGCACTGATAGATCAAGATA

THEO CCCTTCAATGCCCCAGAATGCAAGAGAGACAGAGACATATAAGGATCCC
FUP  CCCTTCAATGCCCCAGAATGCAAGAGAGACAGAGACATATAAGGATCCC
    
```

Figure 25: Sequence alignment between FUP sequence of obtained pD62XET16A gene (FUP) and theoretical pD62XET16A sequence (THEO). In blue characters signal peptide sequence, in red characters *Ptt*-XET16A catalytic domain are presented.

2.2.- Expression attempts with the pD62-XET16A construct.

This part of the work was done in collaboration with other members of our group^{120,121}.

To express *Ptt*-XET16A as an extracellular and constitutively expressed enzyme, BL21 SI *E. coli* cells were transformed with the expression plasmid pD62XET16A. Different culture medium (2YT and LB) and different expression conditions (temperatures) were used. No expression was detected in any case by SDS-PAGE gels.

No activity was detected using a plate assay. In these plate assays, an *E. coli* colony or an extract of an expression experiment was incubated at 37°C overnight with XG and XGos. After that, the plate was stained using I₂ to observe a halo where XET activity exists due to depolymerization of XG by transglycosylation to XGos. In all the experiments, only for the positive controls using a XET expressed in *Pichia pastoris*, this halo was observed.

Because of the lack of positive results, no further work with this expression system was continued.

3.- pET15XET16A construct.

3.1.- pET15XET16A design and construction.

The commercial available pET system is an *E. coli* heterologous protein expression system based on cloning of target genes under the control of strong bacteriophage T7 transcriptional signals. Expression is induced by providing a source of T7 RNA polymerase in the host cell. T7 RNA polymerase is so selective and active that when fully induced, almost all of the cell's resources are converted to target gene expression. Another important benefit of this system is the ability to maintain target genes transcriptionally silent in an uninduced state (http://wolfson.huji.ac.il/purification/PDF/Expression_Systems/NovagenPETSysMan ual.pdf)

We selected the plasmid pET15b, because it was used before with success to express a mammalian α -galactosyltransferase catalytic domain in our laboratory¹²²⁻¹²⁴. It was decided to clone the *Ptt*-XET16A gene between the existing restriction sites *Nde*I and *Bam*HI. Both are unique restriction sites in the pET15b plasmid and are not found in the *Ptt*-XET16A gene. The final construct will have an N terminal 6xHis tag followed by an eight amino acid tail, before the *Ptt*-XET16A gene. (Figure 26).

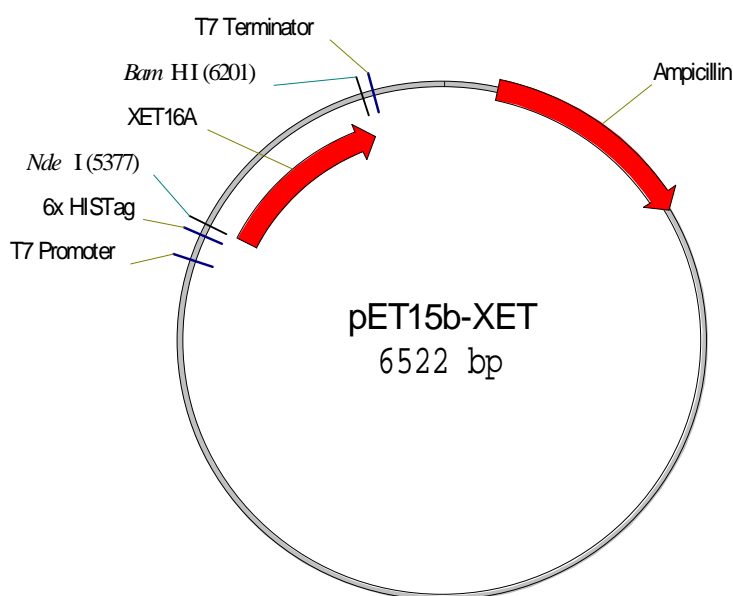


Figure 26: pET15XET16A scheme showing the cloning restriction sites, promoter and termination zones, 6 x His tag, ampicillin resistance gene, and *Ptt*-XET16A catalytic domain.

The *Ptt*-XET16A catalytic domain was amplified by PCR from pPIC9-XET16A using the designed flanking primers to add *Nde*I and *Bam*HI restriction sites (Figure 27) necessary to clone *Ptt*-XET16A gene in the pET15b plasmid.

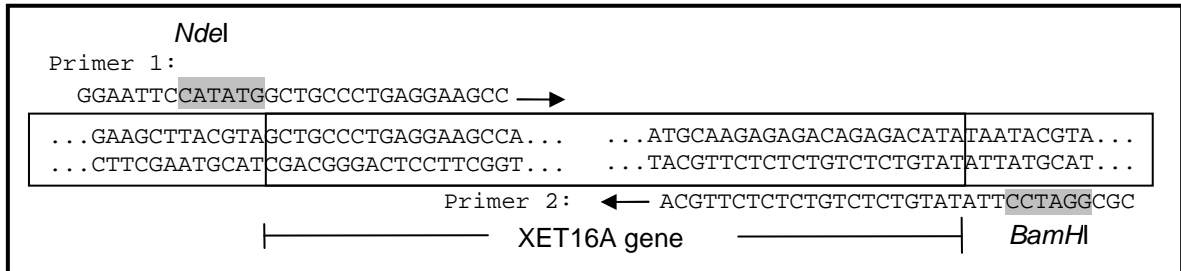


Figure 27: Representation of pPIC9-XET16A plasmid hybridization zones for flanking primers which add to *Ptt*-XET16A gene the necessary restriction sites for cloning (*Nde*I and *Bam*HI). Restriction enzymes recognized sequences were highlighted.

The obtained *Ptt*-XET16A gene fragment and the pET15b plasmid were digested sequentially with *Nde*I and *Bam*HI restriction enzymes. Linear fragments were ligated and ligation products were transformed in DH5 α cells. Resulting colonies were screened for correct insertion by on-colony PCR and insertion in positive colony was verified by restriction analysis on agarose gel (Figure 28).

In this picture it could be observed the increase of size of linearized pET15XET16A 6.5 kDa (D) comparing with linearized pET15b 5.7 kDa (B) and confirmed by the double digestion analysis with *Pst*I & *Stu*I (only present in *Ptt*-XET16A gene sequence) of both plasmids (C, D respectively).

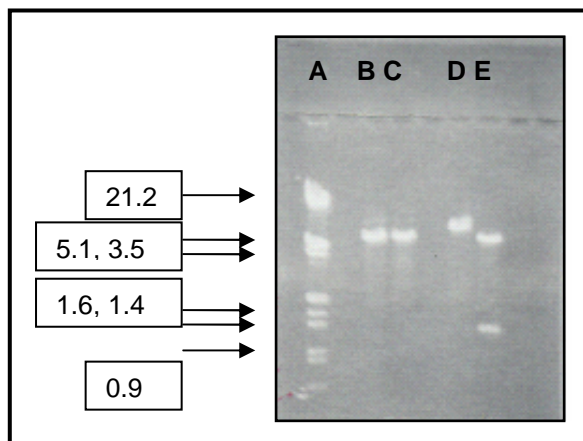


Figure 28: Scan of restriction analysis of pET15XET16A construct, in lane A the molecular weight marker is observed; in lane B, pET15b linearized with *Pst*I (5.7 kDa); in lane C, pET15b digested with *Pst*I & *Stu*I (5.7 kDa); in lane D, pET15XET16A construct linearized with *Pst*I (6.5 kDa), and in lane D, pET15XET16A digested with *Pst*I & *Stu*I (5.2, 1.3 kDa).

The clone showing gene insertion by restriction analysis were sequenced to verify the final construct (Figure 29).

```

theo GAAGTGGCGAGCCCGATCTTCCCATCGGTGATGTCGGCGATATAGGCGC
theo CAGCAACCGCACCTGTGGCGCCGGTATGCCGGCCACGATGCGTCCGGCG
theo TAGAGGATCGAGATCTCGATCCCAGCAAATTAATACGACTCACTATAGGG
theo GAATTGTGAGCGGATAACAATTCCCCTCTAGAAATAATTTTGTTTAACTT
theo TAAGAAGGAGATATACCATGGGCAGCAGCCATCATCATCATCACAGC
prom TAAGAAGGAGATATACCATGGGCAGCAGCCATCATCATCATCACAGC
theo AGCGGCCTGGTGC CGCGCGGCAGCCATATGGCTGCCCTGAGGAAGCCAGT
prom AGCGGCCTGGTGC CGCGCGGCAGCCATATGGCTGCCCTGAGGAAGCCAGT
theo GGATGTGGCGTTCCGGTAGGAACTATGTTCCCTACATGGGCTTTTGACCACA
prom GGATGTGGCGTTCCGGTAGGAACTATGTTCCCTACATGGGCTTTTGACCACA
theo TTAAGTACTTCAATGGAGGCAATGAGATTCAGCTGCACCTGGATAAAATAC
prom TTAAGTACTTCAATGGAGGCAATGAGATTCAGCTGCACCTGGATAAAATAC
term TTAAGTACTTCAATGGAGGCAATGAGATTCAGCTGCACCTGGATAAAATAC
theo ACAGGTACTGGTTTCCAATCAAAAAGGTTTCATACTTATTTGGCCATTTTCAG
prom ACAGGTACTGGTTTCCAATCAAAAAGGTTTCATACTTATTTGGCCATTTTCAG
term ACAGGTACTGGTTTCCAATCAAAAAGGTTTCATACTTATTTGGCCATTTTCAG
theo TATGCAAATGAAGTTGGTTCTGGTGACTCAGCTGGAACAGTCACTGCCT
prom TATGCAAATGAAGTTGGTTCTGGTGACTCAGCTGGAACAGTCACTGCCT
term TATGCAAATGAAGTTGGTTCTGGTGACTCAGCTGGAACAGTCACTGCCT
theo TCTATCTATCCTCACAAAACCTCGGAGCATGACGAGATAGACTTTTGAGTTC
prom TCTATCTATCCTCACAAAACCTCGGAGCATGACGAGATAGACTTTTGAGTTC
term TCTATCTATCCTCACAAAACCTCGGAGCATGACGAGATAGACTTTTGAGTTC
theo TTAGGAAACAGGACTGGCCAGCCCTACATTTTGAGACAATGTTTTTCAC
prom TTAGGAAACAGGACTGGCCAGCCCTACATTTTGAGACAATGTTTTTCAC
term TTAGGAAACAGGACTGGCCAGCCCTACATTTTGAGACAATGTTTTTCAC
theo AGGAGGCAAGGGGGATAGAGAACAGAGGATTTACCTCTGGTTTGACCCAA
prom AGGAGGCAAGGGGGATAGAGAACAGAGGATTTACCTCTGGTTTGACCCAA
term AGGAGGCAAGGGGGATAGAGAACAGAGGATTTACCTCTGGTTTGACCCAA
theo CCAAGGAATTCCACTACTATTCTGTCTCTGGAACATGTACATGATAGTG
prom CCAAGGAATTCCACTACTATTCTGTCTCTGGAACATGTACATGATAGTG
term CCAAGGAATTCCACTACTATTCTGTCTCTGGAACATGTACATGATAGTG
theo TTCCTCGTGGATGACGTGCCAATCAGAGTGTTCAGAAGTCAAGGATTT
term TTCCTCGTGGATGACGTGCCAATCAGAGTGTTCAGAAGTCAAGGATTT
theo GGGAGTTAAGTTTCCATTCAACCAGCCAATGAAGATCTACTCAAGCCTAT
term GGGAGTTAAGTTTCCATTCAACCAGCCAATGAAGATCTACTCAAGCCTAT
theo GGAATGCCGATGATTGGGCTACCAGGGGTGGACTCGAGAAGACAGACTGG
term GGAATGCCGATGATTGGGCTACCAGGGGTGGACTCGAGAAGACAGACTGG
theo TCCAAGGCACCGTTCATTGCCCTCTACAGGAGCTTCCACATAGATGGGTG
term TCCAAGGCACCGTTCATTGCCCTCTACAGGAGCTTCCACATAGATGGGTG
theo CGAGGCCTCCGTGGAAGCCAAGTTCTGCGCCACACAGGGTGCTAGATGGT
term CGAGGCCTCCGTGGAAGCCAAGTTCTGCGCCACACAGGGTGCTAGATGGT
theo GGGACCAGAAGGAGTTCCAAGATCTGGATGCCTTCCAGTACAGGAGGCTC
term GGGACCAGAAGGAGTTCCAAGATCTGGATGCCTTCCAGTACAGGAGGCTC
theo AGCTGGGTCCGCCAGAAATATACCATCTACAATTACTGCACTGATAGATC
term AGCTGGGTCCGCCAGAAATATACCATCTACAATTACTGCACTGATAGATC
theo AAGATACCCTTCAATGCCCCAGAATGCAAGAGAGACAGAGACATATAAG
term AAGATACCCTTCAATGCCCCAGAATGCAAGAGAGACAGAGACATATAAG
theo GATCCGGCTGCTAACAAAGCCCGAAAGGAAGCTGAGTTGGCTGCTGCCAC

```

Figure 29: Sequence alignment between experimental sequence obtained from terminator (term) and promoter (prom) sequencing and theoretical sequence of pET15b-XET16A (theo).

3.2.- Expression attempts with pET15b-XET16A construct:

In the expression experiments done with this construct, culture was induced with 1 mM IPTG at the stationary phase and incubated 4 hours for expression. Different growing temperatures and induction temperatures were assayed. Samples were taken, lysed by sonication and centrifuged to obtain the intracellular soluble and insoluble fractions. All fractions were analyzed by SDS-PAGE but in all cases it was concluded that *Ptt*-XET16A was expressed at very low levels, always in an inactive form and in the intracellular insoluble fraction, probably as inclusion bodies as it was described for other XETs^{49,50,113}.

3.3.- Purification by affinity chromatography:

Purification of His-tagged-*Ptt*-XET16A was attempted in different experiments, both by standard affinity purification protocols for soluble proteins and by denaturing purification followed by on-column refolding protocols for inclusion bodies.

We were not able to purify *Ptt*-XET16A neither from soluble fractions by Ni affinity chromatography nor from insoluble inclusion bodies by Ni affinity chromatography in denaturing conditions followed by on column refolding. This could be explained by the extremely low expression levels, or proteolytic cleavage of His-Tag.

At the same time we are working in the *E. coli* expression of *Ptt*-XET16A, the KTH group (EDEN partner), was attempting to express and purify this enzyme from *Pichia pastoris*. They finally obtained an optimized protocol for glycosylated and active *Ptt*-XET16A expression production⁴⁷ and we continued our work with the glycosylated enzyme produced in *P. pastoris* to kinetically characterize the *Ptt*-XET16A and study its substrate specificity.

CHAPTER 2:
Development of a XET-activity assay

CHAPTER 2: development of XET-activity assay.

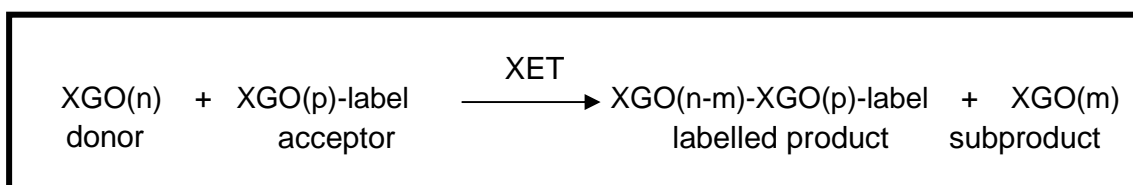
1.- Introduction.

Since now, all enzymatic assays described to study and characterize XET enzymes use XG polymer as donor. As it was presented in the introduction, these assays monitor physical changes due to the resulting XG depolymerization (iodine staining, viscosity, changes in molecular weight distribution⁴²⁻⁴⁷) or use labeled xyloglucan oligosaccharides (XGOs) acceptors measuring label incorporation on XG (by separation of labeled XG from labeled XGOs by cellulose affinity binding, precipitation, GPC, etc.^{40-42,44,46-53}).

XG is a poly-disperse mixture of molecules with different molecular weights. Each molecule can experience multiple turnovers rendering complex behaviors and preventing detailed kinetic evaluation of XET activity. Another drawback of currently used XET enzymatic assays is that they are not able to screen small donors with defined structure, preventing detailed analysis of substrate specificity.

Therefore, to study XET mechanism of action and evaluate small molecules as donors, a novel enzymatic assay was needed. Encouraged by the observation that the tetrasaccharide XXXGXXXG^{71,85} is a donor for a XET from germinating nasturtium seeds, we proposed a new XET enzymatic assay based on HPCE (High Performance Capillary Electrophoresis) to kinetically study XETs using low-molecular-mass xyloglucan oligosaccharide donors. The enzymatic assay should be versatile enough to be used to explore new donors for XETs.

The idea is to use a low-molecular-mass XGO as donor and labeled low-molecular-weight XGO as acceptor as presented in Scheme 1, and monitor the formation of a labeled transglycosylation product.



Scheme 1: Schematic representation of the proposed XET reaction to be analyzed by HPCE.

This method is based on similar assays developed for Leloir glycosyl transferases which use a labeled acceptor bearing a charged chromophore^{122,125-127}. In previous studies on XETs, it has been demonstrated that the non reducing end of the acceptor could be modified without a drastic effect on activity^{40,53,64,91,98-101}. Molecules as big as 2-aminopyridine⁴⁰, sulphorhodamine^{53,99,101}, and fluorescein⁹⁸ have been extensively used to produce labeled acceptors for XETs.

We proposed different structures as putative donors and acceptors for *Ptt*-XET16A which will be analyzed in the following chapters:

Donors:

- a) Xyloglucan polymer.
- b) β -fluorides of xyloglucan oligosaccharides.
- c) Xylogluco-oligosaccharides.

Acceptors:

- a) Labeled xyloglucan oligosaccharide mixtures (XXXG-label, XLG-label, XLXG-label and XLLG-label).
- b) Isolated XXXG-label.

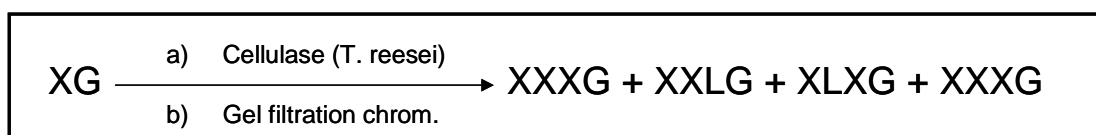
HPCE allows separation of charged analytes through a capillary by application of a voltage difference between both ends of the capillary, due to their different electrophoretic mobilities^{128,129}. Then, for carbohydrates that normally do not have charge, it is necessary to derivatize them with a molecule that give charge to the carbohydrate to allow electrophoretic separation and at the same time it should be a chromophore or a fluorophore to allow detection^{130,131}. We have chosen ANTS (8-aminonaphtalene-1,3,6-trisulfonic acid) as label because of its extensive use for sugar labeling in HPCE analysis^{122,132}.

2.- HPCE method development: separation of XGOsANTS⁽¹⁾.

2.1.- Synthesis of XGOs-ANTS.

2.1.1.- Synthesis of XGOs.

The XGOs mixture was obtained by fractioning the crude obtained by cellulase digestion of XG from Tamarind seeds (Scheme 2) using gel filtration chromatography to remove the enzyme and other XG oligomers as it was previously described by several authors^{42,71,90,134-141}. In this work XGOs were recovered with an overall yield of 73%.



Scheme 2: Synthetic pathway to obtain XGOs mixture, based on the structure of tamarind seeds xyloglucan, the XGOs fraction obtained is a mixture of XXXG (10), XXLG (11), XLXG (12) and XLLG (13).

2.1.2.- XGOs ANTS-labeling.

The XGOs fraction obtained above was ANTS labeled by reductive amination (Scheme 3) using ANTS in AcOH/water and NaCNBH₃ in THF. The resulting crude mixture was purified from non labeled XGOs and from the excess of ANTS by gel filtration chromatography. The major problem of this synthesis was the difficulty to completely separate the labeled acceptors from the huge excess of ANTS. Finally, a partially purified mixture of XXXG-ANTS, (XXLG-ANTS, XLXG-ANTS) and XLLG-ANTS (XGOs-ANTS) (1:6:6 molar ratio) (Figure 30) was recovered with approximately 8% yield from XG.

¹ This part of the Ph.D. is included in the article published in the Biochemical Journal with the title **Kinetic analysis with low molecular mass xyloglucan oligosaccharides defines the catalytic mechanism of a *Populus* Xyloglucan Endotransglycosylase**, by Marc Saura-Valls, Régis Fauré, Sergi Ragàs, Kathleen Piens, Harry Brumer, Tuula T. Teeri, Sylvain Cottaz, Hugues Driguez, and Antoni Planas¹³³.



Scheme 3: ANTS labeling of XGOs mixture.

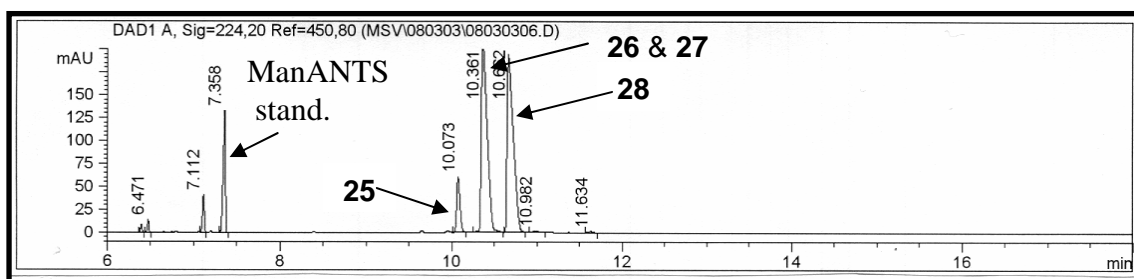


Figure 30: Electropherogram of partially purified mixture of XXXGANTS (25), XXLGANTS (26), XLXGANTS(27) and XLLGANTS (28).

2.2.- HPCE conditions.

Electrophoretic conditions were optimized with the previously described mixture of ANTS-labeled xyloglucan oligosaccharides (XGOs-ANTS). The mixture was analyzed under different electrophoretic conditions to evaluate analysis time, resolution, and efficacy using a fused silica 72 cm effective length capillary with 50 μm internal diameter, with an extended light path bubble (150 μm) in the detection window¹⁴². Previous studies with ANTS-labeled low molecular mass linear oligosaccharides showed that low resolution is attained when using basic buffers and direct electroosmotic flow (EOF)¹²². Electrophoretic methods using acidic buffers with suppressed and inverted EOF were then assayed. Suppressed EOF conditions were obtained with sodium phosphate buffer at pH 2.5, but inverted EOF conditions, generated with triethylamine (TEA) as EOF modifier, gave shorter analysis time (Figure 31) and were chosen for further method optimization. TEA is able to neutralize capillary superficial charge or form a double layer, thus inverts the sign of the exposed charge on the capillary surface.

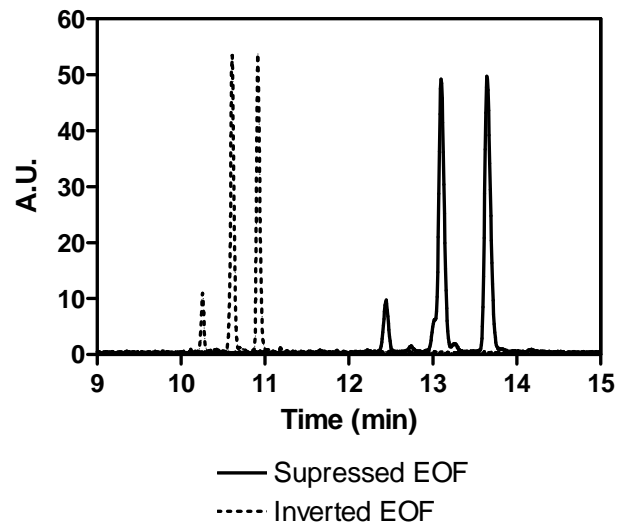


Figure 31: Electropherograms for suppressed (solid line) and inverted EOF (dashed line) conditions of XGOs-ANTS (XXXGANTS + (XXLGANTS and XLXGANTS) + XLLGANTS)

Migration times increased with increasing concentration of the phosphate-TEA buffer (25, 50, and 100 mM, pH 2.5) (Figure 32), efficacy increased with higher buffer concentrations, but resolution was optimal at 50 mM buffer (Table 2).

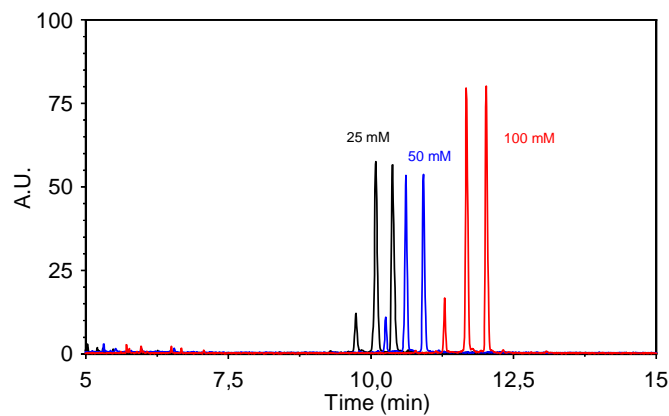


Figure 32: Electropherograms at different buffer concentrations (25, 50, 100 mM).

	Concentration (mM)			pH		
	25	50	100	2.0	2.5	3.0
t_m (min)	9.6	10.2	11.2	10.1	10.2	10.7
resolution ¹	5.88	6.39	2.71	23.13	6.40	4.51
efficacy ²	211762	309408	392690	185418	309407	233824

Table 2: Migration times (t_m) for XXXG-ANTS peak, resolution (Rs) between XXXG-ANTS and XLG-ANTS peaks and efficacy (N) for XXXG-ANTS peak at pH 2.5 different phosphate-TEA concentrations (25, 50 and 100 mM) and different pH values for 50 mM buffer.

¹ Equation 1:

$$\text{Resolution(Rs)} = 1.18 \cdot \frac{tm_2 - tm_1}{w_{1/2}(2) - w_{1/2}(1)}$$

where 1 and 2 the peaks corresponding to compounds XXXG-ANTS and XLG-ANTS, respectively, t_m is the migration time, and $w_{1/2}$ is the peak width.

² Equation 2:

$$\text{Efficacy (N)} = 5.54 \cdot \left(\frac{tm}{w_{1/2}} \right)^2$$

where t_m is the migration time, and $w_{1/2}$ is the peak width for compound XXXG-ANTS.

At 50 mM buffer concentration, as the pH of the buffer increased (2.0, 2.5, and 3.0), migration times increased (Figure 33), resolution decreased, but efficacy resulted optimal at pH 2.5 (Table 2).

Therefore, 50 mM phosphoric acid, adjusted to pH 2.5 with TEA, was selected for all further analyses.

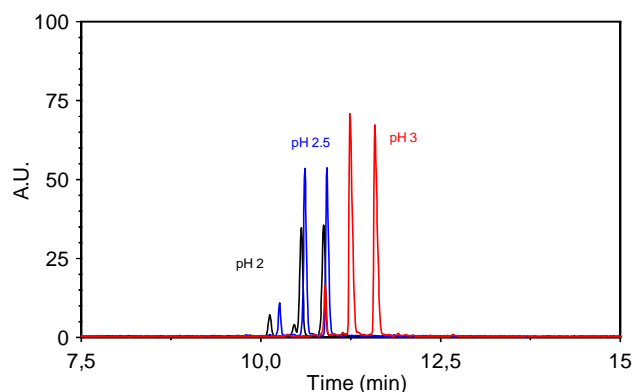


Figure 33: Electropherograms at different buffer pH (2, 2.5, 3).

The XGOs-ANTS mixture was analyzed at three different voltages (-30, -20, and -10 kV). Electropherograms are shown in Figure 34. A large increase in migration times is observed as voltage is reduced.

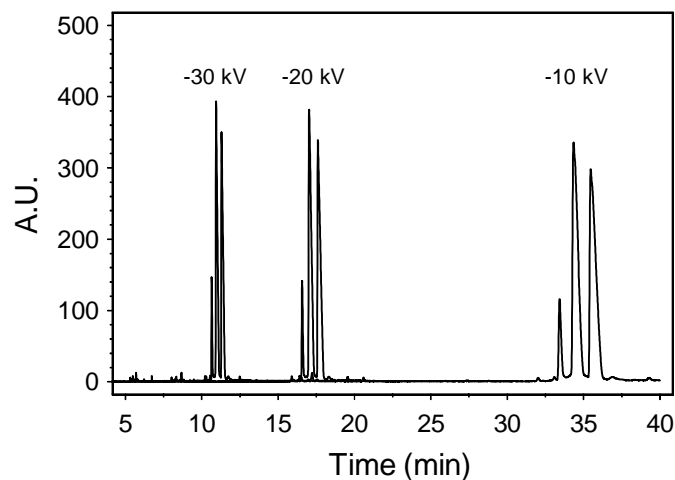


Figure 34: Electropherograms of XGOs-ANTS at -30, -20 and -10 kV applied voltage.

Measured current intensities follow a linear relationship with the applied voltage ($V=I \cdot R$) (Figure 35), meaning that heat generation by Joule effect is negligible, which otherwise would result in a loss of resolution¹⁴³. Therefore, -30 kV was selected as the working voltage to maintain short analysis time.

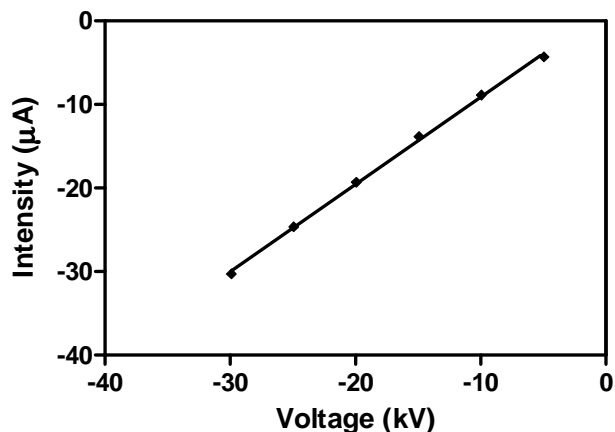


Figure 35: Resulting intensities at different applied electrophoretic voltages, showing a linear relationship between them.

The optimal amount of sample loaded into the capillary was evaluated by varying the injection time (from 3 to 15 s) during hydrodynamic injection. An injection time of 6 s at 40 mbar pressure was chosen as a compromise between low detection limit and reduced resolution at longer injection times (Figure 36).

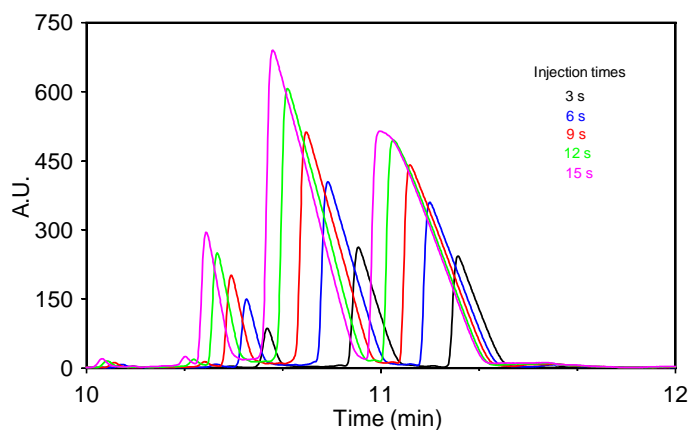


Figure 36: Electropherograms obtained by different hydrodynamic injection times (from 3 to 15 s) at 40 mbar.

In conclusion, HPCE analyses of ANTS-labeled oligosaccharides are performed on a Hewlett-Packard HP^{3D} CE G1600 AX system equipped with a diode array UV-Vis detector. The capillary (72 cm effective length, 50 μm internal diameter, fused silica with an extended light path bubble (150 μm) in the detection window) was pretreated or regenerated with 0.1 M NaOH, H₂O milliQ, and running buffer (for 30, 10, and 10 min respectively). Samples were loaded into the capillary under hydrodynamic injection mode at 40 mbar pressure during 6 s. The conditioning between injections consisted of a 5 min equilibration step with running buffer. Running buffer was 50 mM phosphoric buffer adjusted at pH 2.5 with triethylamine (TEA) as EOF modifier obtaining an inverted EOF method. Electrophoresis was performed at -30 kV and constant temperature of 30°C. The detector was a UV/Vis diode array and the electropherograms were recorded at 214 nm (20 nm slit), 224 nm (20 nm slit) and 270 nm (20 nm slit), but only record at 224 nm was used.

3.- Monitoring XET activity: Xyloglucan as donor and XGOs-ANTS as acceptor⁽²⁾.

To demonstrate that the developed HPCE method is adequate to monitor XET reactions, *Ptt*-XET16A catalyzed transglycosylation between polymeric XG as donor and the mixture of XGOs-ANTS as acceptor was monitored (Figure 37). Several peak clusters were observed in the electropherograms, corresponding to dimmers, trimmers, tetramers, etc. They result from transfer of the basic units of XG polymer (XXXG, XXLG, XLXG, and XLLG) (Figure 38), all generated after extensive depolymerization of the XG donor, to the XGO-ANTS acceptors.

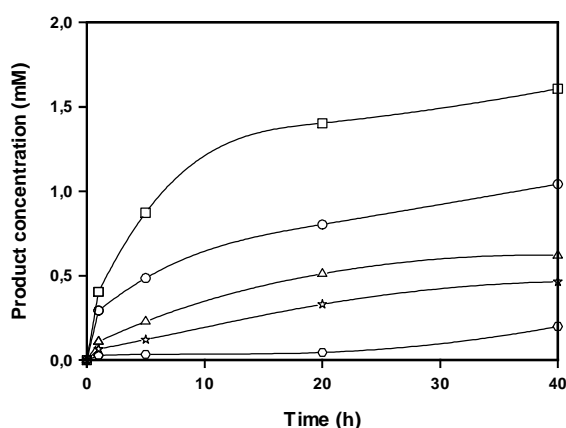


Figure 37: Evolution of different transglycosylation products formed during *Ptt*-XET16A catalyzed reaction between XG and XGOs-ANTS. Dimmers concentration (□), trimmers concentration (○), tetramers concentration (Δ), pentamers concentration (☆), hexamers concentration (⬡).

Theoretically, 16 different dimmers (4 donors x 4 acceptors) can be produced, with 5 unique molecular masses. Indeed, exactly 5 peaks are precisely detected in the dimer cluster of the electropherogram (Figure 38, inset). This demonstrates that XGOs-ANTS are good acceptors indicating that the acidic tag does not prevent binding to the acceptor subsites of the enzyme and that the HPCE method has enough resolution to monitor XET activity.

² This part of the Ph.D. is included in the article published in the Biochemical Journal with the title **Kinetic analysis with low molecular mass xyloglucan oligosaccharides defines the catalytic mechanism of a *Populus* Xyloglucan Endotransglycosylase**, by Marc Saura-Valls, Régis Fauré, Sergi Ragàs, Kathleen Piens, Harry Brumer, Tuula T. Teeri, Sylvain Cottaz, Hugues Driguez, and Antoni Planas¹³³.

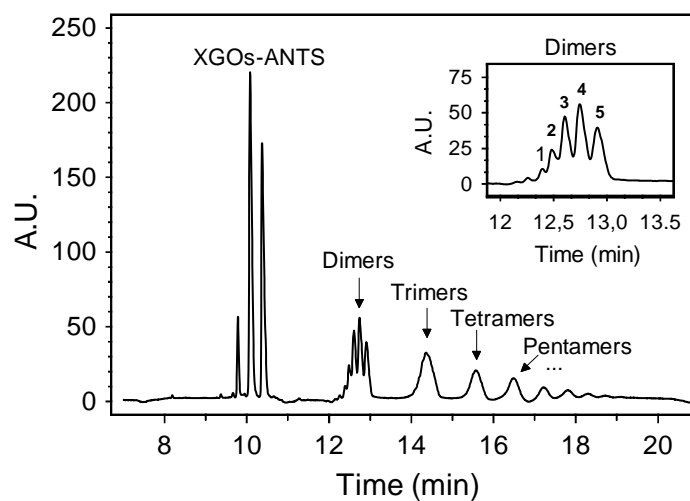


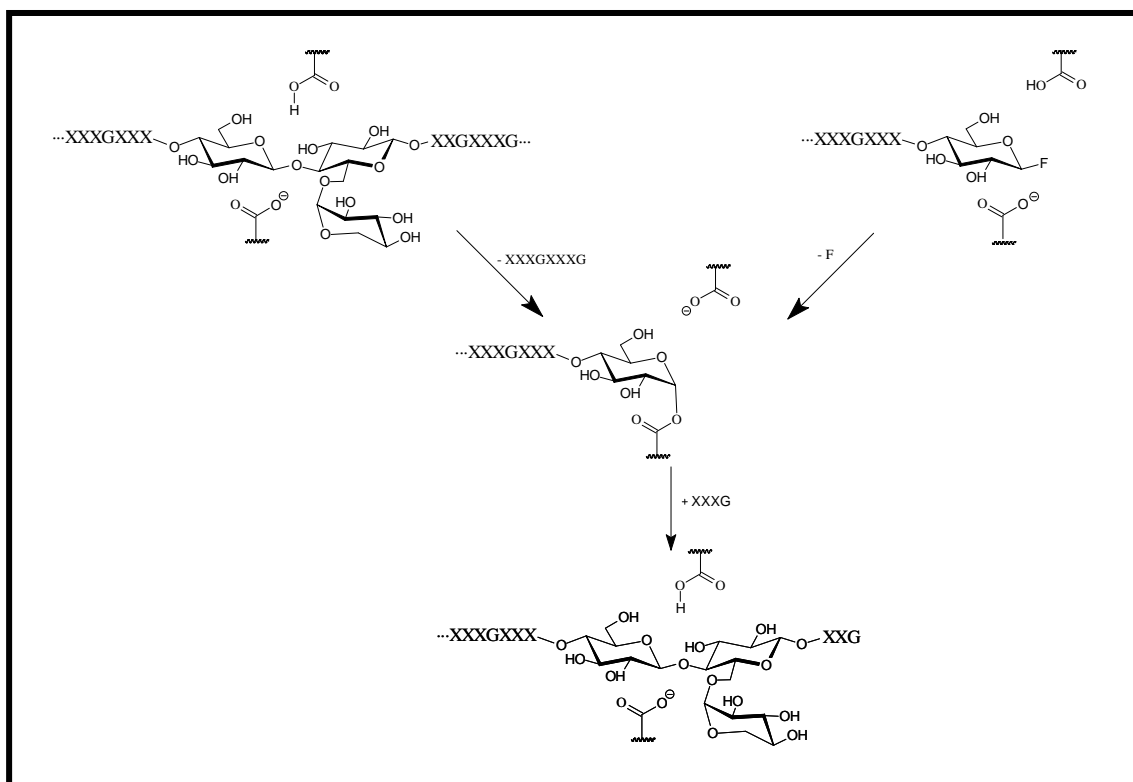
Figure 38: Electropherogram of the *Ptt*-XET16A-catalyzed transglycosylation using XG-polymer as donor and a mixture of XGOs-ANTS as acceptor substrates, after 48 h reaction. Inset: Magnification of the dimers region in which five peaks are resolved.

However, the polydisperse nature of the donor xyloglucan, together with the multiple catalytic events occurring before end products are obtained, limits this experimental design for enzymological studies of XET action. For that reason it is necessary to find low molecular-mass donors to study *Ptt*-XET16A using this HPCE method.

4.- Search of a minimal donor for *Ptt*-XET16A.

4.1.- Hypothesis 1: β -xylogluco-oligosaccharidyl fluorides as donors.

β -glycosyl fluorides are common glycosyl donors in transglycosylation reactions catalyzed by retaining β -glycosidases using kinetically controlled conditions^{77,102,144,145}. In the same way, we have proposed that β -glycosyl fluorides can act as donors for XETs, in this case the fluoride atom mimics the donor fragment liberated in the first part of the reaction (leaving group) (Scheme 4).



Scheme 4: Comparative scheme for proposed XET catalyzed transglycosylation using XG oligosaccharides or β -xylogluco-oligosaccharidyl fluorides as donors. XET catalytic residues are shown.

Three putative XET β -fluoride donors were proposed GG β F(1), XG β F(2) and XXXG β F(14).

4.1.1.- Synthesis of GG β F(1), XG β F(2), and XXXG β F(14).

Once different low molecular weight β -oligosaccharidyl fluorides as putative XET donors were proposed, we have embarked their synthesis. Initially three different fluorides were synthesized: GG β F (1), XG β F(2), and XXXG β F(14) presented in the following figure.

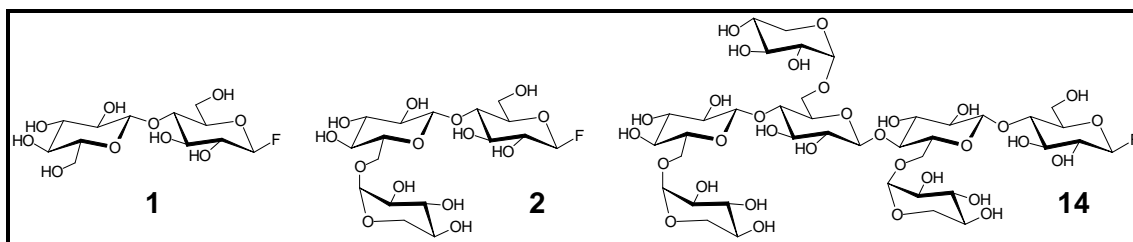
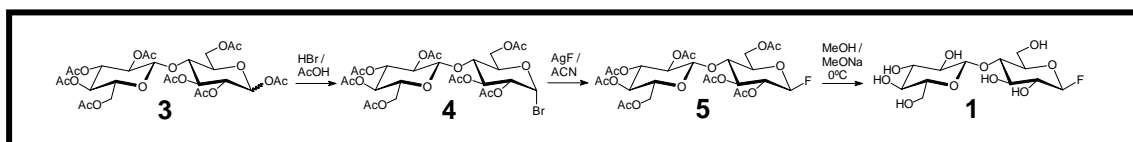


Figure 39: β -fluorides proposed as potential new donors for XETs.

a) Synthesis of GG β F(1).

GG β F (1) was synthesized starting from cellobiose octaacetate (3) by traditional chemical approaches. First of all, per-O-acetylated cellobiose was activated as the anomeric α -bromide (4), which was substituted by a β -fluoride using AgF in freshly dried acetonitrile with an overall yield of 80% after purification. Finally deprotection by Zemplén transesterification afforded 1 (Scheme 5).



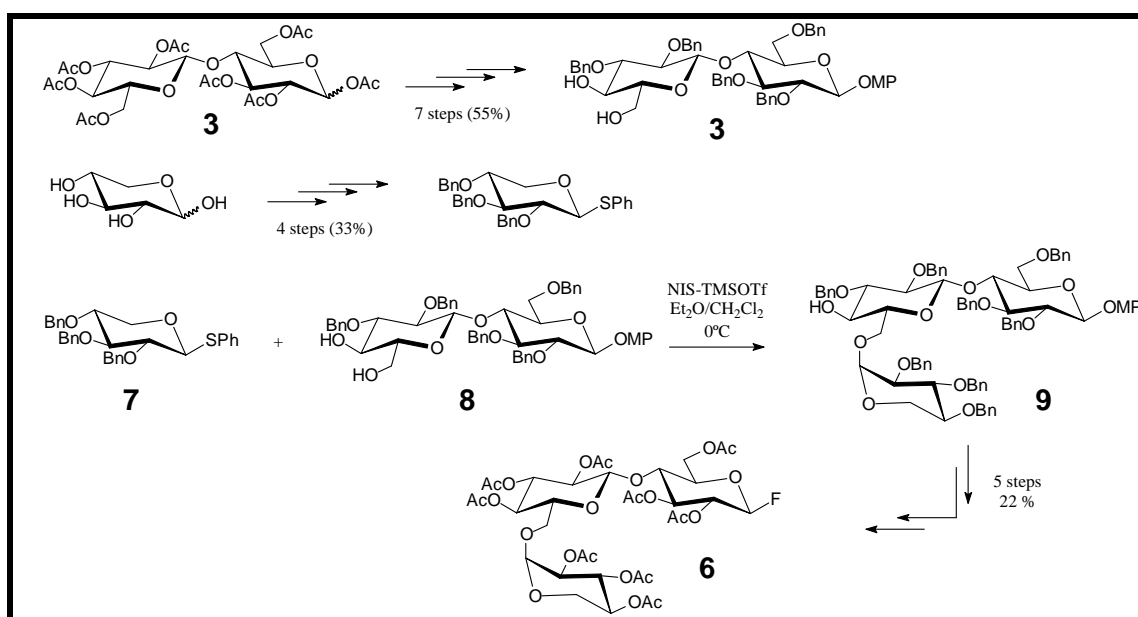
Scheme 5: Synthesis of β -cellobiosyl fluoride (1).

The last step, deprotection, was the most sensitive step of this synthesis. In previous studies in our group it has been shown that best deprotection results were obtained using Zemplén transesterification at 0 °C¹⁰². The deprotection step has to be done immediately before use, because deprotected β -fluorides are rather unstable.

Protected β -cellobiosyl fluoride (5) was characterized by ¹H and ¹³C NMR, observing the characteristic signal at 5.36 ppm (dd) with a F-H geminal coupling constant of 52.8 Hz corresponding to the anomeric proton on the same carbon that has the fluoride (Glc¹) and a coupling constant of 5.7 Hz assignable to H-1 to H-2 axial-axial coupling, demonstrating the β configuration of the fluoride.

b) Synthesis of XGβF(6).

Per-O-acetylated XGβF (**6**) was synthesized by Régis Fauré at CERMAV-CNRS (EDEN partner)¹⁴⁶ using a concurrent synthetic pathway in which the key step was the glycosylation between activated α -xylosyl donor (**7**) and 4^{II},6^{II}-dihydroxyl protected cellobiose acceptor (**8**) to obtain de XG structure (Scheme 6). The per-O-acetylated XGβF (**6**) was deprotected prior to use by Zemplén transesterification at 0°C, again this was a key step due to the instability of β -fluoride-glycosides.



Scheme 6: Summarized synthetic pathway to obtain XGβF (**6**).

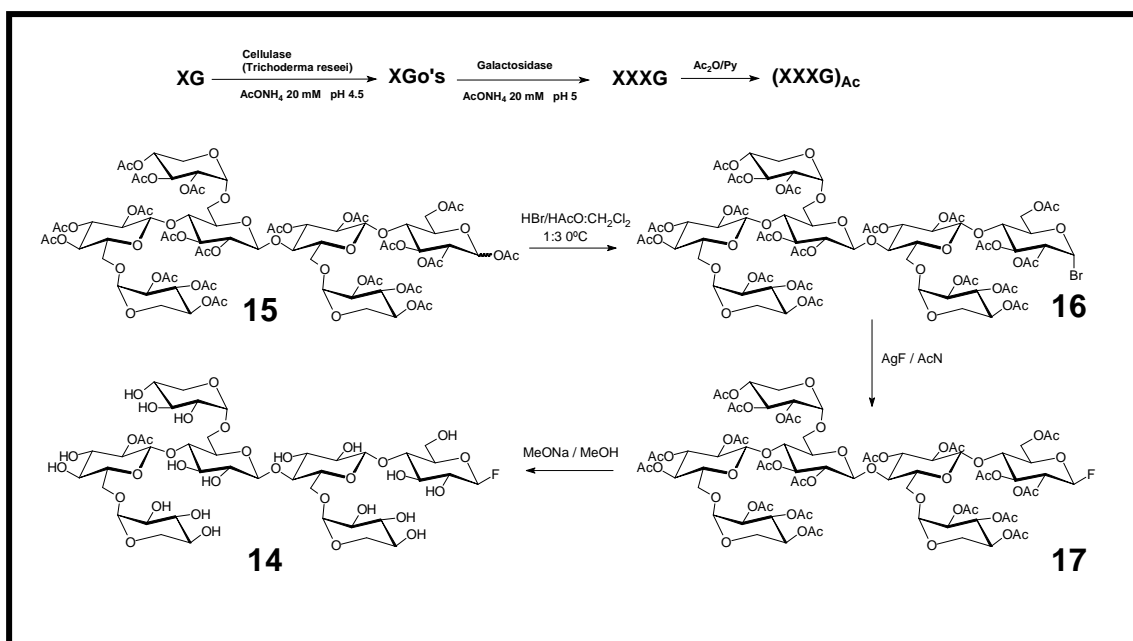
c) Synthesis of XXXGβF(14):

The XXXGβF substrate (**14**) (Figure 39) was synthesized starting from XG polymer by digestion with a *Trichoderma reesei* cellulase (Scheme 7). The resulting product was freeze-dried and degalactosylated by the action of β -galactosidase from *Aspergillus niger*. Product was freeze-dried again, per-O-acetylated and purified to obtain per-O-acetylated XXXG (**15**) with an overall yield of 40%. This product was characterized by NMR: ¹H-NMR showed two doublets at 6.21 ($J_{1,2}=3.6$ Hz) and 5.67 ppm ($J_{1,2}=8.4$ Hz) corresponding to GlcI ^{α} and β anomeric protons, ¹³C-NMR showed between 170.2 and 168.3 signals corresponding to CO of acetyl groups, between 100.3 and 99.9 ppm signals of anomeric carbons of Glc^{II,III,IV}, at 96.8-95.7 anomeric carbons of Xyl^{II,III,IV}, at 91.0 and 88.6 ppm anomeric carbons of GlcI ^{β} and α respectively.

Functionalization of per-O-acetylated XXXG (**15**) at the anomeric position was done using the same synthetic pathway presented for GG β F (Scheme 5). The pure protected β -fluoride **17** was obtained in 38 % yield but also some additional unpurified XXXG β F (**17**) was recovered.

Per-O-acetylated XXXG β F (**17**) was characterized by mass spectrometry, obtaining a molecular mass $[M-3H]^{3-}$ of 475.442, theoretical 475,425; by 1H -NMR, and ^{13}C -NMR. The dd signal at 5.41 ppm with a 53.2 Hz geminal H-F coupling constant in the 1H spectra demonstrate the presence of a fluoride in the anomeric position. The β -fluoride configuration was demonstrated by the typical axial-axial coupling constant (5.0 Hz) between H-1¹ and H-2¹. Relative integral values in the 1H spectra and signals in the ^{13}C spectra match with the expected signals for per-O-acetylated XXXG β F.

Like for other β -oligosaccharidyl fluorides, deprotection was done by Zemplén transesterification at 0°C immediately before use. Purity of the deprotected β -glycosyl fluoride was verified by 1H -NMR.



Scheme 7: Synthetic pathway to obtain XXXG β F(14**) starting from XG polymer.**

4.1.2.- Evaluation of β -glycosyl fluorides as donors of *Ptt*-XET16A.

All synthesized β -glycosyl fluorides (GG β F (1), XG β F (2), XXXG β F (14)) were evaluated as putative new *Ptt*-XET16A donors using the developed HPCE assay presented in this chapter (p. 59) at 1 mM donor and 5 mM XGOsANTS, pH 5.5, 30°C and 3.2 μ M enzyme. Reactions were monitored taking aliquots at different time points, diluting them 1:2 with ManANTS internal standard, quenching reactions by heating at 100 °C during 10 minutes, and analyzing them by HPCE. In Figure 40, electropherograms of reaction crudes after 45 h of reaction are presented. In all cases no new transglycosylation products appeared indicating that **XGOs β F are not donors**.

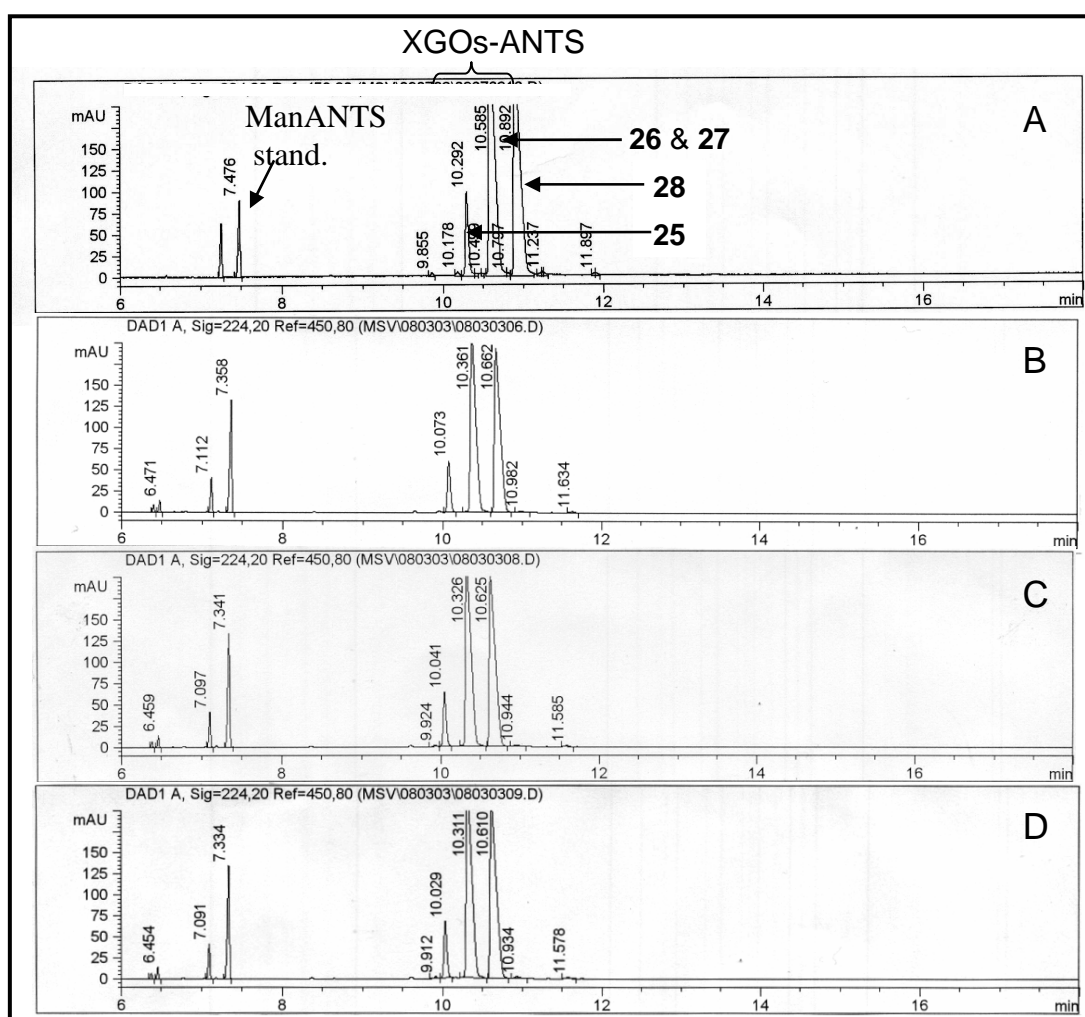


Figure 40: Electropherograms obtained after 45 h reaction, showing (A) example of control reaction without *Ptt*-XET16A, equivalent for all reactions; (B) GG β F(1) + XGOsANTS *Ptt*-XET16A reaction, (C) XG β F(2) + XGOsANTS *Ptt*-XET16A reaction, (D) XXXG β F(14) + XGOsANTS *Ptt*-XET16A reaction.

Another enzymatic assay based on fluoride release was used to evaluate XXXG β F (**14**) as putative donor for *Ptt*-XET16A. Fluoride release was monitored using a fluoride selective electrode (FSE) which monitors total fluoride release arising from spontaneous hydrolysis, enzymatic hydrolysis or transglycosylation of XXXG β F (**14**). For that reason, some control reactions must be done.

Spontaneous hydrolysis was measured with a reaction mixture containing only buffer and **14**. Enzymatic plus spontaneous hydrolysis was measured with a reaction mixture containing *Ptt*-XET16A, buffer and **14** in the absence of acceptor. Finally, enzymatic transglycosylation plus hydrolysis was monitored with a reaction mixture containing enzyme, buffer, XXXG β F (**14**) and XGOs. Initial rates for all these reactions were measured by FSE obtaining equivalent values for all of them as it is shown in Table 3. It indicates that there is no enzymatic catalysis and only spontaneous hydrolysis of XXXG β F (**14**) was observed.

Assay	[XXXG β F] (mM)	[XGOs] (mM)	<i>Ptt</i> -XET16A (μ M)	V _(fluoride release) (mM/h)
Spontaneous hydrolysis	1	0	0	0.162
Control XGOs	1	5	0	0.168
Enzymatic hydrolysis	1	0	3.2	0.160
Enzymatic transglycosylation	1	5	3.2	0.162

Table 3: Fluoride release initial rates of in different reaction: Spontaneous hydrolysis of XXXG β F(14**), control of XGOs mixtures hydrolytical activity, *Ptt*-XET16A hydrolytical activity, and *Ptt*-XET16A transglycosylase activity.**

Negative results obtained using different enzymatic assays with all proposed xylogluco-oligosaccharyl fluorides (GG β F (**1**), XG β F (**2**) and XXXG β F (**14**)) could be interpreted in different ways: For GG β F and XG β F it is possible that the structural requirements for an oligosaccharide to act as donor are not accomplished; they are too small considering that XXXGXXXG and GXXGXXXG are the smallest donors reported for XETs^{71,85} up to now.

On the other hand XXXG β F (**14**) has the minimal XG-like structure which should bind negative subsites in XETs, as when using XXXGXXXG and GXXGXXXG as donors. Therefore, when comparing donors XXXGXXXG and our XXXG β F, it is expected that the later occupies only negative subsites of the enzyme and the fluoride

atom is located in subsite +I, whereas XXXGXXXG occupies all positive and negative subsites⁸⁵.

We can hypothesize that maybe at least some glycosyl units should be present in subsite +I or other positive subsites to make the enzyme active. It is possible that this glycosyl unit at +I has some role in the positioning of catalytic residues. With this working hypothesis, we have proposed a new serie of putative glycosyl donors, which should present at least one glucose unit at the predicted +I subsite.

4.2.- Hypothesis 2: XGOs with at least one glucosyl unit at the positive subsites.

A new group of xylogluco-oligosaccharides as putative donors for XETs were designed with the condition to have at least a glycosyl group at predicted +I subsite(s) (Figure 41). Taking into account that XET cut the glycosydic bond of a non branched glucosyl unit some of these substrates have different proposed +I subsites which can be occupied with a non branched Glc unit or a α -Xyl-(1 \rightarrow 6)- β -Glc unit, note that glycosyl units proposed to be located at +I subsite are underlined (they are located at the reducing end site of a non-branched glucosyl unit).

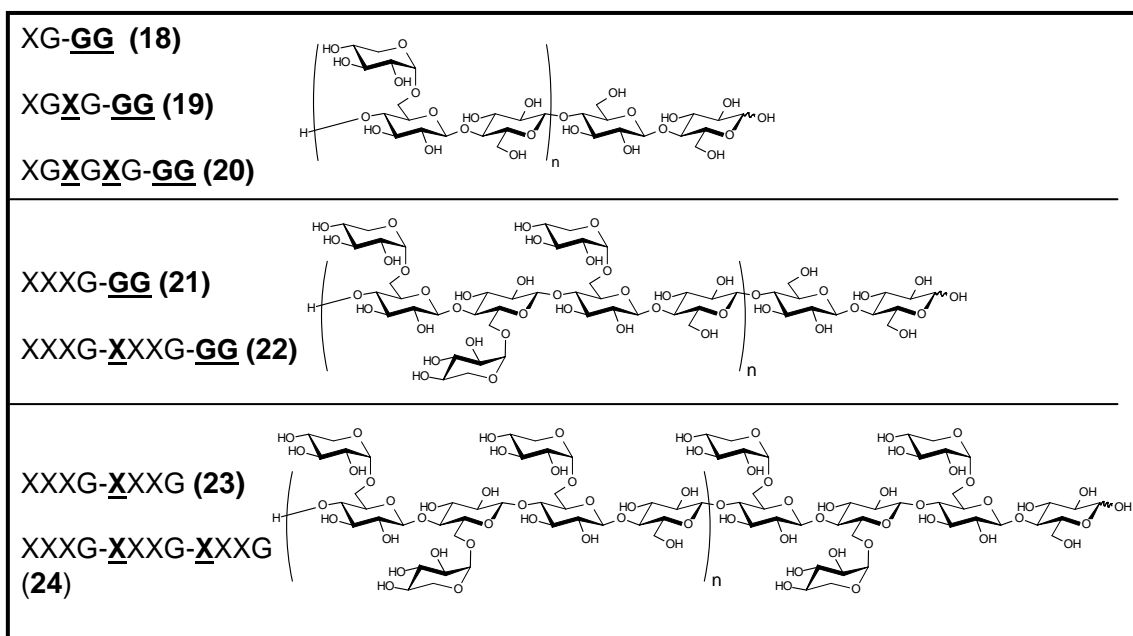
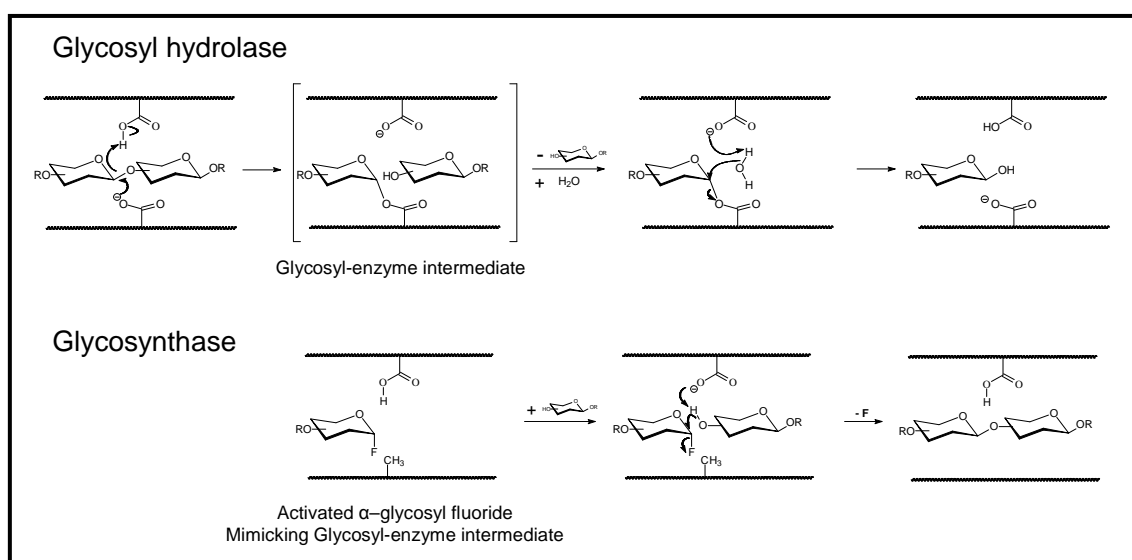


Figure 41: Structure of second group of putative glycosyl donors for *Ptt*-XET16A, in bold and underlined the glycosyl unit or units proposed to be located in the +I subsite.

These substrates were designed in our consortium (EDEN project) and they were synthesized by Régis Fauré at CERMAV-CNRS in Grenoble using the **glycosynthase technology**.

Glycosynthases are engineered retaining glycosyl hydrolases genetically modified by substitution of the catalytic nucleophile by a non acidic amino acid residue that cannot establish a glycosyl-enzyme intermediate, and therefore are hydrolytically inactive enzymes. However, these mutated enzymes can catalyze the transfer of a sugar moiety from an α -glycosyl fluoride (which effectively mimics the glycosyl-enzyme intermediate) to various acceptors (Scheme 8)^{147,148}.

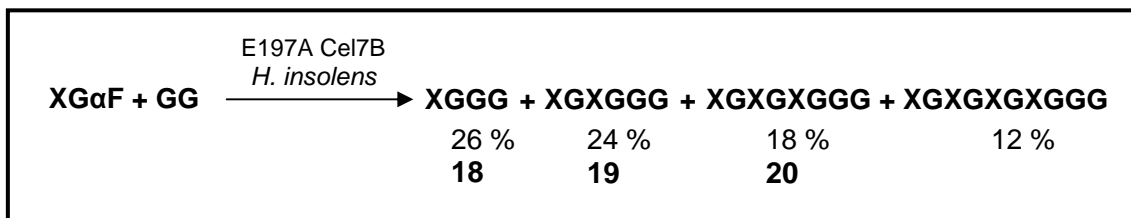


Scheme 8: Comparative scheme of glycosyl hydrolase and glycosynthase catalysed reactions. Note the structural mimicking of glycosyl-hydrolase intermediate by the α -glycosyl fluoride in glycosynthases.

Since the appearance of this technology different authors have studied different nucleophile-less glycosyl hydrolases to evaluate them as novel “glycosynthases”. It has been demonstrated that not all nucleophile-less glycosyl hydrolases become glycosynthases, but several glycosynthases endo and exo type have been described presenting different substrate specificities and different stereo-specificities¹⁴⁹⁻¹⁶⁵. It has been previously demonstrated that 6^{II}-substituted α -cellobiosyl fluorides are efficient substrates for coupling reactions catalyzed by the Cel7B E197A glycosynthase from *Humicola insolens*¹⁴⁹, this finding makes Cel7B E197A glycosynthase a good candidate for XG related structure synthesis.

4.2.1.- (XG)_nGG synthesis.

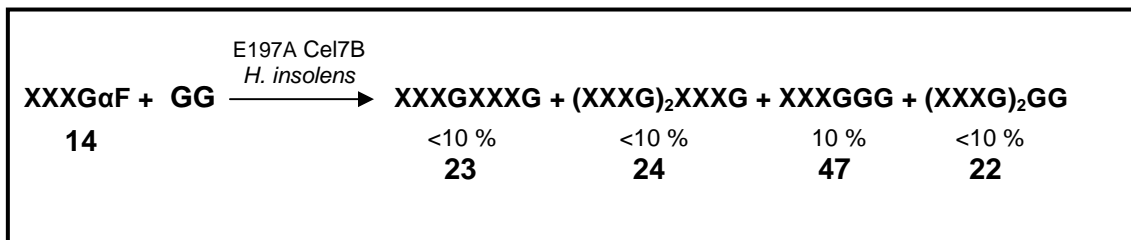
The (XG)_nGG (n=1,2,3) family was obtained by glycosynthase coupling between XGαF (**2**) and GG using the E197A Cel7B from *Humicola insolens*, using 1:5 ratio α-fluoride donor:acceptor (Scheme 9)¹⁴⁶.



Scheme 9: Glycosynthase coupling reaction to obtain (XG)_nGG family of putative donors for XETs.

4.2.2.- (XXXG)_n and (XXXG)_nGG synthesis.

Other families of putative donors (XXXG)_n and (XXXG)_nGG (n=1,2) were obtained by glycosynthase coupling between XXXGαF (**14**) and GG using again the E197A Cel7B from *Humicola insolens*, using 1:5 ratio α-fluoride donor:acceptor (Scheme 10)¹⁴⁶.



Scheme 10: Glycosynthase coupling reaction to obtain (XXXG)_nGG and (XXXG)_n families of putative donors for XETs.

4.2.3.- Evaluation of (XG)_nGG and (XXXG)_n(GG)_m as putative donors for Ptt-XET16A.

These putative donors (XGGG (**18**), XGXGGG (**19**), XGXGXGGG (**20**), XXXGGG (**47**), XXXGXXXG (**23**) and XXXGXXXGXXXG (**24**)) were screened as substrates for Ptt-XET16A using the developed HPCE method at 1 mM donor and approx. 5 mM XGOs-ANTS, and 3.2 μM Ptt-XET16A. Reactions were monitored by taking aliquots of the reaction mixtures at different time points, diluting them 1:2 with ManANTS internal

standard, stopping reaction by heating for 10 minutes at 100°C, and analyzing them by HPCE. Electropherograms obtained after 21 h reaction were presented in Figure 42.

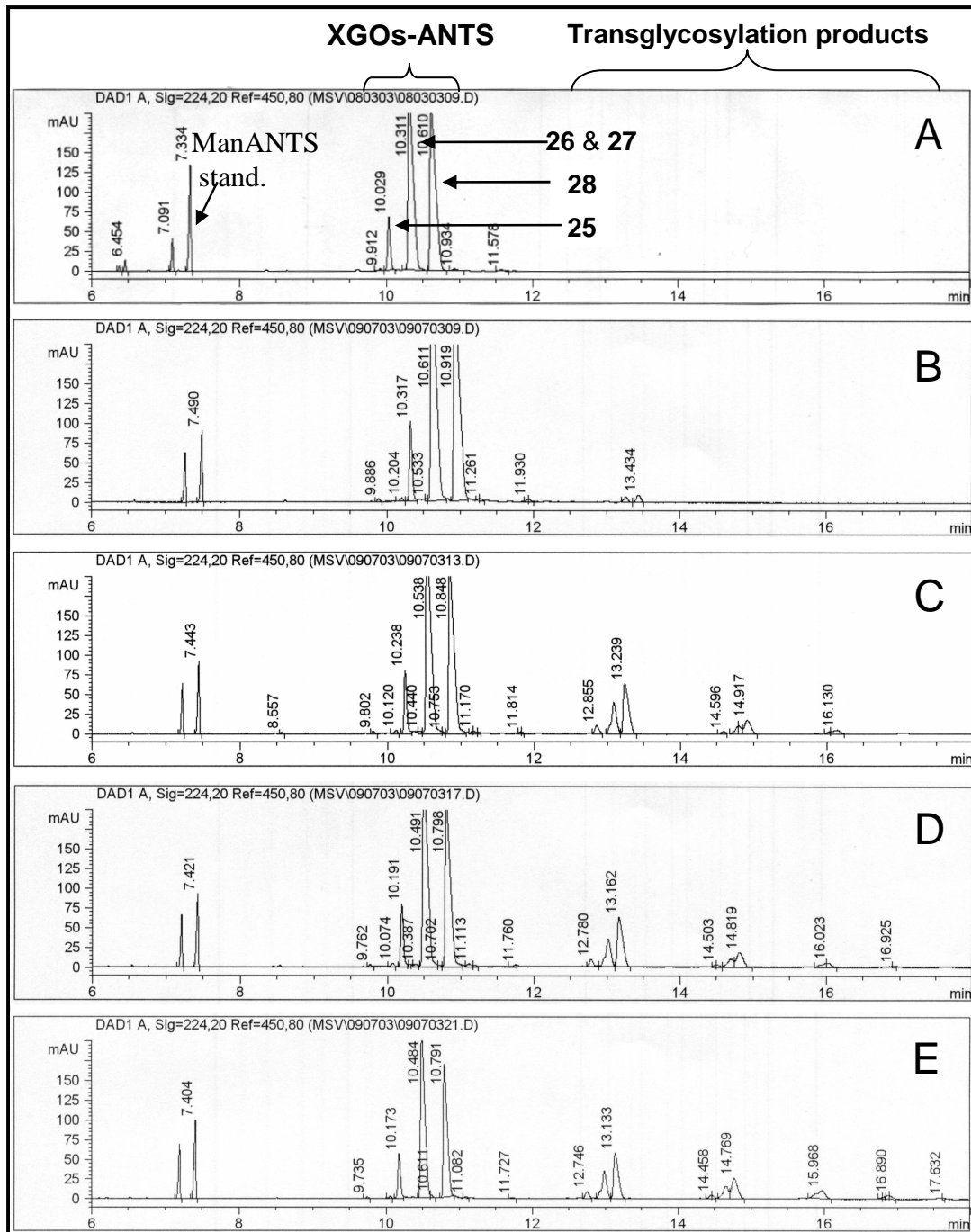


Figure 42: Electropherograms obtained after 21 hours reaction of XGGG (18), XGXGGG (19), XGXGXGGG (20) at 1 mM and 5 mM XGOsANTS. Blank reaction (A). Electropherograms resulting from reaction of XXXGGG (47) (B), XXXGXXXG (23) (C), XXXGXXXGGG (22) (D), XXXGXXXGXXXG (24) (E)

These electropherograms (Figure 42) showed no reaction for XGGG (**18**), XGXGGG (**19**), XGXGXGGG (**20**). In contrast, for XXXGGG (**47**) a moderate reactivity was detected, and for XXXGXXXGGG (**22**), XXXGXXXG (**23**) and XXXGXXXGXXXG (**24**) transglycosylation products were detected. Identification of reaction products will be discussed in chapter 4 (p. 124).

These results have demonstrated that low molecular weight substrates are substrates for *Ptt*-XET16A. Similar results were shown by Fanutti *et al.*^{71,85} for XXXGXXXG (**23**) and GXXGXXXG (**53**) with a xyloglucan endotransglycosylase / hydrolase from germinating nasturtium seeds, although there are other studies that seemed to indicate that this enzymes s do not tolerate substrates as small as XXXGXXXG (**23**)^{40,64}.

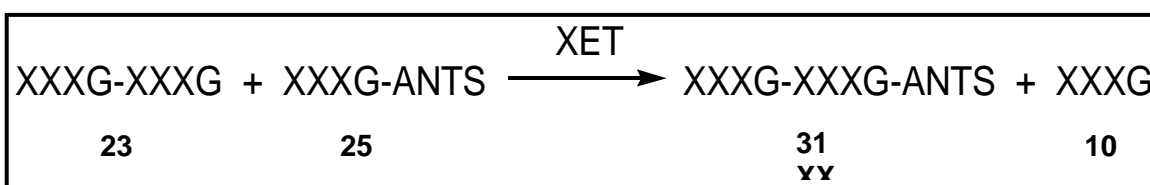
With our results, we have found the smallest donor for XETs ever described **XXXGGG (47)**, although its reactivity compared to XXXGXXXG (**23**) seems to be very low.

It was also observed that the use of a mixture of XGOs-ANTS increases complexity of electropherograms, moreover when different transglycosylation events occurred. For example, in Figure 42 C, it can be observed formation of different dimmers due to the mixture of XGOsANTS containing (XXXG-ANTS (**25**), XLG-ANTS (**26**), XLXG-ANTS (**27**) and XLLG-ANTS (**28**)) and also different clusters of labeled transglycosylation products (apart from these dimmers). This could indicate polymerization events which will increase difficulties on electropherogram interpretation, for that reason it is preferably to use a single acceptor instead of an acceptor mixture. These experiments showed that a single labeled acceptor should be desirable for XET kinetic studies.

5.- HPCE assay for kinetic characterization of *Ptt*-XET16A⁽³⁾:

To kinetically characterize *Ptt*-XET16A we decided to use a low molecular mass xyloglucan oligosaccharide as glycosyl donor and a labeled heptasaccharide as acceptor obtained by reductive amination with 8-aminonaphtalene-1,3,6-trisulfonic acid (XXXG-ANTS (**25**)). Once we have demonstrated the need of occupying acceptor subsites with saccharidic units, XXXGXXXG(**23**) has been chosen as a good substrate with small and defined structure to characterize this enzyme (*Ptt*-XET16A). Even though the compound XXXGGG (**47**) has been found to be the minimal donor for *Ptt*-XET16A, it is a poor substrate compared with the chosen donor XXXGXXXG (**23**).

Under initial rate assay conditions, *Ptt*-XET16A is expected to catalyze a single transglycosylation reaction to form the labeled product XXXGXXXGANTS (Scheme 11):



Scheme 11: Scheme of transglycosylation reaction between the tetradecasaccharide donor 23 and the heptasaccharide labeled acceptor 25 showing the proposed transglycosylation products.

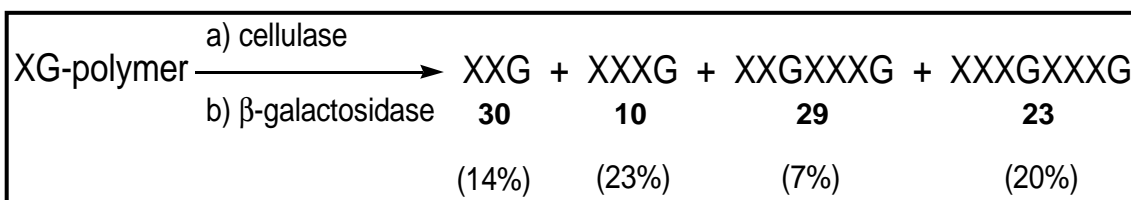
5.1.- XXXGXXXG (**23**) synthesis.

The tetradecasaccharide donor **23** was synthesized in preparative scale by Régis Fauré at CERMAV-CNRS (EDEN partner) using two strategies.

- a) Controlled hydrolysis of XG polymer.
- b) Glycosynthase catalyzed coupling.

³ This part of the Ph.D. is included in the article published in the Biochemical Journal with the title **Kinetic analysis with low molecular mass xyloglucan oligosaccharides defines the catalytic mechanism of a *Populus* Xyloglucan Endotransglycosylase**, by Marc Saura-Valls, Régis Fauré, Sergi Ragàs, Kathleen Piens, Harry Brumer, Tuula T. Teeri, Sylvain Cottaz, Hugues Driguez, and Antoni Planas¹³³.

In the first method (Scheme 12), tamarind seed XG-polymer was incubated with cellulase from *Trichoderma reesei* as essentially described by Fanutti⁷¹, but in such a way that the preparation of mixed monomers (hepta-, octa-, and nonasaccharides) and mixed dimmers (tetradeca-, pentadeca-, hexadeca-, heptadeca-, and octodecasaccharides) was optimized. After de-galactosylation using β -galactosidase from *Aspergillus niger* and purification on silica gel chromatography, penta- (**30**), hepta- (**10**), dodeca- (**29**) and tetradecasaccharides (**23**) were obtained in 14, 23, 7 and 20% yield, respectively, and characterized by MS, ¹H- and ¹³C-NMR. For further characterization of compounds **29** and **23** their reducing ends were coupled with 4-aminobenzoic acid ethyl ester (ABEE) by reductive amination using the sodium cyanoborohydride (NaBH₃CN) procedure, and these derivatives were analyzed by LC/MS¹⁶⁶.

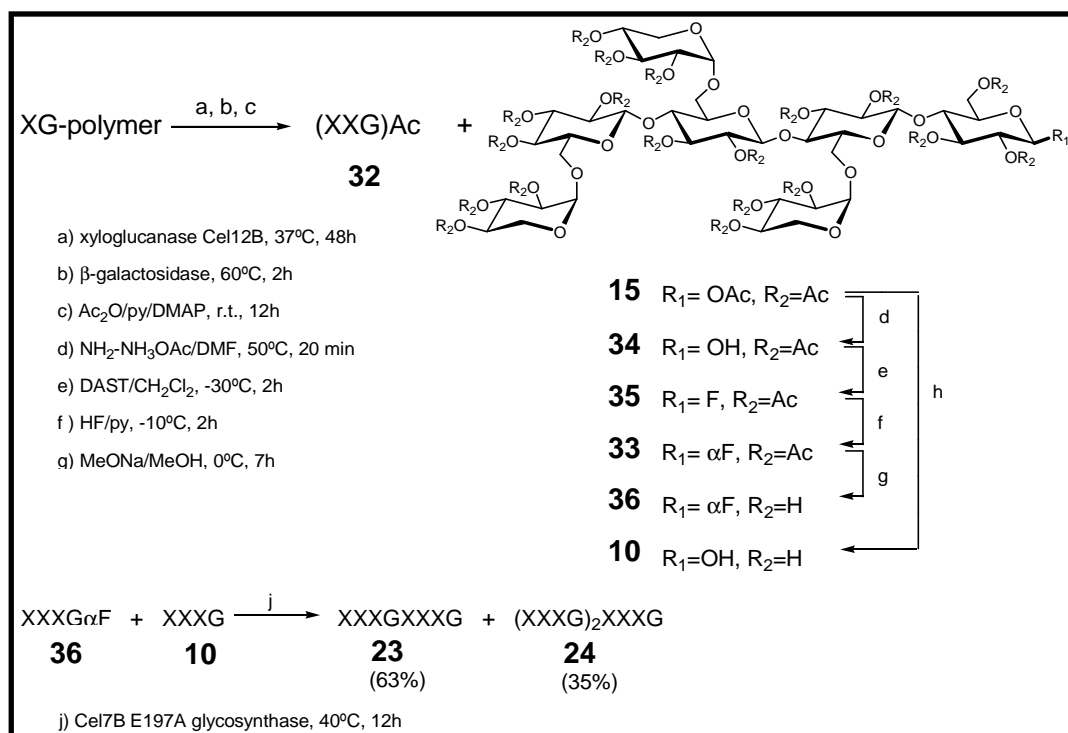


Scheme 12: Reaction of depolymerization and degalactosidation of xyloglucan polymer to obtain the tetradecasaccharide **23.**

Because preparation of pure tetradecasaccharide (XXXGXXXG (**23**)) by controlled enzymatic hydrolysis of xyloglucan is tedious, requiring precise control of reaction parameters and long purification steps, a procedure using glycosynthase technology has been developed. This method was based on full enzymatic degradation of XG-polymer down to its repetitive units, chemical activation of the anomeric reducing end, and glycosynthase-catalyzed condensation (Scheme 13).

Tamarind seed XG was first incubated with pure recombinant xyloglucan-specific *endo*- β -(1→4)-glucanase from *Aspergillus aculeatus*¹⁶⁷ until TLC analysis showed only three major spots (XXXG, XXLG, XLLG), then β -galactosidase from *A. niger* was added to the reaction mixture to hydrolyze all the galactose groups obtaining XXXG as main product.

At this stage, the products of the reaction were acetylated and purified by flash chromatography on silica gel. Acetylated XXG (**32**) and XXXG (**15**) were isolated in 14 and 56% yield, respectively. Compound **32** was formed by contaminant enzymatic activities found in the commercially available β -galactosidase¹⁶⁸.



Scheme 13: Scheme of the synthesis of the activated donor XXXG α F and posterior coupling of this donor and the heptasaccharide acceptor 10 to obtain the tetradecasaccharide 23 objective, by glycosynthase catalysed coupling.

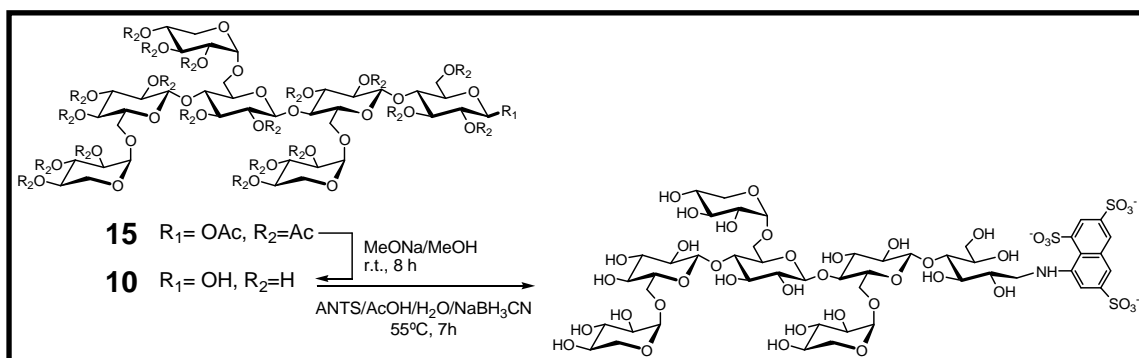
Coupling of two XXXG units to produce the target tetradecasaccharide (**23**) was achieved using the glycosynthase technology by condensation of the corresponding xyloglucan oligosaccharyl α -fluoride **36** with the heptasaccharide **10**.

The α -fluoride donor **36** for glycosynthase catalyzed synthesis of XXXGXXXG (**23**) was obtained as follows Scheme 13: standard hydrazine acetate treatment of acetylated XXXG (**15**) led to selective de-*O*-acetylation of the anomeric position in 84% yield. Compound **34** was then subjected to DAST treatment to yield an anomeric mixture of fluorides **35**. Anomerization with commercially available HF/pyridine reagent gave the pure α -fluoride **33**, which was isolated in 68% yield over the two steps. Catalytic de-*O*-acetylation gave the donor **36** in quantitative yield. The enzymatic condensation catalyzed by Cel7B E197A mutant was conducted by coupling **36** and **10** using previously described conditions¹⁴⁹. The dimer XXXGXXXG (**23**) and the trimer XXXGXXXGXXXG (**24**) were isolated in 63 and 35% yield, respectively. The calculated overall yield from xyloglucan, 20%, is similar to that obtained by enzymatic hydrolysis, but glycosynthase procedure is more reproducible and readily scalable.

5.2.- XXXG-ANTS(25) synthesis.

Up to now we have used a mixture of XGOs-ANTS to screen possible new donors. But once it has been demonstrated that they are good acceptors for XETs it is further more interesting to obtain a unique ANTS labeled acceptor to be used for kinetic analysis of XETs by HPCE. We have chosen XXXG-ANTS as standard acceptor because it is the easiest xyloglucan oligosaccharide to be obtained from tamarind XG, although there are other XGOs that normally are better acceptors for XETs^{41,90}.

The ANTS-labeled xyloglucan heptasaccharide (XXXG-ANTS (**25**)) acceptor was synthesized starting from the per-*O*-acetylated XXXG (**15**) obtained above (Scheme 12). Full de-*O*-acetylation by treatment with sodium methoxide in methanol afforded **10** in quantitative yield. **10** was derivatized by reductive amination with ANTS and sodium cyanoborohydride (Scheme 14), using conditions set up before in our group¹²² for analytical derivatization of oligosaccharides.



Scheme 14: Scheme of labeling reaction of XXXG(10).

Although widely used on analytical scale for HPCE analysis, ANTS-saccharide conjugates have not, to our knowledge, been produced in a preparative scale. The present method allows routine preparation of XXXG-ANTS **25** on a gram scale.

Preparative-scale production of the ANTS-labeled XXXG (**25**) required the optimization of a purification protocol consisting of three chromatographic steps:

a) gel filtration chromatography to remove the large excess of unreacted ANTS, eluted with water.

b) anion exchange chromatography to separate traces of underivatized XXXG (**10**), the labeled product was eluted with sodium hydroxide 0.1 N.

c) a second gel filtration step for desalting and further purification of the final XXXG-ANTS (**25**), eluted with water.

The final product was > 95% pure (as assessed by HPCE) and was isolated with an overall yield of 55 % from XXXG (**10**).

XXXG-ANTS (**25**) was characterized by mass spectrometry and by ^1H and ^{13}C NMR.

In the ^1H spectra doublets between 8.61 and 7.61 ppm of aromatic protons demonstrate the presence of the naphthalene label, the 3H multiplet at 4.94 ppm of anomeric protons demonstrates the presence of three xylosyl groups by comparison with XXXG ^1H spectra¹⁴⁶ and the presence of three glucopyranosyl groups was demonstrated by doublets at 4.60, 4.53 and 4.51 ppm corresponding to β -1,4-glucosyl units. Relative integrals are in concordance with expected structure.

In the ^{13}C spectra signals between 135.9 and 115.0 correspond to ten aromatic carbons from the naphthalene label. Signals at 104.2, 102.9 and 102.4 corresponding to substituted glucose anomeric carbons prove the presence of three glucopyranosyl units, and signals at 99.1, 98.9 and 98.4 are assigned to anomeric carbons of three xylopyranosyl units by comparison with the ^{13}C spectra of XXXG¹⁴⁶. Finally the signal at 46.6 ppm indicate the presence of a $-\text{CH}_2\text{-NH-}$ carbon, demonstrating the amine linkage with reduced Glc¹.

5.3.- HPCE method validation.

The HPCE method developed in chapter 2 (p. 59) for the separation of ANTS-labeled oligosaccharides is validated with purified XXXG-ANTS to be used in kinetic monitoring of XET reaction.

Linearity, repeatability, detection and quantification limits were evaluated to validate the HPCE method. Method response (area vs. concentration plot) is linear between 0.01 and 1 mM XXXGANTS (**25**) with response factors (relative area/concentration) within $\pm 10\%$ of the mean response factor¹⁶⁹ (Figure 43).

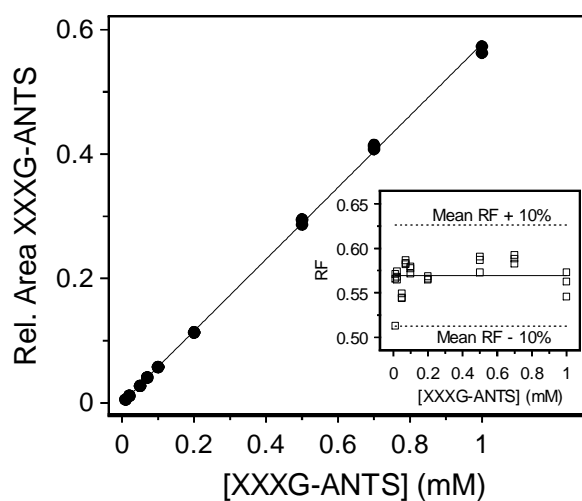


Figure 43: Standard curve and response factors for XXXG-ANTS (25) as analyte. Peak areas for 25 in the electropherograms are relative to the peak area of ANTS-labeled mannose as internal reference. Inset. Response factors (RF) in relative area/concentration, mean response factor (mean RF) (solid line), $\pm 10\%$ of mean RF limits (dashed lines).

Detection and quantification limits were 0.005 mM and 0.01 mM¹⁶⁹, respectively. Repeatability was determined at three concentration levels, 0.01, 0.1 and 1 mM, analyzing 6 samples for each concentration. Variation coefficients were lower than 5% within all the concentration range (Table 4).

conc (mM)	Average Rel. area	St. Dev.	CV (%)
1	0.58263	0.01801	3.09154
0.1	0.05604	0.00177	3.16554
0.01	0.00618	0.00024	3.96282

Table 4: Repeatability of the HPCE method at low, medium, and high concentration levels within the linearity range for the analysis of compound XXXG-ANTS (25).

Finally, response factor comparison between XXXG-ANTS (**25**) (used as analyte in the method validation, and standard acceptor for *Ptt*-XET16A catalyzed reaction) and XXXGXXXG-ANTS (**31**) (the XET-catalyzed reaction product) was done by parallel labeling of both substrates (XXXG (**10**), XXXGXXXG(**23**)) with ANTS and analysis of both stocks. In Figure 44, relative areas of each compound **25** and **31** at the same concentration showed a slope of one, indicating that both compounds have the same response factor.

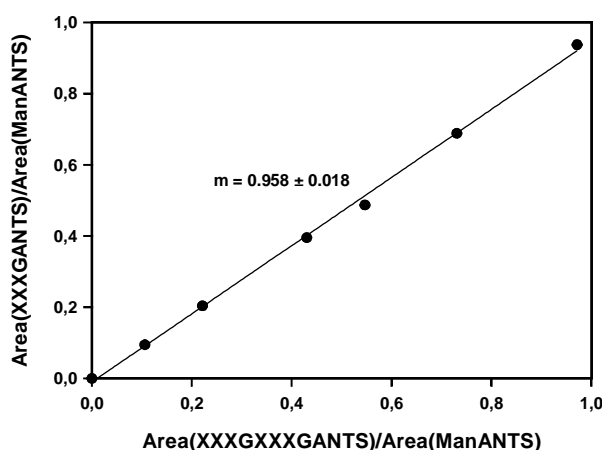
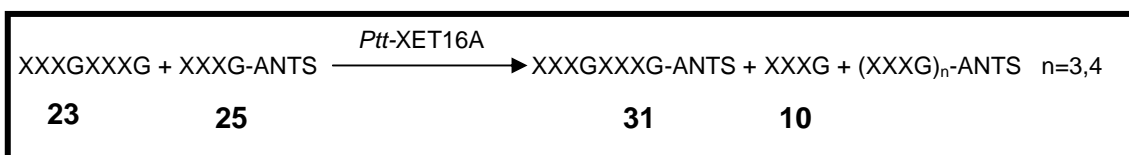


Figure 44: Comparison of relative areas of XXXG-ANTS (**25**) and XXXGXXXG-ANTS (**31**) at 0.1, 0.2, 0.4, 0.5, 0.7, 1 mM.

5.4.- *Ptt*-XET16A reaction monitoring and product identification.

The tetradecasaccharide **23** was assayed as low molecular weight donor for the transglycosylation reaction catalyzed by *Ptt*-XET16A using purified XXXG-ANTS (**25**) as the acceptor substrate (Scheme 15). HPLC analysis (Figure 45) shows the formation of a dimer, a trimer, and traces of a tetramer.



Scheme 15: Scheme of transglycosylation reaction between the tetradecasaccharide donor (**23**) and the heptasaccharide labeled acceptor (**25**), showing the transglycosylation products.

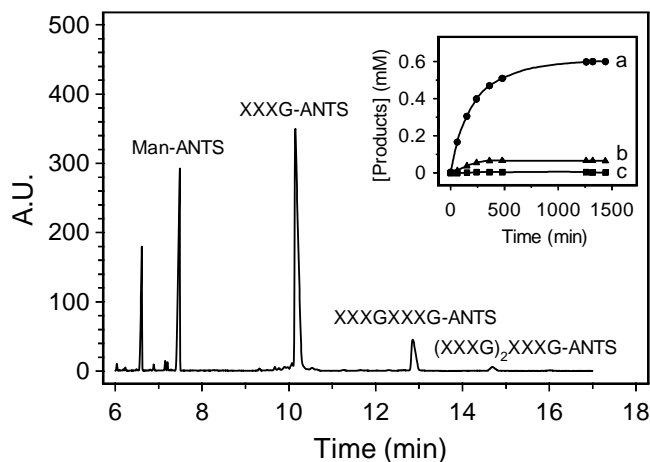


Figure 45: HPCE analysis of the transglycosylation reaction between XXXGXXXG donor (23, 1 mM) and XXXG-ANTS acceptor (25, 5 mM) catalyzed by *Ptt*-XET16A at pH 5.5, 30°C. ManANTS is the internal reference for peak area integration. Inset: Time course of the reaction. a: XXXGXXXG-ANTS (31); b: (XXXG)₂XXXG-ANTS (37); c: (XXXG)₃XXXG-ANTS.

The dimer and trimer were identified as XXXGXXXG-ANTS (31) and (XXXG)₂XXXG-ANTS (37) respectively, by co-injection with chemically synthesized standards⁽⁴⁾ (Figure 46). The dimer (31) is the initial product formed by transfer of the non-reducing end repeating unit from donor 23 to the acceptor (Figure 45, inset), whereas larger oligomers (minor products) arise probably from transglycosylation of donor 23 to the initially formed product (31) acting as an acceptor, although other reaction pathways could be proposed (Scheme 16). This can indicate that transglycosylation products can compete with ANTS labeled heptasaccharide substrate for the acceptors subsites. Taking into account that the XXXG-ANTS (25) concentration was higher than the first transglycosylation products and donor, it could be hypothesized that transglycosylation products, and the donor may be better acceptors than the XXXG-ANTS acceptor (25). For that reason, it can be proposed that the acidic ANTS tag can have some negative effect on binding.

⁴ Synthesis of ANTS-labeled xyloglucan oligosaccharides as standards for product identification is described in chapter 4 (p.123).

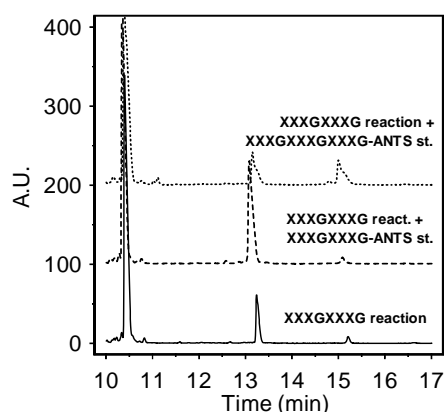
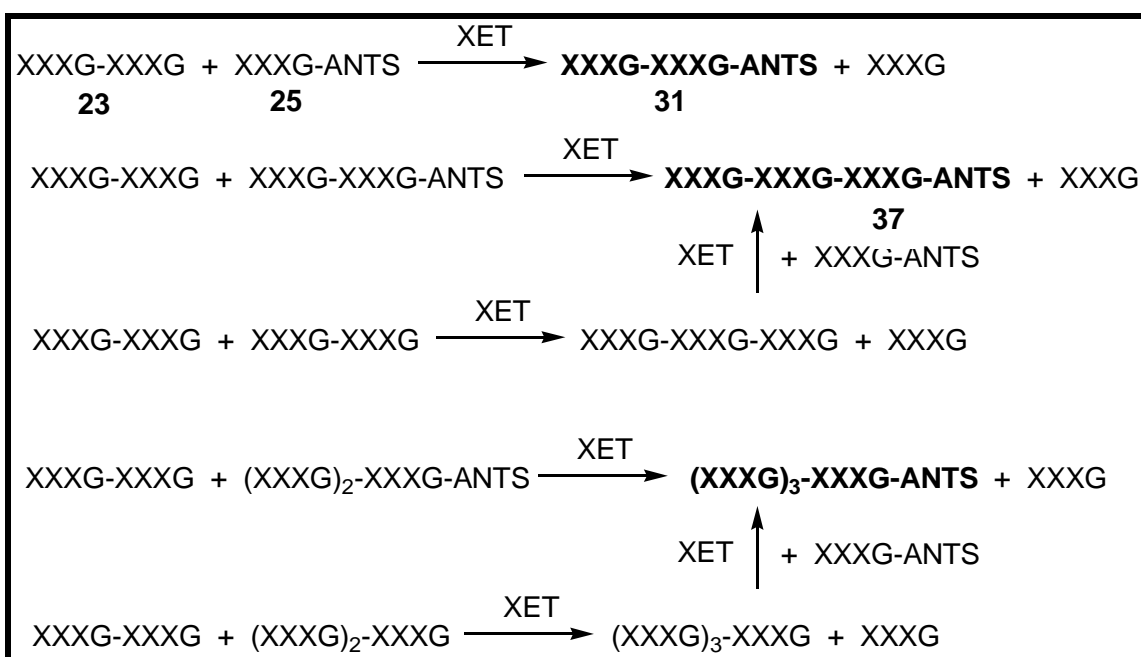


Figure 46: HPCE electropherograms showing identification by coinjection of XXXGXXX-ANTS (31) and XXXGXXXGXXXG-ANTS (37).



Scheme 16: Proposed reaction pathways to explain the formation of detected transglycosylation products in XXXGXXXG (23) + XXXGANTS (25) reaction.

A new HPCE activity assay for XETs was developed using low molecular weight XGos as substrates (XXXGXXXG (23) as donor and XXXGANTS (25) as acceptor) to monitor XET activity and to characterize kinetically *Ptt*-XET16A.

CHAPTER 3:
Ptt-XET16A enzyme characterization

CHAPTER 3: *Ptt*-XET16A enzyme characterization.**1.- Introduction.**

Ptt-XET16A was kinetically characterized using the HPCE method developed and validated in the present work. Kinetics were performed in citrate/phosphate buffer at constant ionic strength to determine pH and temperature profile with the tetradecasaccharide **23** and XXXG-ANTS (**25**) as donor and acceptor substrates, respectively. Initial rates were determined as the slope of the linear region of the time course (product concentration vs. reaction time) normally corresponding to < 5% conversion. Loss of linearity appears when transglycosylation products of higher DP than XXXGXXXGANTS (**31**) are observed (Figure 47). *Ptt*-XET16A has no detectable xyloglucanase (hydrolytic) activity (EC 3.2.1.151) under standard conditions⁴⁷.

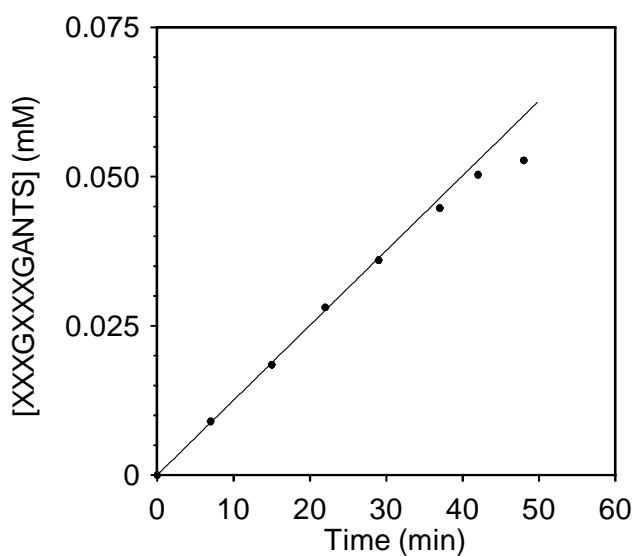


Figure 47: Example of initial rate determination, where linearity is lost at high conversions.

2.- Specific activity.

The linear relationship between initial rate and enzyme concentration (Figure 48) shows that a normal enzyme behavior is observed in all the range of enzyme concentrations studied. Reactions were done at pH 5.5 and 30°C using 1 mM donor **23** and 5 mM acceptor **25**.

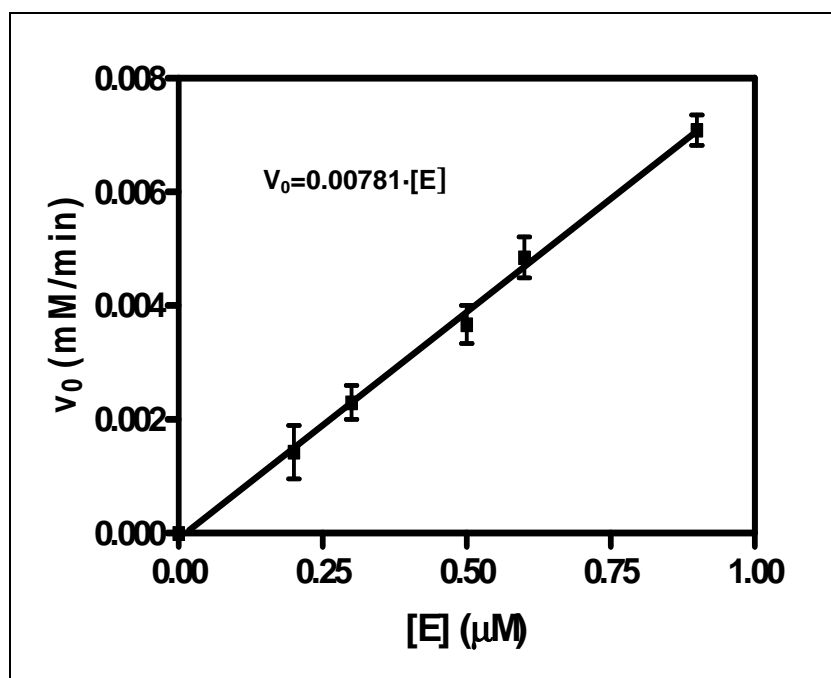


Figure 48: Enzyme standard curve v_0 vs. enzyme concentration. Conditions: citrate/phosphate buffer pH 5.5, 30°C, 1 mM donor **23**, 5 mM acceptor **25**.

Active enzyme concentration of each batch of *Ptt*-XET16A was determined by interpolation in the enzyme standard curve (Figure 48) of the initial rate obtained at 1 mM XXXGXXXG (**23**) and 5 mM XXXGANTS (**25**) at pH 5.5 and 30°C.

3.- pH profile.

The pH-dependence of the enzyme activity (Figure 49) was analyzed at 30°C using 1 mM donor **23** and 5 mM acceptor **25**. Maximum activity was detected between pH 5.0 and 5.5. Activity follows a single ionization curve at high pH values with a kinetic pK_a of 6.1 corresponding to general acid catalysis. At lower pH values, a rapid loss of activity is clearly observed. Enzyme inactivation at $pH < 5$ has previously been observed for *Ptt*-XET16A using standard iodine assays with XG substrate⁴⁷, and it appears to be a common feature of *XTHs*, that normally have a pH optima between 5 and 7.

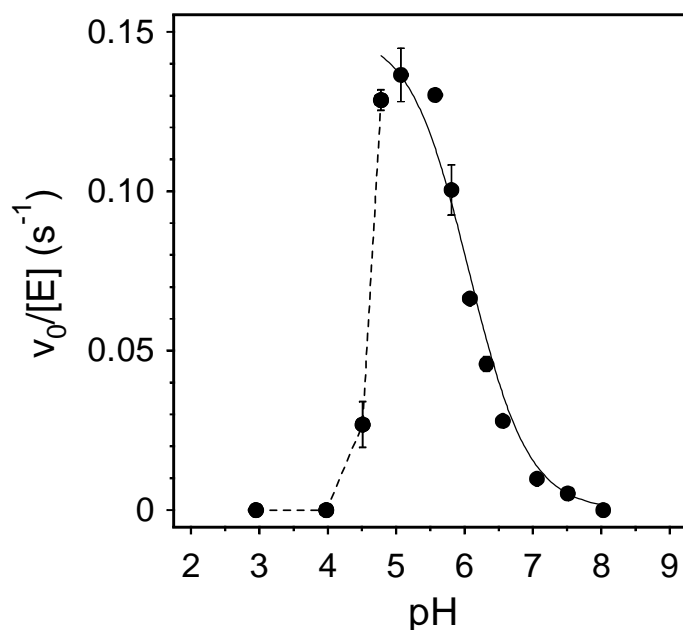


Figure 49: pH-Dependence of *Ptt*-XET16A activity at 30°C, 1 mM donor **23, 5 mM acceptor **25**.**

A general characteristic of *XTHs* is that more or less all enzymes present rapid decrease in activity below pH 5 and total loose of activity at 3.5.

There are *XTHs* which present a **broad pH profile** (>50% activity between pH 4.5-8), for example *At*-*XTH24*⁷⁰ or *Tropaeolum majus* *XTHs*⁸⁷ or some Mung bean seeds *XTHs*⁹⁰.

In contrast, other *XTHs*, including the *Ptt*-XET16A studied in this project, present **sharp pH profiles** maintaining more than 50% of maximum activity only between 2 or 2.5 units of pH. Some of them have the **pH optimum centered at pH 5-5.5**, for example some cauliflower *XTHs*^{46,90}, one *XTH* from Mung bean seeds⁹⁰, or one enzyme from pea stems⁴¹ and the studied *Ptt*-XET16A. Another group of enzymes have sharp pH profiles with the **maximum of activity more centered at pH 6-6.5**, for example *At*-*XTH4*, *At*-*XTH14* and *At*-*XTH22*^{50,70}. And finally another group of enzymes present a **pH optimum between 5.5 and 6** as one *XTH* from ripe kiwifruit (*Actinidia deliciosa*) *Ad*-*XTH6*⁴⁹ and another from azuki bean epicotyls⁶⁴.

4.- Temperature profile.

The temperature dependence of *Ptt*-XET16A (Figure 50) was evaluated at pH 5.5. Maximum activity was obtained between 30 and 40°C, followed by a rapid inactivation at higher temperature as previously observed using standard assays with XG polymer as substrate⁴⁷.

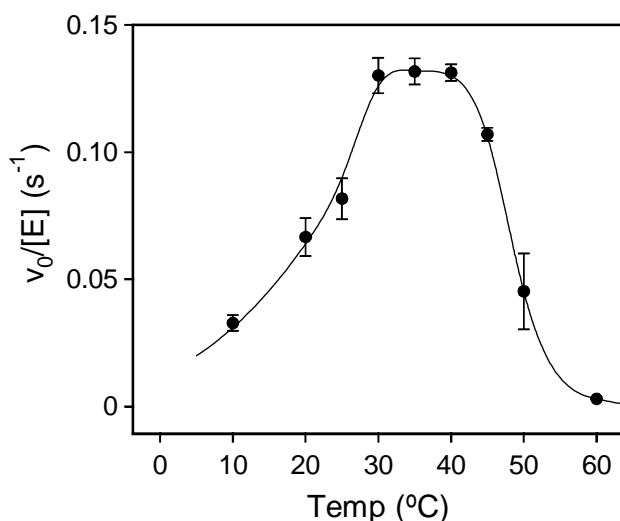


Figure 50: Temperature dependence of *Ptt*-XET16A activity at pH 5.5, 1 mM donor 23, 5 mM acceptor 25.

In general all *XTHs* present a broad temperature profile, where 50% of activity is maintained between at least 25 °C. But *XTHs* can be classified depending on the temperature at which activity is maximal.

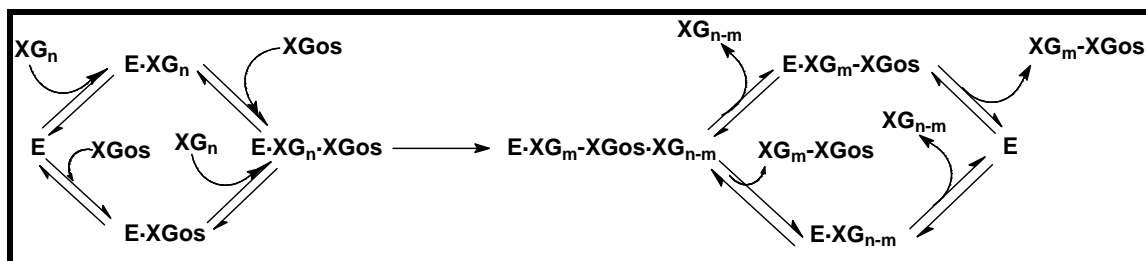
There are some **cold tolerant *XTHs***, for example *At*-*XTH22* heterologously expressed in *E. coli* and purified on denaturing conditions followed by refolding which have maximum activity between 12-18 °C showing more than 50% of activity at -5 °C⁵⁰. Likewise, *At*-*XTH14* and *At*-*XTH22* heterologously expressed in baculovirus/insect cells systems have maximum activity near 18 °C⁷⁰.

There is another group of *XTHs* which have their activity **maximum between 20-30 °C**, some of them having higher thermo tolerance, for example, *At*-*XTH4* and *At*-*XTH24*, they **maintain 80% of activity at 45 °C**⁷⁰, and others in the group present a relative **fast inactivation at higher temperatures**, for example *XTH* from cauliflower^{46,90}, some from mung bean seeds⁹⁰, and *Ptt*-XET16A here reported.

5.- Kinetic mechanism of *Ptt*-XET16A.

5.1.- Background.

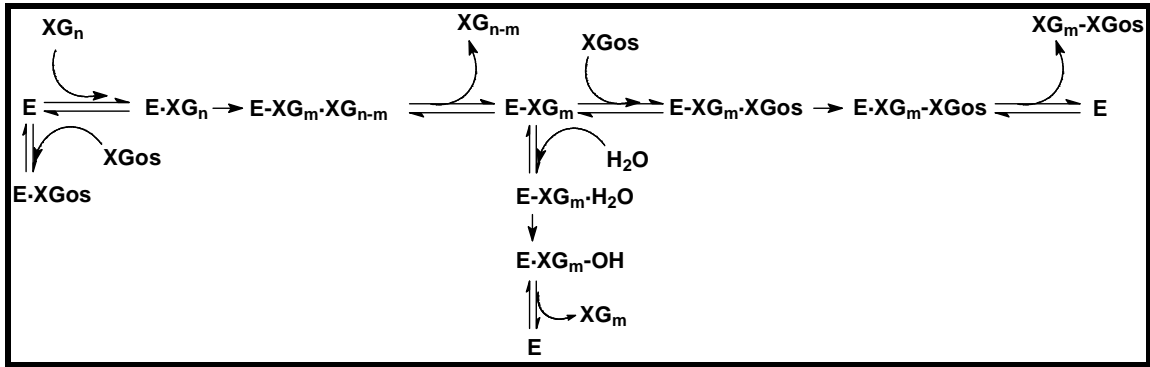
One open discussion in XET studies is the kinetic mechanism of action. Kinetic parameters using xyloglucan as donor substrate have been reported for xyloglucan endotransglycosylase activity of extracts from suspension-cultured poplar cells⁹⁷. A sequential mechanism was proposed, in which both XG as glycosyl donor and XGO as glycosyl acceptor associate with the enzyme to form a ternary complex before cleavage of the XG and transglycosylation to the acceptor occurs (Scheme 17).



Scheme 17: Schematic representation of a sequential *bi bi* mechanism, where donor and acceptor can bind the enzyme randomly and a trivalent complex (enzyme, donor and acceptor) is formed.

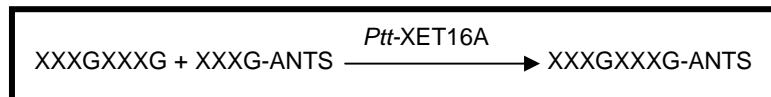
However, the original mechanism postulated for XET involves a double displacement mechanism with formation of a glycosyl-enzyme intermediate⁴². This is in keeping with the observed mechanism of GH16 hydrolases^{78,119} and the retaining mechanism of glycoside hydrolases in general¹⁷⁰. The double displacement mechanism on XETs is supported by different observations as it was presented in the introduction (p. 27)⁷⁹⁻⁸².

Some time later, Farkas and coworkers⁵² analyzed the kinetics of nasturtium seed *XTH* obtained with xyloglucan as donor and radiolabeled ³H-XGOs acceptors by fitting the data to modified ping pong *bi bi* kinetic models. They tried to adjust some variant of ping pong models (donor or acceptor or both acting as competitive inhibitors) and they concluded that the best model explaining the experimental data was a “modified ping-pong mechanism with oligosaccharides acting as dead-end inhibitors and with two alternative fates for the glycosyl-enzyme intermediate: either hydrolysis or transglycosylation” (Scheme 18).



Scheme 18: Schematic representation of a bi-bi ping pong mechanism with XG oligosaccharides acting as competitive inhibitor with respect to xyloglucan and presenting a branching point due to XG hydrolysis.

All previous attempts to obtain kinetic constants provided apparent kinetic parameters and failed to find an ideal model because of the molecular heterogeneity of the xyloglucan donor, the multiple turnovers taking place with the polymeric XG substrate, and the undetectable transfer reactions to other XG-polymer molecules as acceptor. For that reason, one of the objectives of the present work is to **characterize kinetically the *Ptt*-XET16A** enzyme with XXXGXXXG as donor and XXXGANTS as acceptor, evaluating the reaction presented in Scheme 19 to establish the kinetic mechanism using the developed HPCE assay.



Scheme 19: Scheme for transglycosylation reaction between the tetradecasaccharide donor 23 and the heptasaccharide labeled acceptor 25, showing the first transglycosylation product.

5.2.- Steady state kinetics.

Steady state kinetics on *Ptt*-XET16A varying both donor **23** (0.2 – 5 mM) and acceptor **25** (0.5 – 10 mM) concentrations were performed at pH 5.5 and 30°C. As example, initial rates varying acceptor **25** concentration at 1mM donor **23** are presented in Figure 51.

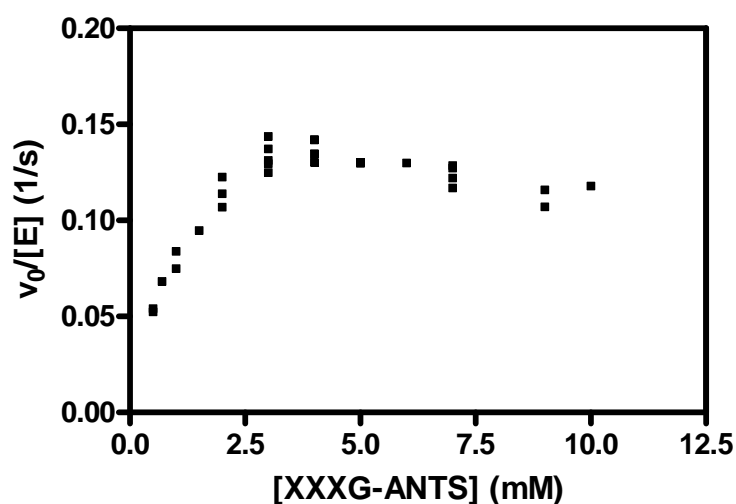


Figure 51: Initial rates obtained at 1 mM XXXGXXXG varying acceptor concentrations.

Full set of initial rates was analyzed according to different variants of ping pong mechanisms^{52,171} (Table 5), where AB is the donor, C is the acceptor, and AC is the labeled transglycosylation product.

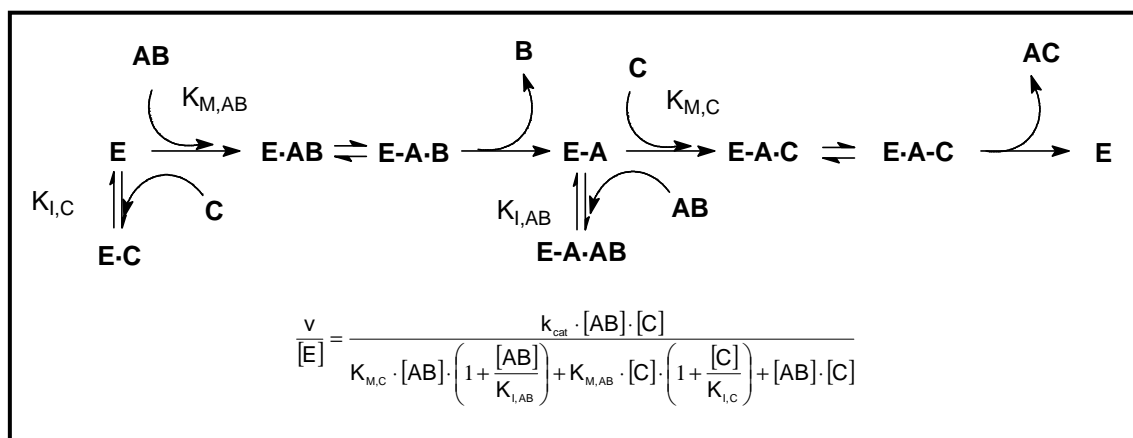
ID	Equation	Results	Eq. ref.
(a)	$\frac{v}{[E]} = \frac{k_{cat} \cdot [AB] \cdot [C]}{K_{MC} \cdot [AB] + K_{MAB} \cdot [C] + [AB] \cdot [C]}$	R = 0,806 R ² = 0,649	171
(b)	$\frac{v}{[E]} = \frac{k_{cat} \cdot [AB] \cdot [C]}{K_{MC} \cdot [AB] + K_{MAB} \cdot [C] + [AB] \cdot [C] + K_{IAB} \cdot K_{MC}}$	Converge to eq. (a)	171
(c)	$\frac{v}{[E]} = \frac{k_{cat} \cdot [AB] \cdot [C]}{K_{MC} \cdot [AB] + K_{MAB} \cdot [C] + [AB] \cdot [C] + K_{IAB} \cdot K_{MAB}}$	Converge to eq. (a)	52
(d)	$\frac{v}{[E]} = \frac{k_{cat} \cdot [AB] \cdot [C]}{K_{MC} \cdot [AB] + K_{MAB} \cdot [C] \cdot \left(1 + \frac{[C]}{K_{IC}}\right) + [AB] \cdot [C]}$	No converge	171
(e)	$\frac{v}{[E]} = \frac{k_{cat} \cdot [AB] \cdot [C]}{K_{MC} \cdot [AB] \cdot \left(1 + \frac{[AB]}{K_{IAB}}\right) + K_{MAB} \cdot [C] + [AB] \cdot [C]}$	R = 0,906 R ² = 0,821	171
(f)	$\frac{v}{[E]} = \frac{k_{cat} \cdot [AB] \cdot [C]}{K_{MC} \cdot [AB] \cdot \left(1 + \frac{[AB]}{K_{IAB}}\right) + K_{MAB} \cdot [C] \cdot \left(1 + \frac{[C]}{K_{IC}}\right) + [AB] \cdot [C]}$	R = 0,9682 R ² = 0,937	171
(g)	$\frac{v}{[E]} = \frac{k_{cat} \cdot [AB] \cdot [C]}{K_1 + K_2 \cdot [C] + K_3 \cdot [C]^2 + K_4 \cdot [AB] + [AB] \cdot [C]}$	No converge	52
(h)	$\frac{v}{[E]} = \frac{k_{cat} \cdot [AB] \cdot [C]}{K_{MC} \cdot \left(1 + \frac{K'_{MAB}}{K_{MABa}}\right) \cdot [AB] + \frac{K_{MC}}{K_{MABa}} \cdot [AB]^2 + K_{MABd} \cdot [C] + [AB] \cdot [C]}$	Converge to eq. (e)	171
(i)	$\frac{v}{[E]} = \frac{k_{cat} \cdot [AB] \cdot [C]}{K_{MC} \cdot \left(1 + \frac{K'_{MAB}}{K_{MABa}}\right) \cdot [AB] + \frac{K_{MC}}{K_{MABa}} \cdot [AB]^2 + K_{MABd} \cdot \left(1 + \frac{[C]}{K_{IC}}\right) \cdot [C] + [AB] \cdot [C]}$	No convergence	Deduced in this study
(j)	$\frac{v}{[E]} = \frac{k_{cat} \cdot [AB] \cdot [C]}{K_{MC} \cdot \left(1 + \frac{K'_{MAB}}{K_{MABa}}\right) \cdot [AB] + \frac{K_{MC}}{K_{MABa}} \cdot [AB]^2 + K_{MABd} \cdot \left(1 + \frac{[C]}{K_{IC}}\right) \cdot [C] + \left(1 + \frac{K'_{MAB} \cdot K_{MC}}{K_{MABa} \cdot K_{IC}}\right) \cdot [AB] \cdot [C]}$	No convergence	Deduced in this study

- Ping Pong bi bi system.
- Ordered bi bi system.
- Sequential ordered system.
- Ping Pong bi bi system where C is competitive inhibitor of AB.
- Ping Pong bi bi system where AB is competitive inhibitor of C.
- Ping Pong bi bi system where AB is competitive inhibitor of C and C is competitive inhibitor of AB.
- Ping Pong bi bi system where C is competitive inhibitor of AB and with a hydrolysis branching point.
- Ping Pong bi bi system where AB is acting as alternative substrate to C.
- Ping Pong bi bi system where AB is acting as alternative substrate to C and C is acting as competitive inhibitor for AB (version 1).
- Ping Pong bi bi system where AB is acting as alternative substrate to C and C is acting as competitive inhibitor for AB (version 2).

Table 5: Kinetic models and results when fitting the experimental data.

AB is the donor XXXGXXXG (23) and C is the acceptor XXXGANTS (25).

Best results were obtained when fitting the data to equation f in Table 5. This equation describes a ping pong *bi bi* mechanism with competitive inhibition by the labeled acceptor binding to the free enzyme, and inhibition by the donor binding on the acceptor subsites of the glycosyl-enzyme intermediate (Scheme 20):



Scheme 20: Proposed kinetic mechanism for the reaction of *Ptt*-XET16A. AB: donor substrate, C: acceptor substrate, AC: labeled transglycosylation product, and equation describing this mechanism (equation f in Table 5).

Figure 52 and Figure 53 present selected kinetic data varying one substrate concentration at fixed concentrations of the other substrate together with fitted model curves. Both figures contain the same experimental data but presented versus each substrate (donor or acceptor) concentrations. Lines represent overall-data-fitted-model (equation f from Table 5) for selected substrate concentrations. Although some variability in data was detected due to experimental deviations, a good fit is obtained rendering the following kinetic parameters: $k_{\text{cat}} = 0.45 \pm 0.04 \text{ s}^{-1}$, $K_{M,AB} = 0.37 \pm 0.09 \text{ mM}$, $K_{M,C} = 1.9 \pm 0.3 \text{ mM}$, $K_{I,AB} = 1.0 \pm 0.1 \text{ mM}$, and $K_{I,C} = 1.5 \pm 0.4 \text{ mM}$.

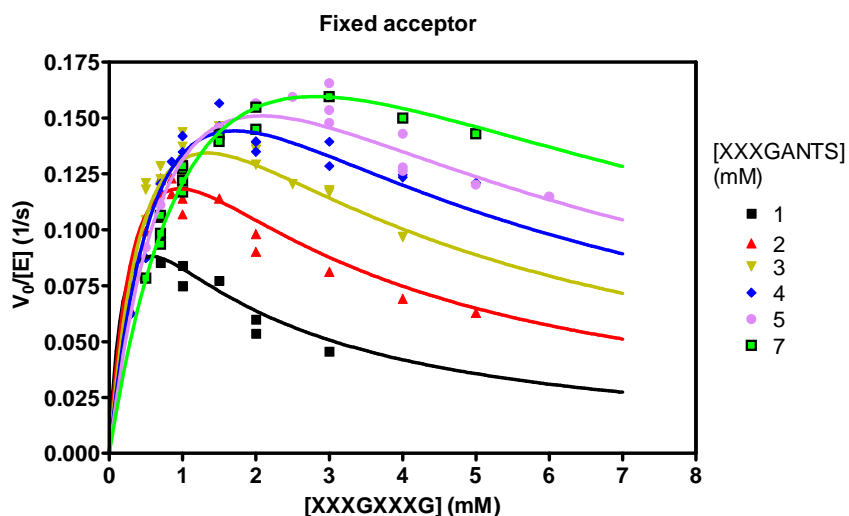


Figure 52: Kinetics (v_0 vs. [donor 23]) at different acceptor 25 concentrations (mM). Initial rates (v_0) were determined by the HPCE method at pH 5.5, 30°C. Plotted lines are the corresponding calculated curves obtained after fitting all kinetic data to equation **f in Table 5.**

Figure 52 shows high donor inhibition phenomena, the lower the acceptor concentration, the higher the donor inhibition. This is explained by the fitted model, where competitive binding of donor to acceptor subsites of glycosyl-enzyme intermediate renders a dead-end complex (Scheme 20).

This dead-end complex (E-A·AB) presented in fitted model (equation **f** in Table 5), may not be really a dead-end complex, because it is possible that the donor (AB) acts as acceptor rendering the non-labeled AAB transglycosylation product. Moreover, taking into account that some high DP labeled transglycosylation products were detected at longer reaction times such as XXXGXXXGXXXGANTS (AAC, **37**) and XXXGXXXGXXXGXXXGANTS (AAAC). Two equations describing a kinetic mechanism where the donor (AB) acts as alternative substrate to acceptor (C) were deduced in the present work (equations **i** and **j**, from Table 5), however it was not possible to adjust kinetic data to the proposed models.

Focusing on experimental data and fitted curves at low acceptor concentrations (1 mM (black) and 2 mM (red)) significant deviations from the model are observed. These deviations could be explained by an undetected donor polymerization reaction occurring when donor binds at acceptor subsites. This polymerization reaction may explain the unusually high inhibitory effect of the donor. Other indications that this reaction occurs is the observation of polymerization at high reaction evolution as presented before (Figure 45).

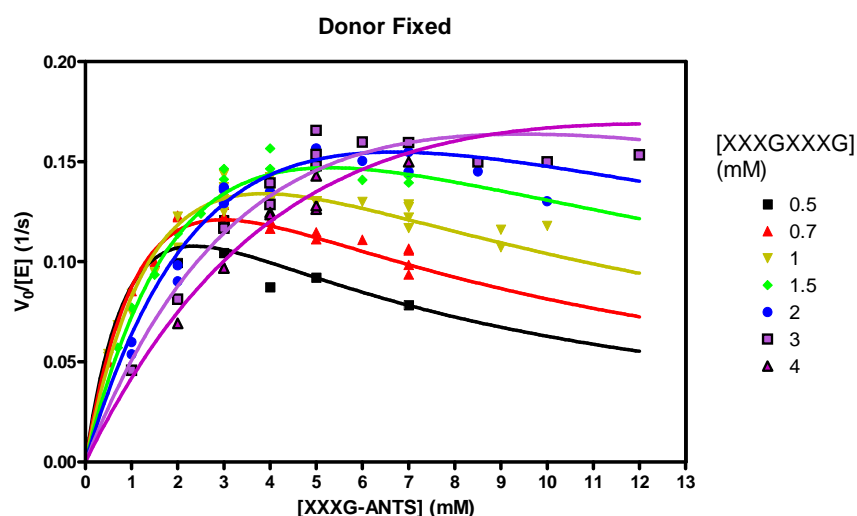


Figure 53: Kinetics (v_0 vs. [acceptor 25]) at different donor 23 concentrations (mM). Initial rates (v_0) were determined by the HPCE method at pH 5.5, 30°C. Plotted lines are the corresponding calculated curves obtained after fitting all kinetic data to equation f in Table 5.

In the complementary representation of experimental data and fitted curves to the model (Figure 53), competitive inhibition of acceptor for donor subsites could be observed.

Reciprocal plots are presented in Figure 54. In contrast to normal ping pong *bi bi* systems where for $1/v_0$ versus $1/[\text{substrate}]$ produces a series of parallel lines at different fixed concentrations of the other substrate, the proposed model shows strong inhibition at high donor and acceptor concentrations.

For the adjusted model, each curve at a fixed concentration of one substrate presents a minimum which moves closer to the $1/v_0$ axis as higher is the concentration of the fixed substrate (as the fixed substrate overcomes the inhibition by the varied substrate) and the slope of the reciprocal plot increases (as the fixed substrate introduces its own inhibitory effect) as it was expected for the adjusted model¹⁷¹.

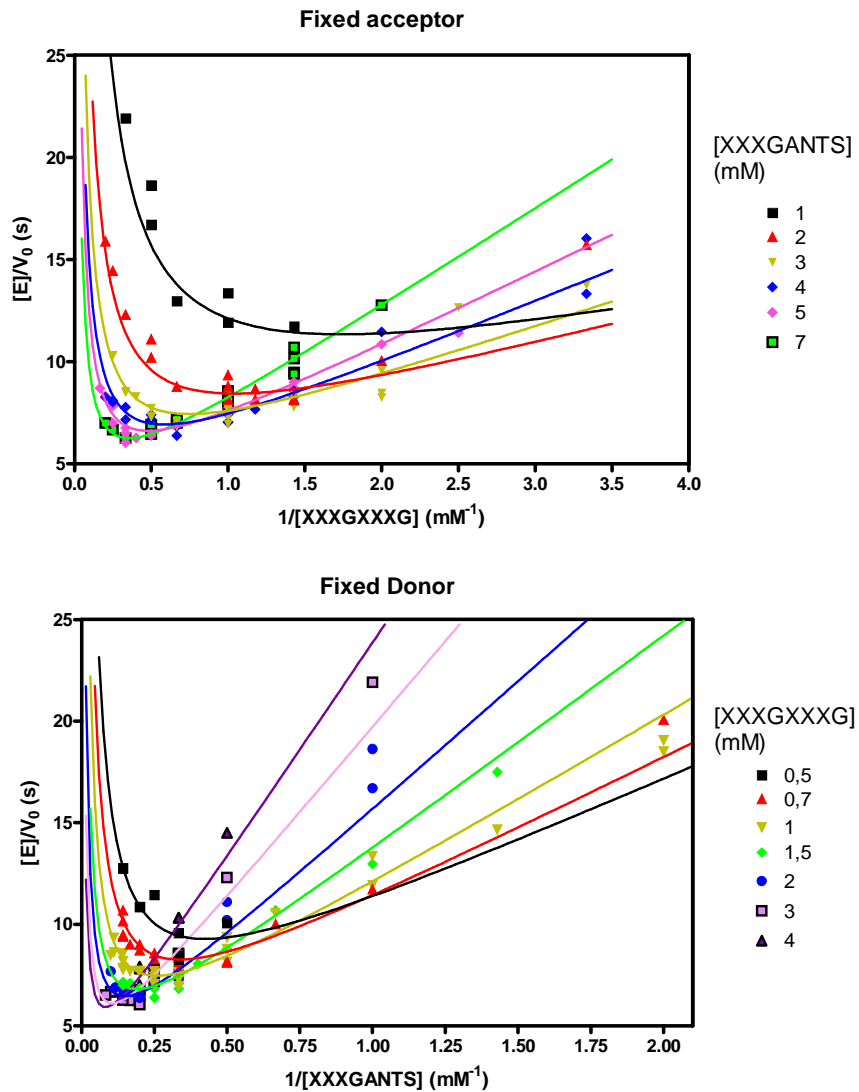


Figure 54: Double reciprocals plot for kinetics of *Ptt*-XET16A using compounds 23 and 25 as donor and acceptor, respectively, concentrations are expressed in mM. Reactions were performed in citrate/phosphate buffer pH 5.5, 30°C, and initial rates determined by the HPCE method.

This fitted model is similar to which Farkas and co-workers proposed for the nasturtium enzyme⁵², except that in the model in our work, donor inhibition is included and hydrolysis of the glycosyl-enzyme intermediate is omitted. Another model considering donor polymerization was deduced in this study (Table 5 equation **i** and **j**) but it was too complex to be adjusted to the experimental data.

This is the first study that allowed obtaining kinetic parameters of a donor different from XG polymer, having a fixed and defined structure. However, donor self-transglycosylation or product polymerization seems to provoke deviations from the fitted model at low acceptor concentration.

To prevent this putative side reaction and to obtain a simpler kinetic mechanism with improved fit to the experimental data, a donor unable polymerize (acting as acceptor) would be desirable. The concept is to use a “blocked” donor in which to 4-OH at the non-reducing end has a different configuration or it is substituted with a protecting group to avoid that the donor acts as acceptor.

5.3.- Steady state kinetic parameters using a blocked donor.

5.3.1.- Background.

In order to obtain this “blocked” donor to prevent the observed side reactions where donor or transglycosylation product act as acceptor, we have designed the blocked substrate GalGXXXGXXXG (**38**) presented in Figure 55. This substrate, derived from XXXGXXXG (**23**), has a galactosyl group in the non reducing end instead of a glucosyl unit. It will prevent donor polymerization because its 4-OH (axial) has the opposite configuration than 4-OH of glucose (equatorial), and therefore it is not correctly positioned to attack the glycosyl-enzyme intermediate.

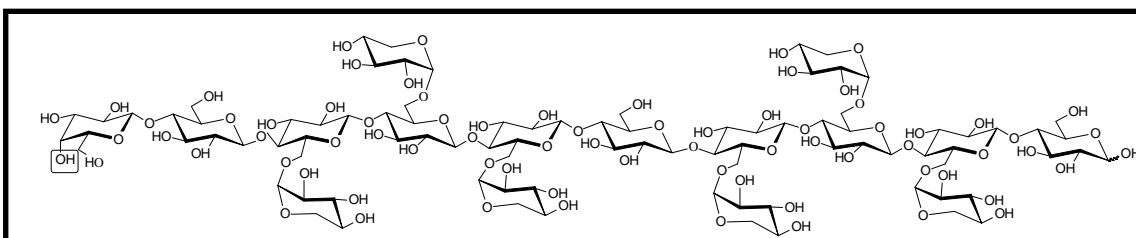
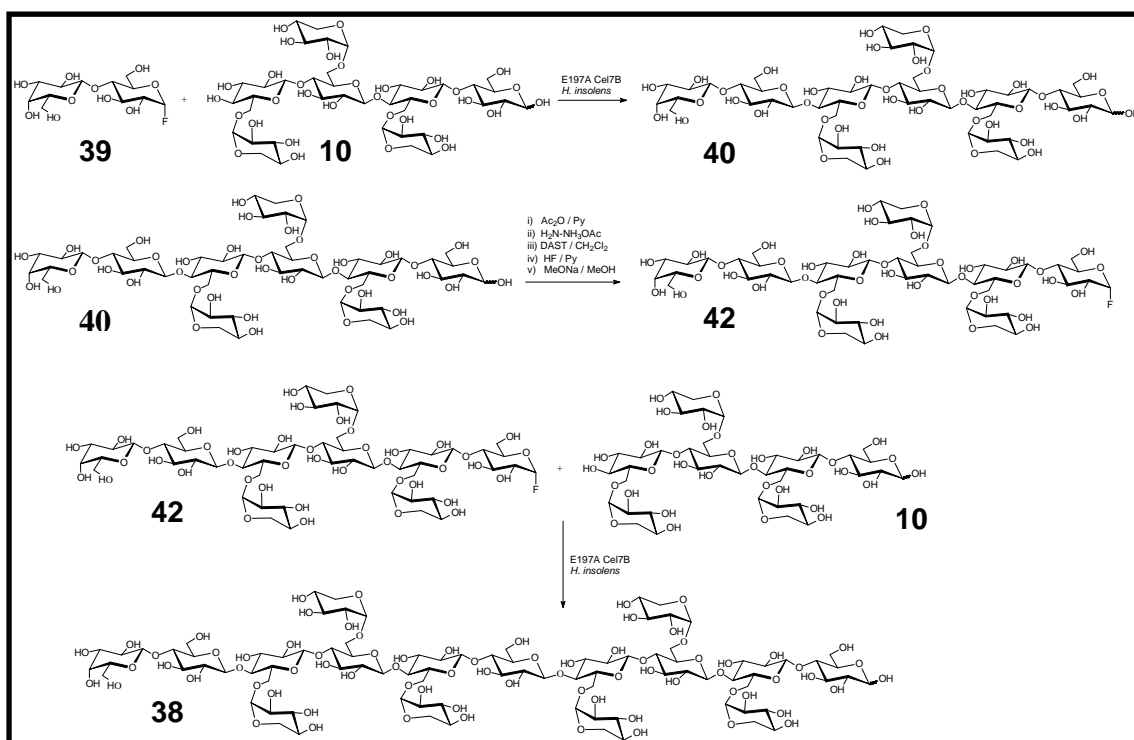


Figure 55: Structure of GalGXXXGXXXG (38), framed the 4-OH of the Gal unit.

The same concept had been applied previously in our and other groups in glycosynthase-catalyzed transglycosylation, demonstrating that a Gal unit on the non-reducing end on substrates for 1,3-1,4- β -glucanase¹⁶³ or for cellulases^{149,150} preventing donor self condensation and polymerization reactions.

5.3.2.- GalGXXXGXXXG (38) synthesis.

The GalGXXXGXXXG (38) substrate was synthesized by Régis Fauré at CERMAV-CNRS (EDEN partner). It was synthesized in two steps by the glycosynthase methodology^{149,150}. First glycosylation was carried out between GalGlc α F (39) and XXXG (10) by the Cel7B E197A from *H. insolens* to render GalGXXXG (40) (Scheme 21). GalGXXXG (40) was per-O-acetylated, purified and activated again as α -fluoride by: standard hydrazine acetate treatment, DAST fluorination and HF/Py anomerization of the fluoride. Finally, de-O-acetylation rendered the donor substrate GalGXXXG α F (42) for the next step. Second condensation between GalGXXXG α F (42) and XXXG (10) was catalyzed again by the Cel7B E197A from *H. insolens* obtaining the blocked *Ptt*-XET16A donor substrate 38.



Scheme 21: Synthetic route to obtain GalGXXXGXXXG (38).

5.3.3.- *Ptt*-XET16A reaction monitoring and product identification with GalGXXXGXXXG as blocked donor.

Ptt-XET16A-catalyzed reaction monitoring using GalGXXXGXXXG (**38**) and XXXGXXXG (**23**) as donors showed different reaction profiles (Figure 56).

For compound **23** different reaction products (polymerization) are formed from the beginning (Figure 56A).

In contrast, for compound **38** no polymerization products were detected at initial reaction times demonstrating that the GalG group is effective in blocking donor (Figure 56B). Only at longer reaction times ($t > 30$ min) when conversion is higher than 70%, and first product (GalGXXXGXXXGANTS (**44**)) is accumulated, other products appeared and were identified (by co-injection with ANTS labeled standards)⁽⁵⁾ as GalGXXXG-ANTS (**43**), XXXGXXXG-ANTS (**31**), and some polymerization products of XXXGXXXG (**23**) (Figure 57).

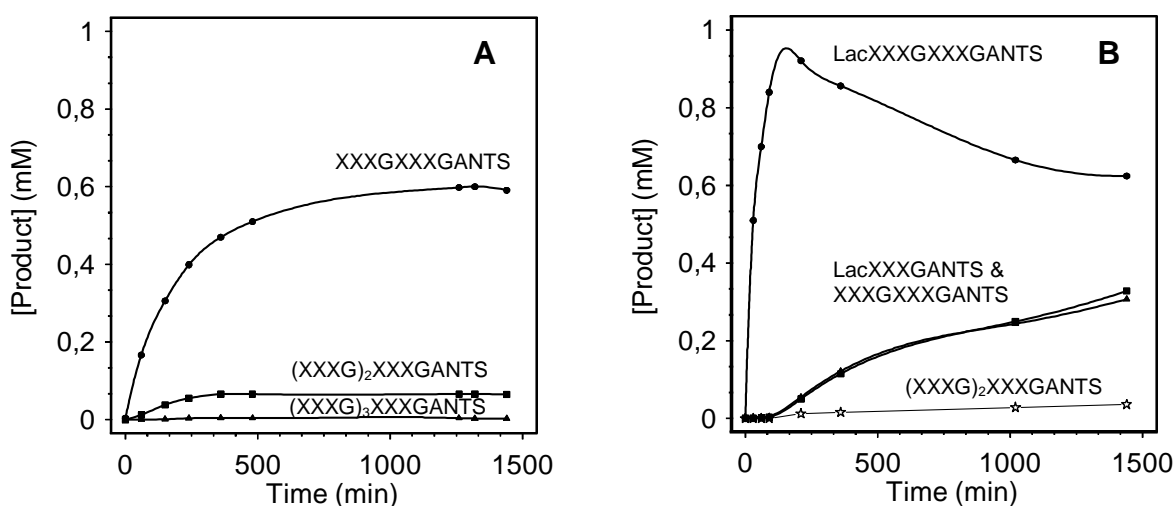


Figure 56: Product evolution for *Ptt*-XET16A catalyzed reaction using 1 mM XXXGXXXG(23**), 5 mM XXXGANTS(**25**) and 6.2 μM *Ptt*-XET16A (A) or 1 mM GalGXXXGXXXG(**38**), 5 mM XXXGANTS and 3 μM *Ptt*-XET16A (B).**

⁵ Synthesis of ANTS-labeled xyloglucan oligosaccharides as standards for product identification is described in chapter 4 (p.123).

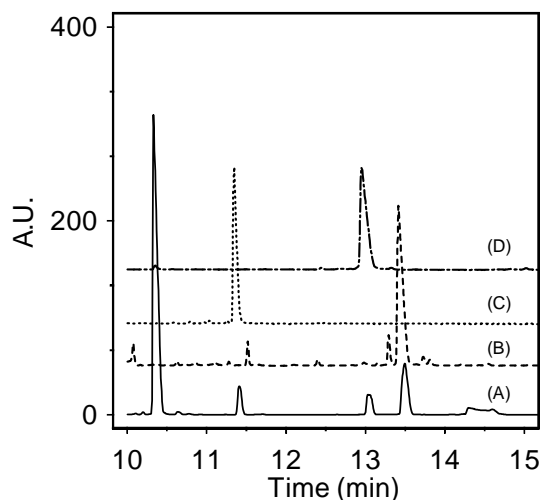
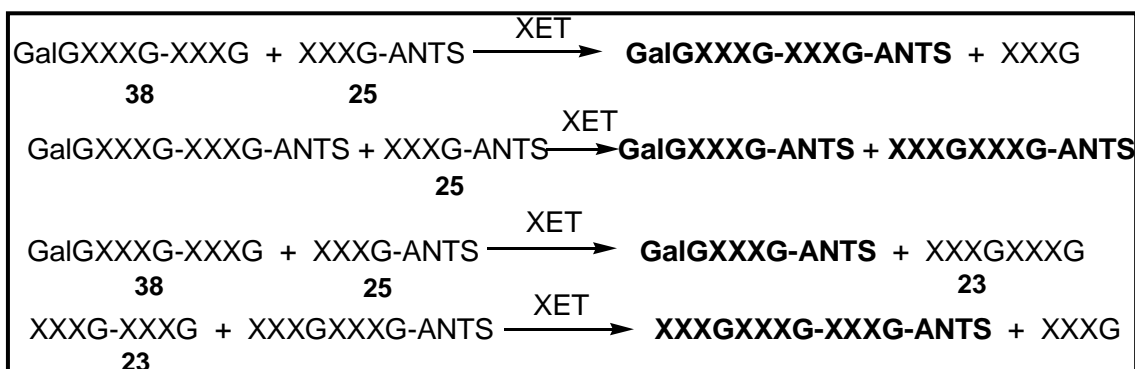


Figure 57: Electropherograms to identify transglycosylation products using GalGXXXGXXXG (38) as donor. (A) GalGXXXGXXXG (38) + XXXGANTS (25) after 24 h reaction. (B) GalGXXXGXXXGANTS (44) standard, (C) GalGXXXGANTS (31) standard, (D) XXXGXXXGANTS (31) standard.

These products could be produced due to the transfer of the GalG moiety from the GalGXXXGXXXG (38) or more probably from the accumulated GalGXXXGXXXGANTS to the acceptor XXXG-ANTS (25) to yield GalGXXXG-ANTS (43) and XXXGXXXG (23) (or XXXGXXXGANTS (31)) (Scheme 22). The latter acts as the original standard donor (XXXGXXXG (23)) giving polymerization products, as it is presented in Scheme 16.



Scheme 22: Possible pathways which could explain detection of different transglycosylation products observed in the *Ptt*-XET16A catalyzed reaction between GalGXXXGXXXG (38) and XXXGANTS (25). In bold the detected ANTS labeled products.

These experiments indicate that the GalGXXXGXXXG (**38**) donor avoids donor polymerization, although at long reaction times when GalGXXXGXXXGANTS is accumulated other reactions can occur. For that reason, the GalGXXXGXXXG (**38**) will be used to study the effects on kinetic parameters of proposed competing reactions (polymerization) when XXXGXXXG (**23**) was used as donor in the kinetic characterization of *Ptt*-XET16A.

5.3.4.- Steady state kinetic parameters of *Ptt*-XET16A using the blocked donor GalGXXXGXXXG (**38**).

Following the same methodology previously applied to XXXGXXXG (**23**), steady state kinetics varying donor **38** (0.5 - 7 mM) and acceptor **25** (0.3 - 7 mM) concentrations were performed in citrate phosphate buffer pH 5.5, I=0.5 M, and 30°C. As example, results obtained at 1 mM GalGXXXGXXXG (**38**) and different XXXG-ANTS (**25**) concentrations are presented in Figure 58. Initial rates for a 6x6 matrix of donor and acceptor concentrations were fitted to different ping-pong *bi-bi* models (Table 5, p. 97), using Sigma-Plot program. Best results were obtained by fitting experimental data to Equation 3 in Scheme 23 which describes a ping pong bi-bi system with acceptor substrate acting as competitive inhibition for donor substrate.

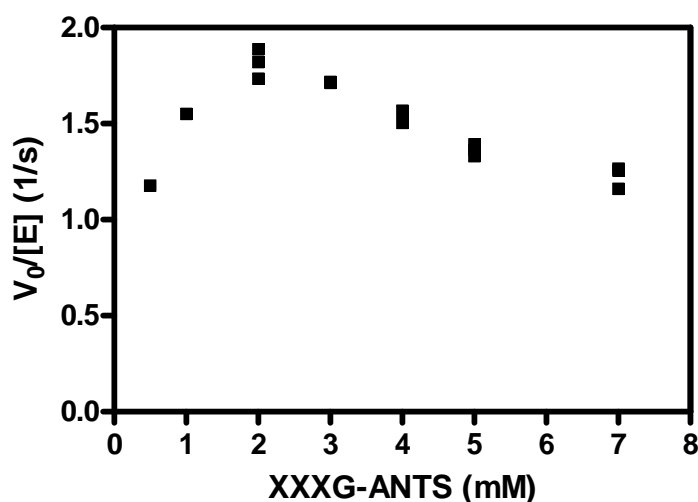
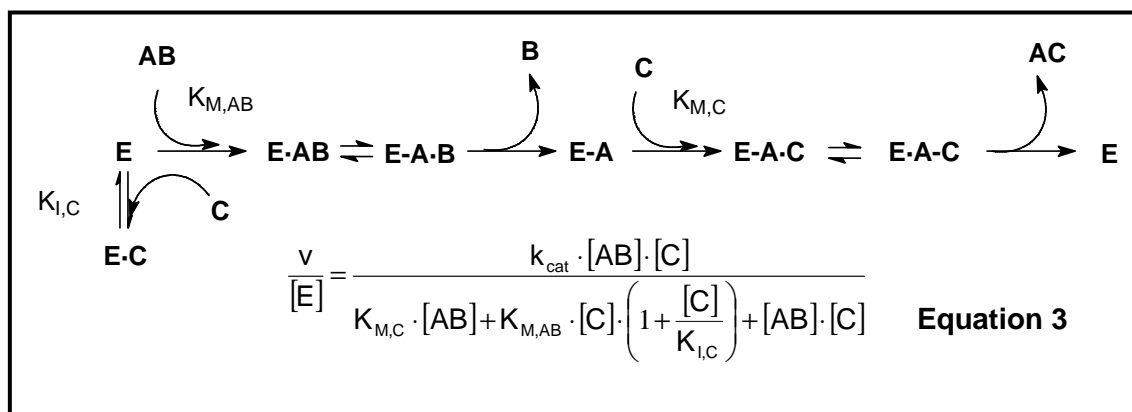


Figure 58: Initial rates obtained at 1 mM GalGXXXGXXXG (**38**) and different acceptor (**25**) concentrations.



Scheme 23: Proposed kinetic mechanism for the *Ptt*-XET16A reaction between GalGXXXGXXXG (38) and XXXG-ANTS (25). AB: donor substrate, C: acceptor substrate, and AC: labeled transglycosylation product. Equation describing the proposed mechanism (ping pong *bi-bi* mechanism with competitive inhibition for acceptor substrate). $K_{M,AB}$ is the K_M for the donor, $K_{M,C}$ is the K_M for the acceptor and $K_{I,C}$ is the inhibition constant for the acceptor.

Experimental initial rates (data points) and fitted model (lines) are presented in Figure 59 and Figure 60. A good fit ($R=0.990$, $R^2=0.981$) was obtained with the following kinetic parameters: $k_{\text{cat}}=4.8 \pm 0.3 \text{ s}^{-1}$, $K_{M,AB}=2.8 \pm 0.2 \text{ mM}$, $K_{M,C}=1.1 \pm 0.1 \text{ mM}$ and $K_{I,C}=1.7 \pm 0.2 \text{ mM}$. In the first representation (Figure 59) initial rates versus donor concentration are presented at different fixed acceptor concentrations. Comparing this representation with Figure 53 in which XXXGXXXG (23) was the donor substrate, it is clear that donor inhibition is suppressed in this case (Figure 59) at least in the concentration range studied. These results proof that GalGXXXGXXXG (38) efficiently avoids binding of donor to acceptor subsites (avoiding donor polymerization and/or donor inhibition).

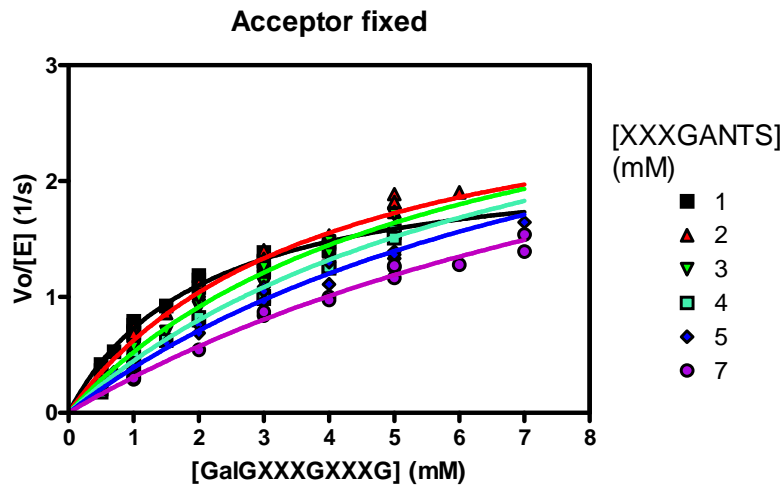


Figure 59: Graphical representation of experimental initial rates varying donor (38) concentration at different fixed acceptor (25) concentrations (points) and fitted model at these acceptor concentrations.

The same experimental data is shown in the second representation (Figure 60), where $v_o/[E]$ vs. $[XXXGANTS]$ (25) at different fixed $[GalGXXXGXXXG]$ (38) are presented. In this graph an evident acceptor inhibition was detected similar to that observed in Figure 53 using $XXXGXXXG$ (23) as donor. This inhibition is caused by binding of acceptor substrate to free enzyme competing with donor binding and rendering an inactive complex.

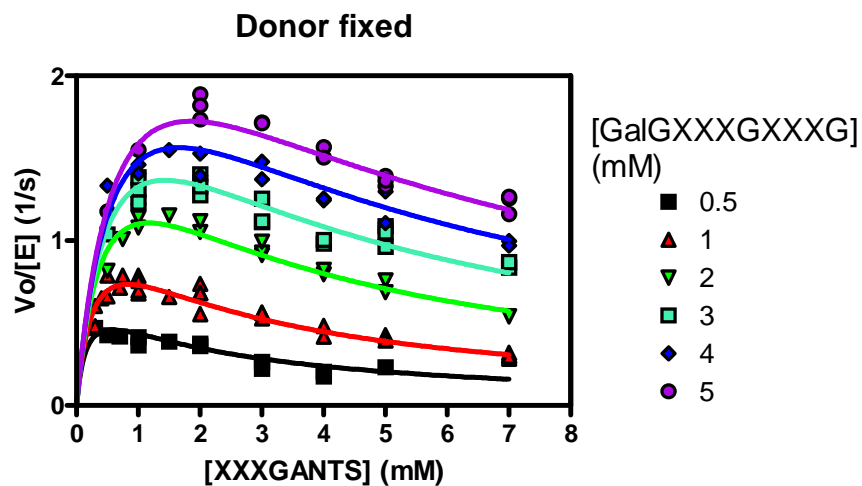


Figure 60: Graphical representation of experimental initial rates varying acceptor (25) concentration at different fixed donor (38) concentrations (points) and fitted model (lines) at these donor concentrations.

Reciprocal plot representations of experimental data points and adjusted models (Figure 61 and Figure 62) show the expected behavior for this model¹⁷¹.

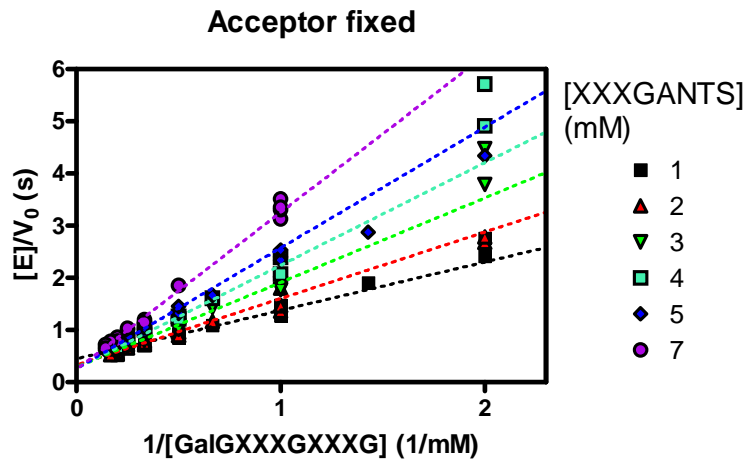


Figure 61: Reciprocal plot representation of experimental $1/v_0$ values versus $1/[\text{GalGXXXGXXXG}(38)]$ at different fixed acceptor (25) concentrations (points) and fitted model at these acceptor concentrations.

Complementary reciprocal plot $1/v$ versus $1/[\text{XXXGANTS}(25)]$ lines appear parallel at high $1/[\text{XXXGANTS}(25)]$ but pass through a minimum and go up when approaching the $1/v_0$ axis. As the $[\text{GalGXXXGXXXG}(38)]$ increases the position of the minimum moves closer to the $1/v_0$ axis and should disappear when $[\text{GalGXXXGXXXG}(38)]$ is saturating¹⁷¹.

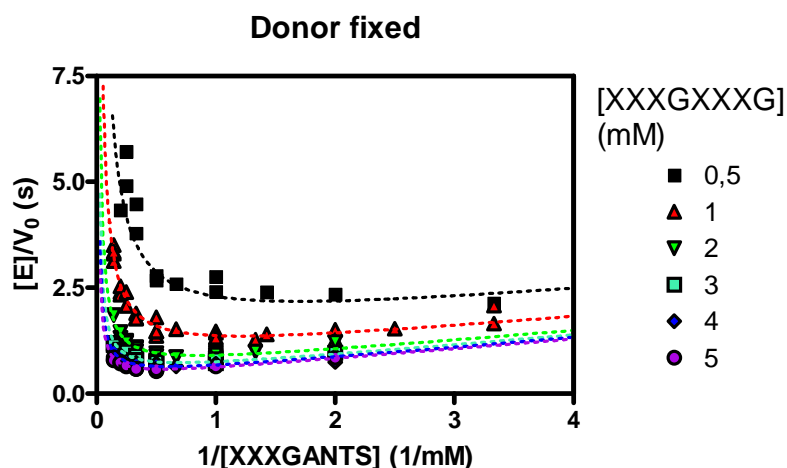


Figure 62: Reciprocal plot representation of experimental $1/v$ values versus $1/[\text{XXXGANTS}(25)]$ at different fixed donor (38) concentrations (points) and fitted model at these donor concentrations.

Comparison between kinetic parameters for XXXGXXXG and kinetic parameter for GalGXXXGXXXG is presented in the following table (Table 6).

Kinetic parameter	XXXGXXXG (23) + XXXGANTS (25)	GalGXXXGXXXG (38) + XXXGANTS (25)
k_{cat} (s^{-1})	0.45 ± 0.04	4.8 ± 0.3
$K_{\text{M,AB}}$ (mM)	0.37 ± 0.09	2.8 ± 0.2
$K_{\text{I,AB}}$ (mM)	1.0 ± 0.1	-----
$K_{\text{M,C}}$ (mM)	1.9 ± 0.3	1.1 ± 0.1
$K_{\text{I,C}}$ (mM)	1.5 ± 0.4	1.7 ± 0.2

Table 6: Comparison between kinetic parameter for steady state kinetic of *Ptt*-XET16A catalyzed reactions of XXXGXXXG (23**) + XXXG-ANTS (**25**) and GalGXXXGXXXG (**38**) + XXXG-ANTS (**25**).**

$K_{\text{M,C}}$ (Michaelis-Menten constant for the acceptor) using both donors XXXGXXXG (**23**) and GalGXXXGXXXG (**38**) are approximately equivalent, because in both experiments the same acceptor XXXG-ANTS (**25**) was used. Likewise, the inhibition constant for the acceptor binding in donor subsites ($K_{\text{I,C}}$) has the same value in both cases.

In the donor concentration range studied no donor inhibition was detected for GalGXXXGXXXG (**38**), as opposite to XXXGXXXG (**23**) (with a $K_{\text{I,AB}} = 1$ mM). This difference can indicate that most donor inhibition observed in XXXGXXXG (**23**) experiment was caused by self-transglycosylation or product polymerization. Once this was avoided using the blocked donor GalGXXXGXXXG (**38**) no donor inhibition was detected.

$K_{\text{M,AB}}$ values are significantly different between both donors. $K_{\text{M,AB}}$ for GalGXXXGXXXG (**38**) is higher than $K_{\text{M,AB}}$ for XXXGXXXG (**23**), what may indicates that *Ptt*-XET16A affinity for GalGXXXGXXXG (**38**) is lower than for XXXGXXXG (**23**).

The k_{cat} increase from XXXGXXXG (**23**) to GalGXXXGXXXG (**38**) demonstrates that k_{cat} for XXXGXXXG (**23**) is sub-estimated due to putative polymerization reactions.

The present work is the first XET kinetic characterization using low molecular weight donors where only a singly transglycosylation event can occur for each donor molecule. It was demonstrated the bi-bi ping-pong kinetic mechanism of XETs.

CHAPTER 4:
Donor screening and subsite mapping

CHAPTER 4: Donor screening and subsite mapping.

1.- Background.

Enzymes that bind oligomeric substrates have an extended binding site composed of subsites. One subsite is defined as the set of amino acid residues in the binding site that interact with one unit of the substrate.

As it was presented in the introduction, subsites are named using negative numbers starting from the catalytic machinery (the scissile glycosidic bond) to the non-reducing end, and with positive numbers starting from the scissile glycosidic bond to the reducing end^{102,103}. In our case, for XET, we use roman numbering for the glucosyl backbone and each xylosyl substitution is named with the same roman number assigned to the branched glucosyl unit with a prime superindex (Figure 63).

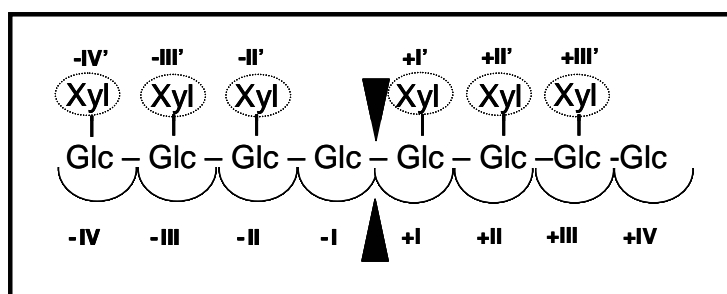


Figure 63: Subsite numbering in *Ptt*-XET16A for standard XXXGXXXG (23) substrate.

For *XTHs*, only some research groups have tried to obtain information about subsite mapping, their hypotheses and conclusion will be discussed in the following paragraphs.

Fanutti *et al.* have studied qualitatively the transglycosylation and hydrolytic activity of a XG endotransglycosylase / hydrolase from germinated nasturtium seeds with different isolated oligosaccharides (XXXGXXXG, XXXGXXLG + isomers, XXLGXXLG + isomers, XLLGXXLG + isomers, XLLGXLLG, GXXGXXXG and GLLGXLLG) and have proposed the substitution requirements at different positions of the donor molecule^{71,85}. Their conclusions are summarized as follows:

a) **At –I subsite it has been shown that a non-substituted Glc has to be present.**

b) GXXGXXXG underwent transglycosylation acting as donor and acceptor at the same time, the same is observed with GLLGXLLG. Therefore **xylosyl substitution was not necessary at -IV' subsite (when acting as donor) and +I subsite (when acting as acceptor)**.

c) With the donor GXXGG-XXGXXXG a hydrolytic cleavage of “-“ glycosidic bond to give GXXGG and XXGXXXG was observed, indicating that **xylosyl substitution at -II' subsite was not a requirement**. In contrast, no hydrolytical cleavage of GLLGG-LLGXLLG was observed, that was proposed as a clear indication that galactosyl-xylosyl substitution at +II prevent chain cleavage.

d) For subsites -III, +II and +III the conclusions they obtained were less clear. Taking into account the observation of transglycosylation with GXXG as acceptor, it could be concluded that **xylosyl substitution at +II' subsite and/or +III' subsite** are required. They had not obtained any direct evidence on which xylosyl substitution at +II and/or +III subsite is required, but taking into account molecular modeling studies which propose that XG polymer have an alternating conformation¹⁰⁴ (similar to the alternative flat “cellulosic” conformation), and the substitution requirements proposed before; Fanutti *et al.* hypothesized that **xylosyl substitution requirement at +III subsite seemed unlikely** (because xylosyl group at +III subsite would lie on the same side of the backbone as non-required xylosyl groups at -IV', -II', and +I' subsites), but xylosyl substitution at -III and +II subsites were proposed to be required (because they would lie on the same side of the backbone) (Figure 64).

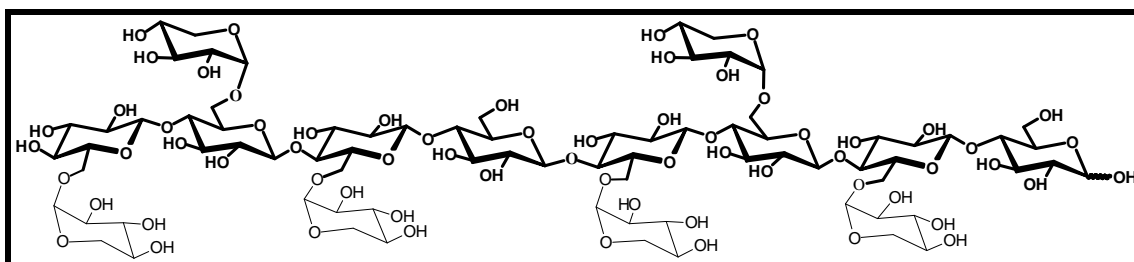


Figure 64: Schematic representation of structural requirements proposed by Fanutti and coworkers^{71,85}: In bold the glycosyl units proposed to be essential.

Other studies analyzed acceptor specificity: Fry *et al.*⁴¹ used a competitive assay to obtain I_{50} for different acceptors and they proposed XXG as simplest structural unit for a molecule to act as acceptor (**xylosyl substitution at +I and +II subsites are required**). The same minimal acceptor (XXG) was proposed by Fry and coworkers with cauliflower and mung bean *XTH*, although for one isoenzyme minimal activity was detected using the trisaccharide XG as acceptor⁹⁰. However higher activities were obtained using larger acceptors (XLLG>XXXG>XXG>XG).

Lorences *et al.*⁹⁵ tried to determine which of the xylosyl residues of XXG were required (xylosyl groups at +I and +II subsites) to act as acceptor. They evaluated GXG and XGG as possible acceptor but neither of them showed activity, concluding that **both xylosyl substitutions were required**. This result is somewhat limited due to the lack of mono-xylosyl-substituted material and seems to be inconsistent with qualitative results from Fanutti *et al.*⁸⁵ which indicate that xylosyl substitution at +I subsite was not required.

These are the first proposals of substitution requirement published up to now, although all conclusion were not totally proved and the analyses were qualitative. This will be the starting point for the quantitative and extensive subsite mapping for XET which is one of the objectives of the present work.

With the HPCE assay here developed, we are able to evaluate different donor substrates as putative XET donors. As shown in chapter 2 (p. 76) different putative donors were screened as possible new donors for *Ptt*-XET16A (XGGG (**18**), XGXGGG (**19**), XGXGXGGG (**20**), XXXGGG (**21**), XXXGXXXGGG (**22**), XXXGXXXG (**23**), XXXGXXXGXXXG (**24**)), finding the smallest donor ever found for XETs (XXXGGG (**21**)).

This chapter describes the design, synthesis and evaluation of a family of new XET donor substrates using the developed HPCE methodology with the objective of studying substrate specificity of *Ptt*-XET16A and obtaining a subsite map of the binding cleft.

2.- Donor library design.

A library of xyloglucan oligosaccharides (Figure 65 and Figure 66) was designed in collaboration with other members in the EDEN project to study substrate specificity of *Ptt*-XET16A. More concretely, our objective is to evaluate the contribution on binding and activity of each glycosyl unit in the standard substrate (XXXGXXXG (23)). This library allows us to study the donor specificity of xyloglucan endotransglycosylases, in this case XET16A from *Populus tremula x tremuloides* (*Ptt*-XET16A).

The putative donor substrates could be divided in two families to study separately the negative and positive subsites of the enzyme. In the first family (Figure 65, left), the group XXXG- was kept constant in the non reducing end part of the molecule and structures at the reducing part end were variable, to study the positive subsites of the enzyme. In the second family (Figure 65, right), the opposite idea was applied, the reducing end part was kept constant (-XXXG) and the non reducing end part was variable allowing the study of negative subsites. In both cases, the acceptor will be XXXGANTS (25).

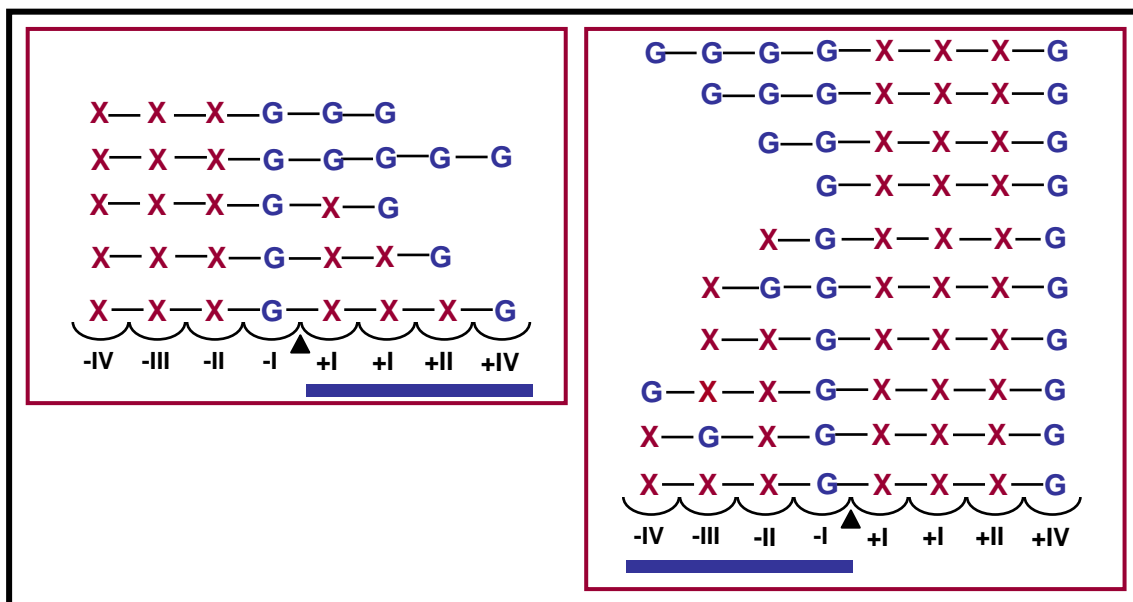
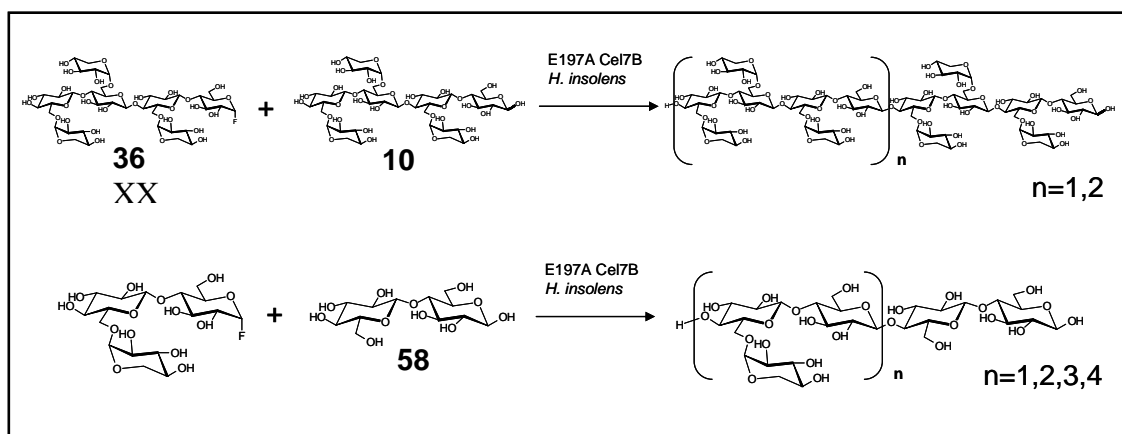


Figure 65: Schematic representation of proposed substrate library positioned in the subsites of binding cleft. On the left, family 1 designed to map positive subsites and on the right, family 2 designed to map negative subsites.

3.- Donor library synthesis⁽⁶⁾.

Substrates were synthesized by Régis Fauré at CERMAV-CNRS (EDEN partner) using the glycosynthase technology described before.

As reported in chapter 2 (p. 74), some drawbacks were detected when using the glycosynthase methodology. When the standard donor XXXGXXXG (**23**) was synthesized by glycosynthase transglycosylation between XXXG α F (**36**) and XXXG (**10**), using the E197A mutant of Cel7B from *Humicola insolens*, other condensation products were produced (polymerization) (Scheme 24, first). Higher is the variability of the transglycosylation products obtained from coupling between XG α F (**57**) and GG (**58**) (Scheme 24, second).

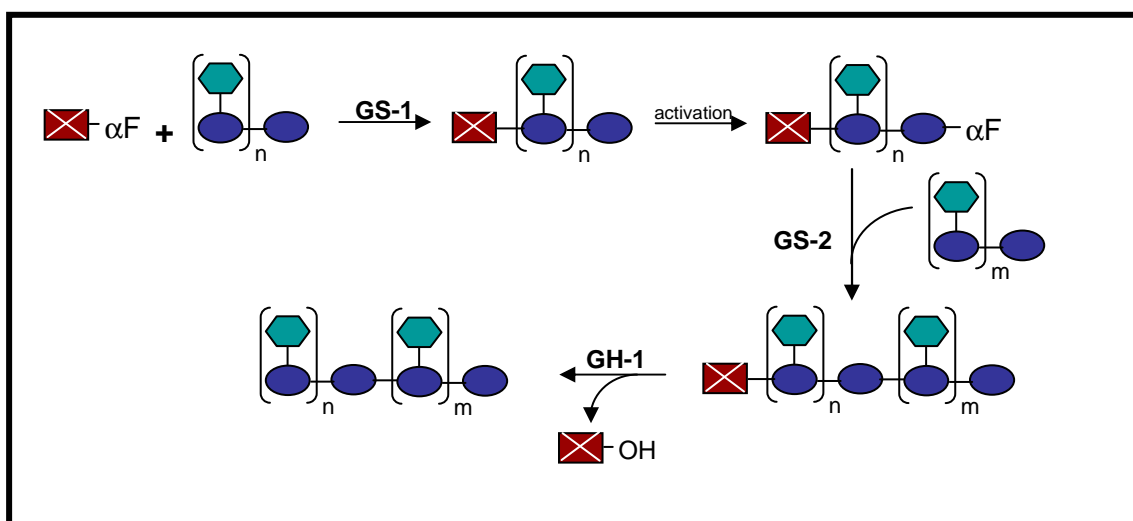


Scheme 24: Examples of coupling reactions using the E197A mutant of Cel7B form *Humicola insolens*.

The formation of different reaction products is caused by two different mechanisms: Donor polymerization and/or product elongation. This behavior is possible because donors have the same Glc conformation in the non reducing end as the acceptors.

⁶ This part of the Ph.D. is included in the article published in the Journal of Organic Chemistry with the title **Synthesis of a Library of Xylogluco-Oligosaccharides for Active-Site Mapping of Xyloglucan endo-Transglycosylase**, by Régis Fauré, Marc Saura-Valls, Harry Brumer III, Antoni Planas, Sylvain Cottaz, and Hugues Driguez¹⁷².

We have proposed a new methodology to avoid these possible competing reactions: the idea was to block the 4-OH position of the non reducing end glucose of the donor, as it was proposed in earlier studies of our group¹⁶³ and also it has been used in this study to obtain a blocked donor for *Ptt*-XET16A characterization. But we are not able to use a normal chemical protecting group with our substrates, at least with most of them due to their complex structures. For that reason, we have proposed the use of a glycosyl blocking group which could be added and removed using specific enzymatic steps (Scheme 25).



Scheme 25: Schematic representation of the proposed glycosynthase strategy using a blocking group (square) which will be added (GS-1 step) and removed (GH-1) using specific enzymes to obtain designed xyloglucan oligosaccharides.

This carbohydrate blocking group should have the 4-OH in the non reducing end with a configuration that will avoid it to act as acceptor again. Our first objective was to evaluate enzyme candidates for adding/removing different blocking oligosaccharides.

First proposal is to use a Gal- β -1,4-Glc (lactose)¹⁷³ group which could be added using the E197A Cel7B synthase from *Humicola insolens*^{149,150,163,174} and removed using specific glycosidases. This lactose group has an axial 4-OH in the non reducing end which will prevent donor self condensation (Figure 67). This strategy applied to XGOs has been evaluated at CERMAV-CNRS from Grenoble by Régis Fauré on XXXG (10), as objective molecule to be blocked.

The second proposal, based on the same idea, was to use the Gal- β -1,4-Glc- β -1,3-Glc group as blocking oligosaccharide which could be coupled using the glycosynthase (E134A mutant) derived from 1,3-1,4- β -glucanase from *Bacillus licheniformis*^{158,163} and removed using the wild type 1,3-1,4- β -glucanase (Figure 67). This proposal was evaluated in this work.

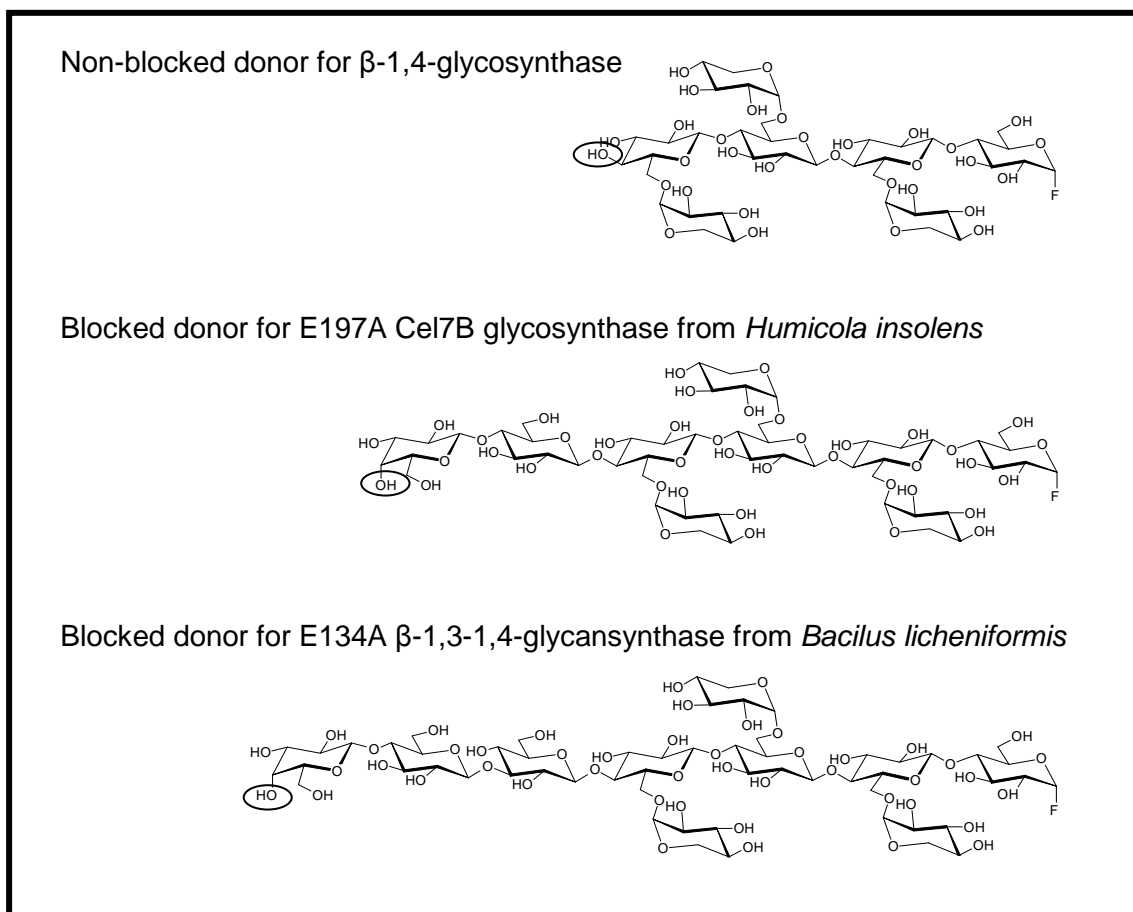
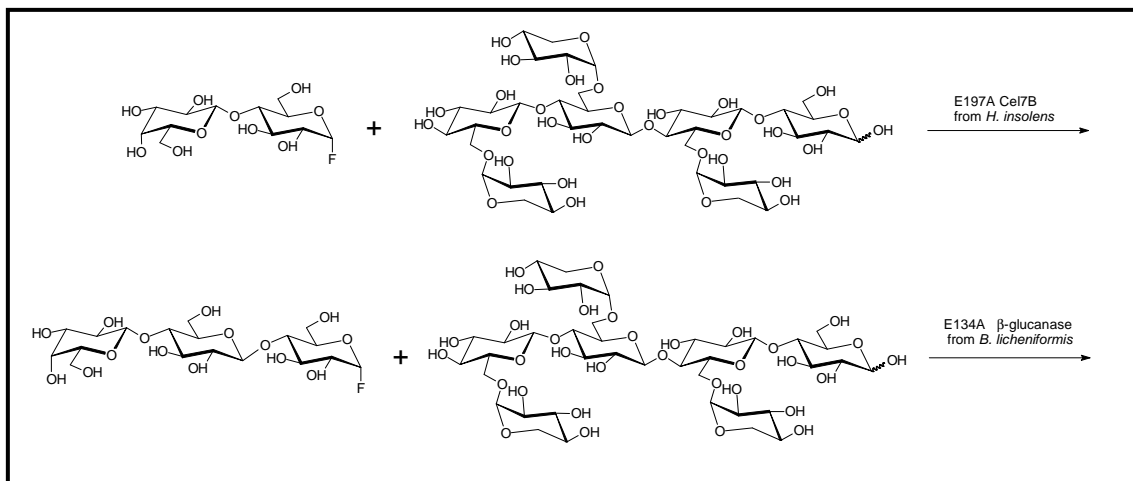


Figure 67: Comparison between examples of blocked and non blocked donors.

Both proposed glycosynthases (E197A Cel7B from *H. insolens* and E134A β -glucansynthase from *B. licheniformis*) were evaluated using the corresponding α -fluoride-oligosaccharidyl blocking groups (Gal4Glc α F and Gal4Glc3Glc α F) as putative XXXG (**10**) protecting tools (Scheme 26).

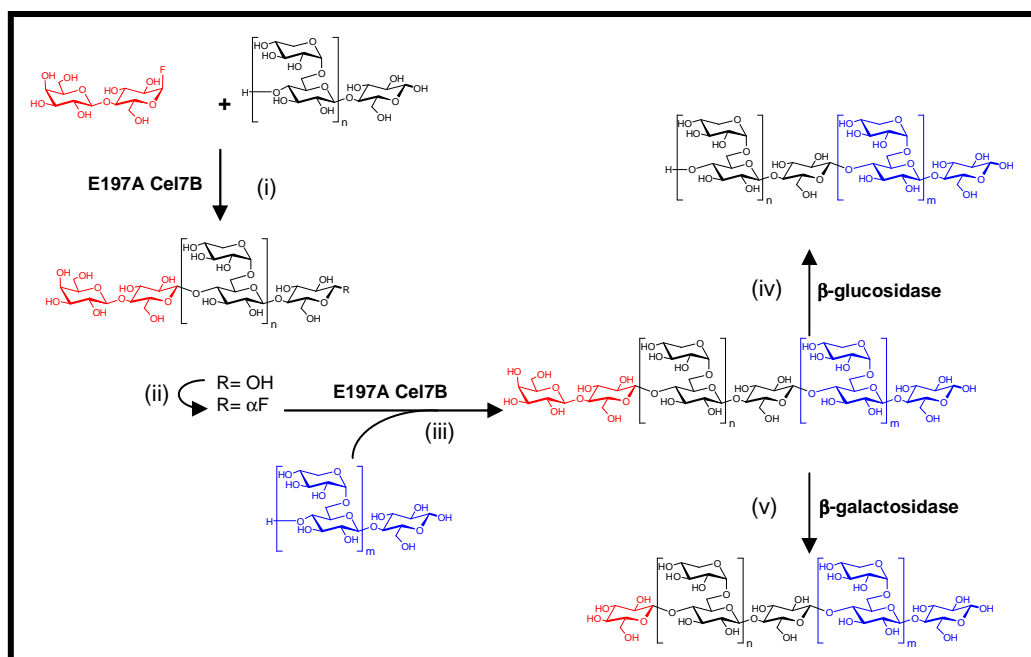


Scheme 26: Screened reactions to obtain blocked XXXG (10) substrates for glycosynthase catalysed reaction to obtain putative XET donors.

It has been demonstrated by TLC that the E197A Cel7B catalyzes blocking of XXXG (10) with the lactosyl group¹⁴⁶. It has also been demonstrated that the β -glucosidase from *Agrobacterium sp.*¹⁷⁵ gift from professor S.G. Withers, is able to nearly quantitatively hydrolyze the protection group Gal4Glc, rendering the unblocked oligosaccharide (XXXG (10)) without detecting any trace of supplementary hydrolysis. Moreover, it has been found that the commercial available β -galactosidase from *Aspergillus oryzae* is able to hydrolyze the terminal galactosyl group of GalGXXXG (40) rendering a substrate with a non-reducing-end-non-branched glucose (GXXXG (49)) unit by kinetically controlled de-galactosidation. Note that this reaction should be kinetically controlled because too much longer reaction times produce hydrolysis of terminal glucose unit

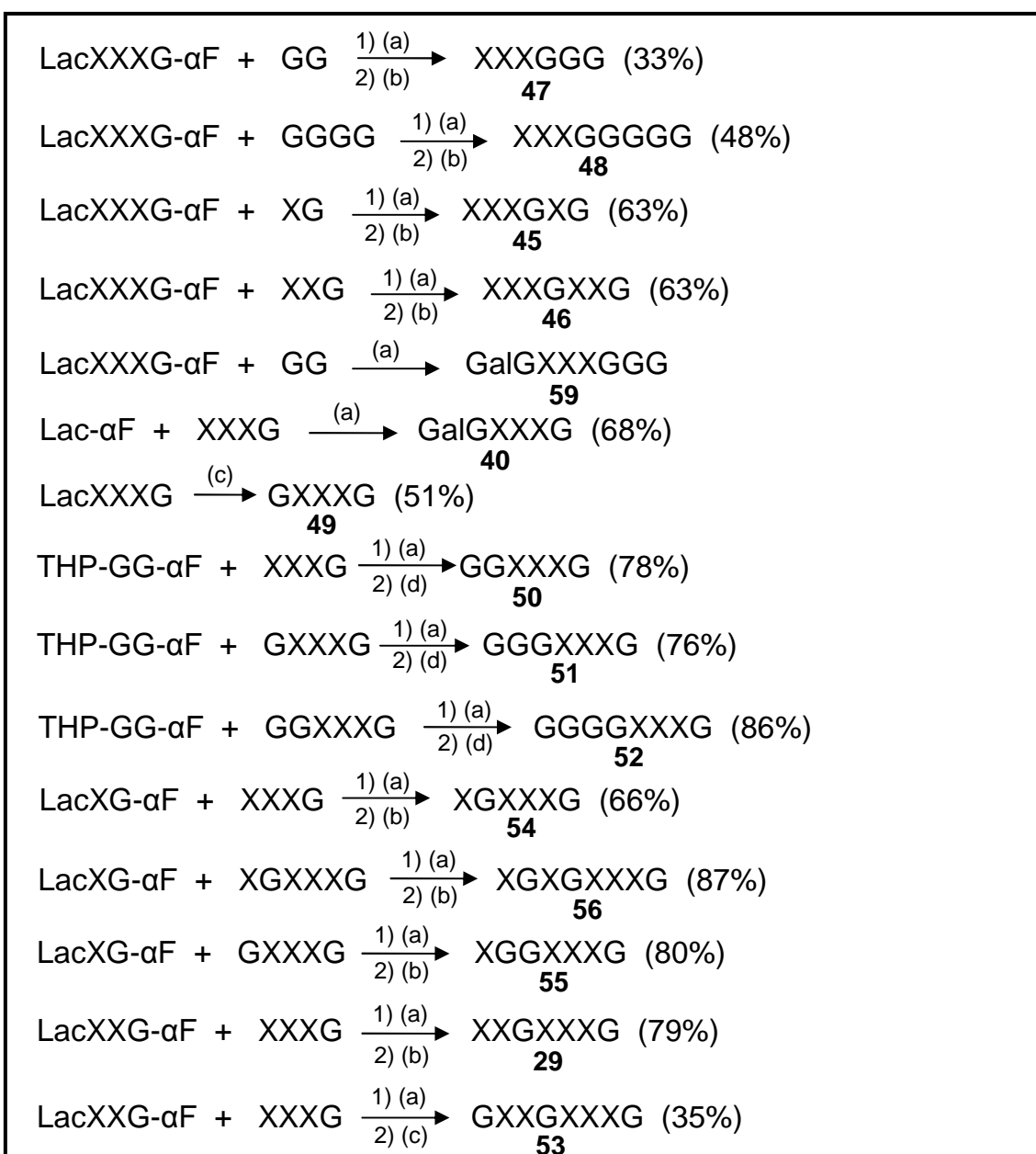
In contrast, in this work, no reaction was observed using the E134A 1,3-1,4- β -glucanase with Gal- β -1,4-Glc- β -1,3-Glc although this oligosaccharide has been demonstrated to be a donor substrate for this glycosynthase¹⁶⁴, the most probable explanation can be that the branched XGO substrate is not a acceptor for E134A 1,3-1,4- β -glucanase.

As conclusion, only E197A Cel7B has demonstrated to be a useful tool to enzymatically block 4-OH position on the non reducing end glucose unit in substrates such as XXXG (**10**), having two possible deblocking tools β -glucosidase from *Agrobacterium sp.* and β -galactosidase from *Aspergillus oryzae* (Scheme 27)^{146,172}.



Scheme 27: Reaction pathway for glycosynthase catalysed coupling: Blocking of donor precursor (i), activation of donor precursor (ii), glycosynthase coupling (iii) and two possible deblocking reactions (iv and v).

Scheme 28 compiles the list of reactions leading to the full set of XET donors obtaining notable high yields¹⁷². XXXGXXXG (**23**) and XXXGXXXGXXXG (**24**) were produced by glycosynthase coupling of XXXG α F (**36**) and XXXG (**10**) without a blocking group as it was described before in this work.



Scheme 28: Reaction pathways to synthesize XET-donor library using glycosynthase catalyzed coupling (a), followed by deblocking reaction using β -glucosidase from *Agrobacterium sp* (b), or α -galactosidase from *Aspergillus oryzae* (c) or acidic deprotection (HCl pH 1) (d).

4.- Donor concentration determination.

Putative XET donors were synthesized in mg scale. In some cases, they needed long purification protocols, causing the presence of some impurities, for example silica contamination. For that reason it was necessary to determine the stock concentration using a no-gravimetric methodology.

The XXXGXXXG (**23**) stock, produced in a gram scale, was extensively purified by gel filtration chromatography. Nominal XXXGXXXG (**23**) stock concentration was determined gravimetrically. After ANTS derivatization of a set of dilutions of XXXGXXXG (**23**), a standard curve (area *versus* concentration) was generated. Then, the actual concentration of each donor substrate was determined by HPCE prior ANTS derivatization by interpolation in this standard curve. It should be noted that the same standard curve (prepared with XXXGXXXG (**23**)) is used for all compounds since all ANTS-labeled oligosaccharides are expected to have the same response factor¹²², as it was demonstrated in this work for XXXG-ANTS (**25**) and XXXGXXXG-ANTS (**31**) (Chapter 2, p. 85).

5.- Synthesis of standard XGOs-ANTS compounds.

All synthetic compounds presented in Figure 66 were derivatized by reductive amination with ANTS to obtain the conjugated XGOs-ANTS. Reaction mixtures were not purified to remove the excess of ANTS since their purity was good enough to be used for qualitative HPCE analysis as reference compounds for product identification in enzymatic reactions.

Interestingly, migration times (t_m) in HPCE follows a linear relationship with $\log(\text{MW})$ as shown in Figure 68.

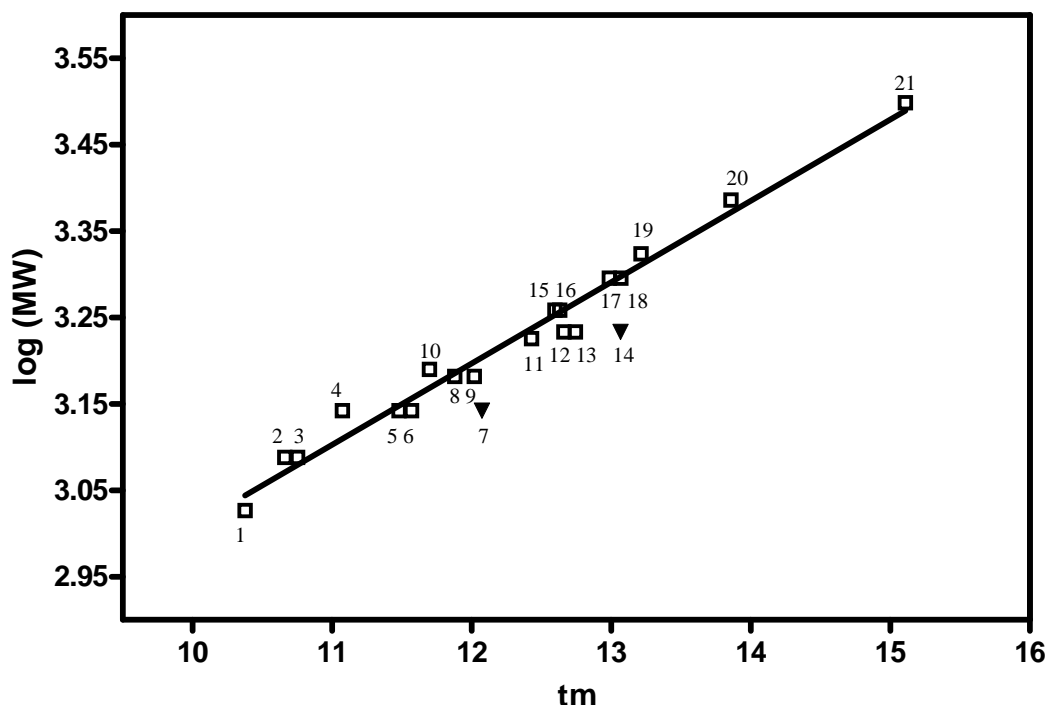
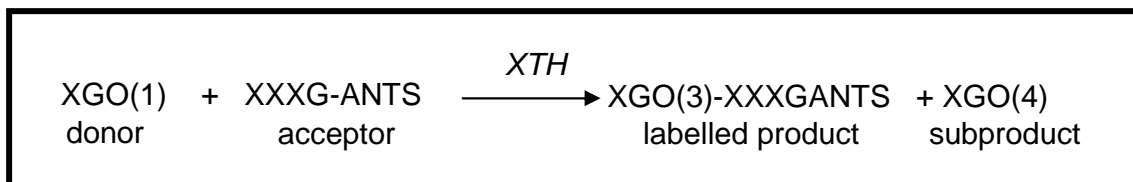


Figure 68: Linear relationship between $\log(\text{MW})$ of putative donor substrates and observed migration time obtained from HPCE electropherograms. 1-XXXG(10), 2-GXXXG(11), 3-XXLG or XLXG(12), 4-XLLG(13), 5-GalGXXXG(40), 6-GGXXXG(50), 7-XXXGGG(21), 8-XGXXXG(45), 9-XXXGXG(54), 10-GGGXXXG(51), 11-XGGXXXG(55), 12-GGGGXXXG(52), 13-GalGXXXGGG(59), 14-XXXGGGGG(48), 15-XXGXXXG(29), 16-XXXGXXG(46), 17-GXXGXXXG(53), 18-XGXGXXXG(56), 19-XXXGXXXG(23), 20-GalGXXXGXXXG(38), 21-XXXGXXXGXXXG(24).

6.- Donor screening.

Enzymatic reactions at 1 mM donor, 5 mM XXXG-ANTS (**25**) and 3 μ M *Ptt*-XET16A were monitored after 24 hours reaction to detect possible different patterns of reactivity of different donors and to identify ANTS-labeled products (Scheme 29).



Scheme 29: General transglycosylation reaction between donors from library and XXXGANTS (25) acceptor.

6.1.- Product identification.

In order to facilitate discussion, donors have been grouped taking into account their reaction behaviors.

Donors within the first family (donors that have invariable the non reducing end fragment (XXXG-)) could be divided in two subgroups depending on the number of transglycosylation products detected: donors which render a single transglycosylation product (XXXGGG (**21**), XXXGXG (**45**), XXXGGGGG (**48**)) and donors which render multiple transglycosylation products (XXXGXXG (**46**), XXXGXXXG (**23**), XXXGXXXGXXXG (**24**)).

Donor belonging to the second family (they have invariable the reducing end fragment (-XXXG)) showed more complicated reaction patterns. First subgroup includes donors with non-branched glucoses at negative subsites (GXXXG (**49**), GGXXXG (**50**), GGGXXXG (**51**), GGGGXXXG (**52**)). Second subgroup is formed by donors which have a terminal galactose unit (GalGXXXG (**40**), GalGXXXGGG (**59**) and GalGXXXGXXXG (**38**)). Third subgroup includes donors aimed to explore the xylosyl substitution requirements of *Ptt*-XET16A in negative subsites (XGXXXG (**54**), XGGXXXG (**55**), XXGXXXG (**29**), GXXGXXXG (**53**), and XGXGXXXG (**56**)).

6.1.1.- Family 1. Single transglycosylation product.

The first group of donors (XXXG-GG (**47**), XXXG-GGGG (**48**), and XXXG-XG (**45**)) showed similar behavior. The same single transglycosylation product was obtained for all of them and identified as XXXGXXXGANTS (**31**) by comparison with XXXGXXXGANTS (**31**) standard. For example, product identification for XXXGGGGG (**48**) + XXXGANTS (**25**) reaction is shown in Figure 69.

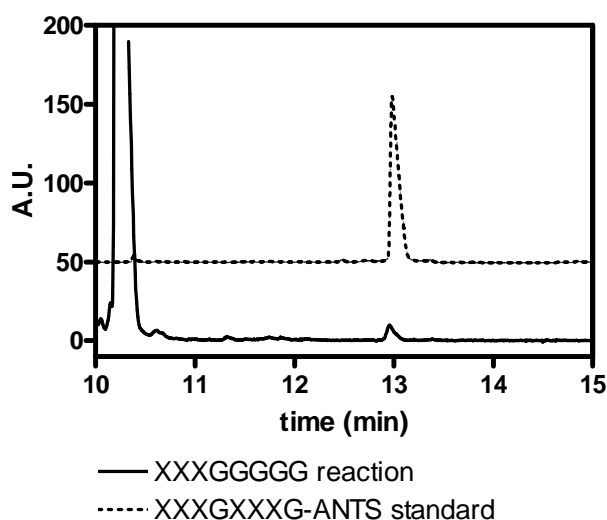
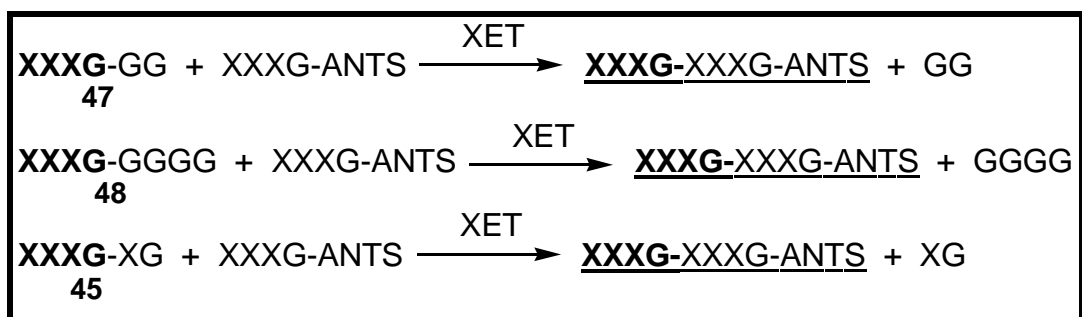


Figure 69: Electropherograms of XXXGXXXG-ANTS (**31**) standard and XXXGGGGG(**48**) + XXXG-ANTS (**25**) *Ptt*-XET16A catalyzed reaction.

The common transglycosylation product arises from transfer of the common non-reducing fragment XXXG- to the acceptor as it is shown in Scheme 30.



Scheme 30: Reaction pathways for XXXG-GG (**47**), XXXG-GGGG (**48**), and XXXG-XG (**45**) + XXXG-ANTS (**25**).

6.1.2.- Family 1. Multiple transglycosylation products.

The second subgroup within the first family is formed by XXXGXXG (**46**), XXXGXXXG (**23**) and XXXGXXXGXXXG (**24**). All of them yielded multiple transfer products with the same migration times (t_m), indicating that they are common for all donors within this group. Products were identified as XXXGXXXG-ANTS (**31**) and XXXGXXXGXXXG-ANTS (**37**) by co-injection with the corresponding standards (Figure 70).

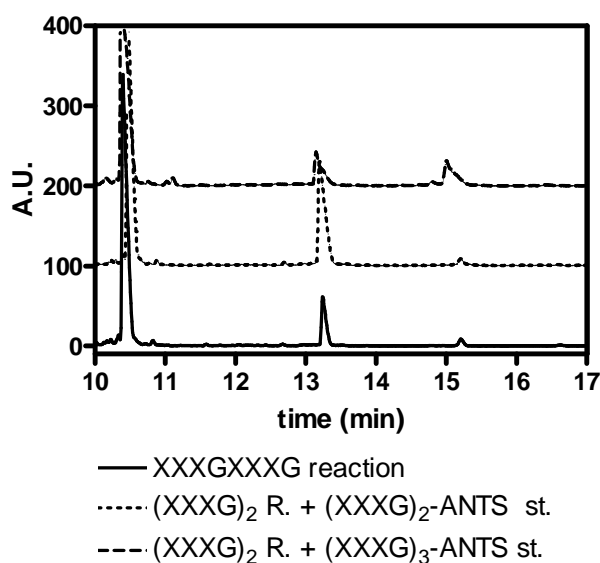
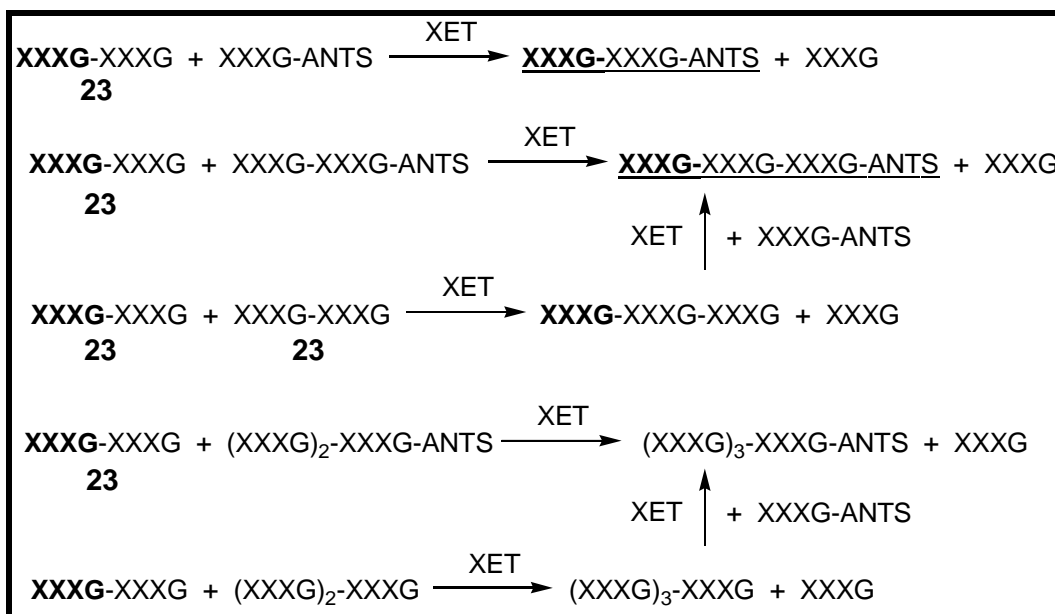


Figure 70: Electropherograms of coinjection of XXXGXXXGXXXG-ANTS (37**) standard and XXXGXXXG (**23**) + XXXG-ANTS (**25**) reaction (up), of coinjection of XXXGXXXG-ANTS and XXXGXXXG (**23**) + XXXG-ANTS (**25**) reaction (middle) and of *Pft*-XET16A catalysed reaction between XXXGXXXG (**23**) and XXXG-ANTS (**25**) (down).**

The major product for the three donors (**46**, **23**, and **24**) was XXXGXXXGANTS (**31**) which arises, in all cases, from transfer of the non-reducing end moiety XXXG- to the acceptor (Scheme 31). Higher oligomers were also obtained which arise from a second transglycosylation reaction in which the first product acts as acceptor, and/or donor self-transglycosylation reaction to render trimeric species that behave as donor substrate. As an example, reaction pathways for XXXGXXXG (**23**) are presented in Scheme 31 and similar behaviors can be proposed for XXXGXXG (**46**) and XXXGXXXGXXXG (**24**).

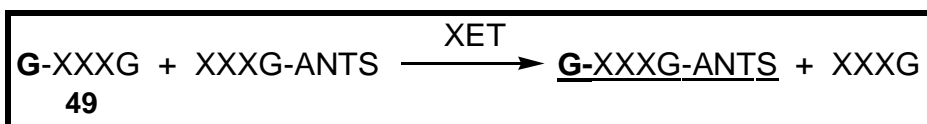
For XXXGXXXGXXXG (**23**) donor, a minor product was also observed at higher t_m , tentatively assigned at XXXGXXXGXXXGXXXGANTS, although we are not able to identify it due to the lack of adequate standards.



Scheme 31: Possible reaction pathways to explain identified transglycosylation products (**XXXGXXXGANTS** (31) and **XXXGXXXGXXXGANTS** (37)) and presumably, but not identified, transglycosylation product **XXXGXXXGXXXGXXXGANTS**. In bold, transferred fragment and underlined, identified products.

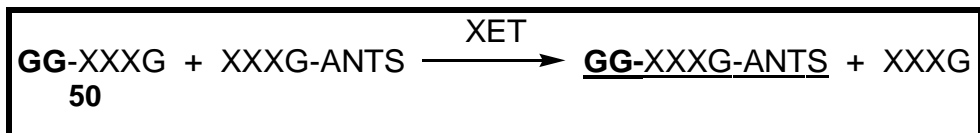
6.1.3.- Family 2. Donors with non branched Glc in negative subsites.

Compound GXXXG (**49**), GGXXXG (**50**), GGGXXXG (**51**), and GGGGXXXG (**52**) contain one to four non-xylosylated β -1,4-glucosyl units on the negative subsites. Compound GXXXG (**49**) is a poor donor, yielding only traces of transglycosylation product which was identified by t_m comparison as GXXXGANTS (Figure 71A). This product arises from a single transfer of the G- group from donor to acceptor (Scheme 32). GXXXG (**49**) is the smallest donor described so far.



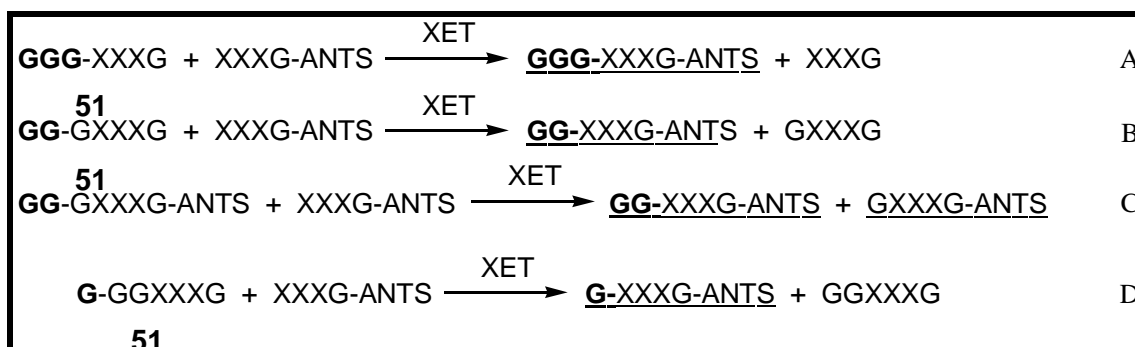
Scheme 32: Transglycosylation reaction between GXXXG (**49**) and XXXGANTS (**25**) catalyzed by *Ptt*-XET16A. The transferred fragment is presented in bold and the identified product, underlined.

For donors **50**, **51**, and **52** the reactivity is higher. For GGXXXG (**50**) a single product was detected and identified as GGXXXGANTS (Figure 71B), which is produced by direct transfer of the GG- moiety to the acceptor (Scheme 33).



Scheme 33: Transglycosylation reaction between GGXXXG (50) and the labeled acceptor XXXG-ANTS (25). In bold, the donor fragment transferred to the acceptor is presented and underlined, the identified product.

In contrast, GGGXXXG (**51**) and GGGGXXXG (**52**) showed multiple transglycosylation products. Major product from GGGXXXG (**51**) reaction is the expected from GGG- transfer, GGGXXXGANTS (Scheme 34A), but also two minor products were detected after 24 hours reaction (Figure 71C), which were identified as GGXXXGANTS and GXXXGANTS. Whereas the first may arise from direct transfer of the GG- moiety to the acceptor (Scheme 34B), the second one is unlikely to come from G- transfer (Scheme 34D), but rather it is produced as subproduct of a GG- transfer from the major transglycosylation product (Scheme 34C).



Scheme 34: Reaction pathways explaining production of main transglycosylation product (GGG-XXXG-ANTS) and the minor ones (GG-XXXG-ANTS, G-XXXGANTS) from reaction between 51 and 25. The donor fragment transferred is presented in bold and the identified transglycosylation products, underlined.

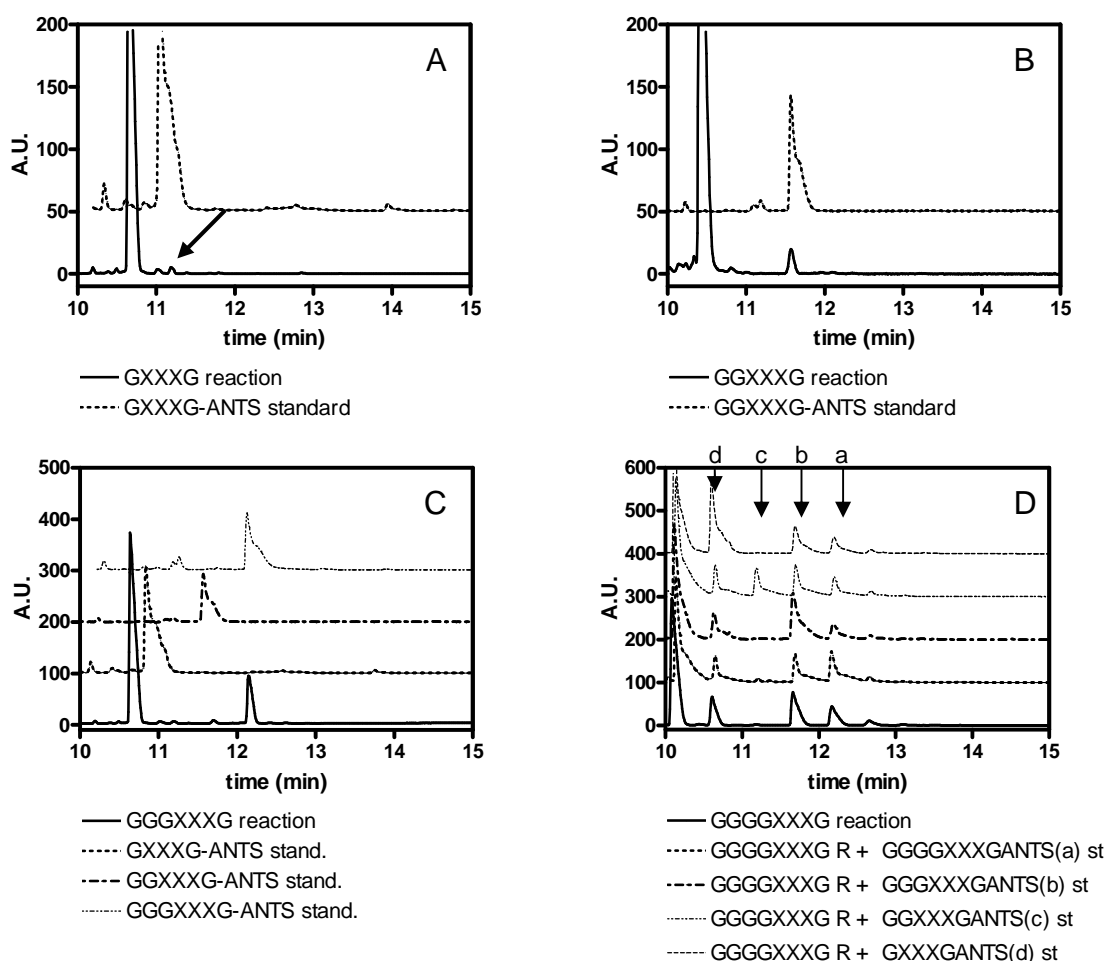
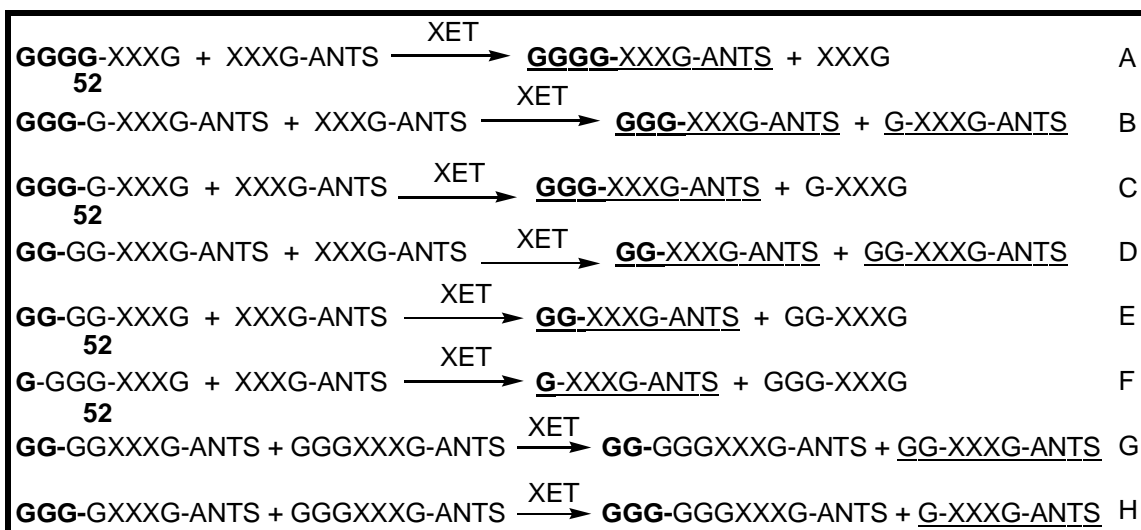


Figure 71: Electropherograms to identify transglycosylation products arising from reactions between GXXXG (49) (A), or GGXXXG (50) (B), or GGGXXXG (51) (C), or GGGGXXXG (52) (D) and XXXGANTS (25). In figures A-C identification was done by t_m comparison in figure D it was done by co-injection with corresponding ANTS standards.

For the longer donor, GGGGXXXG (52), three major products and at least three minor ones were detected after 24 hours reaction. Some of them could be identified by co-injection with adequate standards as GGGGXXXGANTS, GGGXXXGANTS, and GXXXGANTS as major products, and GGXXXGANTS as one of the minor products (Figure 71D).

GGGGXXXGANTS was formed as first product by direct GGGG- transfer (Scheme 35A) at initial reaction times, but the other two major compounds GGGXXXGANTS and GXXXGANTS were later obtained as it is visualized by the time course of the reaction (Figure 72).



Scheme 35: Some of the possible pathways that could explain different transglycosylation products detected in the reaction between GGGGXXXG (52) and XXXGANTS (25): some of them were identified and other ones only as proposed structures. The donor fragment transferred is presented in bold, and the identified transglycosylation products, underlined.

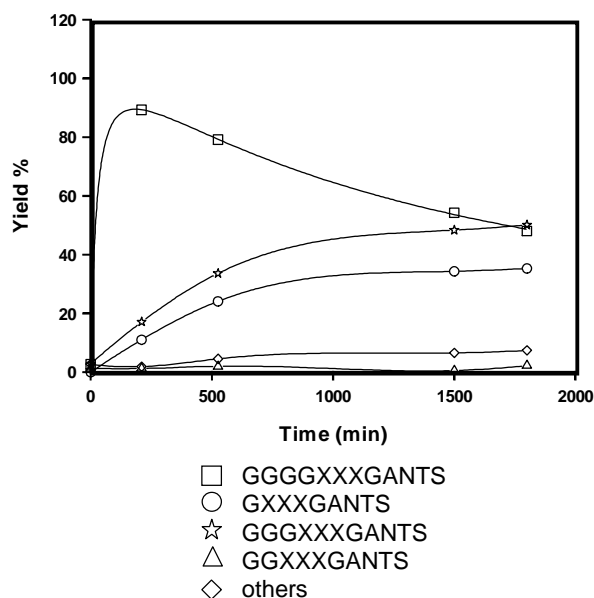


Figure 72: Product evolution of reaction between GGGGXXXG (52) and XXXGANTS (25).

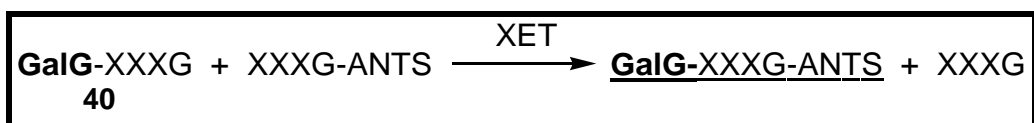
GGGXXXGANTS can be formed by direct GGG- transfer from donor (Scheme 35C); however GXXXGANTS is unlikely to be formed by direct G- transfer from donor (Scheme 35F), whereas it could be formed as byproduct of a second GGG-transfer reaction from the GGGGXXXGANTS product (Scheme 35B).

The identified minor product, GGXXXGANTS, may be formed by GG- transfer from donor and/or product to acceptor (Scheme 35D, E) although produced in very low extent. Structures for non identified minor products are proposed taking into account linear relationship between log (MW) and t_m , and expected polymerization reactions (Scheme 35G and Scheme 35H).

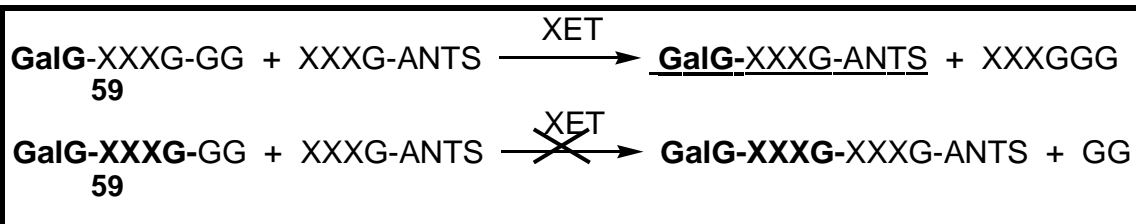
6.1.4.- Family 2. Donors with a terminal Gal group.

Three donors, GalGXXXG (**40**), GalGXXXGGG (**59**) and GalGXXXGXXXG (**38**), were designed to prevent donor-self transglycosylation and product elongation as observed on highly reactive donors such as XXXGXXXG (**23**) or XXXGXXXGXXXG (**24**).

For GalGXXXG (**40**) and GalGXXXGGG (**59**) a single transglycosylation product was detected and identified as GalGXXXGANTS by t_m comparison (Figure 73A and Figure 73C), both products arising from direct GalG- transfer (Scheme 36 and Scheme 37). Although for GalGXXXG (**40**) no other transfer (different from GalG- one) could be proposed, for GalGXXXGGG (**59**), another transfer (the GalGXXXG- one) might be expected taking into account that for XXXG-GG (**21**) the XXXG- transfer occurs. This GalGXXXG- transfer (Scheme 37) is negligible.



Scheme 36: Transglycosylation reaction between GalGXXXG (40) and XXXGANTS (25) catalysed by Ptt-XET16A. In bold it is presented the fragment of the donor transferred and underlined, the identified transglycosylation product.



Scheme 37: Possible reaction pathways for GalGXXXGGG (59) as donor, only the first one occurs. The fragment of the donor proposed to be transferred in each reaction is presented in bold and underlined, the identified transglycosylation product.

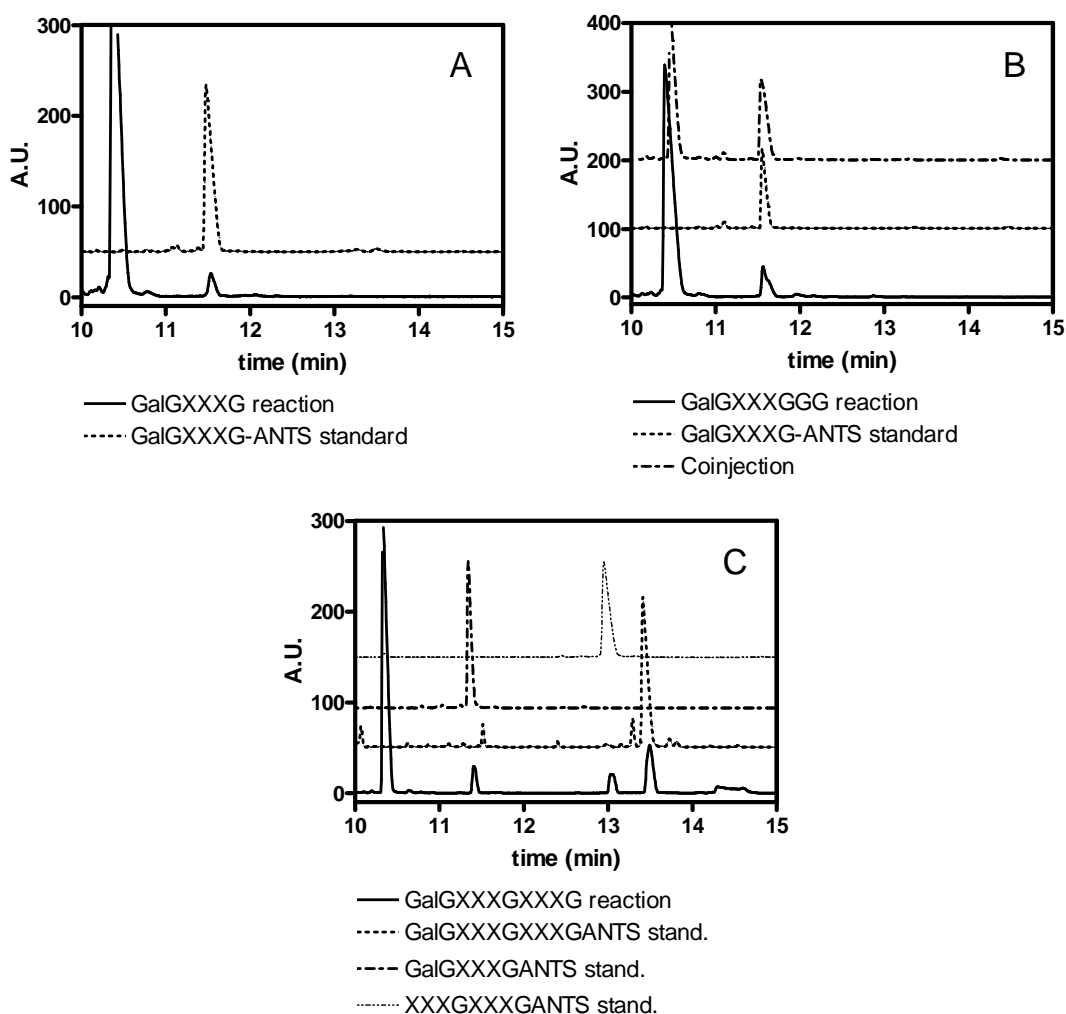


Figure 73: Electropherograms to identify transglycosylation products arising from reactions between GalGXXXG (40) (A), or GalGXXXGGG (59) (B), or GalGXXXGXXXG (38) (C), and XXXGANTS (25). In figures A and C identification was done by t_m comparison. In figure B it was done by co-injection with the corresponding ANTS labeled standards.

The larger donor within this subgroup GalGXXXGXXXG (**38**), designed to kinetically characterize *Ptt*-XET16A avoiding inhibition caused by donor and/or product polymerization showed, after 24 hours reaction, three major transglycosylation products identified by t_m comparison as GalGXXXGANTS, GalGXXXGXXXGANTS and XXXGXXXGANTS (Figure 73C). At initial stages of reaction, GalGXXXGXXXGANTS was formed and accumulated, this product could react again transferring GalGXXXG- what will render the same product or transferring GalG- moiety rendering GalGXXXGANTS and XXXGXXXGANTS as it is represented in Scheme 38.

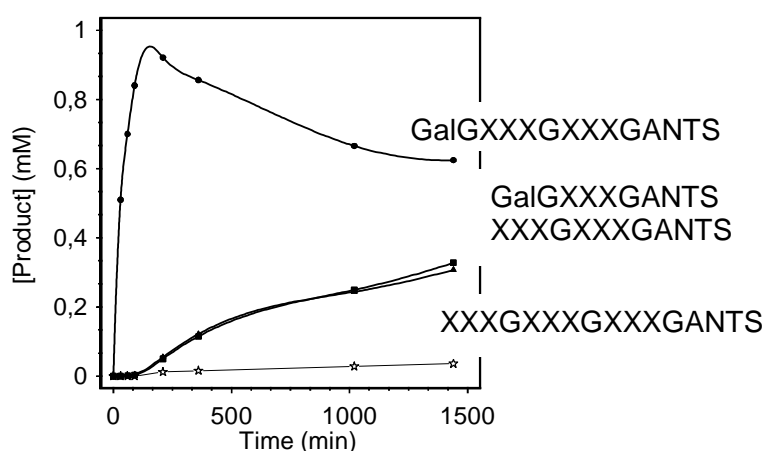
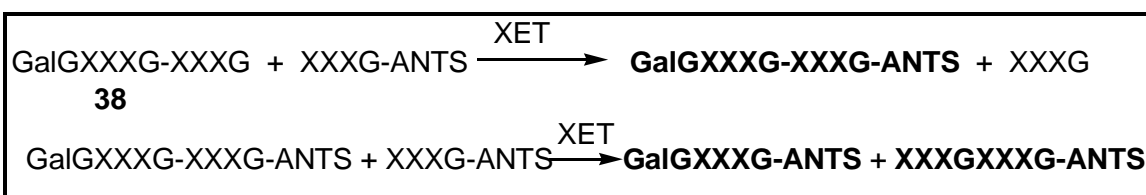


Figure 74: Product evolution of reaction between GalGXXXGXXXG (38**) and XXXGANTS (**25**).**

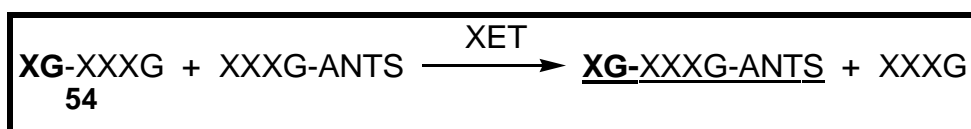


Scheme 38: Reaction pathways which explain transglycosylation products observed after 24 hours reaction between GalGXXXGXXXG (38**) and XXXGANTS (**25**).**

6.1.5.- Family 2. Donors with branched chain in the non reducing end fragment.

Five donors were designed to study the xylosyl substitution requirements of *Ptt*-XET16A in negative subsites: XGXXXG (**54**), XGGXXXG (**55**), XXGXXXG (**29**), XGXGXXXG (**56**), GXXGXXXG (**53**).

Whereas XGXXXG (**54**) gave a single transglycosylation product, identified as XGXXXGANTS (Figure 75A) by transfer of the XG- moiety (Scheme 39), the other ones rendered multiple transfers.



Scheme 39: Transglycosylation reaction between XGXXXG (54) and XXXGANTS. In bold transferred donor fragment and underlined the transglycosylation product identified.

For XXGXXXG (**55**) one major product and one minor product were detected (Figure 75B). The major product, identified as XXGXXXGANTS (Figure 75B), is produced by direct transfer of XXG- fragment (Scheme 40A). The minor one could not be directly identified due to the lack of appropriate standards, however, interpolation of migration time in the linear relationship between $\log(\text{MW})$ and t_m resulted in a MW approximately of 2500 Da which correlates with the proposed XXGXXGXXXGANTS structure, resulting from donor or product polymerization (Scheme 40B and/or Scheme 40C+D).

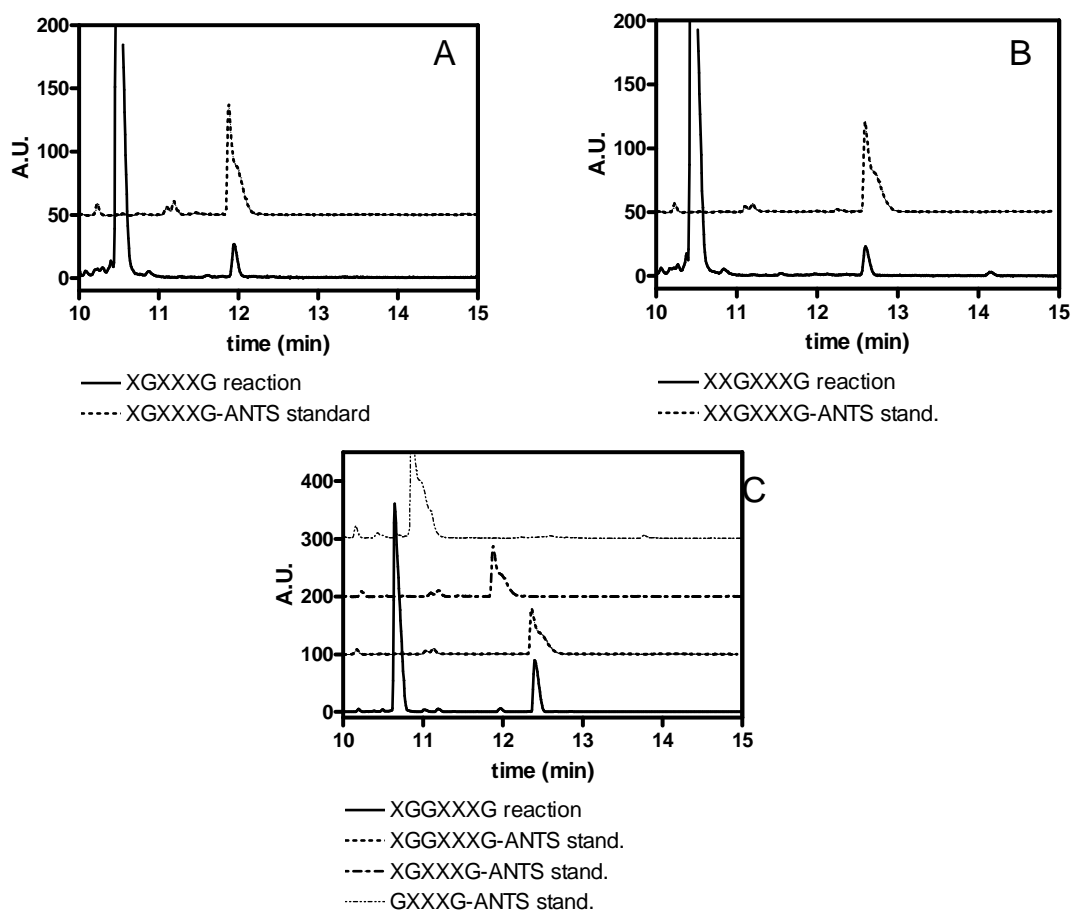
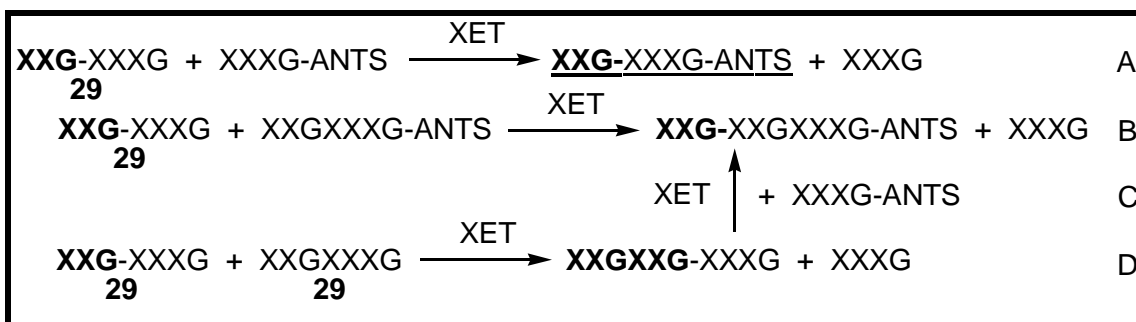
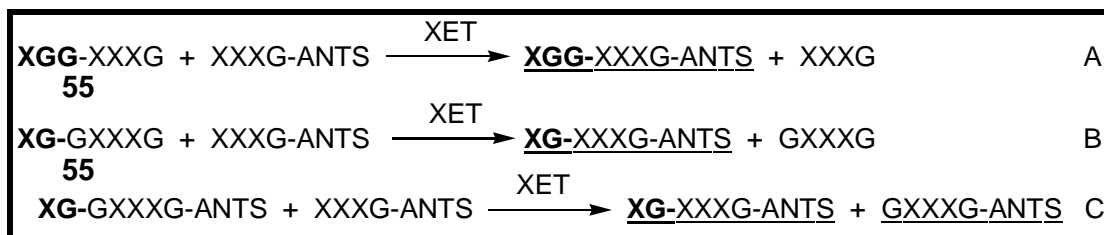


Figure 75: Electropherograms to identify transglycosylation products arising from reactions between XGXXXG (54) (A), or XXGXXXGGG (29) (B), or XGGXXXG (55) (C), and XXXGANTS (25). Identification was done by t_m comparison with corresponding ANTS standards.



Scheme 40: Reaction pathways which explain the formation of the detected products from reaction between XXGXXXG (29) and XXXGANTS (25) due to single transglycosylation reaction (XXGXXXGANTS), or due to different reaction steps (XXGXXGXXXGANTS).

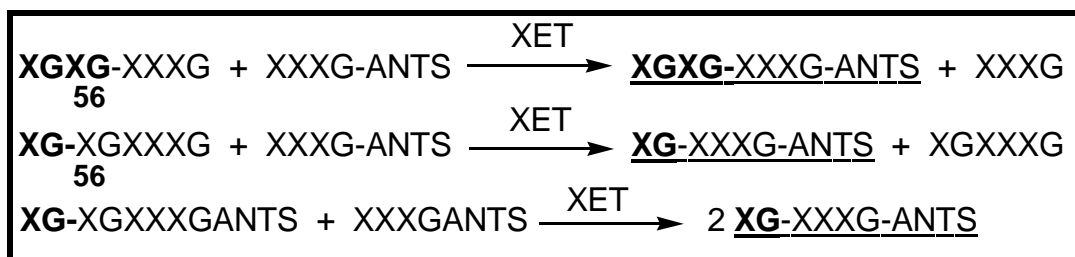
XGGXXXG (**55**) rendered also different transglycosylation products (Figure 75C): XGGXXXGANTS produced by direct XGG- transfer (Scheme 41A), but also two minor products identified as XGXXXGANTS and GXXXGANTS (Figure 75C). Both minor products can arise from XG- transfer from XGGXXXGANTS product to acceptor (Scheme 41C), but XGXXXGANTS could also be produced by direct XG- transfer from donor to acceptor (Scheme 41B).



Scheme 41: Possible reactions of XGGXXXG (55) with XXXGANTS (25).

The donor fragment transferred is presented in bold, and the identified products, underlined.

Other two donors XGXGXXXG (**56**) and GXXGXXG (**53**) showed different reaction products: XGXGXXXG (**56**) rendered only two transglycosylation products XGXGXXXGANTS (Figure 76A) by direct transfer of XGXG- moiety (Scheme 42) and XGXXXGANTS as minor product by XG- transfer from donor or product to the acceptor.



Scheme 42: Reaction pathways that explain formation of two different products XGXGXXXGANTS and XGXXXGANTS. In bold, transferred fragment from donor and underlined, identified product.

GXXGXXXG (**53**) showed three major transglycosylation products and some minor products (Figure 76B). Major products were identified as GXXGXXXGANTS (Figure 76B), produced by direct GXXG- transfer (Scheme 43), GXXXGANTS and XXGXXXGANTS (Figure 76B).

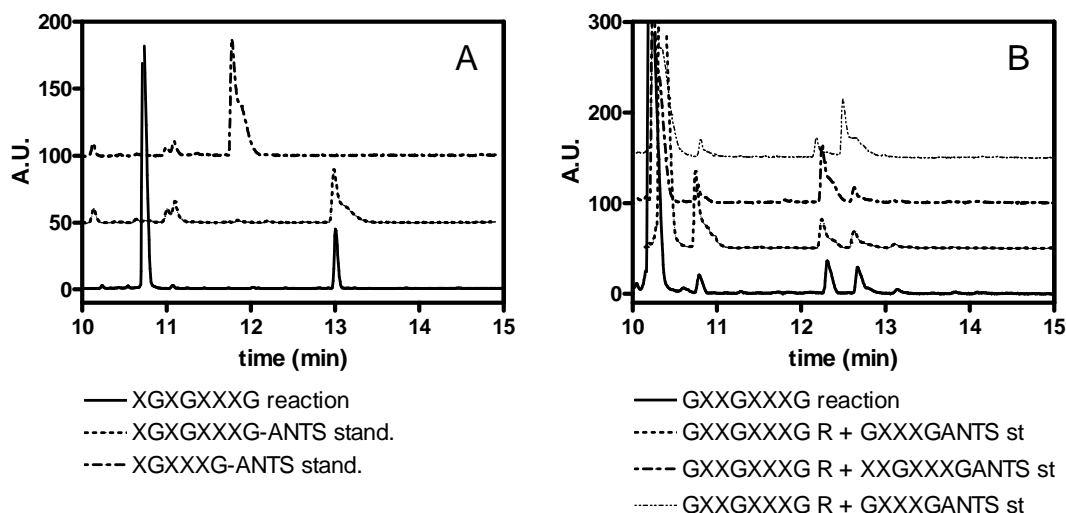


Figure 76: Electropherogram showing identification of transglycosylation products from XGXGXXXG (56**) + XXXGANTS and GXXGXXXG (**53**) + XXXGANTS (**25**) reactions. In figure A identification was done by t_m comparison and in figure B by standard co-injection.**

At initial reaction times GXXGXXXGANTS was produced by direct GXXG-transfer (Scheme 43A) and accumulated in the reaction medium as shown in Figure 77. Production of GXXXGANTS and XXGXXXGANTS products is not expected to occur *via* direct G- transfer from donor or initial product (Scheme 43 B & D) followed by XXG- transfer from XXGXXXG byproduct (Scheme 43C) taking into account the low reactivity of GXXXG (**49**) donor. More reliable is that product polymerization occurs (Scheme 43E) forming an observed but not identified GXXGGXXGXXXGANTS product. This secondary product could act as donor transferring the GXXGG- moiety to render another minor, but not identified product (GXXGGXXXGANTS) and the identified XXGXXXGANTS as byproduct (Scheme 43F). This not identified tertiary product (GXXGGXXXGANTS) is represented in Figure 77 with the symbol (\diamond), firstly, it is accumulated in the reaction medium but afterwards its concentration decreased (Figure 77) probably rendering GXXGXXXGANTS and the identified GXXXGANTS as byproduct (Scheme 43G).

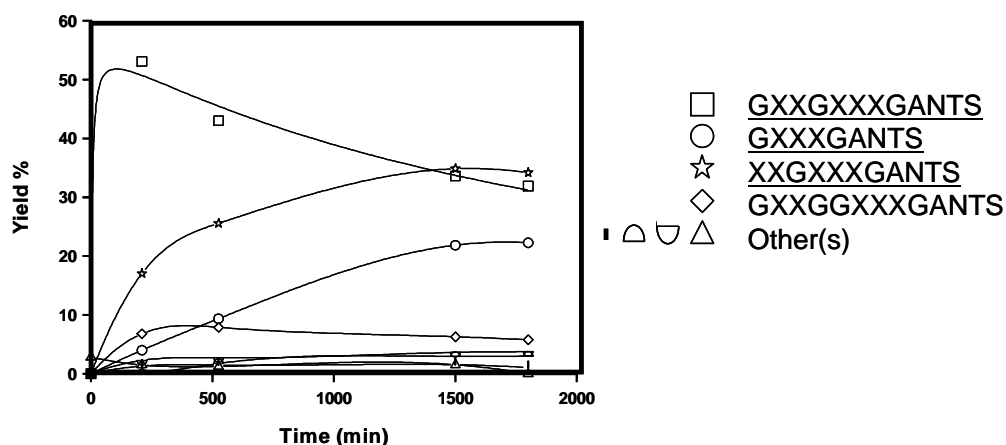
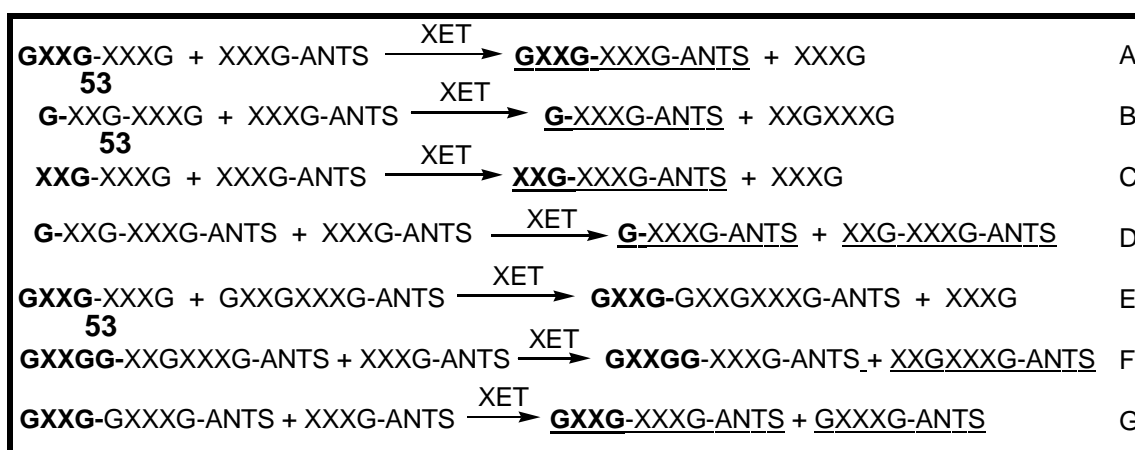


Figure 77: Product evolution of reaction between GXXGXXXG (53) and XXXGANTS (25).



Scheme 43: Reaction pathways that explain the obtaining of different trangucosylation products in the reaction between GXXGXXXG (53) and XXXGANTS (25). Transferred fragments were presented in bold, and identified products, underlined.

6.2.- Relative reactivity after 24 hours reaction.

Once different transglycosylation products were identified (summarized in Table 7), relative reactivity between donors could be obtained by direct comparison of reaction yields of different products after 24 hours reaction.

Yields (%) are expressed as concentration of each product detected relative to the maximum concentration that could be obtained for that transglycosylation product.

Donor	Products	Normalized yield %
XXXG-GG (21)	XXXG-XXXG-ANTS	1.4
XXXG-GGGG (48)	XXXG-XXXG-ANTS	7.8
XXXG-XG (45)	XXXG-XXXG-ANTS	1.1
XXXG-XXG (46)	XXXG-XXXG-ANTS	84.1
	XXXG-XXXG-XXXG-ANTS	16.2
XXXG-XXXG (23)	XXXG-XXXG-ANTS	82.5
	XXXG-XXXG-XXXG-ANTS	29.6
	XXXG-XXXG-XXXG-XXXG-ANTS	3.6
XXXG-XXXG-XXXG (24)	XXXG-XXXG-ANTS	67.4
	XXXG-XXXG-XXXG-ANTS	36.2
	XXXG-XXXG-XXXG-XXXG-ANTS	12.0
G-XXXG (49)	G-XXXG-ANTS	0.7
GG-XXXG (50)	GG-XXXG-ANTS	20.8
GGG-XXXG (51)	GGG-XXXG-ANTS	102.0
	G-XXXG-ANTS	1.2
	GG-XXXG-ANTS	3.6
GGGG-XXXG (52)	GGGG-XXXG-ANTS	48.1
	G-XXXG-ANTS	8.9
	GG-XXXG-ANTS	1.7
	GGG-XXXG-ANTS	37.6
GalG-XXXG (40)	GalG-XXXG-ANTS	31.5
GalG-XXXG-GG (59)	GalG-XXXG-ANTS	33.5
GalGXXXGXXXG (38)	GalG-XXXGXXXG-ANTS	54.5
	GalG-XXXG-ANTS	19.3
	XXXGXXXG-ANTS	18.6
XG-XXXG (54)	XG-XXXG-ANTS	30.4
XGG-XXXG (55)	XGG-XXXG-ANTS	96.9
XXG-XXXG (29)	XXG-XXXG-ANTS	32.0
	XXG-XXG-XXXG-ANTS	9.4
GXXG-XXXG (53)	GXXG-XXXG-ANTS	40.4
	G-XXXG-ANTS	20.9
	XXG-XXXG-ANTS	38.8
XGXG-XXXG (56)	XGXG-XXXG-ANTS	69.5
	XG-XXXG-ANTS	

Table 7: Yields after 24 h reaction at 3 μ M *Ptt*-XET16A, 1 mM donor, 5 mM XXXGANTS in citrate:phosphate buffer 50:50 mM, I=0.5M, pH 5.5 and 30°C.

From identification of transglycosylation products and relative reactivities, some conclusion can be inferred.

a) **The scissile bond for transfer to the acceptor is always the glycosidic bond at an unbranched glucosyl unit.** This is in keeping with the original conclusion by Fanutti and coworkers⁷¹ for an enzyme from germinated nasturtium seeds, based on product analysis of the reaction between XG polymer and XGOs. Moreover, our study shows that if more than one unsubstituted glucosyl unit exists in the donor, several transfer products may be detected, depending on the size and binding preferences for each multiple productive enzyme-donor complexes in which, again, cleavage and transfer occurs from an unbranched glucosyl unit.

b) Comparing donors with the same molecular mass, **donors that have xyloglucan-like structure on the acceptors subsites (-XXXG) are better than the corresponding donors that have this structure on the donor subsites (XXXG-).** This is clearly shown comparing yields after 24 h reaction of similar structures from different donor families (Table 8):

	XG-like in donor subsites	XG-like in acceptor subsites
Donor	XXXG-GG (21)	GG-XXXG (50)
Yield (%)	1.4	20.8
Donor	XXXG-XG (45)	XG-XXXG (54)
Yield (%)	1.1	30.4
Donor	XXXG-GGGG (48)	GGGG-XXXG (52)
Yield (%)	7.8	>100

Table 8: Comparison of yields on transglycosylation reactions of donors from different families depending on where is located the XG-like fragment of it.

The same conclusion arises from the observation that the transglycosylation product of the reaction between GalGXXXGGG (59) and XXXG-ANTS (25) was only the GalGXXXGANTS product, where -XXXG- moiety occupied acceptor subsites and the GalG- unit was transferred to acceptor. This result indicates that **the XXXG moiety is preferably located in the acceptors (positive) subsites than in the donor (negative) ones** as it is shown in Figure 78, second structure.

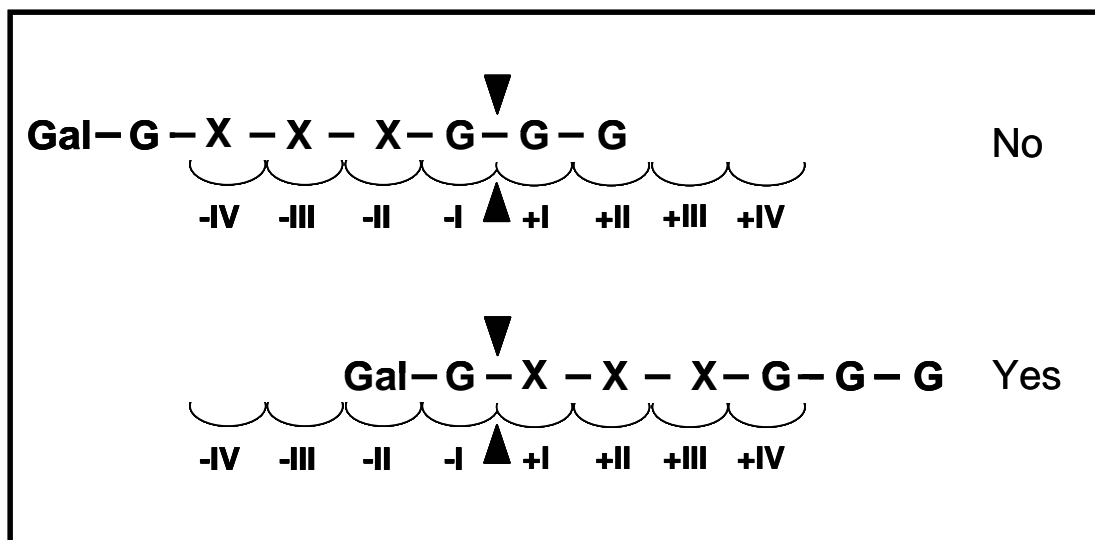


Figure 78: Schematic representation of GalG-XXXG-GG (59) possible modes of binding.

Our conclusion explains the results achieved by other members of EDEN consortium observing the crystallographic structure of *Ptt*-XET16 with XLLG (**13**). In this 3D structure, only the complex *Ptt*-XET16A-XLLG bound in acceptor subsites could be observed (Figure 79) and no electronic density for binding in the negative subsites was detected^{89,105}. Although this binding of XLLG in the positive subsites of the *Ptt*-XET16A obtained by crystal soaking can be an artifact of crystal packing due to the presence of a second molecule of enzyme preventing binding in the negative subsites; our results confirm a higher affinity of positive subsites for XG-like structures.

In the 3D structure^{89,105}, only some glycosyl units of XLLG (**13**) could be observed, specifically glucosyl groups at subsites +I, +II, and +III, xylosyl groups at subsites +I' and +II', and galactosyl group at subsite +II'' which indicates that non observed saccharidic-units are not fixed by enzyme and may adopt several configurations.

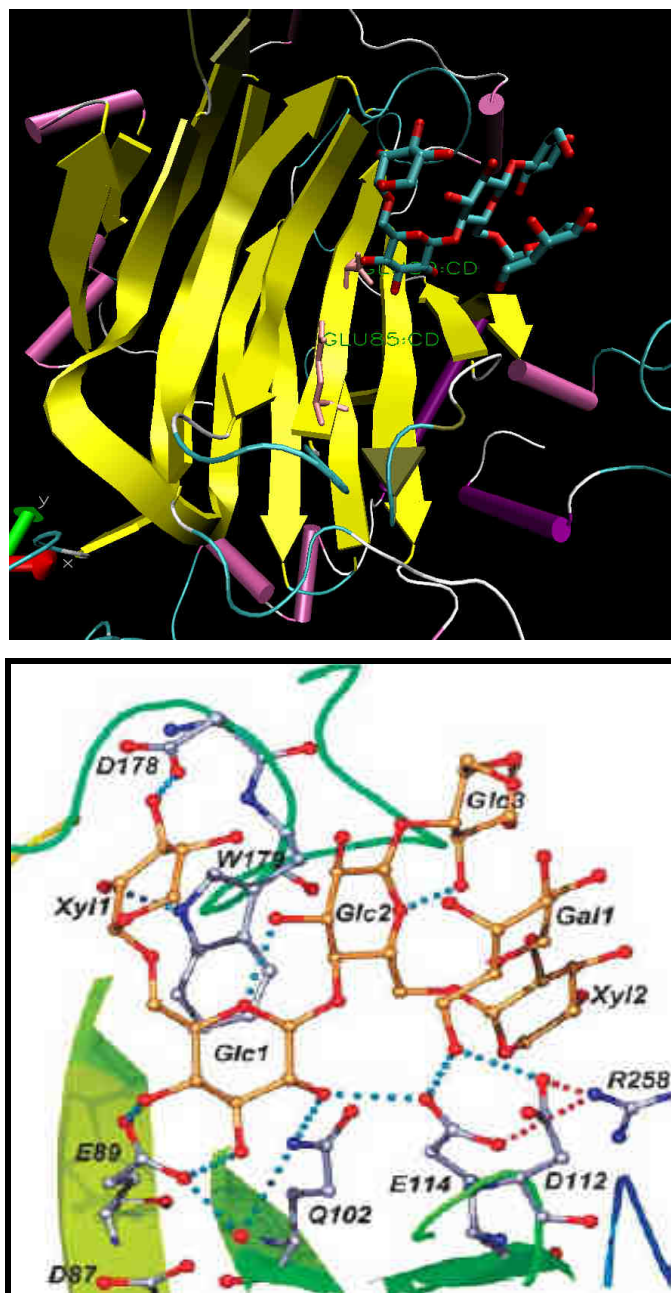


Figure 79: Three-dimensional structures for *Ptt-XET16A* – XLLG complex, from Johansson *et al.* (2003 and 2004)^{89,105}.

c) Donors that have consecutive non-branched glucosyl units and at the same time are good substrates (GGGXXXG (51), GGGGXXXG (52) having the –XXXG at the positive subsites) render different products which arise from bond cleavage at each unsubstituted glucosyl unit, except for the terminal glucosyl unit on the non-reducing end.

d) **Oligomerization reactions arising from multiple transfers were observed for good substrates (XXXGXXXG (23), XXXGXXXGXXXG (24), XXGXXXG (29)) because the first transglycosylation product is accumulated in enough concentration to compete with the acceptor.** Moreover, the transglycosylation product may be a better acceptor due to its larger size and distant location of the ANTS label from the binding cleft.

Product analyses have provided information on enzyme specificity and relative reactivity of donor substrates. But under initial rate conditions, a single transglycosylation product was formed; therefore kinetic parameters are assignable to a single productive binding mode. And we may be able to analyze the contribution of different structural moieties in binding and activity of substrates, by comparison of kinetic parameters between two different substrates.

7.- Subsite mapping.

7.1.- Background.

In the subsite mapping of the binding cleft of an enzyme, often described in glycoside hydrolases acting on polymeric substrates, the objective is to evaluate the contribution of each individual subsites to binding and catalysis.

In polymeric substrates, binding to a multi-site binding cleft may lead to different positional and non productive complexes. All these positional isomers contribute to steady state parameters, but the second order rate constant (k_{cat}/K_M) is independent of the formation of unproductive complexes¹¹⁶ being only dependent of the formation of productive complexes.

The effect of occupying a subsite on k_{cat}/K_M is the contribution of that individual subsite to transition state stabilization, and can be expressed by the difference in transition state activation energy between two substrates differing in one glycosyl unit. This contribution can be assigned to the stabilization of transition state given by the glycosyl unit in which both substrates differ. This contribution is expressed by Equation 4, where **a** and **b** are two substrates differing in the occupancy of subsite **i**.

$$\Delta\Delta G^{\ddagger}_{\text{subsite } i} = \Delta G^{\ddagger}_a - \Delta G^{\ddagger}_b = -R \cdot T \cdot \ln \frac{(k_{cat}/K_M)_a}{(k_{cat}/K_M)_b}$$

Equation 4: Contribution to transition state stabilization caused by the structural difference between substrate a and substrate b, which is the glycosyl unit in subsite i.

As example consider two donors, **23** and **56** (Figure 80), which differ in the xylosyl substitution at subsite -III', therefore the contribution of this subsite is given by Equation 5.

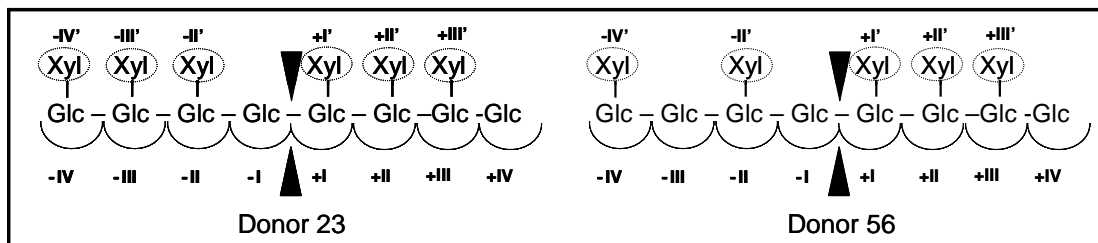


Figure 80: Structures of substrates 23 and 56 designed to evaluate contribution of subsite -III in stabilization of transition state.

$$\Delta\Delta G^{\ddagger}_{\text{subsite -III}'} = \Delta G^{\ddagger}_{23} - \Delta G^{\ddagger}_{56} = -R \cdot T \cdot \ln \frac{(k_{\text{cat}}/K_M)_{23}}{(k_{\text{cat}}/K_M)_{56}}$$

Equation 5: Contribution to transition state stabilization caused by xylosyl substitution at subsite -III.

7.2.- k_{cat}/K_M determination.

Enzymatic initial rates were determined at different donor concentrations (between 0.3 and 1 mM) and 5 mM XXXGANTS (**25**). The slope of v_0 versus [donor] gives the k_{cat}/K_M value for each donor. As an example, in Figure 81 k_{cat}/K_M determination for compound GGXXXG (**50**).

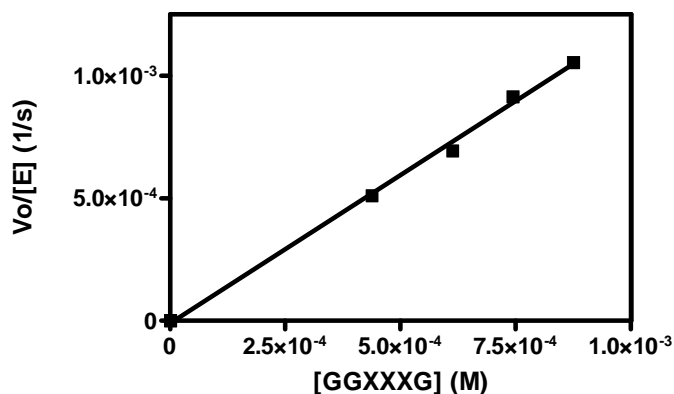


Figure 81: k_{cat}/K_M determination for GGXXXG (50**).**

In all kinetic experiments a single transglycosylation event was produced, except for XXXGXXXGXXXG (**24**) as donor, case in which two products (XXXGXXXGANTS (**31**) and XXXGXXXGXXXGANTS(**37**)) appeared at the same time (Figure 82).

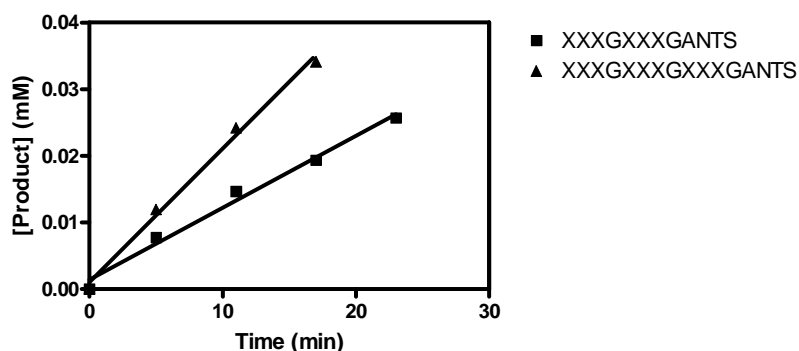


Figure 82: Initial rate determination of *Ptt*-XET16A (1 μ M) transglycosylation reaction between XXXGXXXGXXXG (24**, 0.35 mM) and XXXGANTS (**25**, 5 mM).**

k_{cat}/K_M values obtained for all substrates within the library are presented in the following table (Table 9).

Donor	Product	k_{cat}/K_M
XXXG-GG (47)	XXXG-XXXG-ANTS	< 0.1
XXXG-GGGG (48)	XXXG-XXXG-ANTS	< 0.1
XXXG-XG (45)	XXXG-XXXG-ANTS	< 0.1
XXXG-XXG (46)	XXXG-XXXG-ANTS	57.8 \pm 4.3
XXXG-XXXG (23)	XXXG-XXXG-ANTS	142.3 \pm 6.7
XXXG-XXXG-XXXG (24)	XXXG-XXXG-ANTS	221.1 \pm 15.8
	XXXG-XXXG-XXXG-ANTS	343.8 \pm 19.1
G-XXXG (49)	G-XXXG-ANTS	< 0.1
GG-XXXG (50)	GG-XXXG-ANTS	1.16 \pm 0.02
GGG-XXXG (51)	GGG-XXXG-ANTS	40.9 \pm 2.6
GGGG-XXXG (52)	GGGG-XXXG-ANTS	96.5 \pm 4.7
XG-XXXG (54)	XG-XXXG-ANTS	1.66 \pm 0.13
XGG-XXXG (55)	XGG-XXXG-ANTS	68.8 \pm 4.1
XXG-XXXG (29)	XXG-XXXG-ANTS	57.1 \pm 6.2
GXXG-XXXG (53)	GXXG-XXXG-ANTS	202.8 \pm 17.4
XGXG-XXXG (56)	XGXG-XXXG-ANTS	83.8 \pm 5.3
GalG-XXXG (40)	GalG-XXXG-ANTS	1.66 \pm 0.07
GalG-XXXG-GG (59)	GalG-XXXG-ANTS	1.70 \pm 0.14
GalG-XXXG-XXXG (38)	GalG-XXXG-XXXG-ANTS	395.0 \pm 25.2

Table 9: k_{cat}/K_M values in $M^{-1}\cdot s^{-1}$ obtained for each evaluated donor. The donor studied and the product formed are presented.

7.3.- Subsite mapping.

Thermodynamic cycles relating different substrates within the library and determining contribution to transition state (TS) stabilization of different structural units of a standard substrate were constructed. In the thermodynamic cycles, $\Delta\Delta G^\ddagger$ (kcal/mol) values (Equation 6) are presented on the arrow between the two related substrates. Under each substrate the k_{cat}/K_M ($\text{M}^{-1}\cdot\text{s}^{-1}$) value is presented.

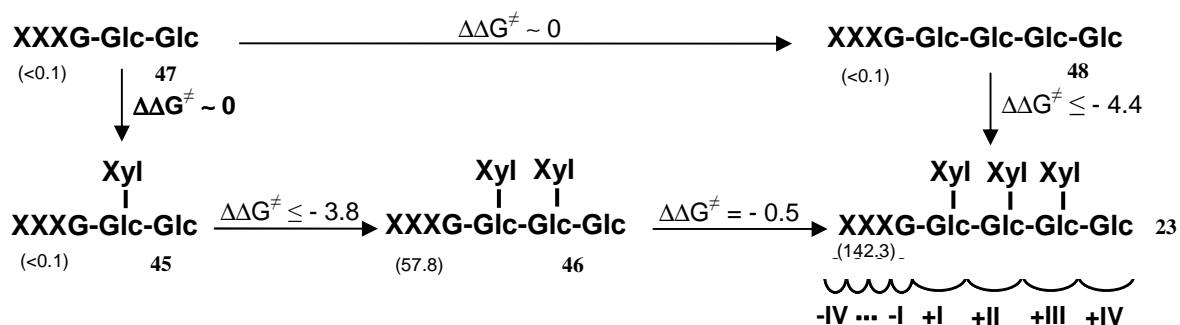
$\Delta\Delta G^\ddagger$ absolute error for each pair of donors was determined as Equation 4 indicates, in all cases obtained errors are near 0.1 kcal/mol or lower and for that reason they are not indicated in the thermodynamic cycles.

$$E_{\Delta\Delta G^\ddagger \text{subsite } i} = R \cdot T \cdot \frac{E_{(k_{\text{cat}}/K_M)_a}}{(k_{\text{cat}}/K_M)_a} + R \cdot T \cdot \frac{E_{(k_{\text{cat}}/K_M)_b}}{(k_{\text{cat}}/K_M)_b}$$

Equation 6: Absolute error determination for $\Delta\Delta G^\ddagger$ contribution of subsite i, determined from k_{cat}/K_M absolute errors for substrate a and b.

7.3.1.- Positive subsites mapping.

In Scheme 44, $\Delta\Delta G^\ddagger$ values for substrates designed to study acceptor subsites (positive subsites) are presented, family 1 of the donor library.



Scheme 44: Subsite mapping of positive subsites, $\Delta\Delta G^\ddagger$ are expressed in kcal/mol between compared donors and k_{cat}/K_M are expressed in $\text{M}^{-1}\cdot\text{s}^{-1}$ in brackets.

a) It is clearly observed that **the minimal structural requirement for positives subsites is the XXG structure**, because XXXGXXG (**46**) is the minimal substrate for which k_{cat}/K_M could be determined and a chain of four Glc on the reducing end is not enough to render a good donor. Combining the $\Delta\Delta G^\ddagger$ values and the yields after 24 hours reaction (XXXG-GG (1.4%), XXXG-XG (1.1%), XXXG-GGGG (4.7%) and XXXG-XXG (84.1%)) it can be proposed **that the highest contribution to TS stabilization is given by Xyl(+II')** taking into account the following observations:

1) $\Delta\Delta G^\ddagger$ (**47**→**45**) between XXXGGG (**47**) and XXXGXG (**45**) is near zero and yields after 24 h reaction for them are approximately equal showing the low contribution of Xyl(+I').

2) $\Delta\Delta G^\ddagger$ (**47**→**48**) between XXXGGG (**47**) and XXXGGGGG (**48**) is near zero and yields after 24 h reaction for **47** (1.4%) and **48** (4.7%) are similar, showing a very slight contribution of Glc(+III and +IV) on TS stabilization.

3) Comparison between XXXGXG (**45**) and XXXGXXG (**46**) renders a $\Delta\Delta G^\ddagger$ (**45**→**46**)= -3.8 kcal/mol showing the high contribution to TS stabilization of Xyl(+II') and/or Glc(+III), since the glucosyl backbone is proposed to give only a very slightly stabilization, then it can be concluded that **the highest contribution on transition state stabilization comes from Xyl(+II')**.

b) Comparison between XXXG-XXG (**46**) and XXXG-XXXG (**23**), renders a $\Delta\Delta G^\ddagger$ (**46**→**23**)= -0.5 kcal/mol showing a **slight contribution of Xyl(+III') and Glc(+IV) units to TS stabilization**.

The conclusion that the highest contribution to TS stabilization is given by Xyl(+II') match with the proposal of branching requirements of a XG endotransglycosylase / hydrolase from germinated nasturtium seeds (the only requirement of xylose substitution at positive subsites is the Xyl(+II'))^{71,85}. Other studies seem to indicate that both substitution (Xyl(+I') and Xyl(+II')) are required for activity⁹⁵.

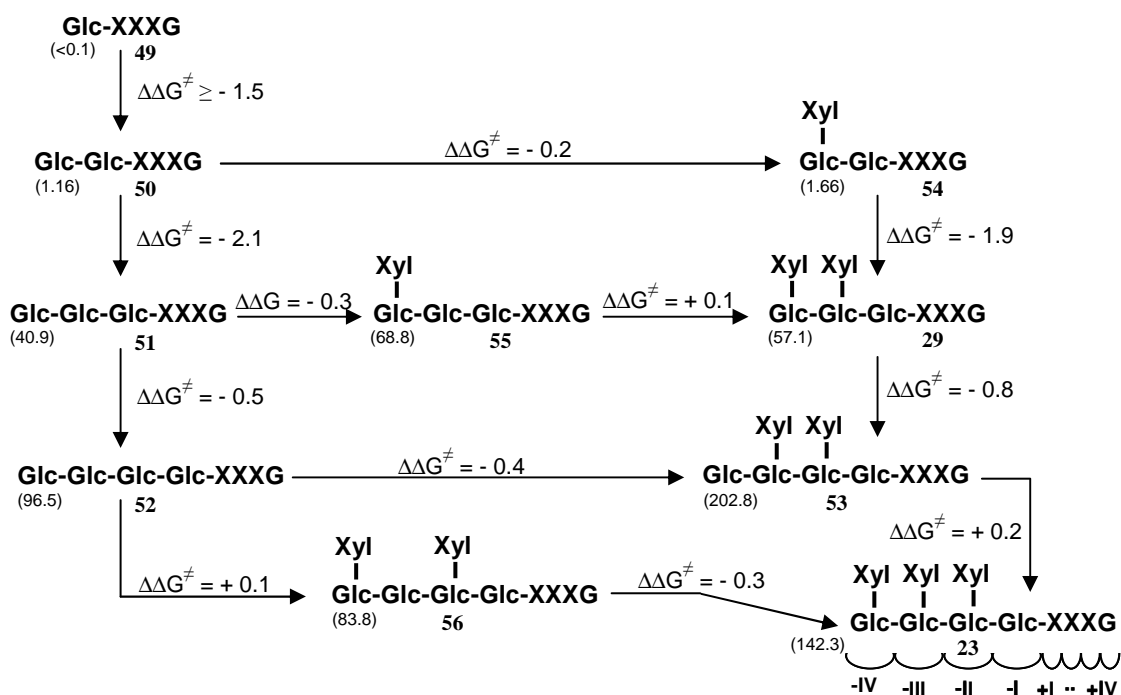
7.3.2.- Negative subsites mapping.

The analysis of donor subsites is presented in Scheme 45, using substrates of family 2 of donor library. This is the first study where donor subsites are studied, because all previous reports have used xyloglucan polymer as donor, and therefore, no information of donor subsites could be obtained.

Contribution to TS stabilization of glucosyl units at each negative subsite was analyzed with the series GXXXG (**49**), GGXXXG (**50**), GGGXXXG (**51**), and GGGGXXXG (**52**).

a) **The largest contribution on TS stabilization comes from glucosyl units at -II and -III (Glc(-II) and Glc(-III))** with given $\Delta\Delta G^\ddagger$ -1.5 and -2.1 kcal/mol (**49**→**50** and **50**→**51**) respectively.

b) **Glc(-IV) have a low contribution on TS stabilization** giving $\Delta\Delta G^\ddagger$ from -0.5 to -0.8 kcal/mol depending on the xylosyl substitution of compared substrates (**51**→**52** and **29**→**53** respectively).



Scheme 45: Schematic representation of subsite mapping, calculated $\Delta\Delta G^\ddagger$, in kcal/mol, were noted on the arrows between compared donors and k_{cat}/K_M values were expressed in $M^{-1}\cdot s^{-1}$ in brackets.

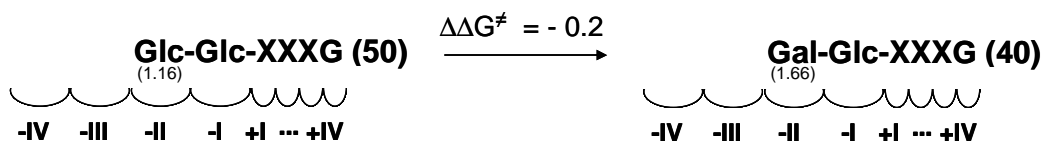
The contribution to TS stabilization of different xylosyl substituents was evaluated. **In all cases xylosyl substitution have a lower contribution than glucosyl units to TS stabilization**, each xylosyl contribution is between $-0.3 < \Delta\Delta G^\ddagger < +0.3$ kcal/mol.

c) The contribution of Xyl(-II') renders $\Delta\Delta G^\ddagger$ of -0.2 or $+0.1$ kcal/mol depending on the compared substrates (**50**→**54** or **55**→**29**), respectively. Both results are very low, near to the error value, showing **the low contribution of Xyl(-II')** in TS stabilization. Although these values are quite similar this difference can indicate that contributions are not fully additives. It can be though that when some subsite is occupied, this could affect interactions in other subsites.

d) For Xyl(-III'), $\Delta\Delta G^\ddagger$ value -0.3 kcal/mol was obtained from **51**→**55** and **56**→**23** indicating some TS stabilizing effect for this xylosyl unit Xyl(-III'). This low value seems not to match with the published proposal that xylosyl substitution at -III' subsite is required for XET / XEH activity^{71,85}.

e) Xyl(-IV') shows some unstabilizing effect with a $\Delta\Delta G^\ddagger = +0.2$ kcal/mol (**53**→**23**).

f) Comparison between GGXXXG (**50**) and GalGXXXG (**40**) shows a slight stabilization of a galactosyl unit compared to a glucosyl unit in the subsite -II, with a $\Delta\Delta G^\ddagger = -0.2$ kcal/mol.

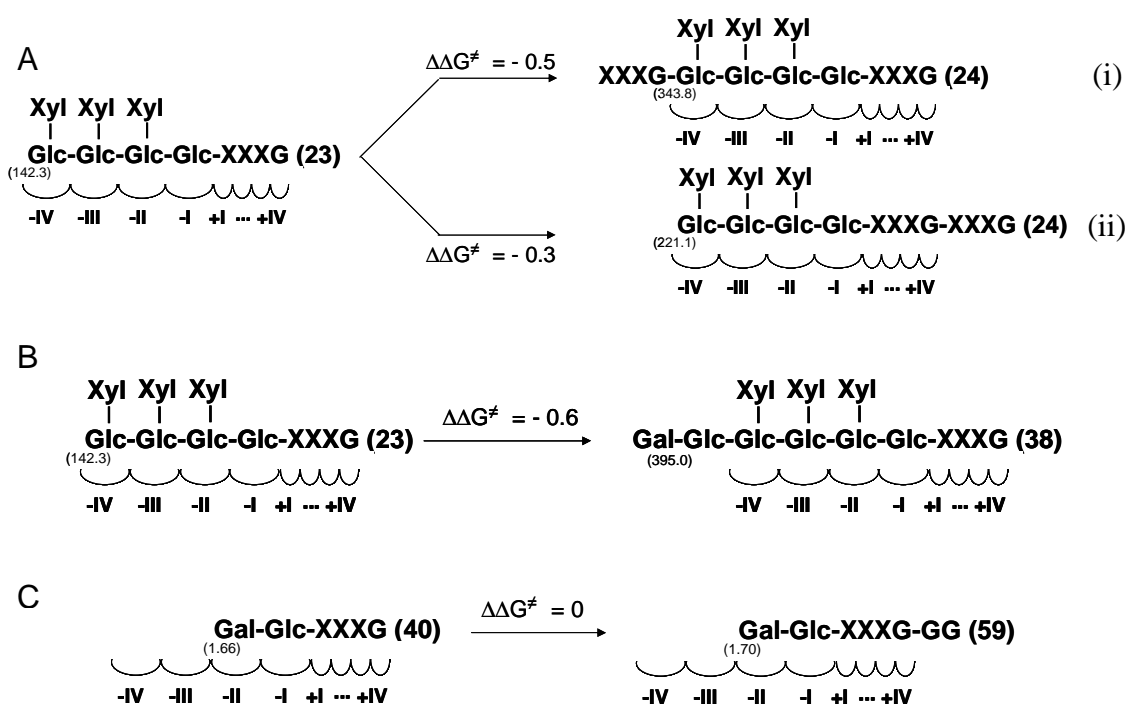


Scheme 46: Effect of galactosyl versus glucosyl residues in subsite -II. $\Delta\Delta G^\ddagger$ in kcal/mol are presented on the arrow between donors and k_{cat}/K_M values in $\text{M}^{-1}\cdot\text{s}^{-1}$ in brackets.

Since now, we have done a subsite mapping only taking into account 4 negative and 4 positive subsites because this is the XG polymer repeating structural unit and other enzymes in family 16 glycosyl hydrolases showed higher contributions on TS stabilization between -IV and +II subsites^{102,116}. However it is possible that these enzymes present more subsites or some surface interactions with substrate outside the binding cleft which can have some contribution to TS stabilization. In the designed library there are only few substrates which can be useful to evaluate the effect of

putative distant subsites other than -IV to +IV: XXXGXXXGXXXG (**24**), GalXXXGXXXG (**38**), and GalXXXGGG (**59**).

h) Comparison of both reaction patterns for donor **24**, with standard donor **23**, (**23**→**24**) render two $\Delta\Delta G^\ddagger$ values -0.3 and -0.5 kcal/mol as shown in Scheme 47A. These negative values indicate that XXXG moiety outside -IV to +IV subsites have a TS stabilizing contribution. Moreover stabilization for -V, -VI, ... subsites if any or unspecific surface interactions on the non reducing end contributes a little bit more Scheme 47A(i) than +V, +VI, ... subsites or unspecific surface interactions on the reducing end Scheme 47A(ii).



Scheme 47: Schematic representation of subsite mapping, where calculated $\Delta\Delta G^\ddagger$ were noted in kcal/mol on the arrows between compared donors and k_{cat}/K_M values were expressed in $\text{M}^{-1}\cdot\text{s}^{-1}$ in brackets.

i) The stabilization of TS due to newly formed interactions between *Ptt*-XET16A and GalG- moiety in the non reducing end, presented in Scheme 47B ($\Delta\Delta G^\ddagger = -0.6$ kcal/mol (**23**→**38**)), is equivalent to the TS stabilization provoked by the non reducing end **XXXG** moiety of **24**, when transferring the **XXXGXXXG**- fragment of **24** to the acceptor (Scheme 47A(i)). This coincidence may indicate that the major contributing interactions of **XXXGXXXGXXXG** (**24**) to TS stabilization are produced between the glucosyl units at -V and -VI subsites and the enzyme, although these interactions might not define a subsite but may be surface interactions.

j) The contribution on TS stabilization of -GG moiety at subsites +V and +VI is negligible (**40**→**59**) (Scheme 47C); which indicates that the slightly stabilization observed for -XXXG moiety of **24** (Scheme 47A(ii)) when transferring XXXG- fragment to acceptor is caused by more distant interactions than these located at subsites +V and +VI.

Subsite mapping results can be resumed in Figure 83 where contributions of different subsites are presented.

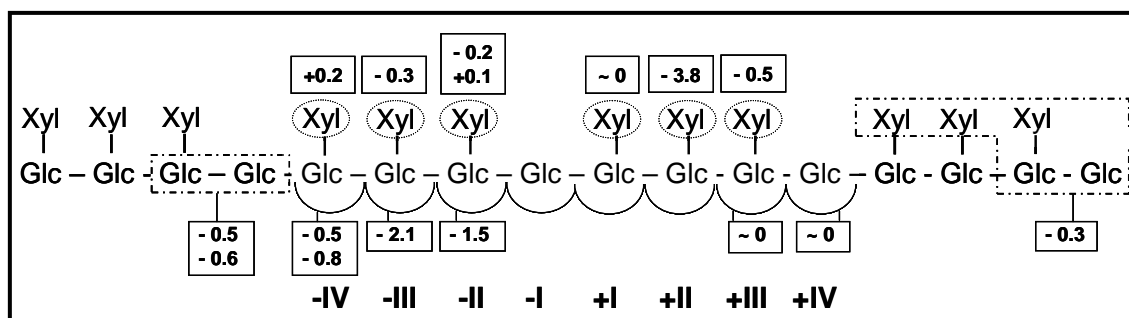


Figure 83: Contribution of different subsites on TS stabilization of *Ptt*-XET16A. Contributions are given in kcal/mol, negative values indicate stabilization and positive one indicate destabilization.

CHAPTER 5:
Design of an assay for transglycosylase /
hydrolase activity measurements for *XTHs*

CHAPTER 5: Design of an assay for transglycosylase /hydrolase activity measurements for *XTHs*.

1.- Background.

In this work we have developed a new enzymatic assay to kinetically characterize xyloglucan endotransglycosylases and to study their substrate specificity. This assay is based in capillary electrophoresis. We were able to monitor ANTS labeled transglycosylation products arising from transfer of a part of a xyloglucan oligosaccharide donor to an ANTS labeled xyloglucan oligosaccharide acceptor (XXXGANTS (25)).

Since *XTHs* were initially discovered, some of them showed different activities: they are able to transfer a fragment of a donor to an acceptor molecule but also they are able to hydrolyze xyloglucan molecules. Some *XTHs* seem to have both activities such as a *XTH* from Nasturtium seed extracts⁴², or a *XTH* from kiwifruit⁴⁹ another group of *XTHs* were proposed only to have hydrolytic activity such as a *XTH* from azuki bean epicotyls^{64,73} (although conditions used there are not the most adequate to monitor transglycosylation activity), and the last *XTHs* group seems to contain only pure transglycosylases such as a XET from cauliflower florets⁴⁶ and XET16A from *Populus tremula x tremuloides*⁴⁷.

Recently, in a new phylogenetic analysis of *XTH* gene products⁶⁸ it has been proposed that *XTH* having hydrolase activity have evolved from xyloglucan endotransglycosylases ancestral enzymes. In this study⁶⁸, the structural requirements of a *XTH* to show endohydrolase activity have been proposed being only subtle changes in the some loops of positive subsites. Once identified this structural requirements they proposed some new *XTH* gene products as putative xyloglucan endohydrolases, but of course further studies are needed to verify this hypothesis.

On the mechanistical point of view, both reactions (hydrolysis and transglycosylation) are equivalent, the only difference is the acceptor molecule. When transglycosylation takes place another XG molecule acts as acceptor. In contrast when hydrolysis occurs a water molecule acts as acceptor. This could let to propose that all *XTH* may have both activities in higher or lower extent⁷⁴.

One of the problems that hinder the classification of *XTHs* between transglycosylase, hydrolase and mixed type ones is that these activities are measured using completely different assays. For hydrolytic activity, different authors use methods normally used for glycosidases (reducing ends, viscosity decrease, etc.)^{42,43,46,47}. For transglycosylase activity different methods were used as it was presented in the introduction. Another possibility is the HPCE method designed and used in this work. Only two different methods could be used to measure simultaneously both activities:

a) The viscometric method⁴³ in which the decrease of viscosity of a solution of XG due to a *XTH* activity (without added acceptor) is monitored to measure hydrolytic activity. This is considered net hydrolytic activity although the XG polymer could act as acceptor, rendering transglycosylation. And when *XTH* and low molecular weight acceptor were added to XG, a measure of both hydrolysis and transglycosylation activities is obtained.

b) The colorimetric method⁴⁵ in which the decrease on absorbance of a complex between high molecular weight XG and iodine is monitored. Then, as in the former method, when only *XTH* is added to the XG solution, a measure of hydrolytic activity is obtained. And when *XTH* and low molecular weight acceptors are added to the XG solution, a measure of competing hydrolysis and transglycosylation activities is obtained.

Both methods are very similar and have the same drawbacks in measuring both activities at the same time. Also note that both methods measure some macromolecular properties, not molecular effects.

Recently, another activity assay based on HPAEC-PAD was published⁶⁸ which allows to measure both activities at the same time: They use as substrates the dimmers (XGO_{Glc8}) arising from XG degradation ($XXXGXXXG$, $XXLGXXXG$, $XLLGXXXG$, $XLLGXXLG$, $XLLGXLLG$, and isomers) and they monitor production of XGO_{Glc12} and XGO_{Glc4} , while XGO_{Glc12} is a direct measure of xyloglucan endotransglycosylase activity, XGO_{Glc4} is a measure of both activities at the same time.

We have decided to design an assay based on Fluorescence (or Förster) Resonance Energy Transfer (FRET) to measure both activities in a single experiment. This technology has the advantage of a high sensibility that would allow to determine and relate both activities although one of them was very low. This methodology has been used to monitor hydrolase enzymatic activities of different enzymes: cellulases^{174,176}, endochitinases, chitobiosidases¹⁷⁷, proteases¹⁷⁸⁻¹⁸¹, helicases¹⁸⁰, phosphatases^{180,182}, etc. On the other hand, FRET has been used to measure conformational changes, binding, etc. in more complex systems such us enzymes, transport channels, etc.¹⁸³

FRET describes a non radiative energy transfer between two fluorescent molecules. A fluorescent donor is excited at its excitation wavelength. Then by a long range dipole-dipole coupling mechanism, this excitation is nonradiatively transferred to a second molecule and, as a result, the donor returns to the ground state and the acceptor is excited. Finally this acceptor decays to the ground state by fluorescence emission at a different wavelength (Figure 84)^{184,185}. The FRET acronym can provoke certain confusion because it is not the fluorescence that is transferred from donor to acceptor but it is the electronic energy of the donor which is transferred to the acceptor, therefore EET (excitation energy transfer or electronic energy transfer) or RET (resonance energy transfer) could be most properly used to refer to this phenomenon¹⁸⁴.

Once this consideration have been done in this work the acronym FRET will be used to refer to the nonradiative transfer of electronic energy from a excited donor to an acceptor.

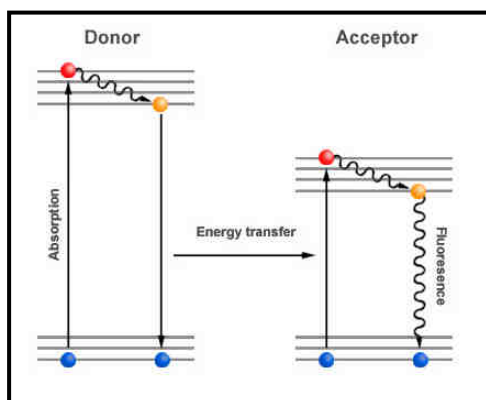


Figure 84: Schematic representation of energy transitions suffered by donor and acceptor fluorophores resulting in a FRET event. From <http://www.mekentosj.com/science/fret/fret.html>, December 2005.

There are some conditions that determine FRET occurrence between two molecules:

- Donor and acceptor molecules must be in close proximity (typically 10-100 Å).
- The absorption spectra of the acceptor must overlap the emission spectra of the donor.
- Donor and acceptor transition dipole orientation should be approximately parallel.

For each donor–acceptor pair, the Förster radius (R_0) can be calculated depending on the spectral properties of donor and acceptor dyes. R_0 is defined as the donor-acceptor distance at which FRET and spontaneous decay of excited donor are equally probable (50% excited donors are deactivated by FRET)^{184,185}.

R_0 depends on:

-An orientation factor which is function of the relative orientation of the donor and acceptor oscillating dipoles.

-The fluoresce quantum efficiency of the donor prove in absence of transfer.

-The refractive index of the medium.

-The overlap of the absorbance spectra of the acceptor and the emission spectra of the donor.

2.- FRET substrate design.

A XTH substrate was designed showing different FRET events depending on which XTH activity occurs (hydrolysis or transglycosylation) (Figure 85).

Exciting at λ_1 the donor does not emit any radiation because the energy from the fluorophore 1 should be transferred by FRET to quencher 1 and no emission should be produced. (the quencher is a molecule that have a wide absorbance spectra and is not once excited, returns to the ground state without fluorescence emission).

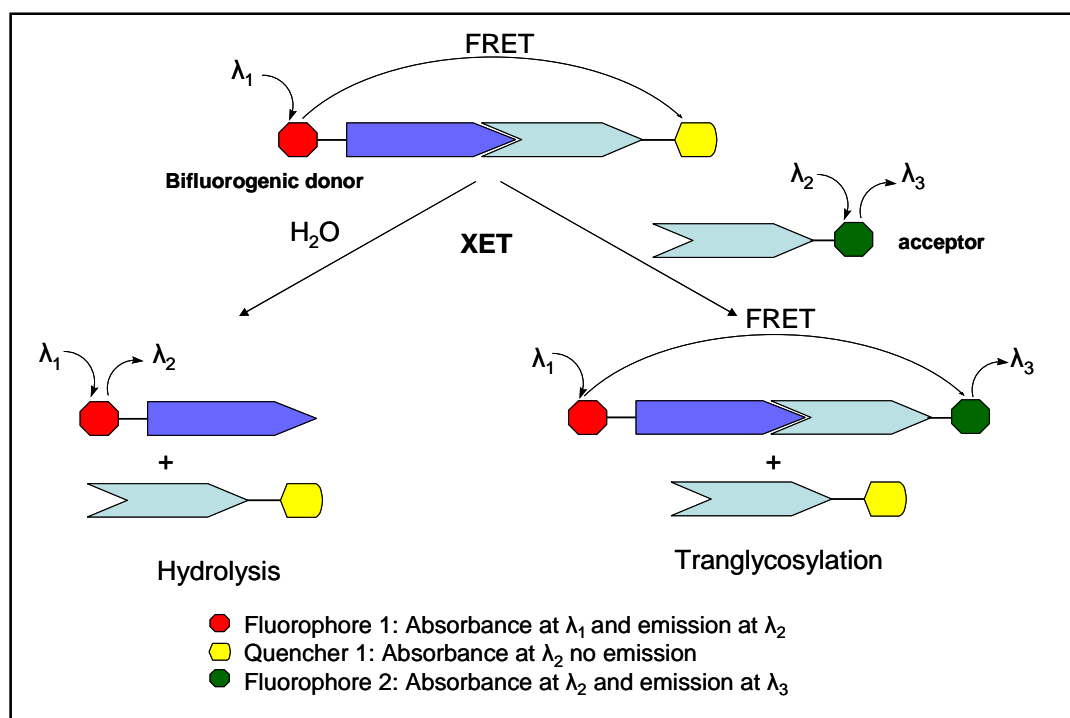


Figure 85: Schematic representation of design of FRET substrate to determine XTH hydrolytic and transglycosylase activity in a single experiment.

When hydrolysis occurs the non reducing fragment of the donor molecule is released separating fluorophore 1 and quencher 1, then irradiation at λ_1 renders emission at λ_2 . So hydrolysis could be measured monitoring only emission at λ_2 vs. time.

When transglycosylation to the acceptor carrying fluorophore 2 occurs, and fluorophore 1 was excited at λ_1 the energy was transferred by FRET to fluorophore 2 which will emit at λ_3 . Therefore transglycosylase activity could be measured by monitoring λ_3 vs. time.

With this combination of substrates both activities could be measured at the same time with only one experiment. Irradiation at λ_1 will not give any signal when no activity was produced, will give emission at λ_2 when hydrolysis is produced and will give emission at λ_3 when transglycosylation is occurring. For that reason, intensity of emission at λ_2 and λ_3 should be a direct measure of hydrolytic and transglycosylase activity, respectively.

To design these substrates we have taken into account the generated knowledge on XET specificity. For the donor we have proposed a XXXGXXXG (**23**) derived oligosaccharide. The quencher 1 should have a reactive amine group to be introduced on the reducing end of XXXGXXXG (**23**) by reductive amination taking advantage of the hemiacetal specific reactive group. To introduce the fluorophore 1 (donor's fluorophore) we have proposed to couple XXXGXXXG (**23**) to a 4th chemically modified cellobiose, concretely, we have proposed to use a 4-azido-4-deoxy-cellobiose, previously used with similar purposes¹⁷⁴. This azido group is an inactive precursor of a reactive amino group and a lot of commercially available fluorophores are designed to react with amines (isothiocyanates, imidates, etc.).

Fluorophore 2 (acceptor's one) should present again a reactive amine group because it is proposed to be introduced to the XXXG (**10**) reducing end by reductive amination.

Structural design for substrates is presented in Figure 86. In these substrates the distance between donor and quencher or donor and acceptor is approximately 50 Å, distance in which it is possible to observe FRET (10-100 Å).

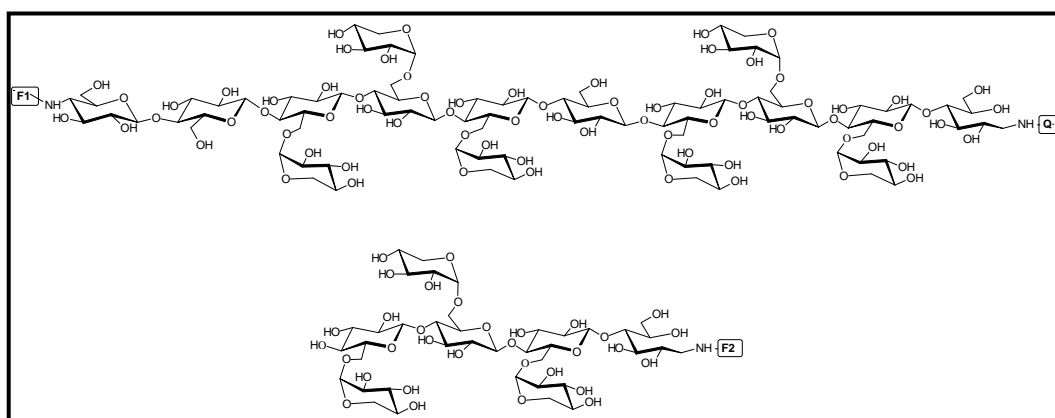


Figure 86: Structure of donor and acceptor designed for XTHs FRET assay. F1 is fluorophore 1, F2 is the fluorophore 2 and Q is the quencher 1.

The second step in FRET substrates design is to find the ideal combination of fluorophores and quencher for both substrates (donor and acceptor). Fluorophore 1 (donor's fluorophore) should absorb at a wavelength λ_1 different from λ_2 and λ_3 . And it should emit at λ_2 different from λ_3 , and it should react with amino groups. Donor's quencher should have a good overlap between its absorbance spectra and emission spectra of fluorophore 1, that is, it should absorb at λ_2 , without any fluorescence emission, and should contain a reactive amino group. Finally, fluorophore 2 should absorb at λ_2 without absorbance at λ_1 and at the same time emit at λ_3 different from λ_1 and λ_2 , and it should contain a reactive amino group.

The final proposal of adequate fluorophores and quencher is presented in Table 10, they were chosen taking into account their water solubility, pH dependence and spectroscopic properties:

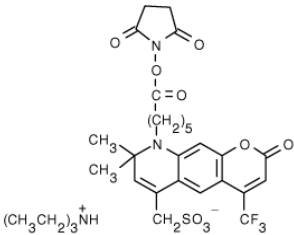
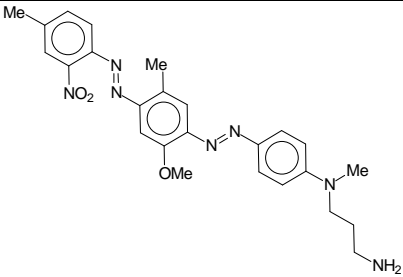
	Fluorophore-1	Quencher	Fluorophore-2
Name	AlexaFluor [®] 430	BHQ-1	AlexaFluor [®] 555
Provider	Invitrogen	Biosearch Technologies	Invitrogen
Structure			
λ max absorbance	430 nm	534 nm	555 nm
Range of absorbance		480-580 nm	
λ max emission	545 nm		572 nm

Table 10: Structures and spectroscopic properties of proposed fluorophores and quencher.

The problem is that all of them are very expensive and are sold in little quantities, making impossible to obtain them for normal chemical reactions.

For that reason it has been decided to design another substrate to use it as proof of concept, using more reasonable proves.

3.- FRET substrate design II.

In this second design, hydrolase and transglycosylase activities will be measured in two different assays.

Donor substrate will have a fluorophore in the reducing end and a quencher in the non reducing end (Figure 87).

When the activity assay is done without acceptor we would monitor the hydrolytic activity, measuring emission at λ_2 vs. time. When the activity assay is performed with acceptor we would monitor the hydrolytic + transglycosylase *XTH* activity, measuring emission at λ_2 vs. time (Figure 87). With both experiments we would be able to obtain comparative measures of hydrolytic and transglycosylase activity of different *XTHs*.

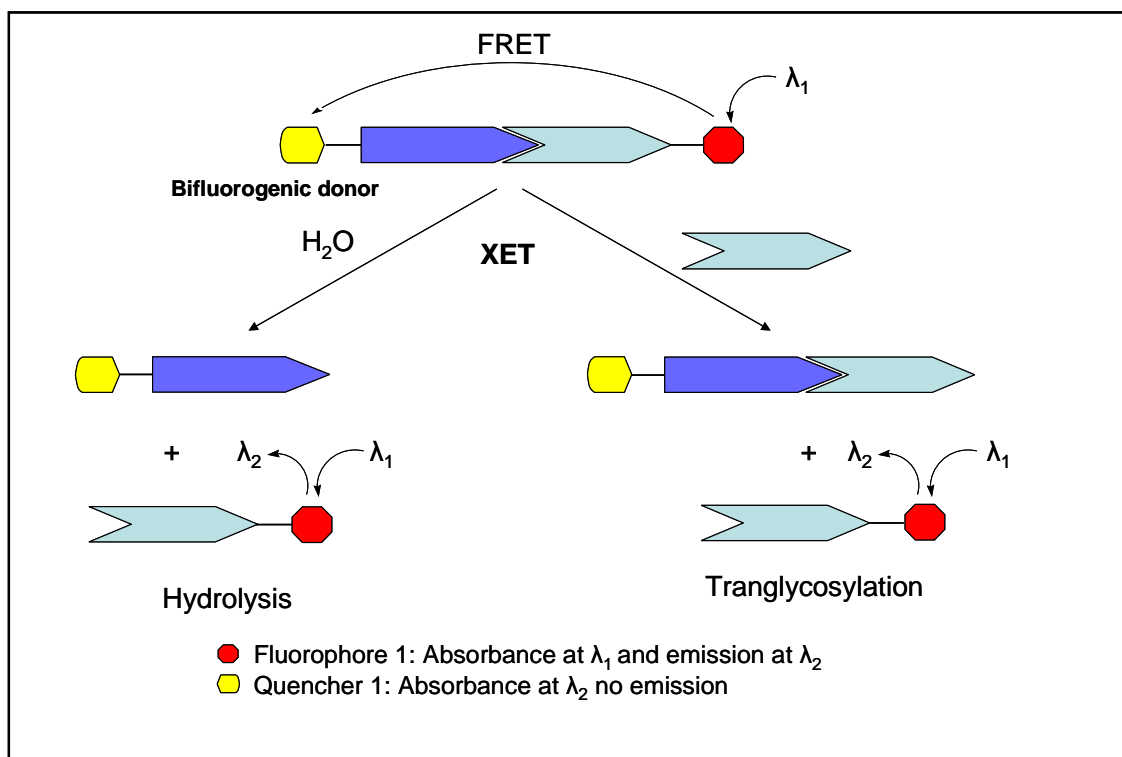


Figure 87: Schematic representation of second design of FRET substrates to determine *XTH* hydrolytically and transglycosylase activity.

The proposed substrate, similar to which it has been proposed in FRET substrate design I, was Q-NH-GG-XXXG-XXXG-F presented in Figure 88.

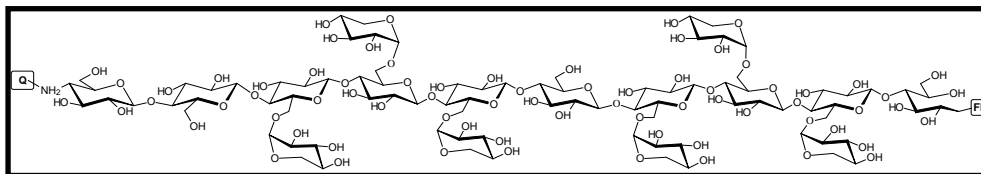


Figure 88: General structure of proposed bifluorogenic donor. Q is the quencher and FI is the fluorophore.

In the search for different fluorophores / quenchers, it has been chosen the commercially available fluorophore: 5-((2-aminoethyl)amino)naphthalene-1-sulfonic acid, sodium salt (EDANS) and two possible quenchers able to react with amino groups: 4-dimethylaminoazobenzene-4'-isothiocyanate (DABITC) and Fluorescein isothiocyanate Isomer I (FITC) (Table 11). The latter is normally considered a fluorophore but at low pH (pH 5.5, maximum activity of *Ptt*-XET16A) it seems not to be very fluorescent and maybe it can be used as quencher.

Combinations of EDANS and DABITC (or other derivatives) and fluorescein were widely used for proteases substrates or DNA probes¹⁸⁶. Although the R_0 described for these FRET pair is 41 Å (EDANS-DAB) and 44.5 Å (EDANS-fluorescein)¹⁸⁵ and the distance between fluorophore and quencher in the designed substrate is approximately 50 Å, it is expected that some quenching occurs and we should be able to detect an increase in fluorescence.

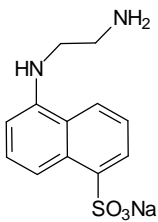
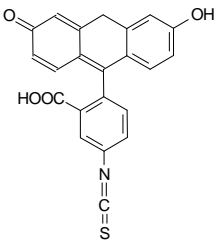
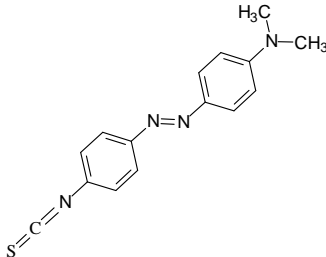
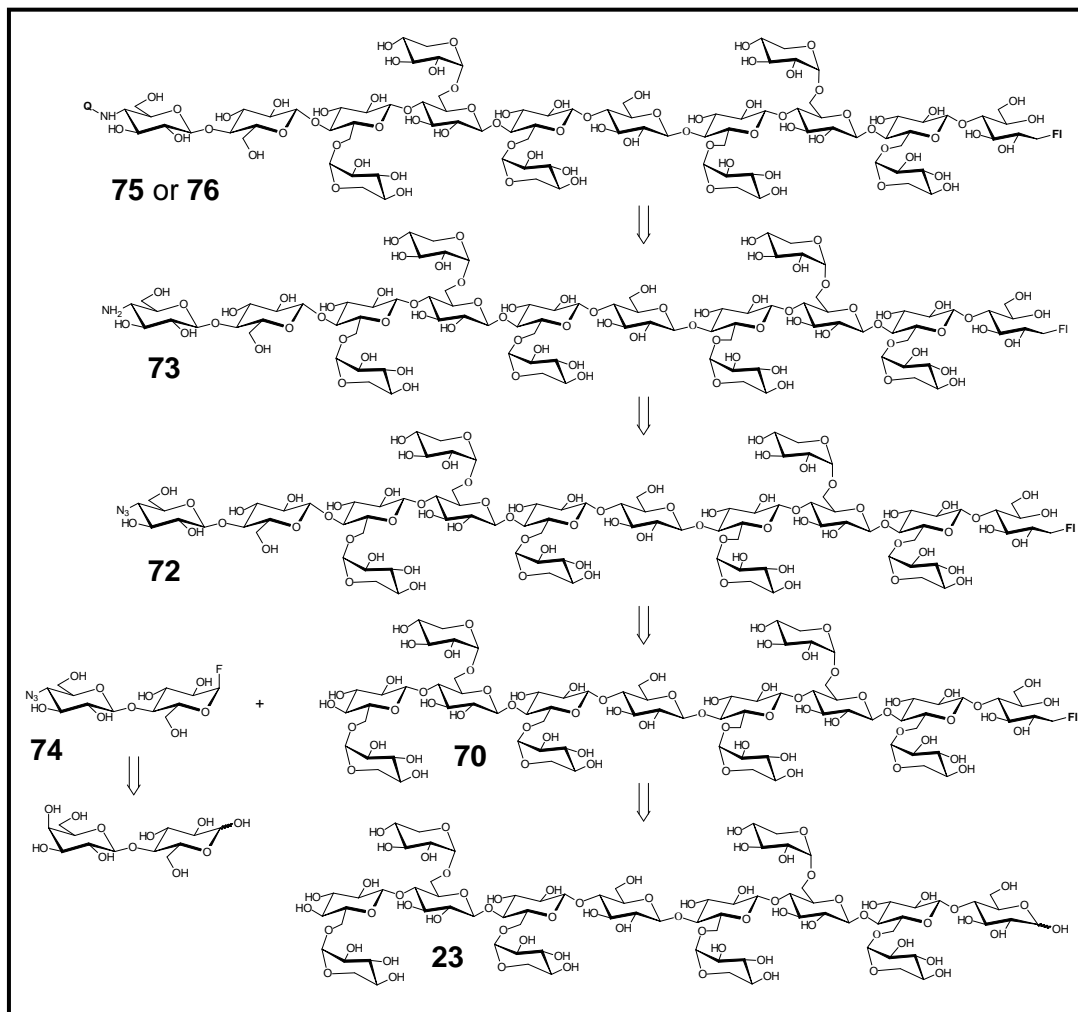
	Fluorophore 1	Quencher option1	Quencher option2
Name	EDANS	FITC	DABITC
Structure			
λ max absorbance	335 nm	490 nm	460 nm
λ max emission	498 nm	514 nm	None

Table 11: Structure and spectroscopic properties of chosen fluorophore and quenchers.

The retro-synthetic strategy proposed to obtain this substrate is presented in the Scheme 48. The final product can be obtained by labeling the nonreducing end amino group of **73** with the adequate quencher (DABITC or FITC), this amino group can be obtained from the azido derivative of **72**. This compound (**72**) can be obtained by a concurrent synthetic strategy by enzymatic coupling of two building blocks: the fluoride of the azido derivative of cellobiose (**74**) with the labeled tetradecasaccharide (**70**).

The labeled tetradecasaccharide can be obtained by reductive amination with EDANS of the tetradecasaccharide **23**. XXXGXXXG (**23**) can be obtained from XG polymer from Tamarind seeds as it is described in this work.

The 4-azido-4-deoxy-cellobiosyl fluoride (**74**) can be synthesized from lactose as described by Baer et al.¹⁸⁷.



Scheme 48: Retro synthetic analysis of the bifluorogenic donor. Q is the quencher (DABITC or FITC) and FI, the fluorophore (EDANS).

Therefore, this convergent synthesis was done in three blocks: 4-azido-4-deoxy-cellobiosyl fluoride (**74**) synthesis, XXXXGXXXG-EDANS (**70**) synthesis, coupling of these building blocks and final labeling.

4.- Synthesis of FRET substrates.

4.1.- Synthesis of 4-azido-4-deoxy-cellobiosyl fluoride (74).

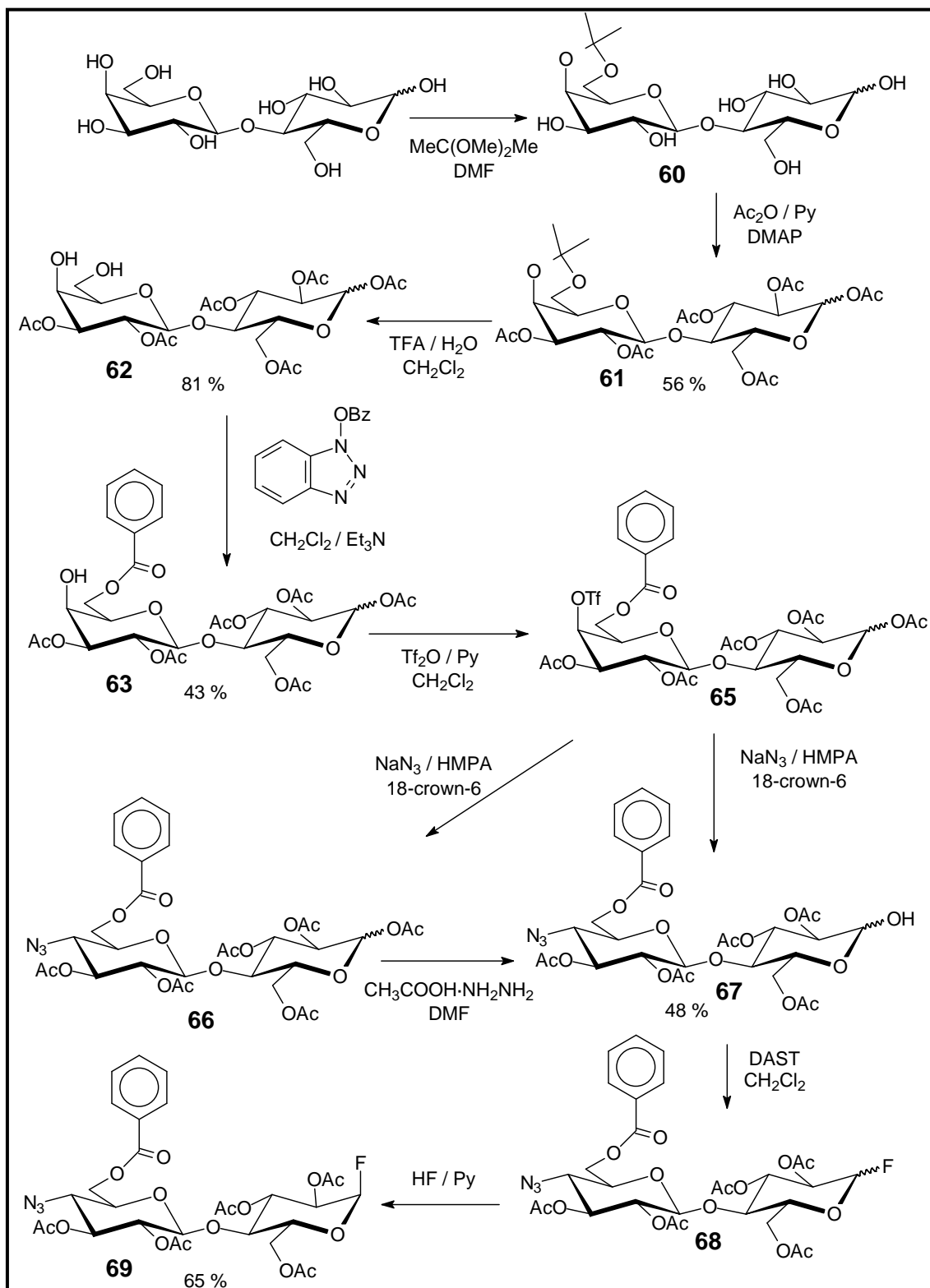
The first part of the synthesis is the obtaining of the of 4-azido-4-deoxy-cellobiosyl fluoride (**74**), following the synthetic pathway described previously¹⁷⁴ (Scheme 49).

In detail, starting from lactose we are able to obtain the diol **62** in three steps, as it was described by Baer *et al.*¹⁸⁷ in 45% overall yield.

First step is the selective protection of 4^{II}, 6^{II} with an isopropylidene group using dimoxypropane in DMF/H⁺ to obtain **60**, followed by complete hydroxyl acetylation by Ac₂O/Py treatment obtaining **61** after purification in 56% yield. The isopropylidene group was removed by acidic treatment (TFA 10%), obtaining the diol **62** in 81% yield upon purification. Part of the totally protected starting material **61** was recovered, because reaction was stopped before completion due to byproducts formation. All these products were identified by TLC comparison with the corresponding standards.

The following step is the 6^{II}-OH selective protection of **62** with a benzoate group using 1-(benzoyloxy)-benzotriazole¹⁸⁸ obtaining **63** in 43% yield after purification. Another product with the same molecular mass but different R_f was also isolated. It was proposed to be 4-benzoylated isomer **64** of **63** obtained in 10% yield.

63 and **64** were characterized by mass spectrometry obtaining a molecular mass [M+Na] of 721, theoretical 721.63. The product of interest **63** was characterized by NMR: in the ¹H-NMR spectra a multiplet at 8.04-7.46 corresponding to aromatic protons of benzoil group was observed which indicates the presence of benzoil group. One singlet at 6.22 ppm and one doubled (J_{1,2}=6Hz) at 5.65 ppm were detected corresponding to anomeric protons of Glc^I of both isomers α and β, respectively. One multiplet was detected between 2.13-1.15 ppm corresponding to 18 protons from 6 acetyl groups demonstrating that 6 hydroxyl groups were acetylated. In the ¹³C-NMR spectra different signals were observed: between 170.3 and 166.3 signals of CO group of acetyls and CO from benzoyl group; between 133.6 and 128.6 signals of aromatic carbons of benzoyl group; at 101.1 ppm Gal anomeric carbon's signal; at 91.6 and 89.0 signal of Glc anomeric carbon for α and β isomers; between 75.5 and 61.4 ppm signal of carbohydrate ring carbons.



Scheme 49: Synthesis of protected 4-azido-4-deoxy- α -D-cellobiosyl fluoride (74).

The 4^{II} position of compound **63** was activated with a triflate group which was displaced by sodium azide in HMPA¹⁸⁹, obtaining a mixture of products **66** and **67** as confirmed by mass spectrometry (746 and 704 respectively), both presenting the azido group. Soli *et al.*¹⁸⁹ have described the substitution of the triflate group by azide but they have observed simultaneously deprotection of the anomeric position. In our case, this anomeric deprotection was not totally achieved although reaction times, temperatures, and reagents concentration were increased.

Anomeric position of product **66** was deprotected to obtain only product **67** by hydrazine acetate treatment¹⁹⁰ obtaining the product **67** with an overall yield of 48% from product **63**. 2,3-di-O-acetyl-4-azido-4-deoxy-6-benzoyl- β -D-glucopyranosyl-(1 \rightarrow 4)-2,3,6-tri-O-acetyl- α/β -glucopyranose (**67**) was identified by NMR: ¹H-NMR spectrum showed between 8.07 and 7.47 ppm a multiplet which correspond to the 5 aromatic protons of benzoil group, at 5.48 ppm a triplet ($J_{1,2}=9.8$ Hz) and at 5.34 ppm a doublet ($J_{1,2}=3.6$ Hz) were observed which correspond to anomeric proton of Glc ^{β} and Glc ^{α} respectively. Finally between 2.09 and 1.89 a multipled was observed corresponding to the 15 protons of 5 acetyl groups. In the ¹³C-NMR spectrum a multiplet between 170.9-166.1 ppm was observed which corresponds to the 6 carbonyl carbons of five acetyl and one benzoyl groups, another multiplet between 133.8 and 128.8 ppm was observed corresponding to 6 aromatic carbons of benzoyl group. Three anomeric carbons were identified at 100.8 ppm corresponding to C-1 of Glc ^{β} and at 95.4 and 90.2 corresponding to C-1 of Glc ^{α,β} . Between 62.0 and 61.8 ppm signals assigned to C-6 of Glc ^{β} were observed and finally, the signal at 60.1 ppm was assigned to C-4 of Glc ^{β} which demonstrates introduction of azido group at C-4. **67** was also characterized by mass spectrometry obtaining a molecular mass [M+Na] of 704, theoretical 704.6.

Finally, the azido derivative was activated for transglycosylation as α -fluoride by initial fluorination with DAST¹⁹¹ followed by isomerization with HF/Py. First step, DAST fluorination, rendered the α/β mixture **68** identified by NMR: in the ¹H-NMR spectra the doublet of doublets (dd) at 5.62 ppm ($J_{1,2}=2.7$ Hz and $J_{1,F}=53.7$ Hz) and the dd at 5.29 ppm ($J_{1,2}=5.4$ Hz and $J_{1,F}=58.2$ Hz) corresponding the anomeric proton of Glc ^{α,β} respectively, demonstrated the introduction of fluoride atom in α and β configuration (0.27:0.73 ratio). This α/β mixture (**68**) was characterized by mass spectrometry obtaining a molecular mass signal [M+NH₃] of 701, being the theoretical 701.6.

Second step, fluoride isomerization with HF/Py¹⁹² rendered the α anomer **69** in an overall yield of 65% from **67**. Per-O-acetylated α -4^{II}-azido-4^{II}-deoxy-cellobiosyl fluoride (**69**) was identified by NMR, detecting its characteristic signals: in the ¹H-NMR spectra it was observed at 5.65 ppm the dd ($J_{1,2}=2.7$ Hz and $J_{1,F}=53.1$ Hz) corresponding to the anomeric proton of α -glucosyl fluoride, also signals corresponding to 5 aromatic protons of the benzoyl group (8.07-7.48 ppm) and to 15 protons from 5 acetyl groups (2.07-1.86 ppm) were observed. In the ¹³C-NMR spectra the signal corresponding to C-4 of Glc^{II} substituted with an azido group was detected at 60.0 ppm. Signals of benzoyl aromatic carbons (133.6-128.7 ppm), benzoyl (165.9 ppm) and acetyl carbonyl carbons (170.4-169.6), Glc^I anomeric carbon (103.6 ppm, $J_{C,F}=218$ Hz) and Glc^{II} (100.6 ppm) were also identified. This α -fluoride **69** was also characterized by mass spectrometry obtaining a [M+Na] of 706, theoretical 706.6.

The α -fluoride **69** was fully deprotected by sodium methoxide/methanol treatment obtaining **74** quantitatively. **74** was characterized by mass spectrometry: a molecular mass plus sodium of 392 was obtained which is equivalent to expected molecular mass (392.3).

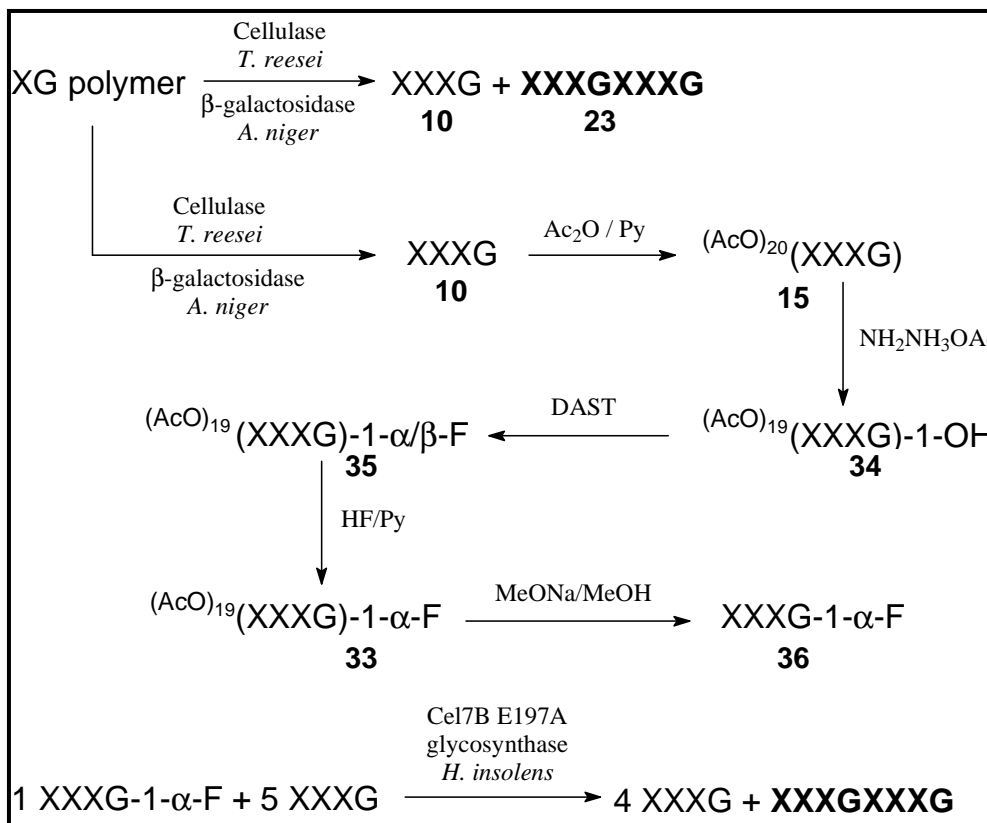
4.2.- Synthesis of XXXGXXXG-EDANS (70)

4.2.1.- Synthesis of XXXGXXXG (23).

The tetradecasaccharide XXXGXXXG (**23**) was obtained in this work using both methodologies presented in chapter 5 (p. 79) (Scheme 50). Using first methodology, controlled degradation of XG with cellulase from *T. reesei* and β -galactosidase from *A. niger*, XXXG (**10**) and XXXGXXXG (**23**) were isolated in 12% and 7 % yield respectively.

XXXG (**10**) was characterized by mass spectrometry obtaining a molecular mass [M+Na] of 1085.31 (theoretical 1085.3) and NMR which match with presented by Régis Fauré¹⁴⁶. Most representative signals in these NMR spectra are: ¹H-NMR: at 5.21 and 4.64 ppm two doublets, with $J_{1,2}=3.6$ and 7.8 Hz respectively, counting for 1 H together, corresponding to anomeric protons of α and β isomers of XXXG (**10**). At 4.92 ppm a complex signal was observed, having a relative area of three, corresponding to anomeric signals of xylosyl groups, and finally at 4.54 ppm another complex signal, having a relative area of three, corresponding to the anomeric signals of glucosyl groups (Glc^{II,III} and ^{IV}). ¹³C-NMR: At 102.3 and 102.0 ppm a complex signal corresponding to anomeric carbons of Glc^{II,III,IV}, at 98.3 ppm a complex signal

corresponding to anomeric carbons of Xyl^{II,III}, at 97.8 ppm a signal corresponding to C-1 of Xyl^{IV}, and finally at 95.2 and 91.3 ppm two signals corresponding to C-1 of Glc^{IB} and ^{Ia} respectively.



Scheme 50: XXXGXXXG (23) synthesis using both methodologies proposed by Régis Fauré^{133,146}.

Using second methodology, per-O-acetylated XXXG (**15**) was isolated from the reaction crude of extensive degradation of XG with cellulase from *T. reesei* and β -galactosidase from *A. niger* followed by acetylation in 40% yield as it was presented in chapter 2 (p. 70).

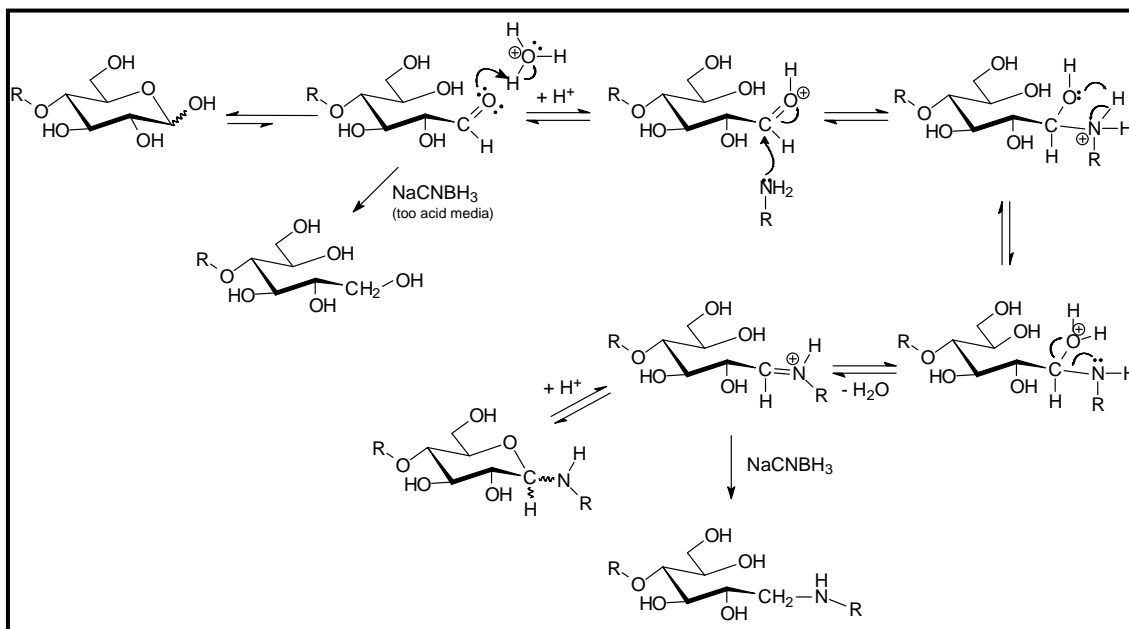
In this work, obtaining of XXXG α F (**36**) by anomeric deprotection, DAST fluorination, HF/Py anomerization and total de-O-acetylation was achieved with 42% yield from **15** over four synthetic steps.

XXXG α F (**36**) was coupled with XXXG (**10**) using the E197A Cel7B synthase maintaining a minimum molar ratio of 1:15 **36**:**10**, by three different additions of 56 μ moles of **36** in a solution of 860 μ moles of **10**. XXXGXXXG (**23**) was obtained after normal phase chromatography in 91% yield, all XXXG (**10**) in excess was recovered.

XXXGXXXG (**23**) obtained with both methods was characterized by mass spectrometry obtaining a molecular mass [M+Na] of 2129.56 (theoretical 2129.7) and by NMR which is equivalent to those obtained by Régis Faure¹⁴⁶: in the ¹H-NMR spectrum, the signal at 5.22 and 4.65 ($J_{1,2}=3.6$ and 7.8 Hz respectively) correspond to anomeric protons of α and β isomers of **23**. Signals corresponding to H-1 of 6 α -xylosyl groups and 6 β -glucosyl groups were observed at 4.93 and 4.53 ppm respectively. In the ¹³C-NMR, signals of anomeric carbons of Glc^{II,III,IV,V,VI,VII} and VIII were observed at 102.3 and 102.0-101.9 ppm. Signals of anomeric carbons of Xyl^{II,III,IV,VI,VII} and VIII were observed at 98.3-97.8 and 95.2 ppm, and signals of C-1 of Glc ^{β} and α were observed at 95.2 and 91.3 ppm respectively.

4.2.2.- EDANS labeling.

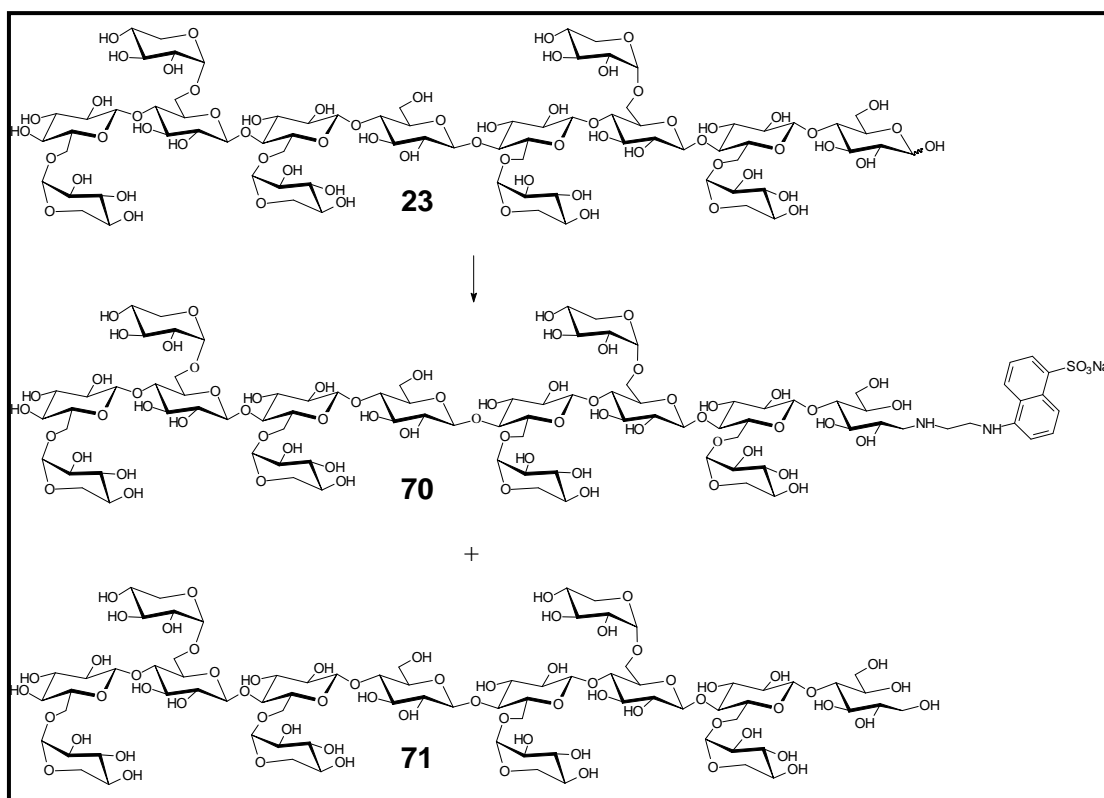
The tetradecasaccharide (**23**) was labeled with EDANS by reductive amination, reaction extensively used for analytical labeling of carbohydrates. This reaction is very sensitive to pH. At basic pH the reaction does not progress because there is an acid dependant step, but at pH<3 there is a competing reaction, reduction of carbohydrate to render de alditol (Scheme 51)¹⁹³⁻¹⁹⁵.



Scheme 51: Mechanism of reductive amination of carbohydrates and competing reactions.

EDANS labeling of XXXGXXXG (**23**) was especially difficult due to EDANS insolubility at acidic pH, and the difficulty to control apparent pH of reaction taking into account it consumes H⁺ and reaction stops at high pH values. Different combinations of solvents were evaluated (water/DMF/AcOH and water/THF/AcOH), obtaining quite similar results. Finally, the later one was used, regulating pH near 4-5 by addition of AcOH.

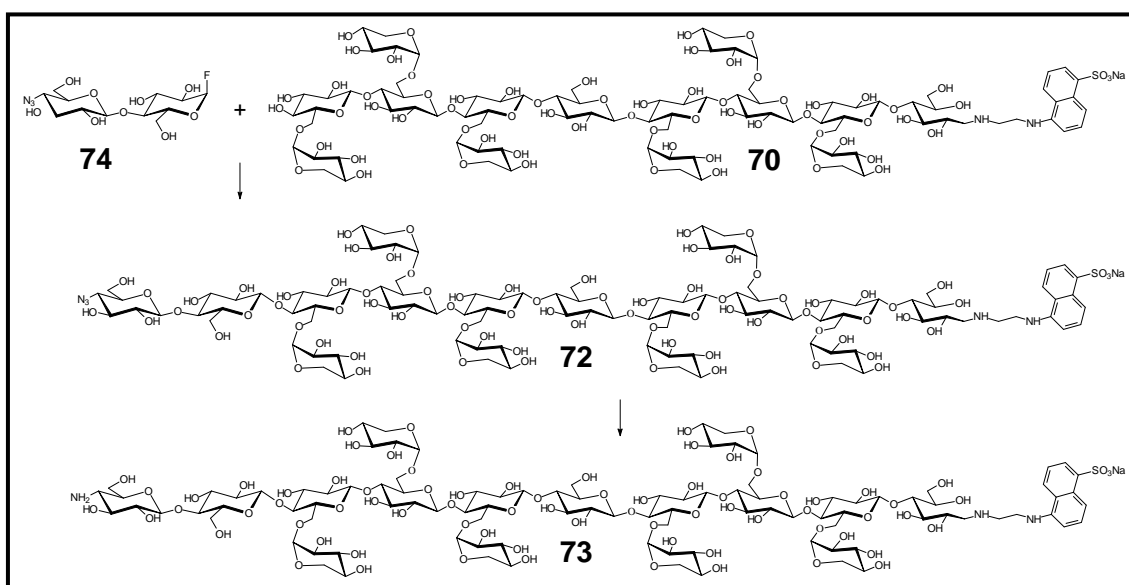
After reaction, main impurities of EDANS labeled tetradecasaccharide **70** were excess of EDANS and tetradecasaccharide alditol **71** (Scheme 52). XXXGXXXGEDANS (**70**) was purified from excess EDANS by normal phase chromatography and from XXXGXXXG alditol (**71**) by reverse phase chromatography obtaining **70** in 36% yield. XXXGXXXGEDANS (**70**) was characterized by mass spectrometry obtaining a molecular mass [M+Na] of 2401.7 matching exactly with theoretical molecular mass.



Scheme 52: EDANS labeling of the tetradecasaccharide XXXGXXXG
(**23**)

4.3.- Coupling of 74 with 70 and final labeling.

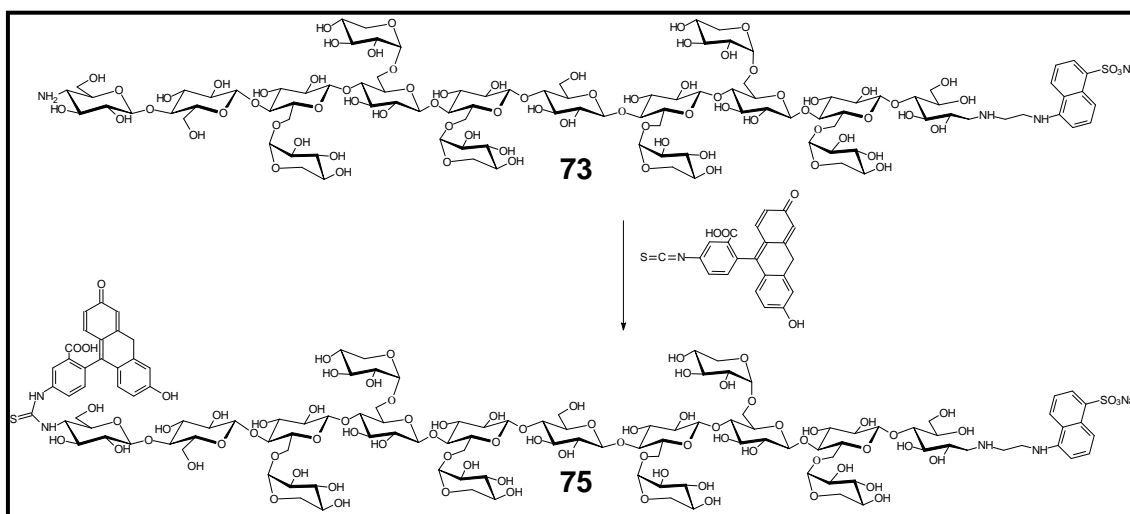
The XXXGXXXG-EDANS (**70**) was coupled with the 4-azido-4-deoxy- α -D-cellobiosyl fluoride (**74**) using the E197A Cel7B synthase (from *H. insolens*) (Scheme 53) and purified by reverse phase chromatography. The coupling product **72**, isolated in 83% yield, was characterized by mass spectrometry obtaining a molecular mass [M+Na] of 2751.7 (theoretical 2750.8).



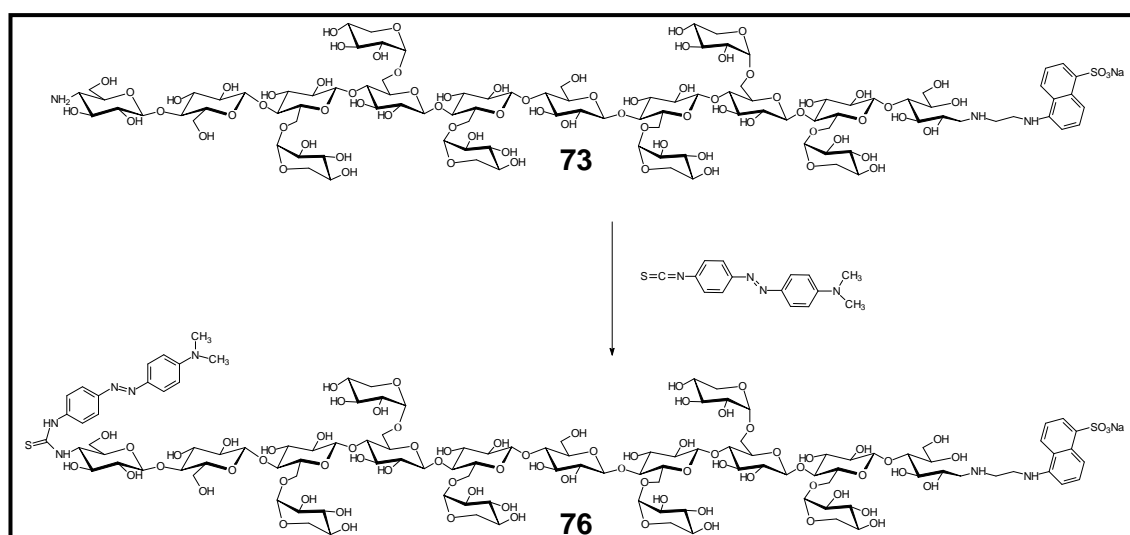
Scheme 53: Coupling of XXXGXXXGEDANS (70**) and 4-azido- α -D-cellobiosyl fluoride (**74**) and posterior modification of azido group to amino group.**

After that, the azido group of **72** was reduced to amino group by H_2S in $\text{Py}/\text{H}_2\text{O}^{196}$ obtaining **73** in 97% yield (Scheme 53), which was characterized by mass spectrometry obtaining a molecular mass [M+Na] 2725.41 (theoretical 2724.86). **73** was used without further purification for coupling with the correspondent isothiocyanate label (FITC or DABITC)¹⁷⁴.

DABITC and FITC labeling are widely described for oligonucleotides and protein labeling where is not necessary to assure total labeling or extensive purification of labeled product. However, some examples describe preparative DABITC or FITC labeling of carbohydrates. Concretely, Cottaz *et al.* and Boyer *et al.* used $\text{DMF}/\text{NaHCO}_3$ (aq) to label similar deoxy-azido carbohydrates with DABITC with acceptable yields^{174,177}. Similar conditions were used to FITC (Scheme 54) and DABITC (Scheme 55) labeling of **73**.



Scheme 54: Fluorescein labeling of NH₂-GGXXXGXXXG-EDANS (73**)**



Scheme 55: DAB labeling of NH₂-GGXXXGXXXG-EDANS (73**)**

Preliminary experiments varying temperature showed, by TLC, the formation of at least two different saccharidic products for each labeling reaction. DAB labeled product (**76**) was detected by mass spectrometry in partially purified fractions of reaction crude, in contrast, fluorescein labeled product (**75**) was not detected in any partially purified fraction of its reaction crude.

For that reason, we have decided to continue the synthesis only to obtain the DAB-GG-XXXG-XXXG-EDANS (**76**) substrate.

A lot of difficulties were found on purification of this product. Normal phase chromatography, reverse phase chromatography and gel filtration chromatography were assayed and only using the last one both carbohydrate reaction products could be isolated.

As conclusion it could be stated that DAB labeling of $\text{NH}_2\text{-GGXXXGXXXG-EDANS}$ (**73**) was achieved in 21 % yield. $\text{DAB-GG-XXXGXXXG-EDANS}$ (**76**) was characterized by mass spectrometry obtaining a molecular mass $[\text{M-Na}] = 2963.01$, theoretical 2962.79.

5.- Ptt-XET16A FRET assays.

5.1.- Preliminary fluorescence assays with 76.

Once the FRET substrate synthesis was achieved, it has to be demonstrated if this substrate was adequate to measure both hydrolytic and transglycosylation activities.

First of all, determination of absorbance and emission spectra of XXXGXXXGEDANS (**70**), and absorbance spectra of DABITC were done as it is showed in the following picture (Figure 89). It can be observed that DABITC absorbs at maximum emission wavelength of **70**. Therefore, if distance and orientation conditions are accomplished, FRET quenching was expected to occur.

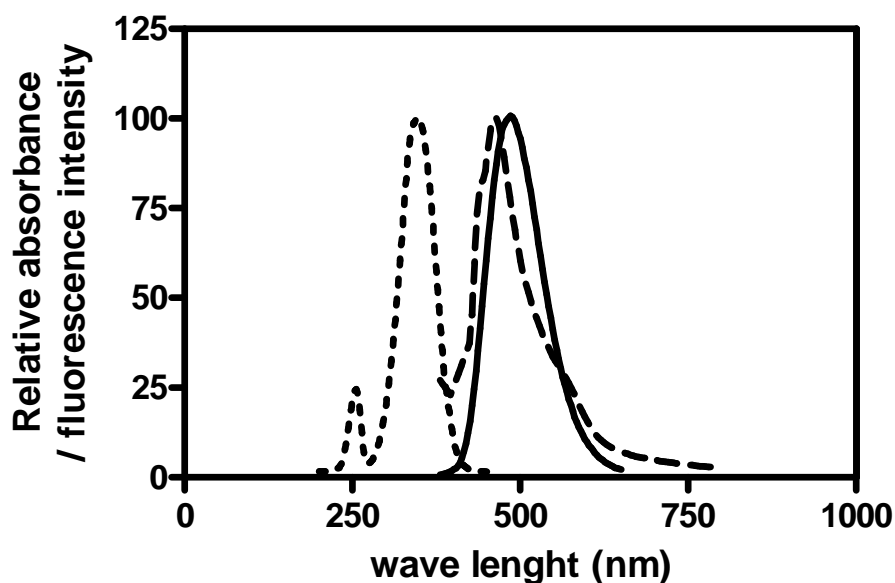


Figure 89: UV absorbance spectra of DABITC (dashed), fluorescence emission spectra of XXXGXXXGEDANS (**70**) ($\lambda_{exc}=345$ nm) (black) and fluorescence absorbance spectra of **70** ($\lambda_{em}=485$ nm) (pointed).

5.2.- Fluorescence characterization of FRET substrate 76.

Comparing intensity of emission at 485 nm of XXXGXXXG-EDANS (**70**) and DAB-GGXXXGXXXG-EDANS (**76**) ($\lambda_{exc}=345$ nm) (Figure 90), FRET efficiency was calculated ($E=1-I/I_0$ where I and I_0 are the fluorescence intensities of 5 μ M solutions of **76** and **70** respectively at 485 nm). Surprisingly, it was obtained a FRET efficiency of **0.97** which was unexpectedly high taking into account the distance between DAB and EDANS group in substrate **76** (50 nm approximately) and FRET efficiencies described for shorter substrates 0.91 (25 Å between DAB and EDANS labels)¹⁷⁷.

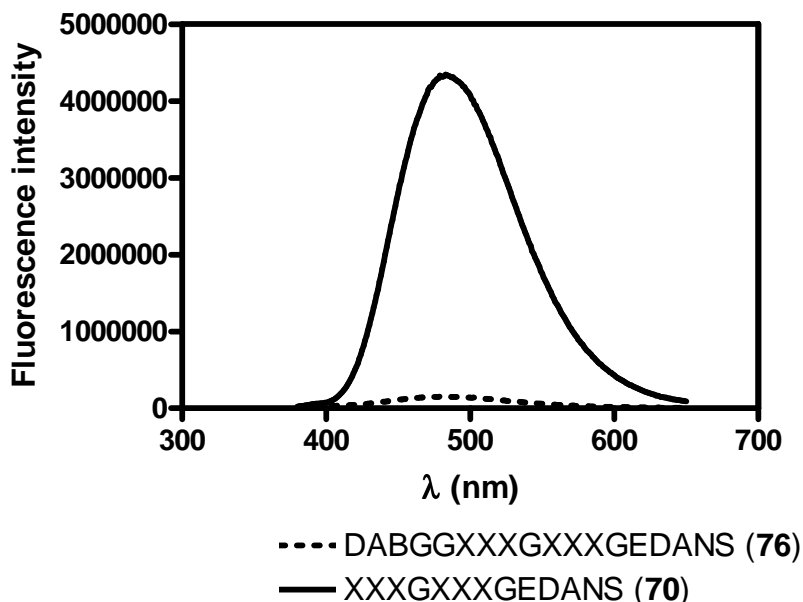
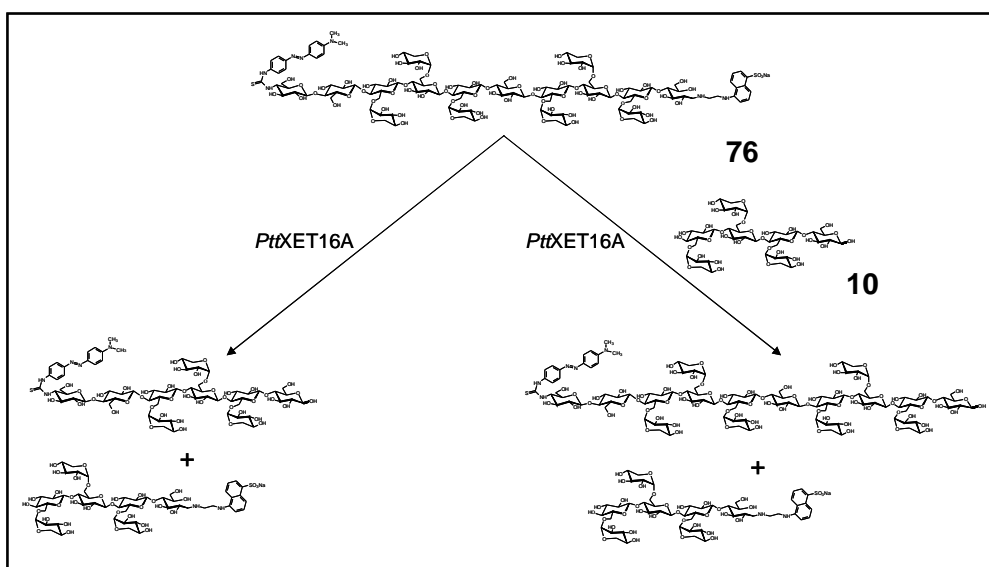


Figure 90: Emission spectra for XXXGXXXG-EDANS (**70**) and DAB-GGXXXGXXXG-EDANS (**76**) ($\lambda_{exc}= 345$ nm (10 nm slit), $\lambda_{em}= 485$ nm (5 nm slit)).

5.3.- Kinetic assays using DAB-GGXXXGXXXG-EDANS (76).

Different conditions (substrate concentration, enzyme concentration, etc.) were assayed to measure *Ptt*-XET16A hydrolytical and transglycosylase activities using **76** and **76+10** as substrates respectively (Scheme 56) as it is described in Table 12.



Scheme 56: *Ptt*-XET16A catalyzed hydrolytic and transglycosylase reaction with DABGGXXXGXXXGEDANS (76) substrate.

DABGGXXXGXXXGEDANS (76) (μM)	XXXG (10) (μM)	[<i>Ptt</i> -XET16A] (μM)
2	0	0.3
5	0	0.3
10	0	0.3
2	5	0.3
5	5	0.3
2	25	0.3
5	25	0.3
10	25	0.3
5	25	0.03
5	25	0.003

Table 12: FRET experiments performed at different substrate and enzyme concentrations (excitation wavelength 345 nm emission wavelength 485 nm)

Unfortunately, we are not able to detect a significant increase in fluorescence intensity in any experiment done.

Three hypothesis were proposed to explain these negative results:

- DABGGXXXGXXXGoI-EDANS (**76**) is not substrate for *Ptt*-XET16A
- The byproduct of *Ptt*-XET16A reaction with DABGGXXXGXXXG-EDANS (**76**) (XXXG-EDANS) is not fluorescent.
- Fluorescence of XXXG-EDANS is quenched by some component of the reaction mixture.

To discard any intramolecular quenching phenomena (between reaction byproduct XXXG-EDANS and another reaction-mixture component such as *Ptt*-XET16A and/or XXXG (**10**) and/or buffer), fluorescence intensities at 485 nm (excitation 345 nm) of different concentration of XXXGXXXGEDANS (**70**) adding different reaction components (XXXG (**10**), *Ptt*-XET16A, buffer) were recorded.

[XXXGXXXGEDANS (70) (μM)	Citrate:phosphate buffer (mM)	[<i>Ptt</i> - XET16A] (μM)	[XXXG(10)] (μM)	Fluorescence intensity
5	-	-	-	4326997
5	50:50	0.3	25	4572187
0.5	-	-	-	396370
0.5	50:50	0.3	25	373290
0.05	-	-	-	40480
0.05	50:50	0.3	25	43370

Table 13: Fluorescence intensities at 485 nm (excitation 345 nm) XXXGXXXG-EDANS (70**) solutions in water and XXXGXXXG-EDANS (**70**) + 0.3 μM *Ptt*-XET16A + 25 μM XXXG (**10**) solutions in citrate phosphate buffer 50 : 50 mM pH 5.5 30°C.**

Fluorescence intensity variations detected in the intramolecular quenching experiments, due to the addition of 0.3 μM *Ptt*-XET16A, 25 μM XXXG (**10**), and citrate:phosphate buffer 50:50 mM pH 5.5 I=0.5 M, were within ± 7 % assignable to experimental variability, therefore intramolecular quenching was discarded.

To demonstrate that XXXG-EDANS is a fluorescent product, a hydrolytic reaction on DABGGXXXGXXXG-EDANS (**76**) using a cellulase from *Trichoderma reesei* and a cellulase from *Aspergillus niger* were monitored by fluorescence emission. No increase in fluorescence intensity at 485 nm was detected, reaction mixtures were analyzed by TLC and no fluorescent spot was detected although two saccharidic spots were observed.

In accordance to these results and taking into account that we have observed fluorescence since the isolation of **76**, it was proposed that in the last reaction step (DAB labeling) or in the purification protocol used to obtain **76** something was happened to EDANS label provoking that it lost its fluorescence.

As conclusion, although DABGGXXXGXXXG-EDANS (**76**) was synthesized and characterized by mass spectrometry, something had happened to the EDANS label that makes it no longer fluorescent. For that reason, we are not able to demonstrate if DABGGXXXGXXXG-EDANS is an adequate substrate to monitor hydrolytical and transglycosylase activities of *XTHs* or not.

.

CONCLUSIONS

CONCLUSIONS:

The presented work was done in the Institut Químic de Sarrià within a the European project E.D.E.N. to study the xyloglucan endotransglycosylase *Ptt*-XET16A from *Populus tremula x tremuloides*.

1. *Ptt*-XET16A gene was cloned into two plasmids for expression in *Escherichia coli*, pD62XEt16A and pET15XET16A. All expression attempts were unsuccessful.

2. On the search of new activity assays to monitor xyloglucan endotransglycosylase activities (XET), different substrates were synthesized and evaluated as putative substrates for *Ptt*-XET16A:

a) A mixture of 8-aminonaphtalene-1,3,6-trisulphonic acid (ANTS) labeled xyloglucan oligosaccharides (XGOs) was obtained in 6% overall yield from xyloglucan and was proved to be an acceptor substrate for *Ptt*-XET16A using xyloglucan as donor. The XGOs-ANTS (**25**, **26+27**, and **28**) mixture was used to optimize a new activity assay based on high performance capillary electrophoresis (HPCE) to monitor XET activity using low molecular weight substrates.

b) The β -fluorides GG β F (**1**, 87% yield), XG β F (**2**), and XXXG β F (**14**, 12% yield) were synthesized and evaluated as putative new donor substrates using the developed HPCE assay and a fluoride selective electrode method but none of them were substrates for *Ptt*-XET16A.

c) Different xylogluco-oligosaccharides (XGGG(**18**), XGXGGG(**19**), XGXGXGGG (**20**), XXXGGG (**21**), XXXGXXXGGG (**22**), XXXGXXXG (**23**) and XXXGXXXGXXXG (**24**)), synthesized by Régis Fauré at CERMAV, were evaluated as putative *Ptt*-XET16A donors using the developed HPCE assay and only with XXXGGG, XXXGXXXG and XXXGXXXGXXXG some XET activity was detected.

d) XXXGANTS (**25**) was synthesized in a semi preparative scale from xyloglucan in 22% yield, being the first published description of semi-preparative synthesis of ANTS labeled oligosaccharides. This labeled substrate was used as standard acceptor for *Ptt*-XET16A catalyzed transglycosylation of a large set of low molecular weight donors.

3. *Ptt*-XET16A was kinetically characterized using the developed HPCE assay with XXXGXXXG (**23**) and XXXGANTS (**25**) as donor and acceptor substrates respectively. Maximum activity was found between pH 5.0-5.5 and 30-40 °C.

It is demonstrated that *Ptt*-XET16A follows a ping-pong *bi bi* kinetic mechanism, where acceptor (XXXG-ANTS(**25**)) acts as competitive inhibitor of donor binding to the free enzyme and donor (XXXGXXXG(**23**)) acts as competitive inhibitor of acceptor binding to the acceptor subsites of glycosyl-enzyme intermediate. The kinetic parameter obtained were: $k_{\text{cat}} = 0.45 \pm 0.04 \text{ s}^{-1}$, $K_{\text{M,AB}} = 0.37 \pm 0.09 \text{ mM}$, $K_{\text{M,C}} = 1.9 \pm 0.3 \text{ mM}$, $K_{\text{I,AB}} = 1.0 \pm 0.1 \text{ mM}$, and $K_{\text{I,C}} = 1.5 \pm 0.4 \text{ mM}$. However, side reactions such as donor self-condensation and product elongation causes some deviation from the model at high donor:acceptor concentration ratio.

Ptt-XET16A ping-pong *bi bi* kinetic mechanism was demonstrated again using the standard acceptor XXXG-ANTS (**25**) and a non-reducing-end-blocked donor (GalGXXXGXXXG (**38**)) as substrates to avoid putative side reactions (donor polymerization and product elongation). In this case, only competitive acceptor inhibition obtaining a simpler kinetic model with the following kinetic parameters: $k_{\text{cat}} = 4.8 \pm 0.3 \text{ s}^{-1}$, $K_{\text{M,AB}} = 2.8 \pm 0.2 \text{ mM}$, $K_{\text{M,C}} = 1.1 \pm 0.1 \text{ mM}$ and $K_{\text{I,C}} = 1.7 \pm 0.2 \text{ mM}$.

4. A library of xylogluco-oligosaccharide donors was designed to study *Ptt*-XET16A substrate specificity with the final objective of mapping the subsites in the binding cleft. This donor library was synthesized by Régis Fauré at CERMAV.

a) After identification of the transglycosylation products using the standard ANTS-labeled heptasaccharide acceptor (XXXGANTS (**25**)) and different xylogluco-oligosaccharide donor substrates it is concluded that:

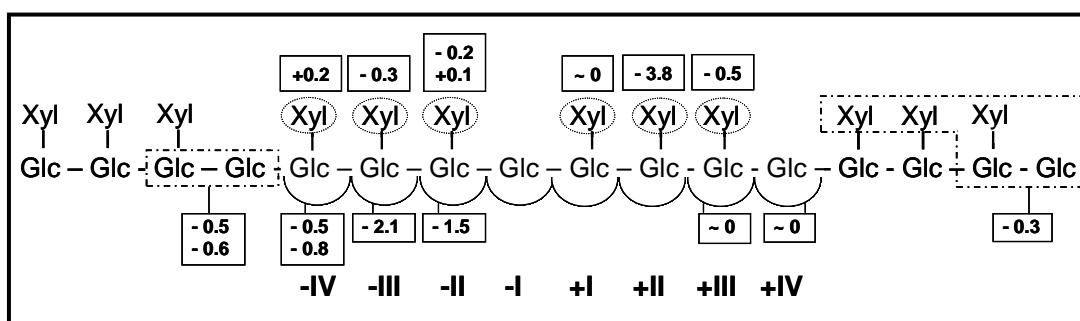
i) The donor scissile bond for transfer to the acceptor is always the glycosidic bond at an unbranched glycosyl unit: if more than one unbranched glycosyl unit is present in the donor, different transfers can be observed.

ii) Binding affinity is higher for xyloglucan like structures on positive subsites than in negative ones, therefore substrates with xyloglucan-like structures to be located in positive subsites are better donors than their isomers having this XG-like structure to be located in negative subsites.

iii) Donors that have consecutive non-branched glucosyl units and at the same time are good substrates render different products which arise from bond cleavage at each unsubstituted glucosyl unit, except for the terminal glucosyl unit on the non-reducing end.

iv) Oligomerization reactions arising from multiple transfers were observed for good substrates because the first transglycosylation product is accumulated in enough concentration to compete with the acceptor.

b) Steady state kinetics with donors within the library and the standard acceptor (XXXG-ANTS (**25**)) render k_{cat}/K_M values for each donor. Thermodynamic cycles were constructed relating different donors and the contribution of individual subsites to transition state stabilization was calculated as the difference in transition state activation energy between two substrates ($\Delta\Delta G^\ddagger$) differing in the occupancy of the evaluated individual subsite. Contribution of each subsite to transition state stabilization is summarized in the following figure (as $\Delta\Delta G^\ddagger$ in kcal/mol).



5. A new activity assay to monitor hydrolase and transglycosylase activities of *XTHs* based on fluorescence resonance energy transfer (FRET) was designed. The bilabeled FRET substrate DAB-GGXXXGXXXG-EDANS (**76**) was synthesized and characterized by mass spectrometry. However, it could not be demonstrated if it is an adequate substrate to measure *XTH* hydrolase and transglycosylase activities, because the fluorescent properties of EDANS label were lost during substrate synthesis.

EXPERIMENTAL PART

1.- Cloning of <i>Ptt</i> -XET16A for Escherichia coli expression.....	183
1.1.- Molecular biology general methods.....	183
1.1.1.- Competent cells preparation.....	183
1.1.2.- Competent cells transformation.....	183
1.1.3.- Sterilization.....	184
1.1.4.- Agarose gel electrophoresis.....	184
1.1.5.- DNA quantification.....	185
1.1.6.- DNA restriction digestion.....	185
1.1.7.- Extraction of DNA fragments from agarose gels.....	185
1.1.8.- DNA sequencing.....	185
1.2.- pET15b-XET16A construct.....	186
1.2.1.- Amplification of <i>Ptt</i> -XET16A gene from pPIC9- <i>Ptt</i> -XET16A.....	186
1.2.2.- NdeI and BamHI digestion of amplified <i>Ptt</i> -XET16A gene fragment and pET15b.....	187
1.2.3.- Cloning of <i>Ptt</i> -XET16A in pET15b.....	188
1.3.- pD6-2- <i>Ptt</i> -XET16A construct.....	190
1.3.1.- Amplification of <i>Ptt</i> -XET16A gene from pPIC9- <i>Ptt</i> -XET16A.....	190
1.3.2.- Introduction of PstI restriction site in pD6-2.....	191
1.3.3.- Introduction of BamHI restriction site in pD6-2(PstI).....	193
1.3.4.- PstI and BamHI digestion of amplified <i>Ptt</i> -XET16A gene fragment and pD6-2(PstI, BamHI).....	194
1.3.5.- Cloning of <i>Ptt</i> -XET16A in pD6-2(PstI, BamHI).....	195
2.- Synthesis.....	197
2.1.- General methods.....	197
2.1.1.- Solvents.....	197
2.1.2.- Chromatography.....	197
2.1.3.- Analytical methods.....	198
2.1.4.- Nuclear magnetic resonance spectroscopy.....	198
2.2.- Bromide of 2,3,4,6-tetra-O-acetyl- β -D-glucopyranosyl-(1 \rightarrow 4)-2,3,6-tri-O-acetyl- α -D-glucopyranoside (4).....	199
2.3.- Fluoride of 2,3,4,6-tetra-O-acetyl- β -D-glucopyranosyl-(1 \rightarrow 4)-2,3,6-tri-O-acetyl- β -D-glucopyranoside (5).....	200
2.4.- Fluoride of β -D-glucopyranosyl-(1 \rightarrow 4)- β -D-glucopyranoside (1).....	200
2.5.- XGOs (XXXG(10), XLXG(12), XXLG(11), and XLLG(13)).....	201
2.6.- [2,3,4-tri-O-acetyl- α -D-xylopyranosyl-(1 \rightarrow 6)]-2,3,4-tri-O-acetyl- β -D-glucopyranosyl-(1 \rightarrow 4)-[2,3,4-tri-O-acetyl- α -D-xylopyranosyl-(1 \rightarrow 6)]-2,3-di-O-acetyl- β -D-glucopyranosyl-(1 \rightarrow 4)-[2,3,4-tri-O-acetyl- α -D-xylopyranosyl-(1 \rightarrow 6)]-2,3-di-O-acetyl β -D-glucopyranosyl-(1 \rightarrow 4)-1,2,3,6-tri-O-acetyl- α/β -D-glucopyranosyl XXXG (15).....	202
2.7.- [(2,3,4-Tri-O-acetyl- α -D-xylopyranosyl)-(1 \rightarrow 6)]-(2,3,4-tri-O-acetyl- β -D-glucopyranosyl)-(1 \rightarrow 4)-[(2,3,4-tri-O-acetyl- α -D-xylopyranosyl)-(1 \rightarrow 6)]-(2,3-di-O-acetyl- β -D-glucopyranosyl)-(1 \rightarrow 4)-1,2,3,6-tetra-O-acetyl-D-glucopyranose (per-O-acetylated XXG (32)) and [(2,3,4-Tri-O-acetyl- α -D-xylopyranosyl)-(1 \rightarrow 6)]-(2,3,4-tri-O-acetyl- β -D-glucopyranosyl)-(1 \rightarrow 4)-[(2,3,4-tri-O-acetyl- α -D-xylopyranosyl)-(1 \rightarrow 6)]-(2,3-di-O-acetyl- β -D-glucopyranosyl)-(1 \rightarrow 4)-[(2,3,4-tri-O-acetyl- α -D-xylopyranosyl)-(1 \rightarrow 6)]-(2,3-di-O-acetyl- β -D-glucopyranosyl)-(1 \rightarrow 4)-1,2,3,6-tetra-O-acetyl-D-glucopyranose (per-O-acetylated XXXG (15)).....	203

2.8.- [(2,3,4-Tri-O-acetyl- α -D-xylopyranosyl)-(1 \rightarrow 6)]-(2,3,4-tri-O-acetyl- β -D-glucopyranosyl)-(1 \rightarrow 4)-[(2,3,4-tri-O-acetyl- α -D-xylopyranosyl)-(1 \rightarrow 6)]-(2,3-di-O-acetyl- β -D-glucopyranosyl)-(1 \rightarrow 4)-1,2,3,6-tetra-O-acetyl-D-glucopyranose (per-O-acetylated XXG (32)).	204
2.9.- [(2,3,4-Tri-O-acetyl- α -D-xylopyranosyl)-(1 \rightarrow 6)]-(2,3,4-tri-O-acetyl- β -D-glucopyranosyl)-(1 \rightarrow 4)-[(2,3,4-tri-O-acetyl- α -D-xylopyranosyl)-(1 \rightarrow 6)]-(2,3-di-O-acetyl- β -D-glucopyranosyl)-(1 \rightarrow 4)-[(2,3,4-tri-O-acetyl- α -D-xylopyranosyl)-(1 \rightarrow 6)]-(2,3-di-O-acetyl- β -D-glucopyranosyl)-(1 \rightarrow 4)-1,2,3,6-tetra-O-acetyl-D-glucopyranose (per-O-acetylated XXXG (15)).	205
2.10.- Bromide of the [2,3,4-tri-O-acetyl- α -D-xylopyranosyl-(1 \rightarrow 6)]-2,3,4-tri-O-acetyl- β -D-glucopyranosyl-(1 \rightarrow 4)-[2,3,4-tri-O-acetyl- α -D-xylopyranosyl-(1 \rightarrow 6)]-2,3-di-O-acetyl- β -D-glucopyranosyl-(1 \rightarrow 4)-[2,3,4-tri-O-acetyl- α -D-xylopyranosyl-(1 \rightarrow 6)]-2,3-di-O-acetyl β -D-glucopyranosyl-(1 \rightarrow 4)-1,2,3,6-tri-O-acetyl- α -D-glucopyranoside (16).	206
2.11.- Fluoride of the [2,3,4-tri-O-acetyl- α -D-xylopyranosyl-(1 \rightarrow 6)]-2,3,4-tri-O-acetyl- β -D-glucopyranosyl-(1 \rightarrow 4)-[2,3,4-tri-O-acetyl- α -D-xylopyranosyl-(1 \rightarrow 6)]-2,3-di-O-acetyl- β -D-glucopyranosyl-(1 \rightarrow 4)-[2,3,4-tri-O-acetyl- α -D-xylopyranosyl-(1 \rightarrow 6)]-2,3-di-O-acetyl β -D-glucopyranosyl-(1 \rightarrow 4)-1,2,3,6-tri-O-acetyl- β -D-glucopyranoside (17).	206
2.12.- Fluoride of the [α -D-xylopyranosyl-(1 \rightarrow 6)]- β -D-glucopyranosyl-(1 \rightarrow 4)-[α -D-xylopyranosyl-(1 \rightarrow 6)]- β -D-glucopyranosyl-(1 \rightarrow 4)-[α -D-xylopyranosyl-(1 \rightarrow 6)]- β -D-glucopyranosyl-(1 \rightarrow 4)- β -D-glucopyranoside (XXXG β F (14)).	207
2.13.- Analytical ANTS labeling of substrates.	208
2.14.- XGOs-ANTS mixture (XXXGANTS (25), XLGANTS(26), XLXGANTS(27), and XLLGANTS(28)).	208
2.15.- ([α -D-xylopyranosyl-(1 \rightarrow 6)]- β -D-glucopyranosyl-(1 \rightarrow 4)-[α -D-xylopyranosyl-(1 \rightarrow 6)]- β -D-glucopyranosyl-(1 \rightarrow 4)-[α -D-xylopyranosyl-(1 \rightarrow 6)]- β -D-glucopyranosyl-(1 \rightarrow 4)- β -D-glucopyranose (XXXG (10)).	209
2.16.- ([α -D-xylopyranosyl-(1 \rightarrow 6)]- β -D-glucopyranosyl-(1 \rightarrow 4)-[α -D-xylopyranosyl-(1 \rightarrow 6)]- β -D-glucopyranosyl-(1 \rightarrow 4)-[α -D-xylopyranosyl-(1 \rightarrow 6)]- β -D-glucopyranosyl-(1 \rightarrow 4)- β -D-1-deoxy-D-glucitol-1-yl)-8-aminonaphthalene-1,3,6-trisulfonic acid, disodium salt (XXXG-ANTS (25)).	210
2.17.- [α -D-xylopyranosyl-(1 \rightarrow 6)]- β -D-glucopyranosyl-(1 \rightarrow 4)-[α -D-xylopyranosyl-(1 \rightarrow 6)]- β -D-glycopyranosyl-(1 \rightarrow 4)-[α -D-xylopyranosyl-(1 \rightarrow 6)]- β -D-glucopyranosyl-(1 \rightarrow 4)- β -D-glucopyranosyl-(1 \rightarrow 4)-[α -D-xylopyranosyl-(1 \rightarrow 6)]- β -D-glucopyranosyl-(1 \rightarrow 4)-[α -D-xylopyranosyl-(1 \rightarrow 6)]- β -D-glucopyranosyl-(1 \rightarrow 4)-[α -D-xylopyranosyl-(1 \rightarrow 6)]- β -D-glucopyranosyl-(1 \rightarrow 4)- β -D-glucopyranose (XXXGXXXG) (23).	211
2.18.- β -D-galactopyranosyl-(1 \rightarrow 4)- β -D-glucopyranosyl-(1 \rightarrow 4)- [α -D-xylopyranosyl-(1 \rightarrow 6)]- β -D-glucopyranosyl-(1 \rightarrow 4)-[α -D-xylopyranosyl-(1 \rightarrow 6)]- β -D-glycopyranosyl-(1 \rightarrow 4)-[α -D-xylopyranosyl-(1 \rightarrow 6)]- β -D-glucopyranosyl-(1 \rightarrow 4)- β -D-glucopyranosyl-(1 \rightarrow 4)-[α -D-xylopyranosyl-(1 \rightarrow 6)]- β -D-glucopyranosyl-(1 \rightarrow 4)-[α -D-xylopyranosyl-(1 \rightarrow 6)]- β -D-glucopyranosyl-(1 \rightarrow 4)-[α -D-xylopyranosyl-(1 \rightarrow 6)]- β -D-glucopyranosyl-(1 \rightarrow 4)- β -D-glucopyranose (GalGXXXGXXXG) (38).	211

2.19.- Donor library: XXXGGG (47), XXXGXG (45), XXXGGGGG (48), XXXGXXG (46), GXXXG (49), GGXXXG (50), GGGXXXG (51), GGGGXXXG (52), XGXXXG (54), XGGXXXG (55), XXGXXXG (29), GXXGXXXG (53), XGXGXXXG (56), GalGXXXG (40), GalGXXXGGG (59).	211
2.20.- 4,6-isopropylene- β -D-galactopyranosyl-(1 \rightarrow 4)- α / β -D-glucopyranose (60).	212
2.21.- 2,3-di-O-acetyl-4,6-isopropylene- β -D-galactopyranosyl-(1 \rightarrow 4)-1,2,3,6- tetra-O-acetyl- α / β -D-glucopyranose (61).	212
2.22.- 2,3-di-O-acetyl- β -D-galactopyranosyl-(1 \rightarrow 4)-1,2,3,6-tetra-O-acetyl- α / β -D- glucopyranose (62).	213
2.23.- 2,3-di-O-acetyl-6-benzoyl- β -D-galactopyranosyl-(1 \rightarrow 4)-1,2,3,6-tetra-O- acetyl- α / β -D-glucopyranose (63).	213
2.24.- 2,3-di-O-acetyl-4-azido-4-deoxy-6-benzoyl- β -D-glucopyranosyl-(1 \rightarrow 4)- 2,3,6-tri-O-acetyl- α / β -D-glucopyranose (67).	214
2.25.- Fluoride of (2,3-di-O-acetyl-4-azido-4-deoxy-6-benzoyl- β -D- glucopyranosyl-(1 \rightarrow 4)-2,3,6-tri-O-acetyl- α / β -D-glucopyranoside) (68)..	215
2.26.- Fluoride of (2,3-di-O-acetyl-4-azido-4-deoxy-6-benzoyl- β -D- glucopyranosyl-(1 \rightarrow 4)-2,3,6-tri-O-acetyl- α -D-glucopyranoside) (69).	216
2.27.- Fluoride of (4-azido-4-deoxy- β -D-glucopyranosyl-(1 \rightarrow 4)- α -D- glucopyranoside) (74).	217
2.28.- [2,3,4-tri-O-acetyl- α -D-xylopyranosyl-(1 \rightarrow 6)]-2,3,4-tri-O-acetyl- β -D- glucopyranosyl-(1 \rightarrow 4)-[2,3,4-tri-O-acetyl- α -D-xylopyranosyl-(1 \rightarrow 6)]-2,3- di-O-acetyl- β -D-glucopyranosyl-(1 \rightarrow 4)-[2,3,4-tri-O-acetyl- α -D- xylopyranosyl-(1 \rightarrow 6)]-2,3-di-O-acetyl β -D-glucopyranosyl-(1 \rightarrow 4)-2,3,6-tri- O-acetyl- α / β -D-glucopyranose (34).	217
2.29.- Fluoride of ([2,3,4-tri-O-acetyl- α -D-xylopyranosyl-(1 \rightarrow 6)]-2,3,4-tri-O- acetyl- β -D-glucopyranosyl-(1 \rightarrow 4)-[2,3,4-tri-O-acetyl- α -D-xylopyranosyl- (1 \rightarrow 6)]-2,3-di-O-acetyl- β -D-glucopyranosyl-(1 \rightarrow 4)-[2,3,4-tri-O-acetyl- α -D- xylopyranosyl-(1 \rightarrow 6)]-2,3-di-O-acetyl β -D-glucopyranosyl-(1 \rightarrow 4)-2,3,6-tri- O-acetyl- α / β -D-glucopyranoside) (35).	218
2.30.- Fluoride of ([2,3,4-tri-O-acetyl- α -D-xylopyranosyl-(1 \rightarrow 6)]-2,3,4-tri-O- acetyl- β -D-glucopyranosyl-(1 \rightarrow 4)-[2,3,4-tri-O-acetyl- α -D-xylopyranosyl- (1 \rightarrow 6)]-2,3-di-O-acetyl- β -D-glucopyranosyl-(1 \rightarrow 4)-[2,3,4-tri-O-acetyl- α -D- xylopyranosyl-(1 \rightarrow 6)]-2,3-di-O-acetyl β -D-glucopyranosyl-(1 \rightarrow 4)-2,3,6-tri- O-acetyl- α -D-glucopyranoside) (33).	219
2.31.- Fluoride of ([α -D-xylopyranosyl-(1 \rightarrow 6)]- β -D-glucopyranosyl-(1 \rightarrow 4)-[α -D- xylopyranosyl-(1 \rightarrow 6)]- β -D-glucopyranosyl-(1 \rightarrow 4)-[α -D-xylopyranosyl- (1 \rightarrow 6)]- β -D-glucopyranosyl-(1 \rightarrow 4)- α -D-glucopyranoside) XXXGaF (36).	219
2.32.- [α -D-xylopyranosyl-(1 \rightarrow 6)]- β -D-glucopyranosyl-(1 \rightarrow 4)-[α -D- xylopyranosyl-(1 \rightarrow 6)]- β -D-glycopyranosyl-(1 \rightarrow 4)-[α -D-xylopyranosyl- (1 \rightarrow 6)]- β -D-glucopyranosyl-(1 \rightarrow 4)- β -D-glucopyranosyl-(1 \rightarrow 4)-[α -D- xylopyranosyl-(1 \rightarrow 6)]- β -D-glucopyranosyl-(1 \rightarrow 4)-[α -D-xylopyranosyl- (1 \rightarrow 6)]- β -D-glucopyranosyl-(1 \rightarrow 4)-[α -D-xylopyranosyl-(1 \rightarrow 6)]- β -D- glucopyranosyl-(1 \rightarrow 4)- β -D-glucopyranose (XXXGXXXG) (23).	220

2.33.-	([α -D-xylopyranosyl-(1 \rightarrow 6)]- β -D-glucopyranosyl-(1 \rightarrow 4)-[α -D-xylopyranosyl-(1 \rightarrow 6)]- β -D-glycopyranosyl-(1 \rightarrow 4)-[α -D-xylopyranosyl-(1 \rightarrow 6)]- β -D-glucopyranosyl-(1 \rightarrow 4)- β -D-glucopyranosyl-(1 \rightarrow 4)-[α -D-xylopyranosyl-(1 \rightarrow 6)]- β -D-glucopyranosyl-(1 \rightarrow 4)-[α -D-xylopyranosyl-(1 \rightarrow 6)]- β -D-glucopyranosyl-(1 \rightarrow 4)-1-deoxy-D-glucitol-1-yl)-5-(2-aminoethylamino)naphthalene-1-sulfonic acid, sodium salt (XXXGXXXG-EDANS (70)).	221
2.34.-	(4-azido-4-deoxy- β -D-glucopyranosyl-(1 \rightarrow 4)- β -D-glucopyranosyl-(1 \rightarrow 4)-[α -D-xylopyranosyl-(1 \rightarrow 6)]- β -D-glycopyranosyl-(1 \rightarrow 4)-[α -D-xylopyranosyl-(1 \rightarrow 6)]- β -D-glucopyranosyl-(1 \rightarrow 4)- β -D-glucopyranosyl-(1 \rightarrow 4)-[α -D-xylopyranosyl-(1 \rightarrow 6)]- β -D-glucopyranosyl-(1 \rightarrow 4)-[α -D-xylopyranosyl-(1 \rightarrow 6)]- β -D-glucopyranosyl-(1 \rightarrow 4)-[α -D-xylopyranosyl-(1 \rightarrow 6)]- β -D-glucopyranosyl-(1 \rightarrow 4)-1-deoxy-D-glucitol-1-yl)-5-(2-aminoethylamino)naphthalene-1-sulfonic acid, sodium salt (N ₃ GGXXXGXXXG-EDANS (72)).	222
2.35.-	(4-amino-4-deoxy- β -D-glucopyranosyl-(1 \rightarrow 4)- β -D-glucopyranosyl-(1 \rightarrow 4)-[α -D-xylopyranosyl-(1 \rightarrow 6)]- β -D-glycopyranosyl-(1 \rightarrow 4)-[α -D-xylopyranosyl-(1 \rightarrow 6)]- β -D-glucopyranosyl-(1 \rightarrow 4)- β -D-glucopyranosyl-(1 \rightarrow 4)-[α -D-xylopyranosyl-(1 \rightarrow 6)]- β -D-glucopyranosyl-(1 \rightarrow 4)-[α -D-xylopyranosyl-(1 \rightarrow 6)]- β -D-glucopyranosyl-(1 \rightarrow 4)-1-deoxy-D-glucitol-1-yl)-5-(2-aminoethylamino)naphthalene-1-sulfonic acid, sodium salt (NH ₂ GGXXXGXXXG-EDANS (73)).	223
2.36.-	(2-N-(4-deoxy-4-dimethylaminophenylazophenylthioureido)- β -D-glucopyranosyl-(1 \rightarrow 4)- β -D-glucopyranosyl-(1 \rightarrow 4)-[α -D-xylopyranosyl-(1 \rightarrow 6)]- β -D-glycopyranosyl-(1 \rightarrow 4)-[α -D-xylopyranosyl-(1 \rightarrow 6)]- β -D-glycopyranosyl-(1 \rightarrow 4)-[α -D-xylopyranosyl-(1 \rightarrow 6)]- β -D-glucopyranosyl-(1 \rightarrow 4)- β -D-glucopyranosyl-(1 \rightarrow 4)-[α -D-xylopyranosyl-(1 \rightarrow 6)]- β -D-glucopyranosyl-(1 \rightarrow 4)-[α -D-xylopyranosyl-(1 \rightarrow 6)]- β -D-glucopyranosyl-(1 \rightarrow 4)-1-deoxy-D-glucitol-1-yl)-5-(2-aminoethylamino)naphthalene-1-sulfonic acid, sodium salt (DAB-NH-CS-NH-GGXXXGXXXG-EDANS (76)).	224
3.-	HPCE method development and validation.	225
3.1.-	HPCE method development.	225
3.2.-	Definitive HPCE method.	226
3.3.-	HPCE method validation.	227
3.3.1.-	Linearity study.	228
3.3.2.-	Detection and quantification limits.	229
3.3.3.-	Repeatability.	229
3.4.-	XXXGANTS standard curve.	230
3.5.-	Comparison of response factor between XXXG-ANTS (25) and XXXGXXXG-ANTS (31).	231

4.- Determination of stock concentrations.....	232
4.1.- Determination of β -glycosyl fluoride stock concentration.	232
4.2.- Determination of XXXG-ANTS (25) stock concentration.	232
4.3.- Determination of donor stock concentration.....	232
4.4.- <i>Ptt</i> -XET16A concentration.	233
4.4.1.- Total enzyme concentration.	233
4.4.2.- Active enzyme concentration.	233
5.- Kinetic studies.....	234
5.1.- Preliminary evaluation of HPLC method to monitor XET activity.	234
5.2.- Screening of putative <i>Ptt</i> -XET16A donors.	234
5.2.1.- Evaluation of β -glycosyl fluorides as putative <i>Ptt</i> -XET16A donors. ...	234
5.2.2.- Evaluation of β -fluorides as new possible donors for <i>Ptt</i> -XET16A, by fluoride release detection.....	234
5.2.3.- Evaluation of the first family of synthetic XGOs as putative <i>Ptt</i> -XET16A donors.	235
5.3.- <i>Ptt</i> -XET16A kinetic characterization.....	235
5.3.1.- <i>Ptt</i> -XET16A specific activity.....	236
5.3.2.- pH profile.	237
5.3.3.- Temperature profile.....	237
5.3.4.- <i>Ptt</i> -XET16A kinetic mechanism using XXXGXXXG (23) as donor... 238	
5.3.5.- <i>Ptt</i> -XET16A kinetic mechanism using GalGXXXGXXXG (38) as donor.	240
5.4.- Donor screening and subsite mapping.	242
5.5.- Yield after 24 h reaction.....	245
6.- Spectroscopic techniques.	246
6.1.- Absorbance spectra.	246
6.2.- Fluorescence spectra.	246

EXPERIMENTAL PART

1.- Cloning of *Ptt-XET16A* for *Escherichia coli* expression.

1.1.- Molecular biology general methods.

1.1.1.- *Competent cells preparation.*

The calcium chloride method described by Sambrook *et al.* is used^{197,198}.

From one single colony, a 3 mL 2YT culture (200 µg/ml ampicillin) is prepared and incubated at 37°C and 300 rpm O.N. 300 µl from this culture is inoculated to 50 mL 2YT media (200 µg/ml ampicillin) until optical density is 0.3 at 600 nm. Then, the culture is cooled at 0°C during 20 minutes, it is centrifuged at 3000 rpm, at 4°C during 10 min. Supernatant is eliminated and pellet is resuspended in 15 mL CaCl₂ 50 mM at 4°C, suspension is maintained at 4°C during 15 minutes, before 3000 rpm centrifugation at 4°C during 10 minutes, supernatant is again eliminated and pellet is resuspended in 3 mL CaCl₂ 50 mM at 4°C. Competent cells obtained can be stored at 4°C or prior addition of 15% glycerol at -20°C.

1.1.2.- *Competent cells transformation.*

The heat-shock transformation protocol described by Sambrook *et al.* is used^{197,198}.

In a tube containing 100 µl competent cells, 50 ng plasmidic DNA are added, and mixture is softly stirred. This tube is incubated 30 min at 0°C, followed by a heat-shock (2 min at 42°C) and again it is incubated at 0°C during 5 min. 300 mL 2YT media (200 µg/ml ampicillin) were added to transformed cells. This culture is incubated 45 min at 37°C and 200 rpm. Finally transformed cells are passed on a LB plate (200 µg/ml ampicillin) and are incubated O.N. at 37°C.

1.1.3.- Sterilization.

Autoclave:

Liquid media and material are steam-sterilized in an autoclave at 121°C during 15 min.

Filtration:

Solutions of labile reagents are sterilized by filtration through a 0.22 µm filter and stored in sterile containers.

1.1.4.- Agarose gel electrophoresis.

Agarose gel electrophoresis allows DNA fragments separation depending on their mobility in a gel under electric field influence. Resolution depends on agarose concentration. Mobility of a DNA fragment is proportional to the logarithm of its molecular weight and it is possible to determine the molecular weight by comparison with a commercial available molecular weight standard.

Standard DNA fragments in this work are within 800-7000 base pairs (bp), then, agarose concentration is varied from 0.8 to 1.2 % by weight.

TAE buffer is used in electrophoresis, adding 5 µg/ml ethidium bromide. Ethidium bromide is a fluorescent molecule which is able to insert itself between DNA bases and allows observation of DNA fragments under UV light (312 nm). Charge buffer was used to charge samples into the gel.

TAE buffer 50x: 242 g Tris-base, 57.1 mL concentrated AcOH, 100 mL EDTA 0.5 M (pH 8.0) in a total volume of 1 liter.

Charge buffer 10x: 500 mg glycerin, 200 µL EDTA 0.5 M (pH 8.0), 100 µL SDS 10%, 200 µL bromphenol blue (Merck, 12.5 mg/ml), 200 µL xilencianol (Eastman Kodak) and adjust volume to 1 ml.

DNA molecular weight markers III and IV from Boehringer Mannheim GmbH.

1.1.5.- DNA quantification.

DNA concentration is determined by comparative electrophoresis with standard markers, when the quantity and/or purity of DNA are low.

DNA concentration is also determined by absorbance at 260 nm, when samples are pure and high concentrated.

1.1.6.- DNA restriction digestion.

Digestion of DNA fragments with restriction endonucleases is done at 37°C during from 1h to 24 h, with the adequate mixture of reagents, following provider instructions. Restriction enzymes, buffers and additives (BSA) from New England Biolabs and Boehringer Mannheim are used.

Digested fragments are analyzed by agarose gel electrophoresis or purified by the same technique followed by extraction of fragments from agarose gels.

1.1.7.- Extraction of DNA fragments from agarose gels.

The kit GeneClean spin purchased at Bio101 is used. It consists in the addition of a glass milk solution on the gel in a spin filter, cleaning of glass milk by centrifugation and elution of purified fragment from it.

Ultrafree-DA purification kit from Millipore is also used. It consist in a filter that retains agarose and DNA passes through it.

1.1.8.- DNA sequencing.

Sequencing is done following Sanger method¹⁹⁹, using dideoxynucleotides labeled with different fluorophores depending on the base, provided in BigDye terminator v2 kit from ABI Prism, PE.

In a autoclaved Eppendorf tube the following components are poured: 1 µL DMSO 50%, 4 µL (200 ng) dsDNA to be sequenced, 1.5 µL primer 5 pmol/µl, 9.5 µL autoclaved water and after heating mixtures for 5 minutes at 98°C 4 µL of the Premix from the kit.

Reaction mixture is incubated in a PCR machine as it is described in the following table:

Denaturing		3 min	94 °C
30 cycles	Denaturing	30 s	96 °C
	Hybridizing	15 s	50 °C
	Elongation	4 min	60 °C
Storage		Till 24h	4 °C

Table 14: PCR program for DNA sequencing

Once finished PCR program, dNTPs in excess are eliminated as follows: 18 µL of reaction crude are poured in a new Eppendorf tube, then 19 µL water and 61 µL EtOH are added. Mixture is cooled for 10 min in an ice-bath, centrifuged at R.T. during 20 min at 13200 rpm and supernatant is eliminated by aspiration. 200 µL of EtOH 70% are added to pellet, and centrifuged again 2 min at 13200 rpm, supernatant is eliminated by aspiration. Pellet is dried in a desiccator and samples are send to Servei Científic tècnic de la Universitat de Barcelona to be sequenced.

1.2.- pET15b-XET16A construct.

1.2.1.- Amplification of *Ptt-XET16A* gene from *pPIC9-Ptt-XET16A*.

Stocks: All reagents were dissolved in previously sterilized Milli-Q water.

InNdeIXET sequence: GGAATTCCATATGGCTGCCCTGAGGAAGCC.

FiBamHIXET sequence: CGCGGATCCTTATATGTCTCTGTCTCTCTTGC.

	Concentration	Provider
Oligo1: InNdeIXET	10 mM (97.4 µg/ml)	Thermo
Oligo2: FiBamHIXET	10 mM (102.3 µg/ml)	Thermo
pPIC9-XET16A	182.2 µg/ml	KTH (EDEN partner)
Mg	10x	New England Biolabs
dNTPs	10 mM	New England Biolabs
Deep Vent polymerase	2000 U/ml	New England Biolabs
Thermo Pol Buffer	10x	New England Biolabs

Table 15: Stock concentration of reagents for PCR to amplify *Ptt-XET16A* gene from *pPIC9XET16A* with flanking primers to introduce *NdeI* and *BamHI* restriction sites.

Reaction: All reagents except Deep Vent polymerase were mixed and preheated 30 s at 95°C, after that, Deep Vent polymerase was added followed by an oil drop and finally, PCR program is started:

	Volume (μL)	
	Reaction	Negative control
Water	81.7	84.7
Buffer (Thermo Pol)	10	10
Oligo1: InNdeIXET	2	0
Oligo2: FiBamHIXET	2	0
pPIC9-XET16A	0.3	0.3
Mg	2, 4, 6	2
dNTPs	2	2
Deep Vent polymerase	1	1

Table 16: Volumes of reagents added to amplify *Ptt*-XET16A gene from pPIC9*Ptt*-XET16A plasmid by PCR.

PCR program: 30 repetitions of the following sequence, and after all cycles, 5 additional minutes at 72°C:

Temperature (°C)	Time (min)
94	1.25
55, 58, 60.1	1.5
72	1

Table 17: PCR program sequence.

Reaction product from amplification at 60.1°C was analyzed by analytical 2% agarose electrophoresis at 80V. Verified product was purified by preparative 2% agarose electrophoresis gel with Gene Clean with Spin kit.

1.2.2.- *NdeI* and *BamHI* digestion of amplified *Ptt*-XET16A gene fragment and pET15b.

Ptt-XET16A gene flanked by *NdeI* and *BamHI* restriction sites and pET15b were sequentially digested with *NdeI* and *BamHI* restriction endonucleases. First of all, *NdeI* digestion was done as it is described below:

NdeI restriction enzyme ($20 \cdot 10^3$ U/ml) from New England Biolabs.

NE-Buffer 4 (10x) from New England Biolabs.

Sample	Volume (µL)			
	DNA	NEBuffer 4	Enzyme	Water
NdeIXETBamHI	50	6	4	0
pET15b	10	2	2	6

Table 18: Digestion of NdeIXETBamHI and pET15b with *NdeI* restriction endonuclease.

Samples were incubated at 37°C during 24 hours. After that, they were purified by 1% preparative agarose electrophoresis and Ultrafree-DA purification kit from Millipore to extract DNA from agarose gel, followed by concentration.

Purified fragments were digested with *BamHI* restriction enzyme as it follows:

Stocks:

BamHI restriction enzyme (20000 U/ml) from New England Biolabs.

NE-BamHI-buffer (10x) from New England Biolabs.

BSA (10x 1 mg/ml) from New England Biolabs.

Sample	Volume (µL)				
	DNA	NE-BamHI buffer	BSA	<i>BamHI</i>	Water
NdeIXETBamHI	50	7	7	6	0
pET15b	50	7	7	6	0

Table 19: *BamHI* digestion of NdeIXETBamHI and pET15b previously digested with *NdeI* with restriction enzyme.

Samples were digested at 37°C during 24 hours. Digested fragments were purified by 1% preparative agarose electrophoresis and Ultrafree-DA purification kit from Millipore and concentrated.

1.2.3.- Cloning of *Ptt-XET16A* in *pET15b*.

Ligation of previously purified fragments were done during 18 hours at 16°C in a 1:10 plasmid insert ratio, using T4 DNA ligase from Boehringer Mannheim GmbH. DH5α Ca²⁺ competent cells were transformed with the resulting ligation reaction product and negative control (without insert). Cells were transferred to LB media plates supplemented with 200 µg/ml ampicillin and incubated O.N. at 37°C.

Colonies obtained were “on colony” screened for insertion using T7 promoter and termination primers by PCR as it is described in the following tables:

Stocks:

T7 promoter primer sequence CCCGCGAAATTAATACGACTCACTAT, from New England Biolabs (10 mM).

T7 terminator primer sequence TGCTAGTTATTGCTCAGCGGTGGC, from New England Biolabs (10 mM).

dNTPs mixture (10 mM) from New England Biolabs.

Deep Vent DNA polymerase (2000 U/ml) from New England Biolabs.

Thermo Pol buffer (10x) from New England Biolabs.

Sample	Volume (µL)					
	Water	Buffer	T7 prom	T7 term	dNTP	Deep Vent
Colony 1	39	5	2	2	1	1
Colony 2	39	5	2	2	1	1

Table 20: Volumes of reagents for on colony screening of insertion of *Ptt-XET16A* gene in pET15b plasmid by PCR amplification of inserted fragment.

All reagents were mixed except the polymerase and incubated 1 minute at 95°C. After that, Deep Vent polymerase was added and the following temperature program was repeated 30 times, final elongation was done, afterwards, at 72°C during 5 minutes.

Temperature (°C)	Time (min)
94	1.25
57.7	1.5
72	1.5

Table 21: PCR program sequence.

Resulting PCR products were analyzed by 2% analytical agarose electrophoresis at 90V. 3 mL 2YT media supplemented with 300 µg/ml ampicillin were inoculated with colonies which have shown insertion. Cultures were grown O.N. at 37°C and 250 rpm, this cultures were used to inoculate 50 mL 2YT media (300 µg/ml ampicillin) for plasmid production. pET15b-XET16A plasmids were purified using the Wizard Midiprep purification kit from Promega. Purified plasmids were firstly verified by analytical restriction analysis and secondly inserted gene was sequenced using BigDye terminator kit from ABI Prism.

1.3.- pD6-2-*Ptt*-XET16A construct.

1.3.1.- Amplification of *Ptt*-XET16A gene from pPIC9-*Ptt*-XET16A.

Stocks: All reagents were dissolved in Milli-Q previously sterilized water.

InPstIXET sequence: AACTGCAGCTGCCCTGAGGAAGCC.

FiBamHIXET sequence: CGCGGATCCTTATATGTCTCTGTCTCTCTTGC.

	Concentration	Provider
Oligo1: InPstIXET	10 mM (77.5 µg/ml)	Thermo
Oligo2: FiBamHIXET	10 mM (102.3 µg/ml)	Thermo
pPIC9-XET16A	182.2 µg/ml	KTH
Deep Vent DNA polymerase	2000 U/ml	New England Biolabs
dNTPs	10 mM	New England Biolabs
Magnesium		
ThermoPol buffer		New England Biolabs

Table 22: Stock concentrations to amplify *Ptt*-XET16A gene from pPIC9XET16A with flanking primers to introduce *Pst*I and *Bam*HI restriction sites, by PCR.

Reaction: All reagents except Deep Vent polymerase were mixed and preheated 30 s at 95°C, after that, Deep Vent polymerase was added followed by an oil drop and finally PCR program is started:

	Volume (µL)	
	Reaction	Negative control
Water	81.7	84.7
Buffer	10	10
Oligo1: InNdeIXET	2	0
Oligo2: FiBamHIXET	2	0
pPIC9-XET16A	0.3	0.3
Mg	0, 2, 4, 6	2
dNTPs	2	2
Deep Vent polymerase	1	1

Table 23: Volumes of reagents to amplify *Ptt*-XET16A gene from pPIC9XET16A with flanking primers to introduce *Pst*I and *Bam*HI restriction sites, by PCR.

PCR program: Reaction mixtures were submitted to 30 repetitions of the following sequence, and after all cycles, 5 additional minutes at 72°C:

Temperature (°C)	Time (min)
94	1.25
59.8	1.5
72	1

Table 24: PCR program sequence.

Reaction product was analyzed by analytical 2% agarose electrophoresis at 80V. Product obtained without magnesium was purified by preparative 2% agarose electrophoresis gel and plasmid extraction from the agarose gel with the Gene Clean with Spin kit.

1.3.2.- Introduction of *Pst*I restriction site in pD6-2.

Stocks: All reagents were dissolved in Milli-Q previously sterilized water by autoclaving:

53PstIpD62 sequence: GCAAGTGCCTCTGCAGAAACGGGCGGGTTCGTTTT

35PstIpD62 sequence: AAAACGACCCGCCGTTTCTGCAGAGGCACTTGC

	Concentration	Provider
Oligo1: 53PstIpD62	10 mM (119.97 µg/ml)	
Oligo2: 35PstIpD62	10 mM (109.27 µg/ml)	
pD6-2	94.3 µg/ml	
dNTPs	10 mM	New England Biolabs
PfuI turbo polymerase	2 U/µl	Stratagene
Quick change buffer	10x	Stratagene

Table 25: Stock concentration of reagents to introduce *Pst*I restriction site in pD6-2 by side directed mutagenesis.

Reaction: All reagents except *PfuI* turbo polymerase were mixed and preheated 30 s at 95°C, after that *PfuI* turbo was added followed by an oil drop and finally PCR program is started:

	Volume (μL)		
	R1	R2	R3
Water	76	41.2	82.4
Buffer	10	5	10
Oligo1: 53PstIPd62	2.5	1.13	2.25
Oligo2: 35PstIPd62	2.5	1.15	2.29
pD6-2	4	0.53	1.06
dNTPs	4	1	2
Pful turbo polymerase	1	1	1

Table 26: Volumes of reagent for side directed mutagenesis to introduce *PstI* restriction site in pD6-2.

PCR program: 16 repetitions of the following sequence:

Temperature ($^{\circ}\text{C}$)	Time (min)
95	1
55	1.5
68	9

Table 27: PCR program sequence.

1 μL of *DpnI* (20000 U/ml) from Quick change kit from Stratagene was added to reaction mixture, which mixture was incubated at 37°C for 1.5 hours. Chemically competent cells were heat-shock-transformed with 2 and 5 μL of reaction mixture and cells were set in LB media plates with 200 $\mu\text{g}/\text{ml}$ ampicillin. Plates were incubated O.N. at 37°C , obtaining approximately 50 colonies in each plate.

Selected grown cells were passed into 3 mL 2YT media supplemented with 200 $\mu\text{g}/\text{ml}$ ampicillin and incubated at 37°C and 250 rpm O.N. A Miniprep purification with Wizard® miniprep DNA purification kit was done with this culture obtaining 50 μl of purified pD6-2(*PstI*) plasmid.

Correctness of mutation was verified by restriction analysis of *PstI*pD6-2 plasmid by electrophoresis at 80V of a 1% agarose gel using *PstI* and *EcoRI* restriction enzymes.

1.3.3.- Introduction of BamHI restriction site in pD6-2(PstI).

Stocks: All reagents were dissolved in Milli-Q previously sterilized water by autoclaving:

53BamHIpD62 sequence: ACACAAAAAGATAACCGGATCCCAAAACCTGTG

35BamHID62 sequence: CACAGTTTTTGGGATCCGGTTATCTTTTTGTGT

	Concentration	Provider
Oligo1: 53BamHIpD62	10 mM (106.5 µg/ml)	Thermo
Oligo2: 35BamHIpD62	10 mM (107.0 µg/ml)	Thermo
pD6-2(PstI)	249.8 µg/ml	
dNTPs	10 mM	New England Biolabs
Pful turbo polymerase		Stratagene
Buffer		Stratagene

Table 28: Stock concentration of reagents to introduce BamHI restriction site in pD62(PstI), by site directed mutagenesis.

Reaction: All reagents except *Pful* turbo polymerase were mixed and preheated 30 s at 95°C, after that, *Pful* turbo polymerase was added followed by an oil drop and finally PCR program is started:

	Volume (µL)	
	Reaction	Negative control
Water	40.5	43.4
Buffer	5	5
Oligo1: 53BamHIpD62	1.17	0
Oligo2: 35BamHIpD62	1.17	0
pD6-2(PstI)	0.3	0.3
dNTPs	1	1
Pful turbo polymerase	1	1

Table 29: Volumes of reagent mixed to introduce BamHI restriction site in pD6-2(PstI), by site directed mutagenesis.

PCR program: 16 repetitions of the following sequence:

Temperature (°C)	Time (min)
95	1
55	1.5
68	9

Table 30: PCR program sequence.

1 µL of *DpnI* from Quick change kit from Stratagene was added to each reaction mixture and they were incubated at 37°C for 1 hour. Chemically competent cells were

heat-shock-transformed with 2 μ L of reaction mixtures. Negative control and transformed cells were set in LB media plates with 200 μ g/ml ampicillin. Plates were incubated O.N. at 37°C, obtaining approximately 3 colonies in each plate.

3 mL 2YT media tubes supplemented with 200 μ g/ml ampicillin were inoculated with grown colonies and incubated at 37°C and 250 rpm O.N. Plasmids from these cultures were purified with the Wizard® miniprep DNA purification kit obtaining 50 μ l of each putative purified pD6-2(PstI,BamHI) plasmid.

Correctness of mutation was verified by restriction analysis of putative pD6-2(PstI,BamHI) plasmids by electrophoresis at 80V of a 1% agarose gel using *BamHI* and *PstI* restriction enzymes.

1.3.4.- *PstI* and *BamHI* digestion of amplified *Ptt-XET16A* gene fragment and pD6-2(*PstI*, *BamHI*).

Amplified *Ptt-XET16A* gene with flanking primers containing *PstI* and *BamHI* restriction sites and pD6-2(*PstI*, *BamHI*) were double digested with *PstI* and *BamHI* restriction enzymes as it is described in the following table:

PstI restriction enzyme (20000 U/ml) from New England Biolabs.

BamHI restriction enzyme (20000 U/ml) from New England Biolabs.

NE-*BamHI*-buffer (10x) from New England Biolabs.

BSA (10x, 1 mg/ml) from New England Biolabs.

Sample	Volume (μ L)					
	DNA	NE- <i>BamHI</i> buffer	BSA	<i>BamHI</i>	<i>PstI</i>	Water
PstIXETBamHI	14	2	2	1	1	0
pD6-2(<i>PstI</i> , <i>BamHI</i>)	14	2	2	1	1	0

Table 31: Reaction preparation to digest PstIXETBamHI and pD6-2(*PstI*,*BamHI*) with *PstI* and *BamHI* restriction endonucleases.

Resulting reaction products were purified by preparative 1% agarose gel electrophoresis followed by extraction of fragments from agarose gel with Gene Clean with Spin kit from BIO101.

1.3.5.- Cloning of Ptt-XET16A in pD6-2(PstI, BamHI).

Purified fragments were ligated using T4 DNA ligase from Boehringer Mannheim GmbH as it is described in the following table, in an insert/template ratio approximately 1:3:

Sample	Volume (µL)				
	DNA template	Buffer	T4 ligase	DNA insert	Water
pD62XET	12	4	1	30	3
Negative control	8	1	1	0	0

Table 32: Preparation of ligation reaction of PstXETBamHI insert and pD6-2(PstI,BamHI) template.

DH5α chemically competent cells were transformed with resulting reaction products. After that, resulting colonies were incubated O.N. at 37°C in LB + 200 µg/ml ampicillin plates. Grown colonies were screened for insertion by “on colony PCR” as it is described below:

Stocks were prepared dissolved in sterilized water:

FUP sequence: GTAAAACGACGGCCAGT from New England Biolabs (10 mM)

RUP sequence: AACAGCTATGACCATG from New England Biolabs (10 mM)

dNTP (10 mM) from New England Biolabs

Deep Vent Polymerase (2000 U/ml), form New England Biolabs.

ThermoPol buffer (10x) from New England Biolabs.

Sample	Volume (µL)					
	Water	Buffer	FUP	RUP	dNTP	Polymerase
Col 1	41	5	1	1	1	1
Col 2	41	5	1	1	1	1
Col 3	41	5	1	1	1	1
Col 4	41	5	1	1	1	1
Col 5	41	5	1	1	1	1

Table 33: Preparation of PCR reaction for “on colony screening” of Ptt-XET16A insertion in pD6-2(PstI,BamHI) plasmid.

All reagents except polymerase were mixed and incubated 1 minute at 95°C, after that, polymerase was added and 30 repetition of the temperature sequence described in the following table was done.

Temperature (°C)	Time (min)
95	1.25
49	1.5
72	9

Table 34: PCR program sequence.

Reaction products were analyzed by 2% agarose gel electrophoresis, looking for insert amplification. Colonies showing positive amplification were used to inoculate 3 mL 2YT media tubes, which were incubated O.N. at 37°C and 300 rpm. Resulting cultures were used to extract and purify pD6-2*Ptt*-XET16A plasmid using the Wizard miniprep purification kit. Cloning of *Ptt*-XET16A gene in pD6-2 plasmid was verified by analytical restriction analysis using *Hind*III, *Stu*I and *Sac*I restriction enzymes. Gene sequence correctness of obtained pD6-2*Ptt*-XET16A plasmid was analyzed by gene sequencing using the BigDye terminator kit from ABI Prism using gene flanking FUP and RUP primers.

2.- Synthesis.

2.1.- General methods.

2.1.1.- Solvents.

Solvents were distilled and stored under recommended conditions²⁰⁰.

Ethyl acetate and acetone were dried on K_2CO_3 , and fractional distilled.

Dichloromethane, cyclohexane, and chloroform were dried with $CaCl_2$ and fractional distilled.

Methanol was dried with magnesium/iodine (5/0.5 w/w), distilled and stored under nitrogen.

Acetonitrile was dried with calcium hydride, distilled and stored in 4 Å molecular sieves.

Pyridine was dried with KOH and fractional distilled under reduced pressure.

Tetrahydrofuran was dried with H_4LiAl , distilled and stored under nitrogen.

2.1.2.- Chromatography.

Reaction progress was followed by thin layer chromatography (TLC) (aluminum silica gel F₂₅₄, from Merck) with the appropriate eluents. TLC were observed under UV light and by revealing with $H_2SO_4:MeOH:H_2O$ (5:45:45) followed by heating at 90°C during 15 min.

Purifications by normal-phase flash chromatography were done under nitrogen or air pressure with silica gel columns (SiO_2 60 ACC 35-70 μm from SDS and Merck Geduran SI 60 40-63 μm) with the appropriate eluent.

Purifications by normal-phase open chromatography were done at atmospheric pressure using silica gel (SiO_2 60 ACC 70-200 μm from SDS and Merck Geduran SI 60 63-200 μm) columns with the appropriate eluent. Fractions were collected using a automatic fraction collector (Redifrac from Pharmacia Biotech).

Purifications by normal-phase or reverse phase prepacked columns were done using Merck Lobar[®] Lichroprep RP-18 and Si-60 40-63 μm columns with different dimensions, with the appropriate eluents, and using a Micro g/5 pulse pump from Prominent. Fractions were collected using an automatic fraction collector (Redifrac from Pharmacia Biotech).

Purifications by gel filtration chromatography were done using a 170 cm long, ID 1.5 cm Econo-column and Bio-Gel P2, P4 or P6 resin from BioRad. Flow rate was regulated using a peristaltic pump from Gilson, and eluent was MilliQ water. Fractions were collected using an automatic fraction collector (Redifrac from Pharmacia Biotech).

Purification by anion exchange chromatography was done using a 20 cm long, ID 1.5 cm Econo-column and Macro-Prep DEAE support from BioRad. Flow rate was regulated using a peristaltic pump from Gilson. Product was charged in water and eluted using a gradient of NaOH. Fractions were collected using an automatic fraction collector (Redifrac from Pharmacia Biotech).

2.1.3.- Analytical methods.

Mass spectra were done in CERMAV-CNRS or in KTH using the quadripole NERMAG R 10-10C version 2000 for ionization by accelerated atom bombardment (FAB) and chemical ionization (DCI); using the spectrometer Water Micromass ZQ for electro-spray ionization and using a Bruker Autoflex for MALDI. Negative ion (ESI-TOF) mass spectra of ANTS labeled oligosaccharides were recorded on Q2-ToF™ mass spectrometer operated a resolution of > 10000 FWHM (Waters corporation micromass ZQ spectrometers) in KTH.

Capillary electrophoresis analyses were performed on a Hewlet-Packard HP^{3D} CE GC 1600 AX system equipped with a diode array UV-VIS detector. The capillary is 72 cm effective length, 50 µm internal diameter fused silica capillary with an extended light path bubble (150 µm) in the detection window.

2.1.4.- Nuclear magnetic resonance spectroscopy.

NMR spectra were recorded in the CERMAV-CNRS with a Bruker AC300 and Avance 400 and in the IQS with a Varian Gemini 300.

Chemical displacements (δ) were expressed in part per million (ppm) referring to tetramethyl silane (TMS) or sodium propionate of tetramethylsilyl. Coupling constants (J) were expressed in Hz. To describe signals the following notation was used: s (singlet), d (doublet), dd (doublet of doublets), t (triplet), m (multiplet), H_{arom}, and C_{arom} (aromatic protons and carbons respectively).

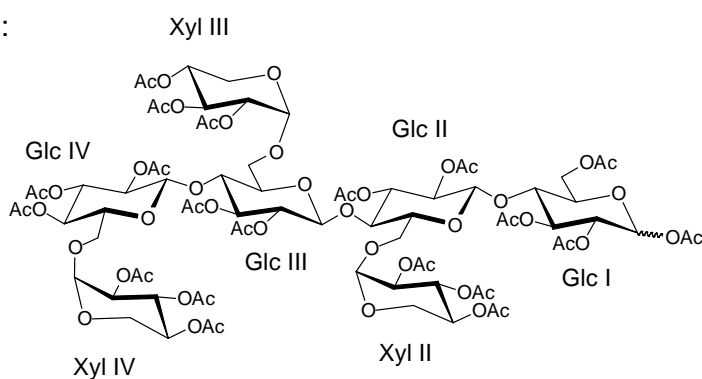
Nomenclature of different monosaccharides which form the characterized oligosaccharide to assign signals in NMR was given as follows.

Each monosaccharide receives a three unit name to indicate the type of monosaccharide (Glc, Xyl, Gal, Fuc...)

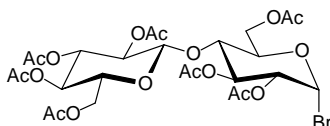
Each monosaccharide in the backbone has a roman number indicating its position starting from the reducing end.

Monosaccharides substituting units in the backbone have the same roman number that the substituted monosaccharide.

For example:

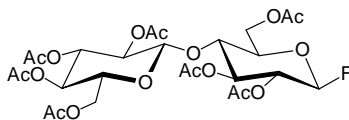


2.2.- Bromide of 2,3,4,6-tetra-O-acetyl- β -D-glucopyranosyl-(1 \rightarrow 4)-2,3,6-tri-O-acetyl- α -D-glucopyranoside (4).



1 g (1.47 mmol, 1 eq) per-O-acetylated cellobiose (**3**) was poured into a round bottomed flask and flushed with N_2 , after that, 14.7 mL HBr/AcOH 33% were added and reaction crude was stirred at R.T. until dissolution of cellobiose (aprox. 45 min). Reaction crude was poured on 75 mL water/ice, insoluble product was filtered, dissolved with $CHCl_3$, dried with $MgSO_4$, and finally, solvent was eliminated at vacuum. This product was immediately used for next step without purification.

2.3.- Fluoride of 2,3,4,6-tetra-O-acetyl- β -D-glucopyranosyl-(1 \rightarrow 4)-2,3,6-tri-O-acetyl- β -D-glucopyranoside (5).

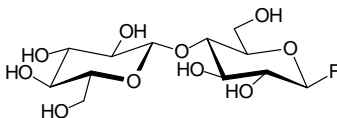


The newly obtained protected cellobiosyl bromide (4) was dissolved in 60 mL fresh dried acetonitrile, then, 1.26 g of AgF (9.9 mmol) were added and reaction suspension was stirred during 3 h at R.T. until total evolution was observed by TLC. Reaction was stopped by filtration on Celite® and solvent was eliminated at vacuum. Product was purified on flash chromatography with AcOEt/CH₂Cl₂ 1:1. Finally, 0.82 g (1.3 mmol) of a white product were recovered. The overall yield over last two steps was 87%.

¹H-NMR (CDCl₃, 300 MHz): δ (ppm) = 5.36 (dd, 1H, $J_{1,2} = 5.7$ Hz, $J_{1,F} = 52.8$ Hz, H-1 of Glc^I); 5.20-4.91 (m, 5H, H-2 and H-3 of Glc^{II} and H-4 of Glc^I); 4.57-4.37 (m, 3H, H-1 of Glc^I, H-5 of Glc^{II}); 4.12-3.93 (m, 3H, H-6a of Glc^{II} and H-4 of Glc^I); 3.85-3.66 (m, 2H, H-6b of Glc^{II}); 2.14-1.99 (m, 21H, CH₃CO).

¹³C-NMR (CDCl₃, 75 MHz): δ (ppm) = 170.3-168.9 (CH₃CO); 105.7 (d, $J_{C,F} = 216.7$ Hz, C-1 of Glc^I); 100.8 (C-1 of Glc^{II}); 75.3 (C-4 of Glc^I); [72.8, 72.6 (d, 2.8 Hz), 72.0, 71.8 (d, 6.8 Hz), 71.5, 71.1 (d, 29.5 Hz)](C-2, C-3 and C-5 of Glc^{II}); 67.7 (C-4 of Glc^{II}); 61.6, 61.5 (C-6 of Glc^{II}); 20.9-20.6 (CH₃CO).

2.4.- Fluoride of β -D-glucopyranosyl-(1 \rightarrow 4)- β -D-glucopyranoside (1).

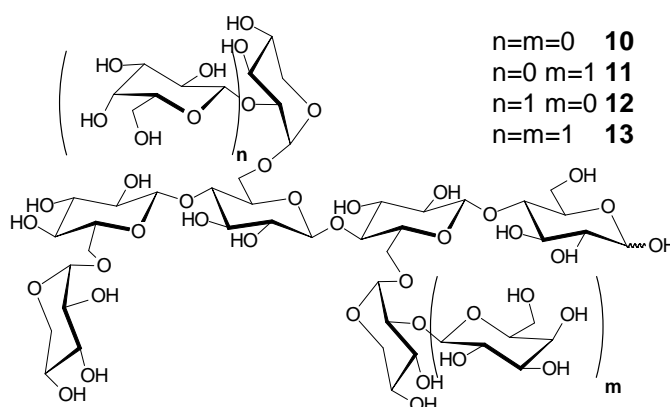


100 mg (0.18 mmol) protected cellobiosyl fluoride (5) were solved in 20 mL freshly dried MeOH, then, 0.3 mL MeONa 1 M were added and reaction mixture was stirred at 0°C until total deprotection judged by TLC (approximately 3 h). Reaction crude was filtered through Amberlyst®15 previously washed with dry MeOH to neutralize. MeOH was eliminated at vacuum maintaining bath temperature below

10 °C. 48.5 mg (0.14 mmol, 90%) were recovered. This product was produced freshly every time prior to use.

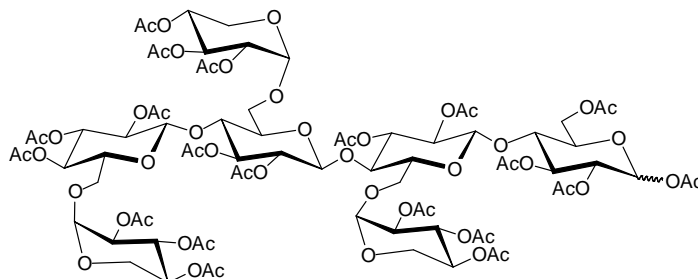
¹H-NMR (D₂O, 300 MHz): δ(ppm)=5.28 (dd, 1H, $J_{1,2} = 7.2$ Hz, $J_{1,F} = 53.1$ Hz, H-1 of Glc^{Iβ}); 4.52 (d, 1H, $J_{1,2} = 7.8$ Hz, H-1 of Glc^{II}); 4.11-3.29 (m, 12H, H-2, H-3, H-4, H-5, H-6a&b of Glc^{I,II}).

2.5.- XGOs (XXXG(10), XLXG(12), XXLG(11), and XLLG(13)).



1.1 g xyloglucan (XG) from Tamarind seeds purchased at Megazyme were solved in 200 mL AcONa 20 mM pH 4.5 previously warmed at 60°C. 60 mg of cellulase from *Trichoderma reesei* were added and reaction mixture was incubated O.N. at 37°C, until all XG was digested. Finally, reaction crude was freeze dried. Recovered white solid was solved in water and purified by gel filtration chromatography using BioGel P6 resin in a 170 cm length and 1.5 cm ID column. Fractions enriched in XGOs were freeze dried and purified again by gel filtration chromatography using BioGel P2 resin in a 170 cm length and 1.5 ID column. XGOs purity was evaluated by HPCE analysis of fractions *prior* ANTS derivatization¹²². Finally, 804 mg purified XGOs (molar ratio 1:6:6, **10:11&12:13**) were recovered (aprox. 73% yield).

2.6.- [2,3,4-tri-O-acetyl- α -D-xylopyranosyl-(1 \rightarrow 6)]-2,3,4-tri-O-acetyl- β -D-glucopyranosyl-(1 \rightarrow 4)-[2,3,4-tri-O-acetyl- α -D-xylopyranosyl-(1 \rightarrow 6)]-2,3-di-O-acetyl- β -D-glucopyranosyl-(1 \rightarrow 4)-[2,3,4-tri-O-acetyl- α -D-xylopyranosyl-(1 \rightarrow 6)]-2,3-di-O-acetyl β -D-glucopyranosyl-(1 \rightarrow 4)-1,2,3,6-tri-O-acetyl- α/β -D-glucopyranosyl XXXG (15).



5 g of XG from Tamarind seeds provided by Megazyme were solved in 4 L double distilled water, 400 mg cellulase from *Trichoderma reesei* from Flucka and 770 μ l (0.67 U/ml) of β -galactosidase from *Aspergillus niger* provided by Megazyme were added, resulting in a final concentration of 1 mg/ml of cellulase and 0.67 U/ml β -galactosidase. Reaction crude was incubated at 37 $^{\circ}$ C until TLC showed mainly two spots, one identified as galactose and the other as XXXG (10). If incubation times are too long, another product with intermediate Rf could be detected indication of unspecific degradation of XXXG. Reaction was stopped and reaction crude was freeze dried.

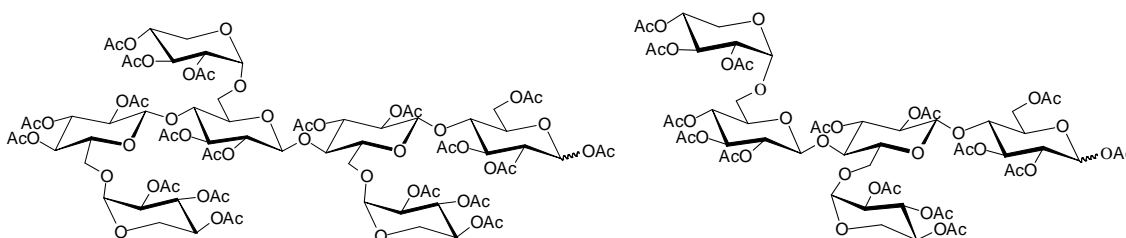
The resulting white solid was poured in a round bottomed flask, 200 mL pyridine and 200 mL acetate anhydride and a catalytic amount of dimethylaminopyridine (DMAP) were added. Reaction mixture was stirred at R.T. during 2 days. Reaction crude was mixed with 800 mL water/ice and stirred during 1 hour. The resulting aqueous suspension was filtered, obtaining a yellow-white solid which was solved with CH_2Cl_2 . The organic phase was dried with MgSO_4 and solvent was eliminated at vacuum, pyridine and AcOH rests were codistilled with toluene.

The obtained white powder was purified by normal phase flash chromatography recovering 3.58 g per-O-acetylated XXXG (15) (1.88 mmol, 40%).

$^1\text{H-NMR}$ (CDCl_3 , 300 MHz): δ (ppm)= 6.21 (d, 0.3 H, $J_{1,2}=3.6$ Hz, H-1 of Glc^{I α}); 5.67 (d, 0.7 H, $J_{1,2}= 8.4$ Hz, H-1 of Glc^{I β}); 5.44-3.37 (m, 45H, H-1 of Glc^{II, III, IV} and Xyl^{II, III, IV}, H-2, H-3, H-4 of Glc^{I, II, III} and Xyl^{II, III, IV}, H-5 of Glc^{I, II, III, IV}, H-5a&b of Xyl^{II, III, IV}, H-6a&b of Glc^{I, II, III, IV})

^{13}C -NMR (CDCl₃, 75 MHz): δ (ppm)= 170.2-168.3 (CH₃CO); 100.3-99.9 (C-1 of Glc^{II,III,IV}); 96.8, 96.8, 95.7 (C-1 of Xyl^{II, III, IV}); 91.0 (C-1 of Glc^{I β}); 88.6 (C-1 of Glc^{I α}); 76.2, 76.0, 75.0, 74.9, 74.5, 74.5, 73.1, 73.1, 72.5, 72.5, 72.4, 71.9, 71.8, 71.7, 71.4, 70.6, 70.5, 70.4, 70.3, 70.2, 69.5, 69.2, 69.1, 69.1, 68.8 (C-2 to C-5 of Glc^{I,II,III,IV} and C-2 to 4 of Xyl^{II,III,IV}), 67.1 (C-6 of Glc^{IV}), 65.4 (C-6 of Glc^{III}), 65.0 (C-6 of Glc^{II}); 61.7, 61.4 (C-6 of Glc^{I \square and I \square}), 59.0, 58.8, 58.6 (C-5 of Xyl^{II,III,IV}), 20.9-20.4 (CH₃CO).

2.7.- [(2,3,4-Tri-O-acetyl- α -D-xylopyranosyl)-(1 \rightarrow 6)]-(2,3,4-tri-O-acetyl- β -D-glucopyranosyl)-(1 \rightarrow 4)-[(2,3,4-tri-O-acetyl- α -D-xylopyranosyl)-(1 \rightarrow 6)]-(2,3-di-O-acetyl- β -D-glucopyranosyl)-(1 \rightarrow 4)-1,2,3,6-tetra-O-acetyl-D-glucopyranose (per-O-acetylated XXG (32)) and [(2,3,4-Tri-O-acetyl- α -D-xylopyranosyl)-(1 \rightarrow 6)]-(2,3,4-tri-O-acetyl- β -D-glucopyranosyl)-(1 \rightarrow 4)-[(2,3,4-tri-O-acetyl- α -D-xylopyranosyl)-(1 \rightarrow 6)]-(2,3-di-O-acetyl- β -D-glucopyranosyl)-(1 \rightarrow 4)-[(2,3,4-tri-O-acetyl- α -D-xylopyranosyl)-(1 \rightarrow 6)]-(2,3-di-O-acetyl- β -D-glucopyranosyl)-(1 \rightarrow 4)-1,2,3,6-tetra-O-acetyl-D-glucopyranose (per-O-acetylated XXXG (15)).



Alternatively, with a similar methodology, Régis Fauré at CERMAV-CNRS^{133,146} have obtained the same product with slightly higher yield, as it follows: An aqueous suspension of tamarind seed xyloglucan (5.0 g in 500 mL) was gently shaken at 60°C for 2 h, then *endo*-glucanase (xyloglucanase Cel12B from *Aspergillus aculeatus*, 5 mg) was added and the reaction mixture was incubated at 37°C for 48 h. The resulting solution was then treated by commercially available β -galactosidase (*Aspergillus niger*, 25 mg, 2800 U) at 60°C for 2 h, then was subject to freeze-drying. Acetylation of the residue (acetic anhydride/pyridine, 1:2 v/v, 225 mL) in the presence of catalytic amount of dimethylaminopyridine (DMAP) was carried out at room temperature and quenched after 12 h by adding MeOH at 0°C. After concentration *in vacuo*, the residue was dissolved in CH₂Cl₂ and washed with 20% aqueous KHSO₄ and brine. The aqueous solutions were back extracted with CH₂Cl₂ (2 x). The organic layers were dried, concentrated and purified by flash chromatography (toluene/acetone, 4:1 then 3:1 v/v).

The per-O-acetylated pentasaccharide XXG (**32**) (0.77g, 0.55 mmol) and the peracetylated heptasaccharide XXXG (**15**) (4.18 g, 2.20 mmol) were isolated in 14 and 56% yield respectively.

2.8.- [(2,3,4-Tri-O-acetyl- α -D-xylopyranosyl)-(1 \rightarrow 6)]-(2,3,4-tri-O-acetyl- β -D-glucopyranosyl)-(1 \rightarrow 4)-[(2,3,4-tri-O-acetyl- α -D-xylopyranosyl)-(1 \rightarrow 6)]-(2,3-di-O-acetyl- β -D-glucopyranosyl)-(1 \rightarrow 4)-1,2,3,6-tetra-O-acetyl-D-glucopyranose (per-O-acetylated XXG (32**)).**

$^1\text{H-NMR}$ (CDCl_3 , 400 MHz): See Table 1.

$^{13}\text{C-NMR}$ (CDCl_3 , 100 MHz): δ (ppm) = 170.3-168.7 (CH_3CO), 100.6, 100.2 (2C : 100.19 and 100.15 ppm), 100.1 (C-1 of Glc^{II} and III), 96.8 (C-1 of Xyl^{II}), 96.3 (C-1 of Xyl^{III}), 91.2 (C-1 of Glc^{IB}), 88.8 (C-1 of Glc^{IA}), 76.1-69.0 (C-2 to C-5 of Glc and C-2 to C-4 of Xyl), 67.1 (C-6 of Glc^{III}), 65.1 (C-6 of Glc^{II}), 61.8, 61.5 (C-6 of Glc^{IA} and ^{IB}), 59.0, 58.8 (C-5 of Xyl), 21.0-20.5 (CH_3CO); ES-HRMS: m/z : calcd. for $\text{C}_{58}\text{H}_{78}\text{O}_{39}\text{Na}$ $[\text{M}+\text{Na}]^+$: 1421.4018, found: 1421.4020.

	H-1	H-2	H-3	H-4	H-5a	H-5b	H-6a	H-6b
Glc ^{IA}	6.19 (3.7)	4.92	5.40	3.82	3.94		4.42	4.06
Glc ^{IB}	5.66 (8.2)	4.94	5.19	3.83	3.72			
Glc ^{II}	4.52 (7.9)	4.70	5.11	3.94	3.44			
	4.51 (7.9)	4.68	5.10	3.91	3.43		3.86	3.74
Glc ^{III}	4.70 (8.0)	4.87	5.17	5.08	3.80		3.79	3.63
Xyl ^{II}	5.10 (3.4)	4.84	5.40 (9.9)	5.02	3.90	3.73		
Xyl ^{III}	5.01 (3.5)	4.78	5.39 (9.9)	4.96	3.78	3.64		

Table 35: Summary of ^1H NMR data (400 MHz, CDCl_3) of per-O-acetylated XXG 5.

2.17-1.96 (m, 45H, CH_3CO).

2.9.- [(2,3,4-Tri-O-acetyl- α -D-xylopyranosyl)-(1 \rightarrow 6)]-(2,3,4-tri-O-acetyl- β -D-glucopyranosyl)-(1 \rightarrow 4)-[(2,3,4-tri-O-acetyl- α -D-xylopyranosyl)-(1 \rightarrow 6)]-(2,3-di-O-acetyl- β -D-glucopyranosyl)-(1 \rightarrow 4)-[(2,3,4-tri-O-acetyl- α -D-xylopyranosyl)-(1 \rightarrow 6)]-(2,3-di-O-acetyl- β -D-glucopyranosyl)-(1 \rightarrow 4)-1,2,3,6-tetra-O-acetyl-D-glucopyranose (per-O-acetylated XXXG (15)).

¹H-NMR (CDCl₃, 400 MHz): See Table 2.

¹³C-NMR (CDCl₃, 100 MHz): δ (ppm) = 170.5-168.5 (CH₃CO), 100.6, 100.5, 100.4, 100.1 (C-1 of Glc^{II, III and IV}), 97.1, 97.0 (C-1 of Xyl^{II and III}), 95.9 (C-1 of Xyl^{IV}), 91.2 (C-1 of Glc^{I β}), 88.8 (C-1 of Glc^{I α}), 76.4, 76.2, 75.2, 75.1, 74.7, 74.6, 73.3, 73.2, 72.7, 72.6, 72.5, 72.0, 71.9, 71.8, 71.6, 70.8, 70.7, 70.5, 70.4, 70.3, 69.6, 69.4, 69.2, 69.1, 69.0 (C-2 to C-5 of Glc and C-2 to 4 of Xyl), 67.3 (C-6 of Glc^{IV}), 65.5 (C-6 of Glc^{III}), 65.0 (C-6 of Glc^{II}), 61.8, 61.5 (C-6 of Glc^{I α and I β}), 59.1, 58.9, 58.7 (C-5 of Xyl), 21.0-20.5 (CH₃CO); ¹H NMR (400 MHz, CDCl₃) and ¹³C NMR (100 MHz, CDCl₃) were identical to the one described²⁰¹. ES-HRMS: *m/z*. calcd. for C₇₉H₁₀₆O₅₃Na [M+Na]⁺: 1925.5497, found: 1925.5494.

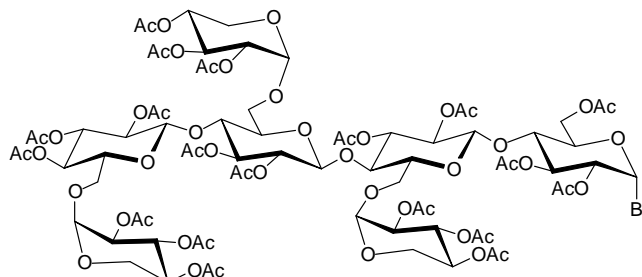
	H-1	H-2	H-3	H-4	H-5a	H-5b	H-6a	H-6b
Glc ^{Iα}	6.18 (3.7)	4.92	5.38	3.79	3.93 (4.8, -)		4.40 (12.2)	4.09
Glc ^{Iβ}	5.65 (8.2)	4.94	5.19 (8.8)	3.80	3.70 (4.9, -)		4.39 (12.2)	4.07
Glc ^{II}	4.51 (7.9)	4.67	5.06	3.98	3.35		3.98	3.65
	4.49 (7.9)	4.64	5.05	3.94	3.34			
Glc ^{III}	4.69	4.66	5.14	4.01	3.72		4.05	3.81
Glc ^{IV}	4.80	4.78	5.18	5.09	3.92		3.82	3.62
Xyl ^{II*}	5.05 (3.7)	4.82	5.34	4.95	3.94	3.69		
Xyl ^{III*}	5.06 (3.4)	4.87 (10.1)	5.38	5.02	3.91	3.77		
Xyl ^{IV}	4.99 (3.7)	4.78	5.37	4.95	3.75	3.64		

* Assignments may be reversed.

2.16-1.94 (m, 60H, CH₃CO).

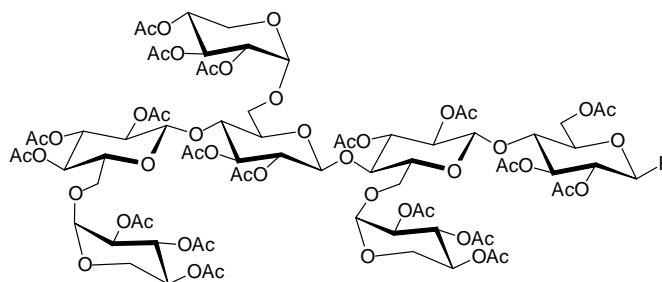
Table 36: Summary of ¹H NMR data (400 MHz, CDCl₃) of per-O-acetylated XXXG 6.

2.10.- Bromide of the [2,3,4-tri-O-acetyl- α -D-xylopyranosyl-(1 \rightarrow 6)]-2,3,4-tri-O-acetyl- β -D-glucopyranosyl-(1 \rightarrow 4)-[2,3,4-tri-O-acetyl- α -D-xylopyranosyl-(1 \rightarrow 6)]-2,3-di-O-acetyl- β -D-glucopyranosyl-(1 \rightarrow 4)-[2,3,4-tri-O-acetyl- α -D-xylopyranosyl-(1 \rightarrow 6)]-2,3-di-O-acetyl β -D-glucopyranosyl-(1 \rightarrow 4)-1,2,3,6-tri-O-acetyl- α -D-glucopyranoside (16).



0.955 g (0.5 mmol) per-O-acetylated XXXG (**15**) were poured in a round bottomed flask. Then, 16 mL of 1:5 previously cooled mixture of HBr/HAcO:CH₂Cl₂ were added and reaction mixture was stirred in an ice bath. Reaction was controlled by TLC and it was stopped, as soon as starting material total consumption was detected, by mixing reaction crude with H₂O/ice. Suspension was stirred 10 min at 0°C and after that, extracted three times with CHCl₃. Organic layer was neutralized 3 x 50 mL NaHCO₃ saturated and dried with MgSO₄. Finally solvent was eliminated by distillation and product was dried at vacuum, obtaining 0.94 g non purified bromide **16** which was immediately used for next step without further purification.

2.11.- Fluoride of the [2,3,4-tri-O-acetyl- α -D-xylopyranosyl-(1 \rightarrow 6)]-2,3,4-tri-O-acetyl- β -D-glucopyranosyl-(1 \rightarrow 4)-[2,3,4-tri-O-acetyl- α -D-xylopyranosyl-(1 \rightarrow 6)]-2,3-di-O-acetyl- β -D-glucopyranosyl-(1 \rightarrow 4)-[2,3,4-tri-O-acetyl- α -D-xylopyranosyl-(1 \rightarrow 6)]-2,3-di-O-acetyl β -D-glucopyranosyl-(1 \rightarrow 4)-1,2,3,6-tri-O-acetyl- β -D-glucopyranoside (17).



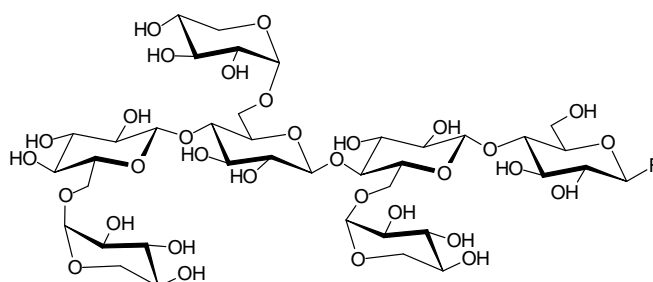
0.94 g of not purified α -bromide **16** were solved in 22 mL previously dried acetonitrile, followed by the addition of 465 mg (3.7 mmol) AgF. Reaction suspension was stirred at room temperature and controlled by TLC. After 4 hours, reaction crude was filtered through Celite[®] and solvent was removed by distillation. Product was purified by normal phase chromatography using a normal phase Lobar[®] Lichroprep prepacked column (AcOEt/Cy 1:1) obtaining protected β -fluoride XXXG- β F (**17**) in 38% yield over last two steps (0.35 g, 0.19 mmol).

Mass spectrometry: ESI-TOF-MS: $[M-3H]^{3-}$, calcd: 475.425, obs. 475.442; $[M-3H+Na]^{2-}$, calcd: 724.633, obs. 724.661.

¹H-NMR (CDCl₃, 300 MHz): δ (ppm)= 5.41 (dd, 1 H, $J_{1,2}=5.0$ Hz, $J_{1,F}=53.2$ Hz H-1 of Glc^{l β}); 5.44-3.34 (m, 45 H, H-1 of Glc^{l β} , ^{II}, ^{III}, ^{IV} and Xyl^{l β} , ^{II,III,IV}, H-2, H-3 and H-4 of Glc^{l β} , ^{II}, ^{III}, ^{IV} and Xyl^{l β} , ^{II,III,IV}, H-5 of Glc^{l β} , ^{II,III,IV}, H-5a&b of Xyl^{l β} , ^{II,III,IV}, H-6a&b of Glc^{l β} , ^{II}, ^{III}, ^{IV})

¹³C-NMR (CDCl₃, 75 MHz): δ (ppm)= 170.3-168.3 (CH₃CO); 105.1 (d, $J_{C,F}=218.3$ Hz C-1 of Glc^l); 100.5 (C-1 of Glc^{l β}); 100.3 (C-1 of Glc^{l β}); 100.3 (C-1 of Glc^{l β}); 97.0, 96.9 (C-1 of Xyl^{l β} , ^{III}); 95.8 (C-1 of Xyl^{l β} , ^{IV}); 75.6, 75.0, 75.0 (C-4 of Glc^{l β} , ^{II,III}); 74.7, 74.6, 73.2, 72.8, 72.7, 72.6, 72.3, 71.9 (2C), 71.7, 71.7, 71.5, 71.0, 70.6 (2C), 70.4, 69.3, 69.2 (3C), 69.1, 68.9 (2C) (C-2, C-3, C-4 of Glc^{l β} , ^{II,III,IV} and Xyl^{l β} , ^{II,III,IV}, C-5 of Glc^{l β} , ^{II,III,IV}); 67.3 (C-6 of Glc^{l β} , ^{IV}); 65.5 (C-6 of Glc^{l β} , ^{III}); 64.9 (C-6 of Glc^{l β} , ^{II}); 61.9 (C-6 of Glc^l) 59.1, 58.9, 58.7 (C-5 of Xyl^{l β} , ^{II,III,IV}); 21.0-20.6 (CH₃CO).

2.12.- Fluoride of the [α -D-xylopyranosyl-(1 \rightarrow 6)]- β -D-glucopyranosyl-(1 \rightarrow 4)-[α -D-xylopyranosyl-(1 \rightarrow 6)]- β -D-glucopyranosyl-(1 \rightarrow 4)-[α -D-xylopyranosyl-(1 \rightarrow 6)]- β -D-glucopyranosyl-(1 \rightarrow 4)- β -D-glucopyranoside (XXXG β F (14**)).**



98,4 mg (53 μ mol) per-O-acetylated XXXG β F (**17**) were solved in 12.5 mL freshly dried MeOH, 2.5 mL MeONa 200 mM were added and reaction mixture was stirred at 0°C until total deprotection judged by TLC (approximately 3 h). Reaction crude was filtered through Amberlyst[®]15 previously washed with dry MeOH to

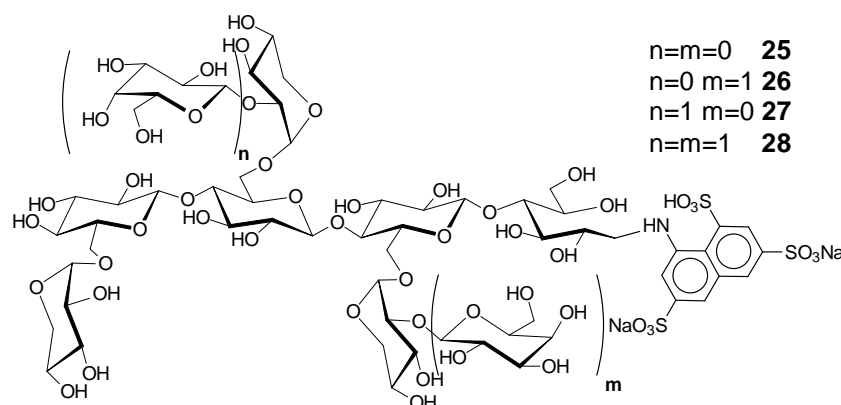
neutralize. Product was dissolved in cold water and freeze dried. Deprotected product (**14**) was recovered in 82% yield (46.2 mg, 43 μ mol).

$^1\text{H-NMR}$ (D_2O , 300 MHz): δ (ppm) = 5.29 (dd, 1H, $J_{1,2} = 7.3$ Hz, $J_{1,F} = 53.1$ Hz, H-1 of Glc^{I β}); 4.85-4.80 (m, 3H, H-1 of Xyl^{II,III,IV}); 4.5-4.35 (m, 3H, H-1 of Glc^{I,II,III}); 4.0-3.1 (m, 39H, H-2, H-3, H-4 of Glc^{I,II,III,IV} and Xyl^{II,III,IV}, H-5 of Glc^{I,II,III,IV}, H-5a&b of Xyl^{II,III,IV}, H-6 of Glc^{I,II,III,IV}).

2.13.- Analytical ANTS labeling of substrates.

A solution of the oligosaccharide to label (coming from chromatographic purifications or being a time point aliquot from a kinetic experiment) was freeze-dried and dissolved in a solution of ANTS (0.15 M) in AcOH/water (20 μ L, 3:17 v/v). Then, a solution of NaCNBH₃ (1 M) in freshly purified THF (20 μ L) was added, and the reaction incubated for 7 h at 55°C in a PCR machine. Derivatized products were re-dissolved with water and then are ready to be analyzed by HPCE.

2.14.- XGOs-ANTS mixture (XXXGANTS (25), XLGANTS(26), XLXGANTS(27), and XLLGANTS(28)).

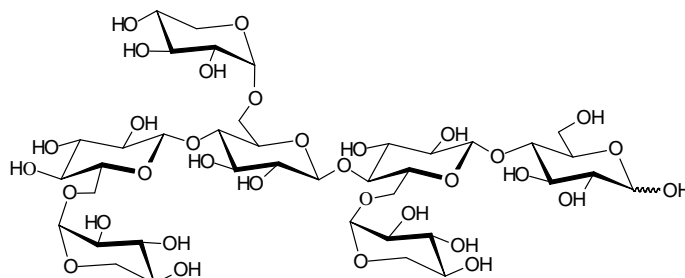


Tamarind seed XG (0.25 g) was dissolved in preheated (50°C) AcONa buffer (20 mM, pH 4.5, 50 mL), then *Trichoderma reesei* cellulase (6 mg) was added. The reaction was incubated overnight at 37°C and freeze-dried. The resulting solid was dissolved in water and purified by gel filtration chromatography on BioGel[®] P2 resin, from which a mixture of XXXG, XLXG, XXLG, and XLLG (0.19 g) was isolated.

Selected fractions were freeze-dried and resulting product was dissolved in a solution of ANTS (0.15 M) in AcOH/water (2 mL, 3:17 v/v). Then, a solution of

NaCNBH₃ (1 M) in freshly purified THF (2 mL) was added, and the reaction incubated for 7 h at 55°C. Reaction crude was concentrated under reduced pressure, and purified by two consecutive gel filtration chromatographic steps on a BioGel P2 resin (170 cm x 1.5 cm ID column, BioRad) to remove the large excess of unreacted ANTS. 88 mg of XGOs-ANTS mixture (XXXGANTS (**25**), (XLXG/XXLG)ANTS (**26/27**) and XLLGANTS (**28**) 1:6:6) were isolated, obtaining an approximately 6% yield from XG polymer.

2.15.- ([α -D-xylopyranosyl-(1 \rightarrow 6)]- β -D-glucopyranosyl-(1 \rightarrow 4)-[α -D-xylopyranosyl-(1 \rightarrow 6)]- β -D-glucopyranosyl-(1 \rightarrow 4)-[α -D-xylopyranosyl-(1 \rightarrow 6)]- β -D-glucopyranosyl-(1 \rightarrow 4)- β -D-glucopyranose (XXXG (10**)).**

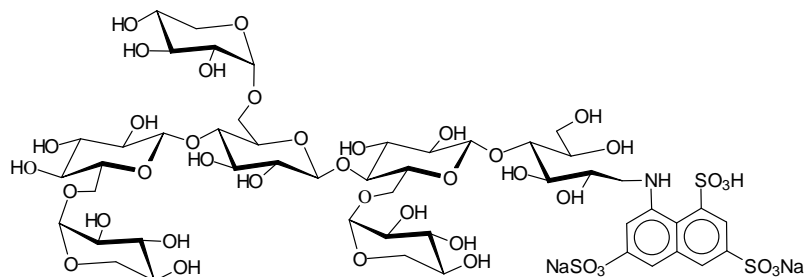


Per-O-acetylated XXXG (**15**) (1.5 g, 0.79 mmol) was solved with 100 mL MeOH, then 2 mL MeONa 1M were added. Reaction crude was stirred at 0°C during 8 hours at room temperature, until reaction completion. Reaction crude was neutralized by filtration through a Amberlyst 15 resin. The neutralized solution was concentrated and product was resuspended with MilliQ water and freeze dried. 0.83 g (0.79 mmol) of **10** were recovered.

¹H-NMR (300 MHz, D₂O): δ (ppm) = 5.21 (d, $J_{1,2}=3,7$ Hz, 0.4H, H-1 of Glc^{I α}); 4.95-4.93 (m, 3H, H-1 of Xyl^{II,III and IV}); 4,64 (d, $J_{1,2}=7.9$ Hz, 0.6H, H-1 of Glc^{I β}); 4.59-4.54 (m, 3H, H-1 of Glc^{I,II,III and IV}); 4.02-3.25 (m, H-2 of Glc^{I,II,III,IV} and Xyl^{II,III,IV}, H-3 of Glc^{I,II,III,IV} and Xyl^{II,III,IV}, H-4 of Glc^{I,II,III,IV} and Xyl^{II,III,IV}, H-5 of Glc^{I,II,III,IV}, H-5a and H5b of Xyl^{II,III,IV}, and H6a and H6b of Glc^{I,II,III,IV})

¹³C NMR (75 MHz, D₂O): δ (ppm) = 103.5-103.0 (C-1 of Glc^{II,III,IV}); 99.5-98.9 (C-1 of Xyl^{II,III,IV}); 96.4 (C-1 of Glc^{I β}); 92.5 (C-1 of Glc^{I α}); 80.0-70.1 (C-2, C-3 and C-4 of Glc^{I,II,III,IV} and Xyl^{II,III,IV}, C-5 of Glc^{I,II,III,IV}); 66.7 (C-6 of Glc^{II,III,IV}); 62.2-61.8 (C-5 of Xyl^{II,III,IV}); 60.7 (C-6 of Glc^{I α and β}).

2.16.- ([α -D-xylopyranosyl-(1 \rightarrow 6)]- β -D-glucopyranosyl-(1 \rightarrow 4)-[α -D-xylopyranosyl-(1 \rightarrow 6)]- β -D-glucopyranosyl-(1 \rightarrow 4)-[α -D-xylopyranosyl-(1 \rightarrow 6)]- β -D-glucopyranosyl-(1 \rightarrow 4)- β -D-1-deoxy-D-glucitol-1-yl)-8-aminonaphthalene-1,3,6-trisulfonic acid, disodium salt (XXXG-ANTS (25)).



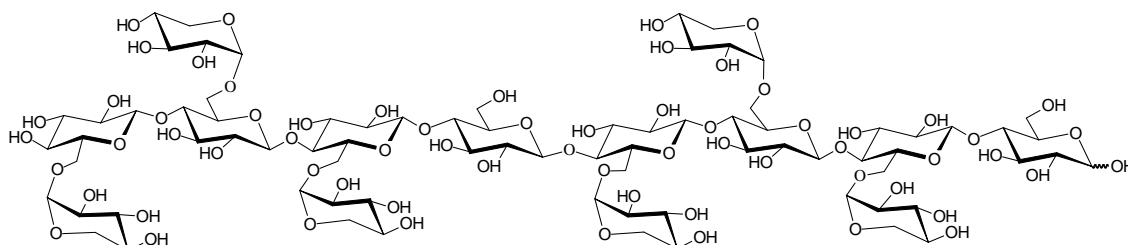
The heptasaccharide **10** (100 mg, 94 μ mol) was dissolved in a solution of ANTS (0.15 M) in AcOH/water (1 mL, 3:17 v/v). Then, a solution of NaCNBH₃ (1 M) in freshly purified THF (1 mL) was added, and the reaction was incubated for 7 h at 55°C. The reaction mixture was concentrated under reduced pressure and the resulting mixture was purified by a sequence of three chromatographic steps: 1) gel filtration on a BioGel P2 resin (170 cm x 1.5 cm ID column, BioRad) to remove the large excess of unreacted ANTS; 2) ionic exchange on a MacroPrep DEAE resin (BioRad) to separate derivatized from underivatized XXXG (**10**); and 3) gel filtration on a BioGel P2 resin for desalting and polishing the final XXXG-ANTS (**25**) (77 mg, 51 μ mol, 55% yield), which was isolated in > 95% purity (as assessed by TLC and HPCE).

Mass spectrometry: ESI⁻-TOF-MS: [M-3H]³⁻, calcd: 475.425, obs. 475.442; [M-3H+Na]²⁻, calcd: 724.633, obs. 724.661.

¹H NMR (300 MHz, D₂O): δ (ppm) = 8.61, 8.46, 7.76, 7.16, 7.15 (4d, J = 1.5 Hz, 4H, H_{arom}), 4.94 (m, 3H, H-1 of Xyl^{II,III,IV}), 4.60, 4.53, 4.51 (3d, $J_{1,2}$ = 8.2 Hz, 3H, H-1 of Glc^{II, III and IV}), 4.3-3.22 (m, 40H, rest of protons);

¹³C NMR (75 MHz, D₂O): δ (ppm) = 145.2, 142.2, 139.9, 135.9, 131.5, 124.6, 120.7, 115.0 (10C, C_{arom}), 104.2 (C-1 of Glc^{IV}), 102.9, 102.4 (C-1 of Glc^{II & III}), 99.1, 98.9 (C-1 of Xyl^{II & III}), 98.4 (C-1 of Xyl^{IV}), 79.8, 79.4, 78.6 (C-4 of Glc^{I, II & III}), 75.7, 74.4, 74.1, 74.1, 73.5, 73.4, 73.2, 73.1, 72.8, 71.6, 71.4, 70.8, 69.6, 69.4, 69.3, 66.2, 66.1, 65.8, 62.3, 61.7, 61.5, 61.4 (C-2 to C-6 of Glc^{I,II,III & IV} and C-2 to C-5 of Xyl^{II, III & IV}), 46.6 (C-1 of Glc^I);

2.17.- [α -D-xylopyranosyl-(1 \rightarrow 6)]- β -D-glucopyranosyl-(1 \rightarrow 4)-[α -D-xylopyranosyl-(1 \rightarrow 6)]- β -D-glycopyranosyl-(1 \rightarrow 4)-[α -D-xylopyranosyl-(1 \rightarrow 6)]- β -D-glucopyranosyl-(1 \rightarrow 4)- β -D-glucopyranosyl-(1 \rightarrow 4)-[α -D-xylopyranosyl-(1 \rightarrow 6)]- β -D-glucopyranosyl-(1 \rightarrow 4)-[α -D-xylopyranosyl-(1 \rightarrow 6)]- β -D-glucopyranosyl-(1 \rightarrow 4)-[α -D-xylopyranosyl-(1 \rightarrow 6)]- β -D-glucopyranose (XXXGXXXG) (23).



XXXGXXXG (23) was synthesized by Régis Fauré at CERMAV-CNRS (Grenoble) as part of collaborating efforts in EDEN project.^{133,146} However it has been synthesized also in this work for FRET substrate (p. 221).

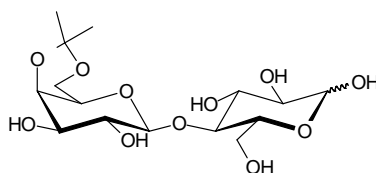
2.18.- β -D-galactopyranosyl-(1 \rightarrow 4)- β -D-glucopyranosyl-(1 \rightarrow 4)- [α -D-xylopyranosyl-(1 \rightarrow 6)]- β -D-glucopyranosyl-(1 \rightarrow 4)-[α -D-xylopyranosyl-(1 \rightarrow 6)]- β -D-glycopyranosyl-(1 \rightarrow 4)-[α -D-xylopyranosyl-(1 \rightarrow 6)]- β -D-glucopyranosyl-(1 \rightarrow 4)- β -D-glucopyranosyl-(1 \rightarrow 4)-[α -D-xylopyranosyl-(1 \rightarrow 6)]- β -D-glucopyranosyl-(1 \rightarrow 4)-[α -D-xylopyranosyl-(1 \rightarrow 6)]- β -D-glucopyranosyl-(1 \rightarrow 4)-[α -D-xylopyranosyl-(1 \rightarrow 6)]- β -D-glucopyranosyl-(1 \rightarrow 4)- β -D-glucopyranose (GalGXXXGXXXG) (38).

GalGXXXGXXXG (38) was synthesized by Régis Fauré at CERMAV-CNRS (Grenoble) as part of collaborating efforts in EDEN project¹⁴⁶.

2.19.- Donor library: XXXGGG (47), XXXGXG (45), XXXGGGGG (48), XXXGXXG (46), GXXXG (49), GGXXXG (50), GGGXXXG (51), GGGGXXXG (52), XGXXXG (54), XGGXXXG (55), XXGXXXG (29), GXXGXXXG (53), XGXGXXXG (56), GalGXXXG (40), GalGXXXGGG (59).

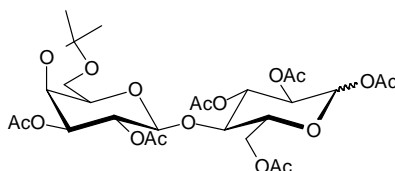
Ptt-XET16A donor library was synthesized by Régis Fauré at CERMAV-CNRS (Grenoble) as part of collaborating efforts in EDEN project¹⁴⁶.

2.20.- 4,6-isopropylene- β -D-galactopyranosyl-(1 \rightarrow 4)- α / β -D-glucopyranose (**60**).



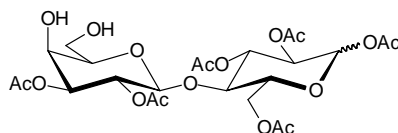
26.3 g β -D-galactopyranosyl-(1 \rightarrow 4)- α / β -D-glucopyranose monohydrate (73 mmol, 1 eq) were suspended in 300 mL DMF, then 50 mL of DMF were distilled under vacuum to dry reaction mixture. After that, 500 mg camphor-10-sulfonic acid were added followed by drop wise addition of 60 mL 2,2-dimethoxypropane (490 mmol, 7 eq) previously diluted with 60 mL DMF during 50 minutes. Reaction was stirred at R.T. till total dissolution of lactose. Finally, reaction crude was neutralized with Amberlite® IR-45. Solvent was eliminated at vacuum codistilled with toluene. Product was not further purified nor characterized, but it was identified by TLC comparison with the correspondent standard.

2.21.- 2,3-di-O-acetyl-4,6-isopropylene- β -D-galactopyranosyl-(1 \rightarrow 4)-1,2,3,6-tetra-O-acetyl- α / β -D-glucopyranose (**61**).



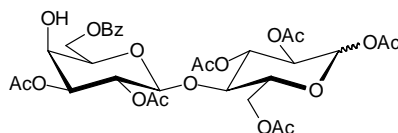
Non purified 4,6-isopropylene- β -D-galactopyranosyl-(1 \rightarrow 4)- α / β -D-glucopyranose (**60**) was suspended in Ac₂O/Py 1:1.5 (440 ml), a catalytic amount of dimethylaminopyridine was added. Reaction crude was stirred at R.T. during 21 hours. Reaction was quenched with 200 mL MeOH in a ice:water bath and solvent was eliminated at vacuum. Product was dissolved in CH₂Cl₂, extracted with KHSO₄ saturated and NaHCO₃ saturated and dried over Na₂SO₄. Solvent was eliminated at vacuum. After normal phase chromatography purification (AcOEt:Petroleum ether 1:1) 26 g (41 mmol, 56 % yield) of product **61** were recovered over last two steps. This product was identified by TLC comparison with the correspondent standard.

2.22.- 2,3-di-O-acetyl- β -D-galactopyranosyl-(1 \rightarrow 4)-1,2,3,6-tetra-O-acetyl- α/β -D-glucopyranose (62).



15 g (23.6 mmol, 1 eq) 2,3-di-O-acetyl-4,6-isopropylene- β -D-galactopyranosyl-(1 \rightarrow 4)-1,2,3,6-tetra-O-acetyl- α/β -D-glucopyranose (**61**) were dissolved in 75 mL CH_2Cl_2 , and 7.5 mL TFA 90% were added. Reaction crude was stirred at R.T. during 75 min, although reaction was not finished, by-products were detected by TLC. Reaction crude was washed with cold water, NaHCO_3 and dried on Na_2SO_4 . Finally solvent was eliminated at vacuum and after normal phase chromatography (Tol:Acetone 7:5) 11.4 g product (19.2 mmol, 81% yield) were recovered which was identified by TLC comparison with the correspondent standard. Also 1.6 g (2.5 mmol) starting material was recovered.

2.23.- 2,3-di-O-acetyl-6-benzoyl- β -D-galactopyranosyl-(1 \rightarrow 4)-1,2,3,6-tetra-O-acetyl- α/β -D-glucopyranose (63).



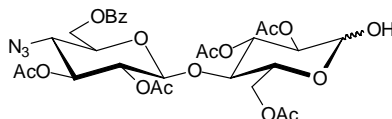
9.6 g (16.1 mmol, 1 eq) 2,3-di-O-acetyl- β -D-galactopyranosyl-(1 \rightarrow 4)-1,2,3,6-tetra-O-acetyl- α/β -D-glucopyranose (**62**) were dissolved in 96 mL dry CH_2Cl_2 , after that, 5.8 g 1-(benzoyloxy)benzotriazole (24.2 mmol, 1.5 eq) and 3.4 mL Et_3N (24.2 mmol, 1.5 eq) were added. Reaction was stirred at R.T. After 19 h reaction, 0.5 g (2.1 mmol, 0.1 eq) 1-(benzoyloxy)benzotriazole and 0.34 mL Et_3N (2.4 mmol, 0.15 eq) were added. Reaction was finally stopped after 39 h. Reaction crude was washed with a saturated solution of KHSO_4 , a saturated solution of NaHCO_3 and a saturated solution of NaCl , finally, it was dried over Na_2SO_4 and dried under vacuum. After purification on normal phase chromatography (AcOEt:Petroleum ether 3:4) 4.9 g product **63** were recovered (7 mmol, 43% yield).

Mass spectrometry (FAB): $m/z = 721[M+Na]$, theoretical: 698.2+23

$^1\text{H-NMR}$ (CDCl_3 , 300 MHz): $\delta(\text{ppm})=8.04-7.46$ (m, 5H, H_{arom} of COPh); 6.22 (s, 0.55H, H-1 of Glc^α); 5.65 (d, $J_{1,2}=6$ Hz, 0.45H, H-1 of Glc^β); 5.55-5.45 (m, 1H); 5.22-4.92 (m, 3H); 4.63-3.77 (m, 9H); 2.13-1.85 (m, 18H, $\text{CH}_3\text{CO-}$)

$^{13}\text{C-NMR}$ (CDCl_3 , 75 MHz): $\delta(\text{ppm})=170.3-166.3$ (CH_3CO); 133.6-128.6 (C_{arom} of COPh); 101.1 (C-1 of Gal); 91.6 and 89.0 (C-1 of $\text{Glc}^{\alpha/\beta}$); 75.5 (C-4 of Gal); 73.6-66.8 (C-2, C-3 & C-5 of Glc and Gal and C-4 of Glc); 62.2-61.4 (C-6 of Glc and Gal)

2.24.- 2,3-di-O-acetyl-4-azido-4-deoxy-6-benzoyl- β -D-glucopyranosyl-(1 \rightarrow 4)-2,3,6-tri-O-acetyl- α/β -D-glucopyranose (67).



4.5 g (6.4 mmol, 1 eq.) 2,3-di-O-acetyl-6-benzoyl- β -D-galactopyranosyl-(1 \rightarrow 4)-1,2,3,6-tetra-O-acetyl- α/β -D-glucopyranose (**63**) were poured in a round-bottomed flask, flushed with argon, dissolved with 220 mL dry CH_2Cl_2 and cooled to 0°C . Then 22 mL of dry Py and 2.5 mL trifluoromethanesulfonic anhydride (15 mmol, 2.4 eq.) were added. Reaction was stirred under argon 30 min at 0°C and after that, 1 h at R.T. Reaction crude was diluted with 100 mL CH_2Cl_2 washed with a solution of NaHSO_4 , a saturated solution of NaHCO_3 and a saturated solution of NaCl . After that, organic layer was dried on Na_2SO_4 and finally solvent was eliminated at vacuum coevaporated with toluene. Product **65** was used without purification for next step.

Yellow solid from previous reaction was dissolved in the minimum quantity of HMPA (15 ml), 4.3g NaN_3 (64 mmol, 10 eq) and a catalytic quantity of 18-crown-6 ether were added. Reaction crude was stirred O.N. at 50°C . After 16.5 hours temperature was increased to 65°C , 2.15g NaN_3 (32 mmol, 5 eq), and more 18-crown-6 ether were added. At 22.5h, 8 mL HMPA were added. At 37 h, 15 mL HMPA, 2.15 g NaN_3 (32 mmol, 5 eq) and more 18-crown-6 ether were added. Due to no reaction evolution, reaction was stopped. Product was precipitated in cold water, filtered on Celite®, and recovered by dissolution in CH_2Cl_2 . Organic layer was dried on Na_2SO_4 and solvent was evaporated at vacuum. 4.7 g of mixture of 2,3-di-O-acetyl-4-azido-4-deoxy-6-benzoyl- β -D-glucopyranosyl-(1 \rightarrow 4)-2,3,6-tri-O-acetyl- α/β -D-glucopyranose (**67**) and

2,3-di-O-acetyl-4-azido-4-deoxy-6-benzoyl- β -D-glucopyranosyl-(1 \rightarrow 4)-1,2,3,6-tetra-O-acetyl- α/β -D-glucopyranosyl (**66**) were recovered.

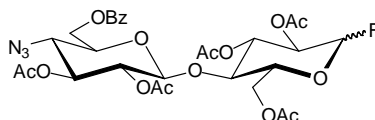
4.4 g of the azido derivative mixture (**66+67**) were solved in 120 mL DMF and 840 mg hydrazine acetate (9.2 mmol, 1.5 eq) were added. Reaction crude was stirred 30 min at 50 °C. After that it was diluted with AcOEt, washed with NaCl saturated, dried on Na₂SO₄, and concentrated at vacuum. After normal phase chromatography (AcOEt/petrol ether 4:5) 2.1 g (3.1 mmol) product **67** were recovered in 48% yield.

Mass spectrometry (DCI): m/z=699[M+NH₃], theoretical: 681.2+18

¹H-NMR (CDCl₃, 300 MHz): δ (ppm)=8.07-7.47 (m, 5H, H_{arom}, COPh); 5.48 (t, J_{1,2}=9.8Hz, 0.55H, H-1 of Glc^{l β}); 5.34 (d, J_{1,2}=3.6 Hz, 1H, H-1 of Glc^{l α}); 5.2-5.12 (m, 1H); 4.93-4.50 (m, 6H); 4.12-4.07 (m, 2H); 3.77-3.53 (m, 4H); 2.09-1.89 (m, 15H, CH₃CO-)

¹³C-NMR (CDCl₃, 75 MHz): δ (ppm)=170.9-166.1 (CH₃CO); 133.8-128.8 (C_{arom} of COPh); 100.8 (C-1 of Glc^l); 95.4 and 90.2 (C-1 of Glc^{l α} and β); 74.1-63.3 (C-2, C-3 and C-5 of Glc^l and ^l, C-4 of Glc^l); 62.0-61.8 (C-6 of Glc^l and ^l); 60.15 (C-4 of Glc^l); 20.6-20.4 (CH₃COO).

2.25.- Fluoride of (2,3-di-O-acetyl-4-azido-4-deoxy-6-benzoyl- β -D-glucopyranosyl-(1 \rightarrow 4)-2,3,6-tri-O-acetyl- α/β -D-glucopyranoside) (**68**).



1.7 g hemiacetal **67** (2.5 mmol, 1 eq) were poured in a round-bottomed flask, flushed with Ar, and dissolved in 87 mL dry CH₂Cl₂. Reaction crude was cooled at -55°C then 1.63 mL DAST (12,6 mmol, 5 eq) were added. Reaction crude was stirred 2 h at -55°C and temperature was increased until 15°C over night. Reaction was quenched with 3 mL MeOH and solvent was eliminated at vacuum. Product was purified by normal phase chromatography (AcOEt:Petroleum ether 1:2) obtaining 1.3 g (1.9 mmol) fluoride **68** in 76% yield.

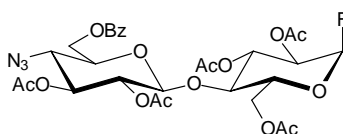
Mass spectrometry (DCI): m/z=701[M+NH₃], theoretical: 683.6 + 18.

¹H-NMR (CDCl₃, 300 MHz): δ (ppm)=8.05-7.45 (m, 5H, H_{arom}, COPh); 5.62 (dd, J_{1,2}= 2.7 Hz, J_{1,F}=53.7 Hz, 0.17H, H-1 of Glc^{l α}); 5.29 (dd, J_{1,2}=5.4 Hz, J_{1,F}=58.2 Hz, 0.83H, H-1 of Glc^{l β}); 5.17-5.11 (m, 1H); 4.97-4.84 (m, 2H); 4.63-4.45 (m, 4H); 4.04 (dd, J=5.1 Hz,

$J=12.3$ Hz, 1H); 3.94-3.88 (m, 1H); 3.80-3.67 (m, 2H); 3.55-3.39 (m, 2H); 2.07-1.86 (m, 15H, $\text{CH}_3\text{CO-}$)

$^{13}\text{C-NMR}$ (CDCl_3 , 75 MHz): $\delta(\text{ppm})=170.2-169.1$ (CH_3CO); 165.9 (COPh); 133.6-128.7 (C_{arom} of COPh); 105.8 (d, $J_{\text{C-F}}=218$ Hz, C-1 of Glc^{I}); 100.7 (C-1 of Glc^{II}); 75.3-71.0 (C-2, C-3, and C-5 of $\text{Glc}^{\text{I and II}}$, and C-4 of Glc^{I}); 63.0-61.5 (C-6 of $\text{Glc}^{\text{I and II}}$); 59.9 (C-4 of Glc^{II})

2.26.- Fluoride of (2,3-di-O-acetyl-4-azido-4-deoxy-6-benzoyl- β -D-glucopyranosyl-(1 \rightarrow 4)-2,3,6-tri-O-acetyl- α -D-glucopyranoside) (69).



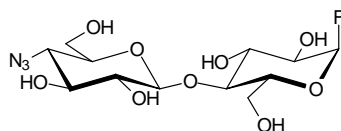
1.3 g fluoride isomers **68** (1.9 mmol, 1 eq) were poured in a plastic tube, 28 mL HF/Py were added and reaction crude was stirred at -50°C 1 hour. Temperature was allowed to increase to -10°C and finally reaction crude was kept at -10°C for 2 h. Reaction crude was diluted with CH_2Cl_2 and neutralized on 100 mL NH_3 (3N) previously cooled. Organic layer was washed twice with NaHCO_3 , dried with Na_2SO_4 , and solvent was eliminated at vacuum. Product was purified by normal phase chromatography (AcOEt :Petroleum ether 1:2) obtaining 1.1 g α -fluoride **69** (1.6 mmol, 85% yield).

Mass spectrometry (FAB): $m/z=706[\text{M}+\text{Na}]$, theoretical: 683.6 +23.

$^1\text{H-NMR}$ (CDCl_3 , 300 MHz): $\delta(\text{ppm})=8.07-7.48$ (m, 5H, H_{arom} , COPh); 5.65 (dd, $J_{1,2}=2.7$ Hz, $J_{1,\text{F}}=53.1$ Hz, 1H, H-1 of Glc^{I}); [5.44 (t, $J=9.9$ Hz, 1H); 5.16 (t, $J=9.9$ Hz, 1H); 4.93-4.76 (m, 2H); 4.66-4.49 (m, 4H); 4.16-4.06 (m, 2H); 3.83-3.71 (m, 2H); 3.59-3.53 (m, 1H)] (H-2, H-3, H-4, H-5, H-6a&b of $\text{Glc}^{\text{I,II}}$); 2.07-1.86 (m, 15H, $\text{CH}_3\text{CO-}$)

$^{13}\text{C-NMR}$ (CDCl_3 , 75 MHz): $\delta(\text{ppm})=170.4-169.6$ (CH_3CO); 165.9 (COPh); 133.6-128.7 (C_{arom} of COPh); 103.6 (d, $J_{\text{C-F}}=218$ Hz, C-1 of Glc^{I}); 100.6 (C-1 of Glc^{II}); 75.5-690.7 (C-2, C-3 and C-5 of $\text{Glc}^{\text{I and II}}$ and C-4 of Glc^{I}); 63.1-61.0 (C-6 of $\text{Glc}^{\text{I and II}}$); 60.0 (C-4 of Glc^{II}).

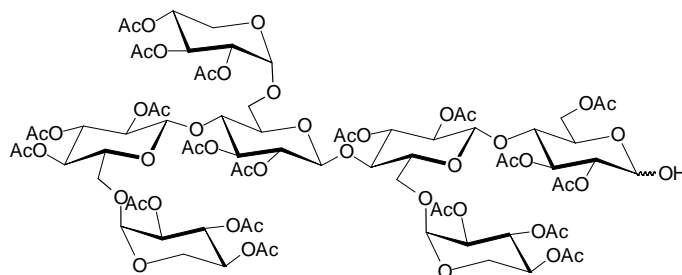
2.27.- Fluoride of (4-azido-4-deoxy- β -D-glucopyranosyl-(1 \rightarrow 4)- α -D-glucopyranoside) (74).



200 mg α -fluoride **69** (0.3 mmol, 1 eq) were dissolved in 28 mL MeOH and cooled at 0°C. After that, 220 μ l of MeONa (1 M) were added and reaction crude was stirred at 0°C O.N. Reaction crude was neutralized with Amberlite® IR-120, solvent was eliminated at vacuum, product was dissolved in cold water and it was freeze dried. 110 mg (0.3 mmol) of α -fluoride **74** were quantitatively obtained.

Mass spectrometry (FAB): $m/z=392[M+Na]$, theoretical 369.3 + 23.

2.28.- [2,3,4-tri-O-acetyl- α -D-xylopyranosyl-(1 \rightarrow 6)]-2,3,4-tri-O-acetyl- β -D-glucopyranosyl-(1 \rightarrow 4)-[2,3,4-tri-O-acetyl- α -D-xylopyranosyl-(1 \rightarrow 6)]-2,3-di-O-acetyl- β -D-glucopyranosyl-(1 \rightarrow 4)-[2,3,4-tri-O-acetyl- α -D-xylopyranosyl-(1 \rightarrow 6)]-2,3-di-O-acetyl β -D-glucopyranosyl-(1 \rightarrow 4)-2,3,6-tri-O-acetyl- α / β -D-glucopyranose (34).

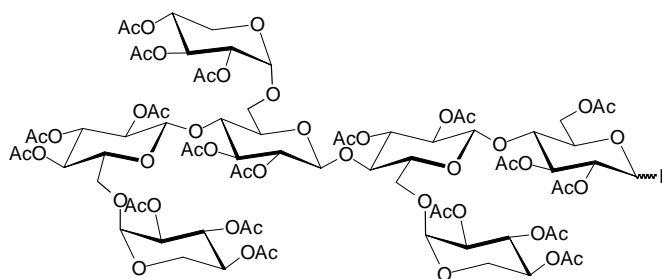


1.46 g (0.77 mmol, 1eq.) per-O-acetylated heptasaccharide XXXG (**15**) were dissolved in 12 mL dry DMF and preheated at 50°C. 106 mg (1.15 mmol, 1.5 eq.) hydrazine acetate were added and reaction mixture was stirred at 50°C during 20 min. Reaction crude was diluted with AcOEt, washed twice with NaCl and dried on Na₂SO₄.

Solvent was eliminated at vacuum, product was purified by normal phase chromatography (Tol:acetone 2:1) obtaining the hemiacetal **34** in 78% yield (1.13 g, 0.61 mmol).

Mass spectrometry (MALDITOF): $m/z=1883.36$ (M+Na), theoretical+Na: $1861.64+23$

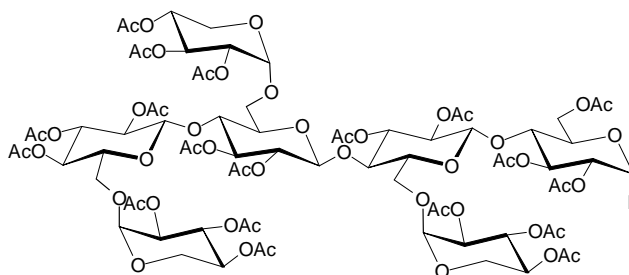
2.29.- Fluoride of ([2,3,4-tri-O-acetyl- α -D-xylopyranosyl-(1 \rightarrow 6)]-2,3,4-tri-O-acetyl- β -D-glucopyranosyl-(1 \rightarrow 4)-[2,3,4-tri-O-acetyl- α -D-xylopyranosyl-(1 \rightarrow 6)]-2,3-di-O-acetyl- β -D-glucopyranosyl-(1 \rightarrow 4)-[2,3,4-tri-O-acetyl- α -D-xylopyranosyl-(1 \rightarrow 6)]-2,3-di-O-acetyl β -D-glucopyranosyl-(1 \rightarrow 4)-2,3,6-tri-O-acetyl- α/β -D-glucopyranoside) (35**).**



1.13 g of hemiacetal **34** (0.61 mmol, 1eq) were dissolved with 21.2 mL dry CH_2Cl_2 and cooled at -50°C . 400 μl of DAST (3 mmol, 5 eq.) were added and reaction mixture was stirred 1 hour at -50°C , after that, temperature was allowed to increase O.N. Reaction was quenched by the addition of 500 μl of MeOH. Solvent was eliminated at vacuum and product was purified by normal phase chromatography (Tol:acetone 4:1) 0.96 g of **35** (0.51 mmol) were recovered in 89% yield.

Mass spectrometry (MALDITOF): $m/z=1884.96$ (M+Na), theoretical+Na: $1863.63+23$

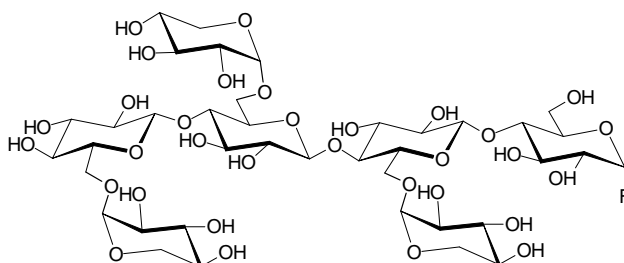
2.30.- Fluoride of ([2,3,4-tri-O-acetyl- α -D-xylopyranosyl-(1 \rightarrow 6)]-2,3,4-tri-O-acetyl- β -D-glucopyranosyl-(1 \rightarrow 4)-[2,3,4-tri-O-acetyl- α -D-xylopyranosyl-(1 \rightarrow 6)]-2,3-di-O-acetyl- β -D-glucopyranosyl-(1 \rightarrow 4)-[2,3,4-tri-O-acetyl- α -D-xylopyranosyl-(1 \rightarrow 6)]-2,3-di-O-acetyl β -D-glucopyranosyl-(1 \rightarrow 4)-2,3,6-tri-O-acetyl- α -D-glucopyranoside) (33**).**



509 mg (0.27 mmol) of α/β fluoride **35** were poured in a plastic tube. 2.7 mL HF/Py 70% were added, reaction was stirred at -50°C for 30 min and then temperature was allowed to increase till -10°C (during 2 hours) and maintained at this temperature for 3 hours. Finally, reaction mixture was diluted with CH_2Cl_2 and poured on a solution of pre-cooled NH_3 (3N), organic layer was washed with NaHCO_3 and dried on Na_2SO_4 . Solvent was eliminated and product was purified by normal phase chromatography (Tol:acetone 3:1) obtaining 360 mg (0.19 mmol, 71%) of α -fluoride **33**.

Mass spectrometry (MALDITOF): $m/z=1884.56$ (M+Na), theoretical+Na: $1863.63+23$.

2.31.- Fluoride of ([α -D-xylopyranosyl-(1 \rightarrow 6)]- β -D-glucopyranosyl-(1 \rightarrow 4)-[α -D-xylopyranosyl-(1 \rightarrow 6)]- β -D-glucopyranosyl-(1 \rightarrow 4)-[α -D-xylopyranosyl-(1 \rightarrow 6)]- β -D-glucopyranosyl-(1 \rightarrow 4)- α -D-glucopyranoside) XXXG α F (36**).**

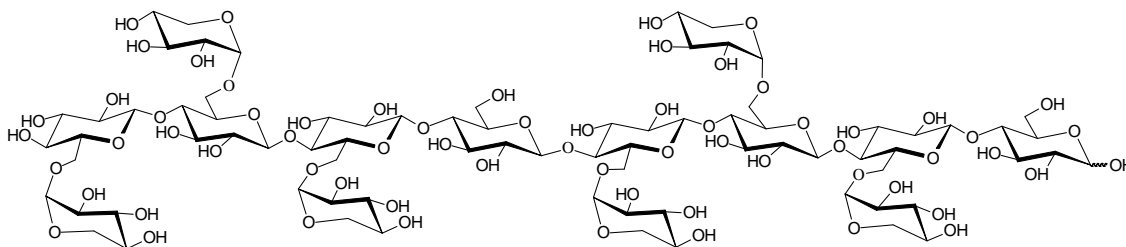


360 mg (0.19 mmol) of per-O-acetylated α -fluoride **33** were dissolved with 43 mL MeOH, 200 μL MeONa (1N) were added and reaction crude was stirred at 0°C

during 8 h. Reaction mixture was neutralized with Amberlite® IR-120 and solvent was eliminated at vacuum. Product was dissolved in water and freeze dried. 178.1 mg (0.17 mmol, 86%) of deprotected α -fluoride **36** were recovered.

Mass spectrometry (ESI+): $m/z=1087.37$ (M+Na), theoretical+Na: 1064.92+23.

2.32.- [α -D-xylopyranosyl-(1 \rightarrow 6)]- β -D-glucopyranosyl-(1 \rightarrow 4)-[α -D-xylopyranosyl-(1 \rightarrow 6)]- β -D-glycopyranosyl-(1 \rightarrow 4)-[α -D-xylopyranosyl-(1 \rightarrow 6)]- β -D-glucopyranosyl-(1 \rightarrow 4)- β -D-glucopyranosyl-(1 \rightarrow 4)-[α -D-xylopyranosyl-(1 \rightarrow 6)]- β -D-glucopyranosyl-(1 \rightarrow 4)-[α -D-xylopyranosyl-(1 \rightarrow 6)]- β -D-glucopyranosyl-(1 \rightarrow 4)- β -D-glucopyranose (XXXGXXXG) (23**).**



Method A:

1.7 g xyloglucan polymer from *Tamarindus indica* seeds were dissolved in 150 mL hot water with gentle stirring and heating. Dissolution was poured into the ultrafiltration cell with a 10 kDa membrane and 3 mg cellulase from *Trichoderma reesei* (5 U/ml) were added. Water was introduced into the cell at 3 bars, maintaining reaction volume constant. Reaction crude was stirred into the ultrafiltration cell during 20 h. Ultrafiltrated dissolution was collected and freeze dried. Resulting white solid was dissolved with 50 mL water. 140 μ l of α -galactosidase from *Aspergillus niger* were added, after 24 h reaction 200 μ l α -galactosidase were added, reaction was stopped after 45 h by boiling of reaction crude. Reaction crude was freeze dried and purified by normal phase chromatography ACN:water 8:2 obtaining 122 mg (57 μ mol, 7% yield) of the tetradecasaccharide **23**. Also 202 mg of heptasaccharide **10** (191 μ mol, 12% yield) were isolated.

Method B:

916 mg (0.86 mmol) of the heptasaccharide **10** were dissolved in 3 mL carbonate/bicarbonate buffer 0.1 M pH 10, then 2.5 mg Cel7B synthase and 60 mg of α -fluoride **36** (56 μ mol, 0.34 eq.) were added, reaction mixture was incubated at 40°C, after 6 h, 60 mg more of α -fluoride **36** (56 μ mol, 0.34 eq.) were added, finally, after 21

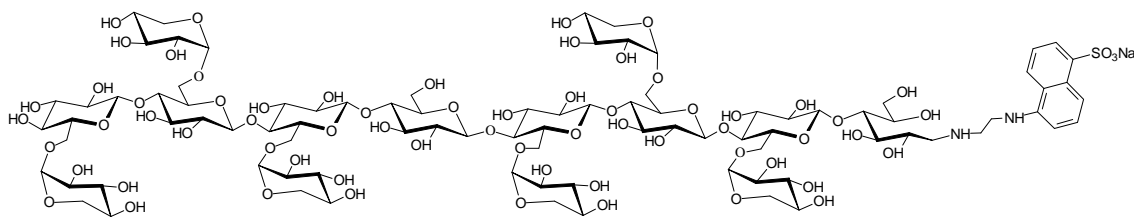
hours the last 58 mg of the α -fluoride **36** were added (54 μ mol, 0.33 eq.). At the end, after 29 hours, reaction crude was freeze dried and purified by normal phase chromatography (ACN:water 75:25) obtaining 318 mg (151 μ mol) of the tetradecasaccharide **23** in 91% yield, and recovering 703 mg (0.7 mmol) of the heptasaccharide **10**.

Mass spectrometry (MALDITOF): $m/z=2129.5$ (M+Na), theoretical+Na: 2107.85+23

$^1\text{H-NMR}(\text{D}_2\text{O}, 300 \text{ MHz}):$ $\delta(\text{ppm})= 5.20$ (d, $J_{1,2}=3.6$ Hz, 0.6H, H-1 of Glc $^{\alpha}$); 4.94-4.91 (m, 6H, H-1 of Xyl $^{\text{II,III,IV,VI,VII,VIII}}$); 4.64 (d, $J_{1,2}=7.8$ Hz, 0.4H, H-1 of Glc $^{\beta}$); 4.56-4.51 (m, 7H, H-1 of Glc $^{\text{II-VIII}}$); 4.01-3.29 (m, 78H, H-2, H-3, H-4 of Glc $^{\text{I-VIII}}$ and Xyl $^{\text{II,III,IV,VI,VII,VIII}}$, H-5a&b of Xyl $^{\text{II,III,IV,VI,VII,VIII}}$, H-5 of Glc $^{\text{I-VIII}}$, H-6a&b of Glc $^{\text{I-VIII}}$)

$^{13}\text{C-NMR}(\text{D}_2\text{O}, 75 \text{ MHz}):$ $\delta(\text{ppm})=102.3-101.9$ (m, 7C, C-1 of Glc $^{\text{II-VIII}}$); 98.3-97.8 (m, 6C, C-1 of Xyl $^{\text{II,III,IV,VI,VII,VIII}}$); 95.2 and 91.3 (2C, C-1 of Glc $^{\alpha}$ and β); 78.9-59.4 (64C, other carbon atoms).

2.33.- ([α -D-xylopyranosyl-(1 \rightarrow 6)]- β -D-glucopyranosyl-(1 \rightarrow 4)-[α -D-xylopyranosyl-(1 \rightarrow 6)]- β -D-glycopyranosyl-(1 \rightarrow 4)-[α -D-xylopyranosyl-(1 \rightarrow 6)]- β -D-glucopyranosyl-(1 \rightarrow 4)- β -D-glucopyranosyl-(1 \rightarrow 4)-[α -D-xylopyranosyl-(1 \rightarrow 6)]- β -D-glucopyranosyl-(1 \rightarrow 4)-[α -D-xylopyranosyl-(1 \rightarrow 6)]- β -D-glucopyranosyl-(1 \rightarrow 4)-[α -D-xylopyranosyl-(1 \rightarrow 6)]- β -D-glucopyranosyl-(1 \rightarrow 4)-1-deoxy-D-glucitol-1-yl)-5-(2-aminoethylamino)naphthalene-1-sulfonic acid, sodium salt (XXXGXXXG-EDANS (70)).

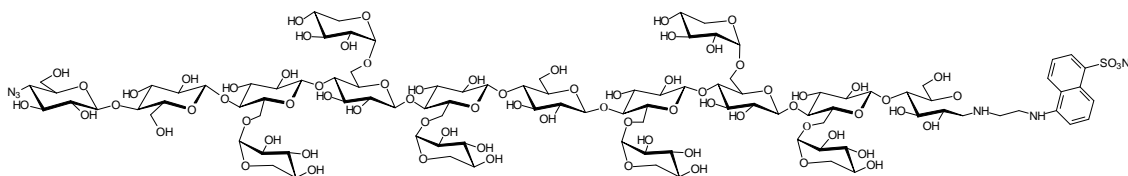


79.8 mg (37.9 μ mol, 1eq.) tetradecasaccharide **23** were dissolved in 2.5 mL water and 2.5 mL dried THF. Then, 54.6 mg 5-((2-aminoethyl)-amino)-naphthalene-1-sulfonic acid (EDANS) (189 μ mol, 5 eq.) and 23.8 mg NaCNBH $_3$ (378 μ mol, 10eq.) were added. pH of reaction crude was adjusted approximately at 5 with AcOH. Reaction mixture was stirred at 60°C, after 20 h, pH was adjusted again and 24 mg NaCNBH $_3$ (378 μ mol, 10 eq.) were added. After 44 h, pH was adjusted again with AcOH. Finally after 64 h, reaction crude was filtered and freeze dried. Product was purified by two chromatography steps using Lobar® prepacked columns, first a normal

phase chromatography (ACN:water, 75:25) and after a reverse phase chromatography (gradient from 500 mL water → 500 mL ACN 20%). 32 mg (13.6 μmol) of the labeled tetradecasaccharide **70** were recovered in a 36% yield.

Mass spectrometry (MALDITOF): $m/z=2401,72(M+Na)$, theoretical+Na: 2378.74+23.

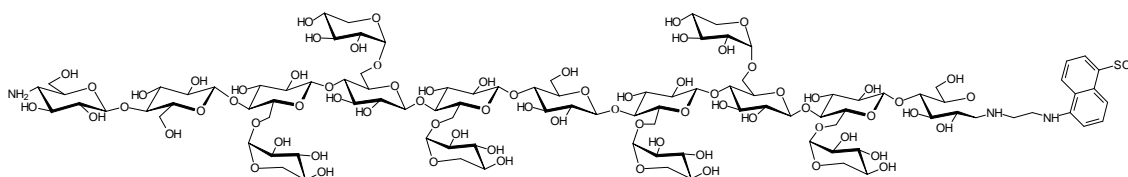
2.34.- (4-azido-4-deoxy-β-D-glucopyranosyl-(1→4)-β-D-glucopyranosyl-(1→4)-[α-D-xylopyranosyl-(1→6)]-β-D-glucopyranosyl-(1→4)-[α-D-xylopyranosyl-(1→6)]-β-D-glycopyranosyl-(1→4)-[α-D-xylopyranosyl-(1→6)]-β-D-glucopyranosyl-(1→4)-β-D-glucopyranosyl-(1→4)-[α-D-xylopyranosyl-(1→6)]-β-D-glucopyranosyl-(1→4)-[α-D-xylopyranosyl-(1→6)]-β-D-glucopyranosyl-(1→4)-1-deoxy-D-glucitol-1-yl)-5-(2-aminoethylamino) naphthalene-1-sulfonic acid, sodium salt (N₃GGXXXGXXXG-EDANS (72**)).**



40 mg (16 μmol, 1 eq.) of XXXGXXXG-EDANS (**70**) and 23.5 mg **69** (60 μmol, 4 eq.) were solved in 3166 μl carbonate buffer 0.1 M pH 10, then 80 μl of Cel7B synthase were added (1 mg). Reaction mixture was incubated at 30 °C during 24 h. Product was purified by reverse phase chromatography (gradient of 400 mL water → 400 mL ACN 20%). Coupling product **72** was recovered in 83% yield (38 mg (14 μmol)).

Mass spectrometry (MALDITOF): $m/z= 2751.7(M+Na)$, theoretical+Na: 2727.85+23

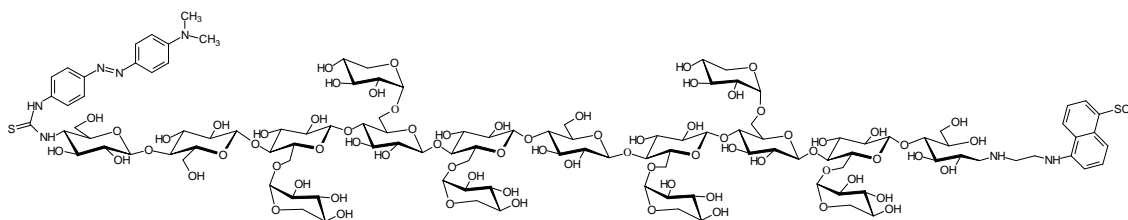
2.35.- (4-amino-4-deoxy- β -D-glucopyranosyl-(1 \rightarrow 4)- β -D-glucopyranosyl-(1 \rightarrow 4)-[α -D-xylopyranosyl-(1 \rightarrow 6)]- β -D-glucopyranosyl-(1 \rightarrow 4)-[α -D-xylopyranosyl-(1 \rightarrow 6)]- β -D-glycopyranosyl-(1 \rightarrow 4)-[α -D-xylopyranosyl-(1 \rightarrow 6)]- β -D-glucopyranosyl-(1 \rightarrow 4)- β -D-glucopyranosyl-(1 \rightarrow 4)-[α -D-xylopyranosyl-(1 \rightarrow 6)]- β -D-glucopyranosyl-(1 \rightarrow 4)-[α -D-xylopyranosyl-(1 \rightarrow 6)]- β -D-glucopyranosyl-(1 \rightarrow 4)-1-deoxy-D-glucitol-1-yl)-5-(2-aminoethylamino) naphthalene-1-sulfonic acid, sodium salt ($\text{NH}_2\text{GGXXXGXXXG-EDANS}$ (73**)).**



34 mg (12.5 μmol , 1 eq) of $\text{N}_3\text{GGXXXGXXXG-EDANS}$ (**72**) were poured in a round-bottomed flask, solved with 2 mL H_2O and 2 mL Py. Reaction mixture was flushed during 10 minutes with H_2S (gas) and stirred at R.T. O.N. protected from light. Reaction crude was neutralized with AcOH 2N, filtered, and solvents were eliminated at vacuum by coevaporation with EtOH. Recovered product was solved in water and freeze dried, obtaining 32.5 mg of **73**, in a 97% yield.

Mass spectrometry (MALDITOF): $m/z = 2725.41(\text{M}+\text{Na})$, theoretical+Na: 2701.9+23

2.36.- (2-N-(4-deoxy-4-dimethylaminophenylazophenylthioureido)- β -D-glucopyranosyl-(1 \rightarrow 4)- β -D-glucopyranosyl-(1 \rightarrow 4)-[α -D-xylopyranosyl-(1 \rightarrow 6)]- β -D-glucopyranosyl-(1 \rightarrow 4)-[α -D-xylopyranosyl-(1 \rightarrow 6)]- β -D-glycopyranosyl-(1 \rightarrow 4)-[α -D-xylopyranosyl-(1 \rightarrow 6)]- β -D-glucopyranosyl-(1 \rightarrow 4)- β -D-glucopyranosyl-(1 \rightarrow 4)-[α -D-xylopyranosyl-(1 \rightarrow 6)]- β -D-glucopyranosyl-(1 \rightarrow 4)-[α -D-xylopyranosyl-(1 \rightarrow 6)]- β -D-glucopyranosyl-(1 \rightarrow 4)-1-deoxy-D-glucitol-1-yl)-5-(2-aminoethylamino)naphthalene-1-sulfonic acid, sodium salt (DAB-NH-CS-NH-GGXXXGXXXG-EDANS (76**)):**



30 mg of **73** (11.1 μ mol) were poured in a round bottomed flask and solved with 1.2 mL NaHCO_3 0.35M (pH 8.1). 6.3 mg (22 μ mol, 2 eq.) DABITC were dissolved with 4.7 mL DMF and added to **73** solution. Reaction mixture was stirred at R.T. and protected from light for 48 hour. Reaction was stopped one all starting material was consumed. Reaction mixture was freeze-dried. Product was purified by gel filtration chromatography using Bio Gel P4 resin from BioRad in a 180 cm long and 1.5 cm internal diameter column. 7 mg (2.3 μ mol) of **76** were recovered, in 21% yield.

Mass spectrometry (MALDITOF, negative mode): $m/z=2963.01$ (M-Na), theoretical-Na: 2962.79.

3.- HPCE method development and validation.

3.1.- HPCE method development.

Capillary electrophoresis was performed on a Hewlett-Packard HP^{3D} CE G1600 AX system equipped with a diode array UV-Vis detector. The capillary (72 cm effective length, 50 μm internal diameter, made of fused silica with an extended light path bubble (150 μm) in the detection window) was pretreated or regenerated with 0.1 M NaOH, double distilled water, and running buffer (for 30, 10, and 10 min respectively). Samples (ANTS-labeled oligosaccharide standards or enzymatic reaction mixtures) were loaded into the capillary under hydrodynamic injection mode at 40 mbar pressure during a fixed time. The conditioning between injections consisted of a 5 min equilibration step with running buffer. The chosen running buffer depended on the electrophoretic method: a) direct EOF (cathodic detection): 50 mM phosphoric acid adjusted to pH 9 with NaOH, b) suppressed EOF (anodic detection): 50 mM phosphoric acid adjusted to pH 2.5 with NaOH, c) inverted EOF (anodic detection): 50 mM phosphoric acid adjusted to pH 2.5 with triethylamine. Electrophoresis was performed at a constant voltage and constant temperature of 30°C. The detector was a UV/Vis diode array and the electropherograms were recorded at 214 nm (20 nm slit), 224 nm (20 nm slit) and 270 nm (20 nm slit).

The purified mixture of ANTS-labeled xyloglucan oligosaccharides XXXG, (XXLG+XLXG), and XLLG (**25**, **26**, **27** and **28**) was analyzed under different electrophoretic conditions using different acidic buffers (File: MSV4007):

Suppressed EOF conditions were obtained with sodium phosphate buffer at pH 2.5. Inverted EOF conditions were generated with the same 50 mM phosphoric buffer adjusted at pH 2.5 with triethylamine (TEA) as EOF modifier.

Buffer concentration and buffer pH were studied using inverted EOF conditions using pH 2.5 phosphate-TEA buffers (25, 50, 100 mM) and also using 50 mM phosphoric buffers adjusted at different pH with TEA (pH 2, 2.5, 3).

For all these assays migration times, efficacy and resolution were evaluated.

	Concentration (mM)			pH		
	25	50	100	2.0	2.5	3.0
t_m (min)	9.6	10.2	11.2	10.1	10.2	10.7
resolution ¹	5.88	6.39	2.71	23.13	6.40	4.51
efficacy ²	211762	309408	392690	185418	309407	233824

Table 37: Migration times (t_m) for XXXG-ANTS (25) peak, resolution (Rs) between XXXG-ANTS (25) and XLG-ANTS (26) peaks and efficacy (N) for XXXG-ANTS (25) peak at pH 2.5 different phosphate-TEA concentrations (25, 50 and 100 mM) and different pH values for 50 mM buffer.

¹ Equation 7:

$$\text{Resolution(Rs)} = 1.18 \cdot \frac{t_{m_2} - t_{m_1}}{w_{1/2}(2) - w_{1/2}(1)}$$

where 1 and 2 the peaks corresponding to compounds XXXG-ANTS (25) and XLG-ANTS (26), respectively, t_m is the migration time, and $w_{1/2}$ is the peak width.

² Equation 8:

$$\text{Efficacy (N)} = 5.54 \cdot \left(\frac{t_m}{w_{1/2}} \right)^2$$

where t_m is the migration time, and $w_{1/2}$ is the peak width for compound XXXG-ANTS (25).

Three different voltages (-30, -20, and -10 kV) were tested analyzing XGOs-ANTS mixture, using pH 2.5, 50 mM phosphate-TEA buffer.

Lineal response of intensity versus voltage was demonstrated by monitoring of intensity at different applied voltages (5, 10, 15, 20, 25, 30 kV).

The optimal amount of sample loaded into the capillary was evaluated by varying the injection time (from 3 to 15 s) during hydrodynamic injection at 40 mbar.

3.2.- Definitive HPCE method.

As it was presented before capillary electrophoresis was performed on a Hewlett-Packard HP^{3D} CE G1600 AX system equipped with a diode array UV-Vis detector. The capillary (72 cm effective length, 50 μ m internal diameter, fused silica with an extended light path bubble (150 μ m) in the detection window) was pretreated or regenerated with 0.1 M NaOH, H₂O milliQ, and running buffer (for 30, 10, and 10 min respectively). Samples (ANTS-labeled oligosaccharide standards or enzymatic reaction mixtures) were loaded into the capillary under hydrodynamic injection mode at 40 mbar pressure

during 6 s. The conditioning between injections consisted of a 5 min equilibration step with running buffer. Running buffer was 50 mM phosphoric buffer adjusted at pH 2.5 with triethylamine (TEA) as EOF modifier obtaining an inverted EOF method. Electrophoresis was performed at -30 kV and constant temperature of 30°C. The detector was a UV/Vis diode array and the electropherograms were recorded at 214 nm (20 nm slit), 224 nm (20 nm slit) and 270 nm (20 nm slit), but only record at 224 nm was used.

3.3.- HPCE method validation.

A stock solution of 50 mM XXXG-ANTS (**25**) was prepared by dissolution of 38.2 mg of synthesized XXXG-ANTS (**25**) in 510.5 μ L double distilled water. Then dilutions were prepared to obtain 5 mM, 0.5 mM and 0.05 mM stock solutions.

Internal standard stock solution was prepared by ANTS labeling of mannose as it follows: 18.2 mg mannose were poured in an Eppendorf tube, then, 1 mL ANTS 0.15 M (in AcOH:H₂O 3:17) and 1 mL NaCNBH₃ 1 M (in recently dried THF) were added. Reaction mixture was incubated at 55°C during 7 h and afterwards it was freeze dried. Yellow solid was dissolved in 50 mL MilliQ water, separated in 1 mL aliquots and stored at -20°C.

3.3.1.- Linearity study.

A serial dilution of XXXGANTS (25) was prepared using the above described stock solutions, as it is presented in the following table (File: MSV3042):

Sample concentration	Stock conc.	XXXGANTS volume	ManANTS volume	Water volume	XXXGANTS/ManANTS Relative area ($\times 10^3$)		
1	5	4	20	16	545.8	573.1	562.7
0.7	5	2.8	20	17.2	411.9	414.7	407.9
0.5	0.5	20	20	0	286.5	295.4	293.6
0.2	0.5	8	20	12	112.9	113.2	114.8
0.1	0.5	4	20	16	58.0	57.9	57.2
0.07	0.5	2.8	20	17.2	41.1	40.8	40.7
0.05	0.05	20	20	0	27.2	27.5	27.2
0.02	0.05	8	20	12	11.5	11.3	11.4
0.01	0.05	4	20	16	5.71	5.66	5.13
0.007	0.05	2.8	20	17.2	3.63	4.68	4.19
0.005	0.05	2	20	18	3.30	3.17	3.07
0		0	20	20	0	0	0

Table 38: Sample preparation to study linearity of HPCE method.

Sample concentration is the concentration of the sample without taking into account the dilution due to 20 μ L ManANTS addition. Each sample was prepared three times. Volumes were expressed in μ L and concentration in mM.

Samples were boiled during 10 min at 100°C in sealed Eppendorf tubes, in a PCR machine, then cooled at room temperature, centrifuged and transferred to HPCE vials and analyzed using the previously described HPCE method.

Integration events in the HPCE ChemStation were fixed at: Slope sensitivity 21.34; peak width 0.025; area reject 1.7; height reject 1.21.

To choose linearity limits, response factors (RF) defined as Relative Area divided by nominal concentration were calculated for each sample. Linearity limits were defined as concentrations of samples that have RF between (mean RF+10%) and (mean RF-10%)¹⁶⁹.

3.3.2.- Detection and quantification limits.

Detection and quantification limits were defined as concentration of samples that have 3 and 10 times, respectively, the height of $\frac{1}{2}$ of the maximum difference in height of noise signal¹⁶⁹.

3.3.3.- Repeatability.

Repeatability was evaluated at three different concentrations as it is presented in the following table (File: MSV3042). Samples were boiled during 10 min at 100°C in sealed Eppendorf tubes in a PCR machine, then cooled at room temperature, centrifuged and transferred to HPCE vial and analyzed using the previously described HPCE method. Mean relative area, standard deviation and variation coefficient were evaluated at each concentration.

Sample conc.	Stock conc.	XXXGANTS volume	ManANTS volume	Water volume	XXXGANTS/ManANTS					
					Relative area ($\times 10^3$)					
1	5	4	20	16	613.1	589.9	566.4	563.2	581.4	581.9
0.1	0.5	4	20	16	54.3	52.8	57.1	55.1	57.2	57.8
0.01	0.05	4	20	16	6.21	6.00	6.52	6.07	6.37	5.87

Table 39: Sample preparation to study repeatability. Sample concentration is the concentration of the sample without taking into account the dilution provoked due to 20 μ l ManANTS addition. Each sample was prepared six times. Volumes were expressed in μ l and concentrations in mM.

3.4.- XXXGANTS standard curve.

Standard curve was prepared for ANTS labeled product quantification with XXXGANTS (25) as it is described in the following table (File: MSV3060):

Sample concentration	Stock conc.	XXXGANTS volume	ManANTS volume	Water volume	XXXGANTS/ManANTS Relative area (x10 ³)		
1	2	10	20	10	632.1	634.5	633.5
0.7	2	7	20	13	452.8	454.3	446.9
0.5	2	5	20	15	317.4	133.3	130.3
0.3	2	3	20	17	199.1	197.8	198.1
0.2	2	2	20	18	128.1	133.3	130.3
0.1	0.2	10	20	10	64.7	63.7	64.5
0.05	0.2	5	20	15	32.9	35.2	33.9
0.02	0.2	2	20	18	13.4	13.9	13.6
0.01	0.02	10	20	10	7.16	6.94	6.92
0		0	20	20	0	0	0

Table 40: Sample preparation to obtain a XXXGANTS (25) standard curve. Sample concentration is the concentration of the sample without taking into account the dilution provoked due to 20 µl ManANTS addition. Each sample was prepared six times. Volumes were expressed in µl and concentrations in mM.

Lineal regression was applied to data and quantification equation was obtained:

$$[\text{XXXGANTS}] = (1,56869 \pm 0,0052503) \cdot A(\text{XXXGANTS}) / A(\text{ManANTS}) - (0,003014 \pm 0,00134667)$$

Equation 9: Standard curve for XXXGANTS (25). Concentration was expressed in mM.

3.5.- Comparison of response factor between XXXG-ANTS (25) and XXXGXXXG-ANTS (31).

2.17 mg XXXG (**10**) were derivatized with 20 μ L ANTS (0.15 M) in AcOH/water (1mL, 3:17 v/v) and 20 μ L NaCNBH₃ (1 M) in freshly purified THF (1 mL), followed by freeze drying and volume was adjusted at 1 mL with water, resulting in a 2.041 mM solution of XXXG-ANTS.

3,86 mg XXXGXXXG (**23**) were derivatized with 20 μ L ANTS (0.15 M) in AcOH/water (1mL, 3:17 v/v) and 20 μ L NaCNBH₃ (1 M) in freshly purified THF (1 mL), followed by freeze drying and volume was adjusted at 1 mL with water, resulting in a 1.831 mM solution of XXXGXXXG-ANTS.

A serial dilution for each labeled oligosaccharide was prepared as it is described in the following table using as internal standard approximately 1 mM maltose-ANTS. (File: MSV5087)

Conc.	XXXGANTS volume	Water volume	Maltose volume		(XXXG) ₂ ANTS Volume	Water volume	Maltose volume
1	9.80	10.20	20		10.92	9.08	20
0.7	6.86	13.14	20		7.65	12.35	20
0.5	4.90	15.10	20		5.46	14.54	20
0.4	3.92	16.08	20		4.37	15.63	20
0.2	1.96	18.04	20		2.18	17.89	20
0.1	0.98	19.02	20		1.09	18.91	20

Table 41: Sample preparation for standard curves of XXXGANTS (25) and XXXGXXXGXXXGANTS (31), to compare response factor of both ANTS labeled oligosaccharides. Volumes are expressed in μ L and concentration in mM.

Samples were analyzed using the previously described HPCE method and response factor comparison was done plotting both relative areas to obtain a slope of one if response factor are equivalent.

4.- Determination of stock concentrations.

4.1.- Determination of β -glycosyl fluoride stock concentration.

β -glycosyl fluoride substrates were solved in double distilled water immediately prior to use and immediately were frozen. Stock concentration is determined as the difference between total fluoride measured after acid hydrolysis of substrate and the free fluoride present in the sample.

Fluoride measurements were done using a fluoride selective electrode (FSE) provided by Sentek and a pHmeter CyberScan 2500.

Free fluoride was measured on 25/500 dilution of substrate dissolution and obtained voltage was interpolated in a fluoride standard curve prepared by dilution in double distilled water of a NaF standard 100 ppm solution.

Acid hydrolysis of substrate solution was done by dilution of 25 μ L of substrate stock in 200 μ L MilliQ water and 25 μ L H₂SO₄ 40 mM. Substrate solution was hydrolyzed during 20 minutes at 100°C, cooled and neutralized with 25 μ L NaOH 80 mM. Total fluoride was measured prior 275:500 dilution in double distilled water. Voltage signal obtained was interpolated in a fluoride standard curve prepared by parallel treatment of dilutions of standard 100 ppm NaF solution.

4.2.- Determination of XXXG-ANTS (25) stock concentration.

Concentration of newly dissolved XXXG-ANTS (25) stock solutions were calculated by interpolation of XXXG-ANTS (25) HPCE areas obtained from analysis of 1:1 dilution of XXXG-ANTS (25) with Man-ANTS internal standard in the XXXG-ANTS (25) standard curve.

4.3.- Determination of donor stock concentration.

Concentration of donor stocks was done by parallel ANTS analytical labeling of a serial dilution of XXXGXXXG (23) (previously extensively purified by normal phase and gel filtration chromatography) and the studied donor stock. Resulting reaction crudes were freeze-dried and analyzed by HPCE prior water dissolution. A standard curve was obtained from the ANTS labeled samples of the serial dilution of XXXGXXXG (23). Areas resulting from evaluated donors were interpolated in this standard curve to obtain stock concentration.

4.4.- *Ptt*-XET16A concentration.

4.4.1.- Total enzyme concentration.

Determination of *Ptt*-XET16A total concentration was done spectrophotometrically at 280 nm using as extinction coefficient the ProtParam calculated value $72970 \text{ M}^{-1}\cdot\text{cm}^{-1}$ this program is available at <http://www.expasy.org/tools/>.

4.4.2.- Active enzyme concentration.

Determination of active *Ptt*-XET16A concentration of newly received or prepared stocks of enzyme was done by interpolation on a *Ptt*-XET16A standard curve of initial rate obtained with the using 1 mM donor **23** and 5 mM acceptor **25** in 50:50 mM citrate:phosphate buffer at pH 5 and 30°C

Ptt-XET16A standard curve was obtained by determination of initial rates of reaction between 1 mM donor **23** and 5 mM acceptor **25** in 50:50 mM citrate:phosphate buffer at pH 5 and 30°C using a recently obtained and purified *Ptt*-XET16A stock, as it is described in the Table 42 (File: MSV4006):

Stocks: XXXGXXXG (**23**): 20 mM, XXXGANTS (**25**): 75.275 mM, *Ptt*-XET16A: 28.995 μM and 2.8995 μM .

[<i>Ptt</i> -XET16A] (μM)	XXXGXXXG volume (μL)	XXXGANTS volume (μL)	Buffer volume (μL)	Enzyme volume (μL)	Water volume (μL)	Initial rate (mM/min)
0.2	5	6.64	50	6.90	31.96	0.00143
0.3	5	6.64	50	10.35	28.01	0.00225
0.5	5	6.64	50	17.24	21.11	0.00367
0.6	5	6.64	50	20.69	17.66	0.0049
0.9	5	6.64	50	<u>3.10</u>	35.25	0.0071

Table 42: Preparation of reaction crudes to obtain the *Ptt*-XET16A standard curve and initial rates obtained at each enzyme concentration.

5.- Kinetic studies.

5.1.- Preliminary evaluation of HPCE method to monitor XET activity.

Ptt-XET16A (3.2 μ M) catalyzed reaction between XG polymer (5 mg/ml) with XGOs-ANTS mixture (**25**, **26+27** and **28**) (approximately 15 mM) in 50 mM citrate 50 mM phosphate buffer at pH 5.5 and $I = 0.5$ M adjusted with NaCl and 30 °C was monitored after during 42 h of reaction. 20 μ L aliquots were taken at different time points, 20 μ L ManANTS (2 mM) were added, samples were heated at 100°C in sealed tubes for 10 minutes, and they were analyzed by HPCE.

5.2.- Screening of putative *Ptt*-XET16A donors.

5.2.1.- Evaluation of β -glycosyl fluorides as putative *Ptt*-XET16A donors.

Reaction mixtures containing 1 mM β -glycosyl fluorides putative *Ptt*-XET16A donors (**1**, **2** and **14**), approximately 5 mM XGOs-ANTS mixture (**25**, **26+27** and **28**) and 3.2 μ M *Ptt*-XET16A in citrate : phosphate buffer 50 mM : 50 mM, $I=0.5$ M, pH 5.5, were incubated at 30°C during 48 hours. 20 μ L aliquots were taken at different time points, 20 μ L of 2 mM ManANTS were added, samples were heated 10 minutes at 100 °C and analyzed by HPCE.

5.2.2.- Evaluation of β -fluorides as new possible donors for *Ptt*-XET16A, by fluoride release detection.

Reaction mixtures and controls to quantify transglycosylase activity using XXXG β F (**14**) as donor, were prepared in citrate:phosphate buffer 50:50 mM, $I=0.5$ M, pH 5.5 and incubated at 30°C, as it is described in the following table. Fluoride release was measured continuously with a fluoride selective electrode (FSE):

Assay	[XXXGβF] (mM)	[XGOs] (mM)	<i>Ptt</i> -XET16A (μM)
Chemical hydrolysis	1	0	0
Control XGos	1	5	0
Enzymatic hydrolysis	1	0	3.2
Enzymatic transglycosylation	1	5	3.2

Table 43: Analysis of XXXGβF (14) as a putative new donor for *Ptt*-XET16A.

Resulting voltages over time were interpolated in a fluoride standard curve prepared by dilution of a 100 ppm fluoride standard in citrate : phosphate buffer 50 mM : 50 mM, I=0.5 M, pH 5.5 and 30°C to obtain mM/s values.

5.2.3.- Evaluation of the first family of synthetic XGOs as putative *Ptt*-XET16A donors.

XGGG (18), XGXGGG (19), XGXGXGGG (20), XXXGGG (21), XXXGXXXGGG (22), XXXGXXXG (23) and XXXGXXXGXXXG (24) have been evaluated as putative new donors for XET using the HPCE method presented before.

Time point aliquots of reaction mixtures containing 5 mM putative donors (18, 19, 20, 21, 22, 23 or 24), approximately 5 mM XGOs-ANTS mixture (25, 26+27 and 28), 3.2 μM *Ptt*-XET16A in 50 mM citrate 50 mM phosphate buffer pH 5.5, I = 0.5 M (adjusted with NaCl) and 30 °C, were analyzed using the previously presented HPCE method.

5.3.- *Ptt*-XET16A kinetic characterization.

All enzymatic reactions were done in 50 mM citrate–50 mM phosphate buffer adjusted to the desired pH with NaOH. Ionic strength was kept constant at I = 0.5 M with added NaCl. Reactions were performed in a final volume of 100 μL in a thermostatic bath at the desired temperature. 20 μL aliquots were withdrawn at different time intervals, mixed with 20 μL of ManANTS 2 mM in water as internal

reference, the mixture heated at 100°C for 10 min in a sealed tube, and finally, samples were analyzed by the HPCE method presented before.

Reactions with XXXGXXXG (**23**) as donor and XXXG-ANTS (**25**) as acceptor substrates for reaction monitoring, product characterization, and enzyme standard curve generation were done at 1 mM **23**, 5 mM **25**, 0.1-1.5 μ M enzyme at pH 5.5, 30°C.

Product concentration from the electropherograms was determined from relative peak areas using Man-ANTS as internal reference by interpolation in the XXXGANTS (**25**) standard curve. Initial rates in product formation (v_0 in mM/min) were calculated as the slope of the linear region of the time course (0 to 20 min) corresponding to < 10% substrate to product conversion.

5.3.1.- *Ptt-XET16A* specific activity.

For enzyme standard curve concretely, concentrations and resulting initial rates were presented in the following table (File: MSV4006)

[<i>Ptt-XET16A</i>] (μ M)	[XXXGXXXG (23)] (mM)	[XXXG-ANTS (25)] (mM)	v_0 (mM/min)
0.9	1	5	0.00709
0.6	1	5	0.00485
0.5	1	5	0.00367
0.3	1	5	0.00230
0.2	1	5	0.00143
0	1	5	0

Table 44: Substrate and enzyme concentrations to determine enzyme standard curve and initial rates obtained.

Data obtained for enzyme standard curve was fitted to lineal regression to obtain specific activity equation (Equation 10) which was used to determine active enzyme concentration of new enzyme stocks.

$$v_0 \left(\frac{\text{mM}}{\text{min}} \right) = 0.00781 \cdot [E] (\mu\text{M})$$

Equation 10: *Ptt-XET16A* specific activity equation at 1 mM **23 and 5 mM **25**.**

5.3.2.- pH profile.

In the study of dependence of activity with pH, reaction mixtures contained 1 mM **23**, 5 mM **25**, 0.3 μ M *Ptt*-XET16A, in the pH range of 3 to 8 at 30°C. Buffers (phosphate 50 mM : citrate 50 mM I = 0.5 M adjusted with NaCl) were prepared as it is indicated by Ellis and Morrison²⁰². Obtained initial rates are presented in the following table (Table 45) (File: pH profile).

Ph	$v_0/[E]$ (1/s)	pH	$v_0/[E]$ (1/s)
2,95	0.000	5,81	0.113
3,98	0.000	6,08	0.066
4,51	0.032	6,08	0.067
4,51	0.022	6,32	0.046
4,78	0.131	6,56	0.028
4,78	0.126	6,56	0.028
5,07	0.136	7,06	0.010
5,57	0.130	7,51	0.005
5,57	0.130	7,51	0.006
5,57	0.130	8,03	0.000

Table 45: *Ptt*-XET16A steady state initial rates at different pH.

Activity follows a single ionization curve at high pH values. Data from pH 5 to 8 were fitted to Equation 11:

$$V_0 = \frac{v_{\max} \cdot \text{pH}}{1 + 10^{\text{pH} - \text{pK}_a}}$$

Equation 11: Equation fitted to *Ptt*-XET16A activity dependence on pH.

5.3.3.- Temperature profile.

The temperature dependence of enzyme activity was performed at 1 mM **23** and 5 mM **25** and 0.3 μ M *Ptt*-XET16A at constant pH 5.5, temperature ranging from 10 to 50°C. Buffers were again prepared as it was indicated by Ellis and Morrison²⁰², results are presented in the following table (Table 46) (File: Temp profile):

Temp. (°C)	$v_0/[E]$ (1/s)
10	0.036
10	0.030
10	0.033
20	0.070
20	0.058
20	0.072
25	0.082
30	0.130
30	0.130
30	0.130

Temp. (°C)	$v_0/[E]$ (1/s)
35	0.128
35	0.135
40	0.133
40	0.128
40	0.133
45	0.109
45	0.105
50	0.035
50	0.056
60	0.003

Table 46: Ptt-XET16A steady state initial rates at different temperatures.

5.3.4.- Ptt-XET16A kinetic mechanism using XXXGXXXG (23) as donor.

Steady-state kinetics, varying donor **23** and acceptor **25** substrate concentrations, were performed at pH 5.5, 30°C, with donor 0.3 – 5 mM, acceptor 0.5 – 10 mM (matrix of approximately 8 donor x 8 acceptor concentrations), and Ptt-XET16A enzyme 0.3 μ M. Kinetic data $v_0/[E]_0=f([\text{donor}],[\text{acceptor}])$ was fitted to modified ping-pong *bi-bi* kinetic models by non-linear regression using the FigP and SigmaPlot software packages. Results were presented in the following table (Table 47) (File: Matrix XXXG2).

[XXXGXXXG] (mM)	[XXXGANTS] (mM)	$V_0/[E]$ (1/seg)	File
0,3	2	0.0636	MSV4084
0,3	3	0.0726	MSV4096
0,3	4	0.0751	MSV4091
0,3	4	0.0623	MSV4095
0,4	3	0.0790	MSV4098
0,4	5	0.0876	MSV4077
0,5	2	0.0994	MSV4084
0,5	3	0.1180	MSV4088
0,5	3	0.1209	MSV4096
0,5	3	0.1044	MSV4098
0,5	4	0.0873	MSV4086
0,5	5	0.0921	MSV4076

[XXXGXXXG] (mM)	[XXXGANTS] (mM)	$V_0/[E]$ (1/seg)	File
1	7	0.1168	MSV4097
1	9	0.1071	MSV4097
1	9	0.1160	MSV4097
1	10	0.1179	MSV4059
1,5	0,7	0.0571	MSV4087
1,5	1	0.0771	MSV4087
1,5	1,5	0.0935	MSV4095
1,5	2	0.1139	MSV4082
1,5	2,5	0.1241	MSV4095
1,5	3	0.1464	MSV4087
1,5	3	0.1412	MSV4088
1,5	4	0.1464	MSV4086

[XXXGXXXG] (mM)	[XXXGANTS] (mM)	V ₀ [E] (1/seg)	File
0,5	7	0.0784	MSV4096
0,7	0,5	0.0498	MSV4085
0,7	1	0.0852	MSV4085
0,7	1,5	0.0998	MSV4085
0,7	2	0.1232	MSV4082
0,7	2	0.1222	MSV4085
0,7	3	0.1197	MSV4085
0,7	3	0.1285	MSV4088
0,7	3	0.1226	MSV4095
0,7	4	0.1165	MSV4085
0,7	4	0.1206	MSV4086
0,7	5	0.1111	MSV4074
0,7	5	0.1147	MSV4095
0,7	6	0.1110	MSV4095
0,7	7	0.1056	MSV4085
0,7	7	0.0935	MSV4087
0,7	7	0.0984	MSV4091
0,7	7	0.1065	MSV4095
0,85	2	0.1227	MSV4082
0,85	2	0.1155	MSV4082
0,85	4	0.1305	MSV4086
1	0,5	0.0540	MSV4059
1	0,5	0.0525	MSV4097
1	0,7	0.0682	MSV4059
1	1	0.0748	MSV4059
1	1	0.0839	MSV4097
1	1,5	0.0947	MSV4059
1	2	0.1069	MSV4059
1	2	0.1137	MSV4082
1	2	0.1225	MSV4097
1	3	0.1249	MSV4059
1	3	0.1313	MSV4096
1	3	0.1437	MSV4097
1	3	0.1296	MSV4098
1	3	0.1373	MSV4098
1	4	0.1421	MSV4078
1	4	0.1418	MSV4097
1	4	0.1302	MSV4097
1	4	0.1348	MSV4098
1	5	0.1302	MSV4072
1	5	0.1302	MSV4073
1	5	0.1302	MSV4074
1	5	0.1302	MSV4076
1	5	0.1297	MSV4077
1	5	0.1302	MSV4078
1	5	0.1302	MSV4097
1	5	0.1302	MSV4098
1	6	0.1299	MSV4098

[XXXGXXXG] (mM)	[XXXGANTS] (mM)	V ₀ [E] (1/seg)	File
1,5	4	0.1566	MSV4087
1,5	5	0.1458	MSV4076
1,5	6	0.1408	MSV4095
1,5	7	0.1428	MSV4087
1,5	7	0.1395	MSV4095
2	1	0.0599	MSV4083
2	1	0.0537	MSV4084
2	2	0.0981	MSV4082
2	2	0.0901	MSV4084
2	3	0.1359	MSV4083
2	3	0.1371	MSV4084
2	3	0.1291	MSV4098
2	4	0.1349	MSV4083
2	4	0.1394	MSV4093
2	4	0.1395	MSV4095
2	5	0.1566	MSV4074
2	5	0.1549	MSV4093
2	6	0.1503	MSV4093
2	7	0.1450	MSV4083
2	7	0.1548	MSV4096
2	8,5	0.1450	MSV4093
2	10	0.1302	MSV4083
2,5	3	0.1204	MSV4098
2,5	5	0.1594	MSV4077
3	1	0.0456	MSV4083
3	2	0.0812	MSV4082
3	3	0.1177	MSV4088
3	3	0.1167	MSV4096
3	4	0.1285	MSV4083
3	4	0.1394	MSV4086
3	5	0.1479	MSV4076
3	5	0.1656	MSV4077
3	5	0.1536	MSV4078
3	6	0.1598	MSV4093
3	7	0.1595	MSV4083
3	8,5	0.1498	MSV4093
3	10	0.1499	MSV4083
3	12	0.1534	MSV4093
4	2	0.0692	MSV4082
4	3	0.0968	MSV4088
4	3	0.0969	MSV4098
4	4	0.1246	MSV4086
4	4	0.1235	MSV4095
4	5	0.1263	MSV4073
4	5	0.1280	MSV4076
4	5	0.1429	MSV4077
4	7	0.1499	MSV4087
5	2	0.0629	MSV4082

[XXXGXXXG] (mM)	[XXXGANTS] (mM)	$V_o/[E]$ (1/seg)	File
1	7	0.1272	MSV4072
1	7	0.1287	MSV4078
1	7	0.1221	MSV4097

[XXXGXXXG] (mM)	[XXXGANTS] (mM)	$V_o/[E]$ (1/seg)	File
5	4	0.1211	MSV4086
5	5	0.1203	MSV4076
5	7	0.1430	MSV4087
6	5	0.1149	MSV4077

Table 47: Initial rates of *Ptt*-XET16A catalyzed reaction between and at different donor 23 and acceptor 25 concentrations.

5.3.5.- *Ptt*-XET16A kinetic mechanism using GalGXXXGXXXG (38) as donor.

Steady-state kinetics, varying donor **38** and acceptor **25** substrate concentrations, were performed at pH 5.5, 30°C, with donor 0.5 – 7 mM, acceptor 0.3 – 7 mM (matrix of approximately 7 donor x 7 acceptor concentrations), and *Ptt*-XET16A enzyme 0.1 μ M. Kinetic data $v_o/[E]_0=f([donor],[acceptor])$ was fitted to modified ping-pong *bi-bi* kinetic models by non-linear regression using the FigP and SigmaPlot software packages. Results were presented in the following table (Table 48) (File: Matrix GalGXXXG2).

[GalGXXXGXXXG] (mM)	[XXXGANTS] (mM)	$V_o/[E]$ (1/seg)	File
0,5	0,3	0,469	MSV5068
0,5	0,5	0,426	MSV5069
0,5	0,7	0,418	MSV5069
0,5	1	0,363	MSV5068
0,5	1	0,415	MSV5069
0,5	1,5	0,386	MSV5069
0,5	2	0,373	MSV5068
0,5	2	0,359	MSV5069
0,5	3	0,223	MSV5068
0,5	3	0,264	MSV5069
0,5	4	0,175	MSV5068
0,5	4	0,204	MSV5069
0,5	5	0,231	MSV5068
0,7	1	0,525	MSV5064
0,7	5	0,348	MSV5064
1	0,3	0,482	MSV5072
1	0,3	0,604	MSV5075
1	0,4	0,652	MSV5072

[GalGXXXGXXXG] (mM)	[XXXGANTS] (mM)	$V_o/[E]$ (1/seg)	File
2	3	0,994	MSV5074
2	4	0,796	MSV5076
2	4	0,823	MSV5074
2	5	0,759	MSV5076
2	5	0,688	MSV5074
2	7	0,540	MSV5076
3	0,5	1,037	MSV5066
3	1	1,309	MSV5066
3	1	1,384	MSV5066
3	1	1,231	MSV5066
3	2	1,403	MSV5065
3	2	1,273	MSV5065
3	2	1,329	MSV5067
3	3	1,112	MSV5065
3	3	1,117	MSV5065
3	3	1,254	MSV5067
3	4	0,981	MSV5074
3	4	1,004	MSV5067

[GalGXXXGXXXG] (mM)	[XXXGANTS] (mM)	Vo/[E] (1/seg)	File	[GalGXXXGXXXG] (mM)	[XXXGANTS] (mM)	Vo/[E] (1/seg)	File
1	0,5	0,662	MSV5072	3	5	1,088	MSV5074
1	0,5	0,788	MSV5075	3	5	1,050	MSV5074
1	0,7	0,714	MSV5075	3	5	0,960	MSV5067
1	0,75	0,788	MSV5075	3	7	0,837	MSV5074
1	1	0,787	MSV5071	3	7	0,870	MSV5074
1	1	0,680	MSV5075	4	0,5	1,334	MSV5070
1	1	0,697	MSV5072	4	1	1,462	MSV5071
1	1	0,756	MSV5075	4	1	1,408	MSV5070
1	1,5	0,658	MSV5075	4	1,5	1,551	MSV5070
1	2	0,737	MSV5071	4	2	1,529	MSV5071
1	2	0,554	MSV5071	4	2	1,395	MSV5070
1	2	0,682	MSV5075	4	3	1,480	MSV5071
1	2	0,683	MSV5067	4	3	1,372	MSV5070
1	3	0,527	MSV5064	4	4	1,246	MSV5071
1	3	0,561	MSV5075	4	4	1,256	MSV5070
1	3	0,564	MSV5067	4	5	1,299	MSV5071
1	4	0,483	MSV5064	4	5	1,107	MSV5070
1	4	0,418	MSV5075	4	7	0,997	MSV5071
1	5	0,417	MSV5064	4	7	0,971	MSV5071
1	5	0,428	MSV5075	5	0,5	1,178	MSV5076
1	5	0,395	MSV5067	5	1	1,550	MSV5076
1	7	0,320	MSV5064	5	2	1,887	MSV5072
1	7	0,303	MSV5064	5	2	1,820	MSV5076
1	7	0,285	MSV5064	5	2	1,734	MSV5076
1	7	0,298	MSV5072	5	3	1,718	MSV5072
1,5	1	0,920	MSV5076	5	3	1,712	MSV5076
1,5	2	0,862	MSV5067	5	4	1,567	MSV5072
1,5	3	0,697	MSV5067	5	4	1,503	MSV5076
1,5	4	0,622	MSV5067	5	5	1,393	MSV5072
1,5	5	0,601	MSV5067	5	5	1,330	MSV5072
2	0,5	0,818	MSV5065	5	5	1,364	MSV5076
2	0,75	1,009	MSV5065	5	7	1,255	MSV5070
2	1	1,183	MSV5065	5	7	1,161	MSV5072
2	1	1,141	MSV5065	5	7	1,267	MSV5066
2	1	1,079	MSV5074	6	2	1,902	MSV5066
2	1,5	1,154	MSV5074	6	7	1,276	MSV5066
2	2	1,052	MSV5065	7	5	1,643	MSV5066
2	2	1,120	MSV5074	7	7	1,389	MSV5066
2	3	0,912	MSV5065	7	7	1,536	MSV5066
2	3	0,927	MSV5065				

Table 48: Initial rates for *Ptt*-XET16A steady state kinetics using GalGXXXGXXXG (38) as donor and XXXG-ANTS (25) as acceptor.

5.4.- Donor screening and subsite mapping.

Kinetics were performed in citrate : phosphate buffer 50 mM : 50 mM I=0.5 M (adjusted with KCl) and pH 5.5, donor concentration was varied between 0.3 and 1 mM, acceptor (XXXG-ANTS (**25**)) was 5 mM, and enzyme concentration between 0.1 and 6.8 μ M. At different time points, 20 μ L of reaction solution was taken, diluted with 20 μ L of approximately 2 mM Man-ANTS internal standard and boiled for 10 minutes to stop reaction. Samples were analyzed on HPCE and initial rate was determined at different donor concentrations. Initial rates at different donor concentration, for each substrate within the library, were presented in the following table (Table 49). Slope of initial rates versus donor concentration determines k_{cat}/K_M value, presented also in the following table (Table 49).

XXXGXXG (46)----- $k_{cat}/K_M = 57.8 \pm 4.3$			
File	[Donor] (mM)	v_0 (mM/min)	$v_0/[E]$ (1/s)
MSV4013	0.465	0.00057	0.03242
MSV4013	0.651	0.00075	0.04207
MSV4013	0.79	0.00084	0.04721
MSV4013	0.93	0.00094	0.05331

XXXGXXXG (23) ----- $k_{cat}/K_M = 142.3 \pm 6.7$			
File	[Donor] (mM)	v_0 (mM/min)	$v_0/[E]$ (1/s)
MSV4011	0.7	0.00205	0.11583
MSV4011	0.85	0.00221	0.12476
MSV4024	0.5	0.00129	0.07649
MSV4024	0.7	0.00186	0.11036
MSV4024	0.85	0.00210	0.12505
MSV4076	0.5	0.00159	0.09208
MSV4074	0.7	0.00194	0.11112
MSV4095	0.7	0.00203	0.11466
MSV5062	0.4	0.00114	0.06882
MSV5062	0.5	0.00132	0.07986
MSV5062	0.7	0.00179	0.10773
MSV5062	0.85	0.00199	0.11985
MSV4060	0.7	0.00182	0.11241
MSV4060	0.85	0.00215	0.13283
MSV4060	1	0.00238	0.14719

XXXGXXXGXXXG (24) first product ----- $k_{cat}/K_M = 221.1 \pm 15.8$			
File	[Donor] (mM)	v_0 (mM/min)	$v_0/[E]$ (1/s)
MSV4011	0.35	0.00155	0.08743
MSV4011	0.425	0.00180	0.10166
MSV4011	0.5	0.00195	0.11013
MSV4022	0.25	0.00112	0.07206
MSV4022	0.35	0.00142	0.09137
MSV4022	0.425	0.00162	0.10424
MSV4022	0.5	0.00176	0.11324

XXXGXXXGXXXG (24)second product ----- $k_{cat}/K_M= 343.8 \pm 19.1$			
File	[Donor] (mM)	v_0 (mM/min)	$v_0/[E]$ (1/s)
MSV4011	0.25	0.00179	0.10132
MSV4011	0.35	0.00219	0.12368
MSV4011	0.425	0.00256	0.14458
MSV4011	0.5	0.00300	0.16943
MSV4022	0.25	0.00160	0.10295
MSV4022	0.35	0.00200	0.12869
MSV4022	0.425	0.00236	0.15185

GGXXXG (50) ----- $k_{cat}/K_M= 1.16 \pm 0.02$			
File	[Donor] (mM)	v_0 (mM/min)	$v_0/[E]$ (1/s)
MSV4019	0.438	0.00025	0.00050
MSV4019	0.613	0.00037	0.00072
MSV4019	0.744	0.00045	0.00089
MSV4019	0.875	0.00052	0.00102
MSV4013	0.875	0.00035	0.00099

GGGXXXG (51) ----- $k_{cat}/K_M= 40.9 \pm 2.6$			
File	[Donor] (mM)	v_0 (mM/min)	$v_0/[E]$ (1/s)
MSV5063	0.400	0.00085	0.01277
MSV5063	0.500	0.00123	0.01857
MSV5063	0.700	0.00163	0.02452
MSV5063	0.850	0.00242	0.03644
MSV5062	0.400	0.00044	0.01341
MSV5062	0.500	0.00067	0.02008
MSV5062	0.700	0.00088	0.02667
MSV5062	0.850	0.00108	0.03269

GGGGXXXG (52)----- $k_{cat}/K_M= 96.5 \pm 4.7$			
File	[Donor] (mM)	v_0 (mM/min)	$v_0/[E]$ (1/s)
MSV4009	0.315	0.00051	0.02903
MSV4009	0.441	0.00072	0.04049
MSV4009	0.536	0.00086	0.04851
MSV4009	0.630	0.00112	0.06310
MSV4015	0.441	0.00060	0.03714
MSV4015	0.630	0.00097	0.06001
MSV4025	0.315	0.00055	0.03241
MSV4025	0.441	0.00077	0.04544
MSV4025	0.630	0.00104	0.06136

XGXXXG (54)----- $k_{cat}/K_M= 1.66 \pm 0.13$			
File	[Donor] (mM)	v_0 (mM/min)	$v_0/[E]$ (1/s)
MSV4017	0.460	0.00049	0.00098
MSV4017	0.644	0.00064	0.00126
MSV4017	0.782	0.00071	0.00141
MSV4017	0.920	0.00079	0.00156
MSV4013	0.920	0.00079	0.00154

XXGXXXG (29) ----- $k_{cat}/K_M= 57.1 \pm 6.2$			
File	[Donor] (mM)	v_0 (mM/min)	$v_0/[E]$ (1/s)
MSV4017	0.468	0.01175	0.03368
MSV4017	0.655	0.01341	0.03843
MSV4022	0.468	0.00157	0.03033
MSV4022	0.655	0.00196	0.03781
MSV4028	0.468	0.00206	0.03394
MSV4028	0.655	0.00227	0.03730

XGGXXG (55)----- $k_{cat}/K_M = 68.8 \pm 4.1$			
File	[Donor] (mM)	v_0 (mM/min)	$v_0/[E]$ (1/s)
MSV4008	0.418	0.00047	0.02677
MSV4008	0.585	0.00070	0.03959
MSV4008	0.710	0.00080	0.04512
MSV4008	0.835	0.00095	0.05365
MSV4015	0.418	0.00041	0.02509
MSV4015	0.710	0.00076	0.04696
MSV4020	0.585	0.00156	0.04474
MSV4020	0.710	0.00177	0.05081
MSV4028	0.418	0.00190	0.03129
MSV4028	0.585	0.00261	0.04302
MSV4028	0.835	0.00370	0.06100

GXXGXXG (53)----- $k_{cat}/K_M = 202.8 \pm 17.4$			
File	[Donor] (mM)	v_0 (mM/min)	$v_0/[E]$ (1/s)
MSV4008	0.314	0.00121	0.06834
MSV4008	0.440	0.00153	0.08641
MSV4008	0.534	0.00189	0.10697
MSV4008	0.628	0.00216	0.12171
MSV4024	0.314	0.00144	0.08585
MSV4024	0.440	0.00169	0.10066
MSV4024	0.534	0.00209	0.12416
MSV4024	0.628	0.00243	0.14430
MSV4020	0.314	0.00142	0.08138
MSV4020	0.534	0.00204	0.11695

XGXGXXG (56)----- $k_{cat}/K_M = 83.8 \pm 5.3$			
File	[Donor] (mM)	v_0 (mM/min)	$v_0/[E]$ (1/s)
MSV4060	0.300	0.00065	0.02413
MSV4060	0.400	0.00087	0.03222
MSV4061	0.300	0.00113	0.02757
MSV4061	0.400	0.00159	0.03869
MSV4061	0.500	0.00164	0.03998
MSV4063	0.300	0.00094	0.02745
MSV4063	0.400	0.00120	0.03510
MSV4063	0.250	0.00085	0.02473
MSV4065	0.350	0.00109	0.03324
MSV4065	0.450	0.00135	0.04111
MSV4065	0.500	0.00141	0.04300

GalGXXG (40)----- $k_{cat}/K_M = 1.66 \pm 0.07$			
File	[Donor] (mM)	v_0 (mM/min)	$v_0/[E]$ (1/s)
MSV4014	0.465	0.00027	0.00082
MSV4014	0.651	0.00033	0.00102
MSV4014	0.791	0.00044	0.00136
MSV4014	0.930	0.00050	0.00154

GalGXXGGG (59)----- $k_{cat}/K_M = 1.70 \pm 0.14$			
File	[Donor] (mM)	v_0 (mM/min)	$v_0/[E]$ (1/s)
MSV4014	0.405	0.00022	0.00069
MSV4014	0.567	0.00030	0.00093
MSV4014	0.689	0.00043	0.00135
MSV4014	0.810	0.00042	0.00131
MSV4019	0.405	0.00028	0.00081
MSV4019	0.689	0.00042	0.00119

GalGXXXGXXXG (38)----- $k_{cat}/K_M = 395.0 \pm 25.2$			
File	[Donor] (mM)	v_0 (mM/min)	$v_0/[E]$ (1/s)
MSV5063	0.400	0.00363	0.21866
MSV5063	0.500	0.00403	0.24327
MSV5063	0.700	0.00529	0.31915
MSV5063	0.850	0.00615	0.37124
MSV5064	0.500	0.00338	0.23062
MSV5064	0.700	0.0051	0.34812
MSV5064	1.000	0.00611	0.41723
MSV5066	1.000	0.00161	0.42814
MSV5071	1.000	0.00135	0.39497

Table 49: Initial rates and k_{cat}/K_M ($M^{-1}\cdot s^{-1}$) obtained for each substrate within the library at different donor concentrations.

5.5.- Yield after 24 h reaction.

Reactions were done on citrate phosphate buffer 50 mM:50 mM I=0.5 M (adjusted with KCl) and pH 5.5. Donor concentration was 1 mM, acceptor (XXXGANTS(25)) was 5 mM, and enzyme concentration was 3 μ M. Samples were taken at 24 h and processed as kinetic time points, on kinetic experiments.

6.- Spectroscopic techniques.

6.1.- Absorbance spectra.

Absorbance spectra were recorded in a Helios- α (Unicam) spectrophotometer, equipped with a thermostated cell holder. All measurements were done at 30°C in a 1 cm light path quartz cuvette.

6.2.- Fluorescence spectra.

Fluorescence spectra were recorded in a Fluoromax-2 spectrofluorimeter, equipped with a thermostated cell holder. All measurements were done at 30°C. Fluorescence measurements were done in a quartz fluorescence cell (3 mm excitation light path and 3 mm emission light path), excitation slit was set up at 10 nm and emission slit at 5 nm.

Excitation maximum wavelength was determined by excitation between 220 and 480 nm recording fluorescence emission at 485 nm. Emission maximum wavelength was determined by excitation at 345 nm and recording emission intensities between 380 and 650 nm.

Kinetic experiments were performed in the same equipment monitoring fluorescence intensity at 485 nm (excitation wavelength 345 nm) each 5 minutes during 30 minutes reaction.

BIBLIOGRAPHY

BIBLIOGRAPHY.

The results presented in this thesis were published in the following papers:

Saura-Valls, M.; Fauré, R.; Ragàs, S.; Piens, K.; Brumer, H.; Teeri, T. T.; Cottaz, S.; Driguez, H.; Planas, A. (2006); **Kinetic analysis using low-molecular mass xyloglucan oligosaccharides defines the catalytic mechanism of a Populus xyloglucan endotransglycosylase**; *Biochemical Journal*; **395**, 99-106.

Fauré, R.; Saura-Valls, M.; Brumer, H., III; Planas, A.; Cottaz, S.; Driguez, H. (2006); **Synthesis of a Library of Xylogluco-Oligosaccharides for Active-Site Mapping of Xyloglucan endo-Transglycosylase**; *Journal of Organic Chemistry*; **71**, 5151-5161.

Saura-Valls, M.; Fauré, R.; Brumer, H.; Driguez H.; Planas, A. **Subsite mapping of a xyloglucan endotransglycosylase**; in preparation.

And they are also presented in the following scientific events:

M. Saura-Valls, R. Fauré, H. Brumer, T. T. Teeri, S. Cottaz, H. Driguez, A. Planas. **Síntesi enzimàtica d'oligosacàrids per l'estudi de xiloglucà endotransglicosilases. IV Trobada de joves investigadors dels països catalans**, Communication 5.4.1, January 2006, Lleida (oral communication).

M. Saura, R. Fauré, H. Brumer, T. Teeri, S. Cottaz, H. Driguez, A. Planas. **Biochemical characterization of a plant xyloglucan endotransglycosylase by synthetically prepared xylogluco-oligosaccharides**. *Journée Chimie Grand Sud-Ouest*, Abs P6, November 2005, Montpellier (oral communication).

M. Saura, R. Fauré, H. Brumer, T. Teeri, S. Cottaz, H. Driguez, A. Planas. **Synthesis of oligosaccharide substrates by chemoenzymatic approaches to study xyloglucan endotransglycosylases** *XI Meeting on Industrial Application of Enzymes*, Abs P6, 244, November 2005, Barcelona (poster).

M. Saura, R. Fauré, H. Brumer, T. Teeri, S. Cottaz, H. Driguez, A. Planas. **Subsite mapping of a xyloglucan endotransglycosylase from *Populus tremula x tremuloides***. *6th Carbohydrate Bioengineering meeting*. Abs P63, 3-6 September 2005, Barcelona (poster).

M. Saura, R. Fauré, H. Brumer, K. Piens, T. Teeri, S. Cottaz, H. Driguez, and A. Planas. **Characterization and substrate specificity of a xyloglucan endotransglycosylase from *Populus tremula x tremuloides***. *VII Jornadas de carbohidratos*, Abs C23, September 2004, Tarragona, (poster).

R. Fauré, M. Saura, K. Piens, H. Brumer, T. Teeri, A. Planas, S. Cottaz, H. Driguez. **Conception et synthesis d'une bibliotèque de xilogluco-oligosaccharides**. *Congres groupe français de glucides*, May 2004, Dourdan (poster).

M. Saura, R. Fauré, H. Brumer, K. Piens, T. Teeri, S. Cottaz, H. Driguez, and A. Planas. **New activity assay for xyloglucan endotransglycosylases based on capillary electrophoresis. Enzyme kinetics and screening of novel substrates**. *22th Internat. Carbohydrate symposium (22th ICS)*, Abs.P-466, July 2004, Glasgow (poster).

R. Fauré, M. Saura, K. Piens, H. Brumer, T. Teeri, A. Planas, S. Cottaz, H. Driguez. **Combinatorial enzymatic coupling for the synthesis of regular xylogluco-oligosaccharides as probes for kinetic and interactions studies of xyloglucan active enzymes**. *22th Internacional Carbohydrate Symposium (22th ICS)*, Abs C18, July 2004, Glasgow (oral communication)

M. Saura, R. Fauré, H. Brumer, T. Teeri, S. Cottaz, H. Driguez, A. Planas. **New activity assay for xyloglucan-endotransglycosylases. The search for minimal donor substrate**. *X Meeting on Industrial Applications of Enzymes*, Abs P-16, p.210., Barcelona, November 2003 (poster).

R. Fauré, M. Saura, H. Brumer, T. Teeri, A. Planas, S. Cottaz, H. Driguez. **Design and synthesis of substrate analogues for xyloglucan endotransglycosylases.** *12th European Carbohydrate Symposium (EUROCARB 12)*, abs PB-086, p.268, Grenoble, July 2003 (poster).

1. Carpita, N. C. and Gibeaut, D. M. (1993); Structural models of primary cell walls in flowering plants: consistency of molecular structure with the physical properties of the walls during growth; *Plant Journal*; **3**, 1-30
2. N. Carpita and M. McCann, in *Biochemistry & Molecular Biology of Plants*, B. Buchanan, W. Gruissem, R. Jones, Eds. (ASPP, 2000).
3. Nishitani, K. (1997); The role of endoxyloglucan transferase in the organization of plant cell walls; *International Review of Cytology*; **173**, 157-206
4. Fry, S. C. (2004); Primary cell wall metabolism: Tracking the careers of wall polymers in living plant cells; *New Phytologist*; **161**, 641-675
5. Aldington, S. and Fry, S. C. (1993); Oligosaccharins; *Advances in Botanical Research*; **19**, 1-101
6. Darvill, A.; Augur, C.; Bergmann, C.; Carlson, R. W.; Cheong, J. J.; Eberhard, S.; Hahn, M. G.; Lo, V. M.; Marfa, V. (1992); Oligosaccharins. Oligosaccharides that regulate growth, development and defense responses in plants; *Glycobiology*; **2**, 181-198
7. Willats, W. G. T.; McCartney, L.; Mackie, W.; Knox, J. P. (2001); Pectin: Cell biology and prospects for functional analysis; *Plant Molecular Biology*; **47**, 9-27
8. Baucher, M.; Monties, B.; van Montagu, M.; Boerjan, W. (1998); Biosynthesis and Genetic Engineering of Lignin; *Critical Reviews in Plant Sciences*; **17**, 125-197
9. Showalter, A. M. (1993); Structure and function of plant cell wall proteins; *Plant Cell*; **5**, 9-23
10. Nishitani, K. (1998); Construction and restructuring of the cellulose-xyloglucan framework in the apoplast as mediated by the xyloglucan-related protein family-A hypothetical scheme; *Journal of Plant Research*; **111**, 159-166
11. Pauly, M.; Albersheim, P.; Darvill, A.; York, W. S. (1999); Molecular domains of the cellulose/xyloglucan network in the cell walls of higher plants; *Plant Journal*; **20**, 629-639
12. Darley, C. P.; Forrester, A. M.; McQueen-Mason, S. J. (2001); The molecular basis of plant cell wall extension; *Plant Molecular Biology*; **47**, 179-95
13. Nishitani, K. and Masuda, Y. (1983); Auxin-induced changes in cell wall xyloglucans: effects of auxin on two different subfractions of xyloglucans in the epicotyl cell wall of *Vigna angularis*; *Plant and Cell Physiology*; **24**, 345-355
14. Hayashi, T. (1989); Xyloglucans in the primary cell wall; *Annual review of plant physiology and plant molecular biology*; **40**, 139-68
15. Edelman, H. G. and Fry, S. C. (1992); Factors that affect the extraction of xyloglucan from the primary cell walls of suspension-cultured rose cells; *Carbohydrate Research*; **228**, 423-431

16. Whitney, S. E. C.; Gothard, M. G. E.; Mitchell, J. T.; Gidley, M. J. (1999); Roles of cellulose and xyloglucan in determining the mechanical properties of primary plant cell walls; *Plant Physiology*; **121**, 657-663
17. Gibeaut, D. M. and Carpita, N. C. (1994); Biosynthesis of plant cell wall polysaccharides; *FASEB Journal*; **8**, 904-15
18. Reiter, W.-D. (2002); Biosynthesis and properties of the plant cell wall; *Current Opinion in Plant Biology*; **5**, 536-542
19. Delmer, D. P. (1999); Cellulose biosynthesis: exciting times for a difficult field of study; *Annual review of plant physiology and plant molecular biology*; **50**, 245-276
20. Perrin, R.; Wilkerson, C.; Keegstra, K. (2001); Golgi enzymes that synthesize plant cell wall polysaccharides: finding and evaluating candidates in the genomic era; *Plant Molecular Biology*; **47**, 115-130
21. Hayashi, T. and Matsuda, K. (1981); Biosynthesis of xyloglucan in suspension-cultured soybean cells. Occurrence and some properties of xyloglucan 4-beta-D-glucosyltransferase and 6-alpha-D-xylosyltransferase; *J.Biol.Chem.*; **256**, 11117-11122
22. Fry, S. C.; York, W. S.; Albersheim, P.; Darvill, A.; Hayashi, T.; Joseleau, J. P.; Kato, Y.; Lorences, E. P.; Maclachlan, G. A.; et al. (1993); An unambiguous nomenclature for xyloglucan-derived oligosaccharides; *Physiologia Plantarum*; **89**, 1-3
23. Ray, P. M. (1980); Cooperative action of beta-glucan synthetase and UDP-xylose xylosyl transferase of Golgi membranes in the synthesis of xyloglucan-like polysaccharide; *Biochim Biophys Acta*; **629**, 431-444
24. White, A. R.; Xin, Y.; Pezeshk, V. (1993); Xyloglucan glucosyltransferase in Golgi membranes from *Pisum sativum* (pea); *Biochemical Journal*; **294**, 231-8
25. Faik, A.; Chileshe, C.; Sterling, J.; Maclachlan, G. (1997); Xyloglucan galactosyl- and fucosyltransferase activities from pea epicotyl microsomes; *Plant Physiology*; **114**, 245-254
26. Gordon, R. and Maclachlan, G. (1989); Incorporation of UDP-[14C]glucose into xyloglucan by pea membranes; *Plant Physiology*; **91**, 373-378
27. Faik, A.; Bar-Peled, M.; DeRocher, A. E.; Zeng, W.; Perrin, R. M.; Wilkerson, C.; Raikhel, N. V.; Keegstra, K. (2000); Biochemical characterization and molecular cloning of an α -1,2-fucosyltransferase that catalyzes the last step of cell wall xyloglucan biosynthesis in pea; *J.Biol.Chem.*; **275**, 15082-15089
28. Sarria, R.; Wagner, T. A.; O'Neill, M. A.; Faik, A.; Wilkerson, C. G.; Keegstra, K.; Raikhel, N. V. (2001); Characterization of a family of *Arabidopsis* genes related to xyloglucan fucosyltransferase1; *Plant Physiology*; **127**, 1595-1606

29. Rose, J. K. and Bennett, A. B. (1999); Cooperative disassembly of the cellulose-xyloglucan network of plant cell walls: parallels between cell expansion and fruit ripening; *Trends Plant Sci*; **4**, 176-183
30. Cosgrove, D. J. (2001); Wall structure and wall loosening. A look backwards and forwards; *Plant Physiology*; **125**, 131-134
31. Rose, J. K. C.; Braam, J.; Fry, S. C.; Nishitani, K. (2002); The XTH family of enzymes involved in xyloglucan endotransglucosylation and endohydrolysis: Current perspectives and a new unifying nomenclature; *Plant and Cell Physiology*; **43**, 1421-1435
32. Cosgrove, D. J. (1999); Enzymes and other agents that enhance cell wall extensibility; *Annual review of plant physiology and plant molecular biology*; **50**, 391-417
33. McQueen-Mason, S.; Durachko, D. M.; Cosgrove, D. J. (1992); Two endogenous proteins that induce cell wall extension in plants; *Plant Cell*; **4**, 1425-1433
34. McQueen-Mason, S. J. and Cosgrove, D. J. (1995); Expansin mode of action on cell walls. Analysis of wall hydrolysis, stress relaxation, and binding; *Plant Physiology*; **107**, 87-100
35. Okamoto-Nakazato, A.; Takahashi, K.; Kido, N.; Owaribe, K.; Katou, K. (2000); Molecular cloning of yieldins regulating the yield threshold of cowpea cell walls: cDNA cloning and characterization of recombinant yieldin; *Plant, Cell and Environment*; **23**, 155-164
36. Okamoto-Nakazato, A.; Nakamura, T.; Okamoto, H. (2000); The isolation of wall-bound proteins regulating yield threshold tension in glycerinated hollow cylinders of cowpea hypocotyl; *Plant, Cell and Environment*; **23**, 145-154
37. McQueen-Mason, S. J.; Fry, S. C.; Durachko, D. M.; Cosgrove, D. J. (1993); The relationship between xyloglucan endotransglycosylase and in-vitro cell wall extension in cucumber hypocotyls; *Planta*; **190**, 327-331
38. Yuan, S.; Wu, Y.; Cosgrove, D. J. (2001); A fungal endoglucanase with plant cell wall extension activity; *Plant Physiology*; **127**, 324-333
39. Fry, S. C. (1995); Polysaccharide-modifying enzymes in the plant cell wall; *Annu.Rev.Plant Physiol.Plant Mol.Biol.*; **46**, 497-520
40. Nishitani, K. and Tominaga, R. (1992); Endo-xyloglucan transferase, a novel class of glycosyltransferase that catalyzes transfer of a segment of xyloglucan molecule to another xyloglucan molecule; *J.Biol.Chem.*; **267**, 21058-64
41. Fry, S. C.; Smith, R. C.; Renwick, K. F.; Martin, D. J.; Hodge, S. K.; Matthews, K. J. (1992); Xyloglucan endotransglycosylase, a new wall-loosening enzyme activity from plants; *Biochemical Journal*; **282**, 821-8

42. Farkas, V.; Sulova, Z.; Stratilova, E.; Hanna, R.; Maclachlan, G. (1992); Cleavage of xyloglucan by nasturtium seed xyloglucanase and transglycosylation to xyloglucan subunit oligosaccharides; *Archives of biochemistry and biophysics*; **298**, 365-70
43. Maclachlan, G. and Brady, C. (1994); Endo-1,4- β -glucanase, xyloglucanase, and xyloglucan endo-transglycosylase activities versus potential substrates in ripening tomatoes; *Plant Physiology*; **105**, 965-74
44. Faik, A.; Desveaux, D.; Maclachlan, G. (1998); Enzymic activities responsible for xyloglucan depolymerization in extracts of developing tomato fruit: In honor of professor G. H. Neil Towers 75th birthday; *Phytochemistry*; **49**, 365-376
45. Sulova, Z.; Lednicka, M.; Farkas, V. (1995); A colorimetric assay for xyloglucan-endo-transglycosylase from germinating seeds; *Analytical Biochemistry*; **229**, 80-5
46. Henriksson, H.; Denman, S. E.; Campuzano, I. D. G.; Ademark, P.; Master, E. R.; Teeri, T. T.; Brumer, H., III (2003); N-linked glycosylation of native and recombinant cauliflower xyloglucan endotransglycosylase 16A; *Biochemical Journal*; **375**, 61-73
47. Kallas, A. M.; Piens, K.; Denman, S. E.; Henriksson, H.; Faeldt, J.; Johansson, P.; Brumer, H.; Teeri, T. T. (2005); Enzymatic properties of native and deglycosylated hybrid aspen (*Populus tremula***tremuloides*) xyloglucan endotransglycosylase 16A expressed in *Pichia pastoris*; *Biochemical Journal*; **390**, 105-113
48. Nishitani, K. (1992); A novel method for detection of endo-xyloglucan transferase; *Plant and Cell Physiology*; **33**, 1159-64
49. Schroder, R.; Atkinson, R. G.; Langenkamper, G.; Redgwell, R. J. (1998); Biochemical and molecular characterisation of xyloglucan endotransglycosylase from ripe kiwifruit; *Planta*; **204**, 242-51
50. Purugganan, M. M.; Braam, J.; Fry, S. C. (1997); The *Arabidopsis* TCH4 xyloglucan endotransglycosylase. Substrate specificity, pH optimum, and cold tolerance; *Plant Physiology*; **115**, 181-190
51. Rose, J. K. C.; Brummell, D. A.; Bennett, A. B. (1996); Two divergent xyloglucan endotransglycosylases exhibit mutually exclusive patterns of expression in nasturtium; *Plant Physiology*; **110**, 493-9
52. Baran, R.; Sulova, Z.; Stratilova, E.; Farkas, V. (2000); Ping-pong character of nasturtium-seed xyloglucan endotransglycosylase (XET) reaction; *General Physiology and Biophysics*; **19**, 427-440
53. Fry, S. C. (1997); Novel "dot-blot" assays for glycosyltransferases and glycosylhydrolases: optimization for xyloglucan endotransglycosylase (XET) activity; *Plant Journal*; **11**, 1141-1150
54. Henrissat, B. (1991); A classification of glycosyl hydrolases based on amino acid sequence similarities; *Biochemical Journal*; **280**, 309-16

55. Campbell, J. A.; Davies, G. J.; Bulone, V.; Henrissat, B. (1997); A classification of nucleotide-diphospho-sugar glycosyltransferases based on amino acid sequence similarities; *Biochem.J.*; **326**, 929-939
56. Coutinho, P. M. and Henrissat, B. (1999); Carbohydrate-active enzymes: an integrated database approach; *Special Publication - Royal Society of Chemistry*; **246**, 3-12
57. Coutinho, P. M.; Deleury, E.; Henrissat, B. (2003); The families of carbohydrate-active enzymes in the genomic era; *Journal of Applied Glycoscience*; **50**, 241-244
58. Coutinho, P. M.; Deleury, E.; Davies, G. J.; Henrissat, B. (2003); An evolving hierarchical family classification for glycosyltransferases; *Journal of Molecular Biology*; **328**, 307-317
59. Henrissat, B.; Deleury, E.; Coutinhosu, P. M.; Davies, G. J. (2004); Sequence families and modular organization of carbohydrate-active enzymes; *Enzyme Functionality*; 15-34
60. Henrissat, B. and Davies, G. J. (2000); Glycoside hydrolases and glycosyltransferases. Families, modules, and implications for genomics; *Plant Physiology*; **124**, 1515-1519
61. Henrissat, B. and Bairoch, A. (1993); New families in the classification of glycosyl hydrolases based on amino acid sequence similarities; *Biochem.J.*; **293**, 781-788
62. Henrissat, B. and Bairoch, A. (1996); Updating the sequence-based classification of glycosyl hydrolases; *Biochem.J.*; **316**, 695-696
63. Henrissat, B. and Davies, G. J. (1997); Structural and sequence-based classification of glycoside hydrolases; *Curr.Opin.Struct.Biol.*; **7**, 637-644
64. Tabuchi, A.; Kamisaka, S.; Hoson, T. (1997); Purification of xyloglucan hydrolase/endotransferase from cell walls of azuki bean epicotyls; *Plant and Cell Physiology*; **38**, 653-658
65. Campbell, P. and Braam, J. (1999); Xyloglucan endotransglycosylases: diversity of genes, enzymes and potential wall-modifying functions; *Trends in plant science*; **4**, 361-6
66. Uozu, S.; Tanaka-Ueguchi, M.; Kitano, H.; Hattori, K.; Matsuoka, M. (2000); Characterization of XET-related genes of rice; *Plant Physiology*; **122**, 853-859
67. Catala, C.; Rose, J. K. C.; Bennett, A. B. (2000); Auxin-regulated genes encoding cell wall-modifying proteins are expressed during early tomato fruit growth; *Plant Physiology*; **122**, 527-534
68. Baumann, M. J.; Eklöf, J. M.; Gurvan, M.; Kallas, A. M.; Teeri, T. T.; Czjzek, M.; Brumer, H., III (2007); Structural evidence for the evolution of Xyloglucanase activity from xyloglucan endo-transglycosylases: Biological implications for cell wall metabolism; *The plant cell preview*;

69. Xu, W.; Campbell, P.; Vargheese, A. K.; Braam, J. (1996); The Arabidopsis XET-related gene family: Environmental and hormonal regulation of expression; *Plant Journal*; **9**, 879-889
70. Campbell, P. and Braam, J. (1999); *In vitro* activities of four xyloglucan endotransglycosylases from *Arabidopsis*; *Plant Journal*; **18**, 371-82
71. Fanutti, C.; Gidley, M. J.; Reid, J. S. G. (1993); Action of a pure xyloglucan endo-transglycosylase (formerly called xyloglucan-specific endo-(1->4)- β -D-glucanase) from the cotyledons of germinated nasturtium seeds; *Plant Journal*; **3**, 691-700
72. de Silva, J.; Jarman, C. D.; Arrowsmith, D. A.; Stronach, M. S.; Chengappa, S.; Sidebottom, C.; Reid, J. S. (1993); Molecular characterization of a xyloglucan-specific endo-(1->4)- β -D-glucanase (xyloglucan endo-transglycosylase) from nasturtium seeds; *Plant Journal*; **3**, 701-11
73. Tabuchi, A.; Mori, H.; Kamisaka, S.; Hoson, T. (2001); A new type of endo-xyloglucan transferase devoted to xyloglucan hydrolysis in the cell wall of azuki bean epicotyls; *Plant and Cell Physiology*; **42**, 154-161
74. Saladie, M.; Rose, J. K. C.; Cosgrove, D. J.; Catala, C. (2006); Characterization of a new xyloglucan endotransglucosylase/hydrolase (*XTH*) from ripening tomato fruit and implications for the diverse modes of enzymic action; *Plant Journal*; **47**, 282-295
75. Smith, R. C. and Fry, S. C. (1991); Endotransglycosylation of xyloglucans in plant cell suspension cultures; *Biochemical Journal*; **279**, 529-35
76. Malet, C.; Jiménez-Barbero, J.; Bernabé, M.; Brosa, C.; Planas, A. (1993); Stereochemical course and structure of the products of the enzymic action of endo-1,3-1,4- β -D-glucan 4-glucanohydrolase from *Bacillus licheniformis*; *Biochem.J.*; **296**, 753-758
77. Viladot, J. L.; de Ramon, E.; Durany, O.; Planas, A. (1998); Probing the mechanism of Bacillus 1,3-1,4-beta-D-glucan 4-glucanohydrolases by chemical rescue of inactive mutants at catalytically essential residues; *Biochemistry*; **37**, 11332-11342
78. Viladot, J. L.; Canals, F.; Batllori, X.; Planas, A. (2001); Long-lived glycosyl-enzyme intermediate mimic produced by formate re-activation of a mutant endoglucanase lacking its catalytic nucleophile; *Biochem.J.*; **355**, 79-86
79. Sulova, Z.; Takacova, M.; Steele, N. M.; Fry, S. C.; Farkas, V. (1998); Xyloglucan endotransglycosylase: evidence for the existence of a relatively stable glycosyl-enzyme intermediate; *Biochemical Journal*; **330**, 1475-1480
80. Sulova, Z. and Farkas, V. (1999); Purification of xyloglucan endotransglycosylase based on affinity sorption of the active glycosyl-enzyme intermediate complex to cellulose; *Protein Expression and Purification*; **16**, 231-235

81. Steele, N. M. and Fry, S. C. (1999); Purification of xyloglucan endotransglycosylases (XETs): a generally applicable and simple method based on reversible formation of an enzyme-substrate complex; *Biochemical Journal*; **341**, 862
82. Sulova, Z.; Baran, R.; Farkas, V. (2001); Release of complexed xyloglucan endotransglycosylase (XET) from plant cell walls by a transglycosylation reaction with xyloglucan-derived oligosaccharides; *Plant Physiology and Biochemistry*; **39**, 927-932
83. Okazawa, K.; Sato, Y.; Nakagawa, T.; Asada, K.; Kato, I.; Tomita, E.; Nishitani, K. (1993); Molecular cloning and cDNA sequencing of endoxyloglucan transferase, a novel class of glycosyltransferase that mediates molecular grafting between matrix polysaccharides in plant cell walls; *J.Biol.Chem.*; **268**, 25364-8
84. Juncosa, M.; Pons, J.; Dot, T.; Querol, E.; Planas, A. (1994); Identification of Active Site Carboxylic Residues in *Bacillus licheniformis* 1,3-1,4- β -D-Glucan 4-Glucanohydrolase by Site-directed Mutagenesis; *J.Biol.Chem.*; **269**, 14530-14535
85. Fanutti, C.; Gidley, M. J.; Reid, J. S. G. (1996); Substrate subsite recognition of the xyloglucan endo-transglycosylase or xyloglucan-specific endo-(1 \rightarrow 4)- β -D-glucanase from the cotyledons of germinated nasturtium (*Tropaeolum majus*) seeds; *Planta*; **200**, 221-228
86. Steele, N. M.; Sulova, Z.; Campbell, P.; Braam, J.; Farkas, V.; Fry, S. C. (2001); Ten isoenzymes of xyloglucan endotransglycosylase from plant cell walls select and cleave the donor substrate stochastically; *Biochemical Journal*; **355**, 671-9
87. Sulova, Z.; Baran, R.; Farkas, V. (2003); Divergent modes of action on xyloglucan of two isoenzymes of xyloglucan endo-transglycosylase from *Tropaeolum majus*; *Plant Physiology and Biochemistry*; **41**, 431-437
88. Campbell, P. and Braam, J. (1998); Co- and/or post-translational modifications are critical for TCH4 XET activity; *Plant Journal*; **15**, 553-61
89. Johansson, P.; Brumer, H., III; Baumann, M. J.; Kallas, A. M.; Henriksson, H.; Denman, S. E.; Teeri, T. T.; Jones, T. A. (2004); Crystal structures of a poplar xyloglucan endotransglycosylase reveal details of transglycosylation acceptor binding; *Plant Cell*; **16**, 874-886
90. Steele, N. M. and Fry, S. C. (2000); Differences in catalytic properties between native isoenzymes of xyloglucan endotransglycosylase (XET); *Phytochemistry*; **54**, 667-680
91. Catala, C.; Rose, J. K.; York, W. S.; Albersheim, P.; Darvill, A. G.; Bennett, A. B. (2001); Characterization of a tomato xyloglucan endotransglycosylase gene that is down-regulated by auxin in etiolated hypocotyls; *Plant Physiology*; **127**, 1180-92

92. Redgwell, R. J. and Fry, S. C. (1993); Xyloglucan endotransglycosylase activity increases during kiwifruit (*Actinidia deliciosa*) ripening. Implications for fruit softening; *Plant Physiology*; **103**, 1399-406
93. Pritchard, J.; Hetherington, P. R.; Fry, S. C.; Tomos, A. D. (1993); Xyloglucan endotransglycosylase activity, microfibril orientation and the profiles of cell wall properties along growing regions of maize roots; *Journal of Experimental Botany*; **44**, 1281-9
94. Potter, I. and Fry, S. C. (1993); Xyloglucan endotransglycosylase activity in pea internodes. Effects of applied gibberellic acid; *Plant Physiology*; **103**, 235-41
95. Lorences, E. P. and Fry, S. C. (1993); Xyloglucan oligosaccharides with at least two α -D-xylose residues act as acceptor substrates for xyloglucan endotransglycosylase and promote the depolymerization of xyloglucan; *Physiologia Plantarum*; **88**, 105-12
96. Hetherington, P. R. and Fry, S. C. (1993); Xyloglucan endotransglycosylase activity in carrot cell suspensions during cell elongation and somatic embryogenesis; *Plant Physiology*; **103**, 987-92
97. Takeda, T.; Mitsuishi, Y.; Sakai, F.; Hayashi, T. (1996); Xyloglucan endotransglycosylation in suspension-cultured poplar cells; *Bioscience, Biotechnology, and Biochemistry*; **60**, 1950-1955
98. Ito, H. and Nishitani, K. (1999); Visualization of EXGT-mediated molecular grafting activity by means of a fluorescent-labeled xyloglucan oligomer; *Plant and Cell Physiology*; **40**, 1172-1176
99. Vissenberg, K.; Martinez-Vilchez, I. M.; Verbelen, J.-P.; Miller, J. G.; Fry, S. C. (2000); In vivo colocalization of xyloglucan endotransglycosylase activity and its donor substrate in the elongation zone of Arabidopsis roots; *Plant Cell*; **12**, 1229-1237
100. Vissenberg, K.; Van Sandt, V.; Fry, S. C.; Verbelen, J. P. (2003); Xyloglucan endotransglucosylase action is high in the root elongation zone and in the trichoblasts of all vascular plants from selaginella to zea mays; *Journal of Experimental Botany*; **54**, 335-344
101. Bourquin, V.; Nishikubo, N.; Abe, H.; Brumer, H.; Denman, S.; Eklund, M.; Christiernin, M.; Teeri, T. T.; Sundberg, B.; Mellerowicz, E. J. (2002); Xyloglucan endotransglycosylases have a function during the formation of secondary cell walls of vascular tissues; *Plant Cell*; **14**, 3073-3088
102. J. L. Viladot, thesis, Universitat Ramon Llull, Institut Quimic de Sarria (1999).
103. Davies, G. J.; Wilson, K. S.; Henrissat, B. (1997); Nomenclature for sugar-binding subsites in glycosyl hydrolases; *Biochemical Journal*; **321**, 557-9
104. Levy, S.; York, W. S.; Stuike-Prill, R.; Meyer, B.; Staehelin, L. A. (1991); Simulations of the static and dynamic molecular conformations of xyloglucan. The role of the fucosylated sidechain in surface-specific sidechain folding; *Plant Journal*; **1**, 195-215

105. Johansson, P.; Denman, S.; Brumer, H.; Kallas, A. M.; Henriksson, H.; Bergfors, T.; Teeri, T. T.; Jones, T. A. (2003); Crystallization and preliminary X-ray analysis of a xyloglucan endotransglycosylase from *Populus tremula x tremuloides*; *Acta Crystallographica, Section D: Biological Crystallography*; **59**, 535-537
106. Thompson, J. E.; Smith, R. C.; Fry, S. C. (1997); Xyloglucan undergoes interpolymeric transglycosylation during binding to the plant cell wall in vivo: evidence from ¹³C/³H dual labelling and isopycnic centrifugation in caesium trifluoroacetate; *Biochem.J.*; **327 (Pt 3)**, 699-708
107. Antosiewicz, D. M.; Purugganan, M. M.; Polisensky, D. H.; Braam, J. (1997); Cellular localization of Arabidopsis xyloglucan endotransglycosylase-related proteins during development and after wind stimulation; *Plant Physiol.*; **115**, 1319-1328
108. Xu, W.; Purugganan, M. M.; Polisensky, D. H.; Antosiewicz, D. M.; Fry, S. C.; Braam, J. (1995); Arabidopsis TCH4, regulated by hormones and the environment, encodes a xyloglucan endotransglycosylase; *Plant Cell*; **7**, 1555-1567
109. Palmer, S. J. and Davies, W. J. (1996); An analysis of relative elemental growth rate, epidermal cell size and xyloglucan endotransglycosylase activity through the growing zone of aging maize leaves; *Journal of Experimental Botany*; **47**, 339-347
110. Saab, I. N. and Sachs, M. M. (1996); A flooding-induced xyloglucan endotransglycosylase homolog in maize is responsive to ethylene and associated with aerenchyma; *Plant Physiol.*; **112**, 385-391
111. Catala, C.; Rose, J. K.; Bennett, A. B. (1997); Auxin regulation and spatial localization of an endo-1,4-beta-D-glucanase and a xyloglucan endotransglycosylase in expanding tomato hypocotyls; *Plant J.*; **12**, 417-426
112. Thompson, J. E. and Fry, S. C. (2001); Restructuring of wall-bound xyloglucan by transglycosylation in living plant cells; *Plant Journal*; **26**, 23-34
113. Arrowsmith, D. A. and de Silva, J. (1995); Characterization of two tomato fruit-expressed cDNAs encoding xyloglucan endo-transglycosylase; *Plant Molecular Biology*; **28**, 391-403
114. Planas, A.; Juncosa, M.; Cayetano, A.; Querol, E. (1992); Studies on *Bacillus licheniformis* endo- β -1,3-1,4-D-glucanase: characterization and kinetic analysis; *Appl.Microbiol.Biotechnol.*; **37**, 583-589
115. Planas, A.; Juncosa, M.; Lloberas, J.; Querol, E. (1992); Essential catalytic role of Glu134 in endo- β -1,3-1,4-D-glucan 4-glucanohydrolase from *B.licheniformis* as determined by site-directed mutagenesis; *FEBS Lett.*; **308**, 141-145
116. A. Planas and C. Malet, in *Carbohydrate Bioengineering*, S. B. Petersen, B. Svensson, S. Pedersen, Eds. (Elsevier, Amsterdam, 1995) ,chap. 8.

117. A. Planas, in *Carbohydrases from Trichoderma reesei and other microorganisms*, M. Claeysens, W. Nerinckx, K. Piens, Eds. (The Royal Society of Chemistry, Cambridge, 1998).
118. A. Planas, J. L. Viladot, M. Faijes, in *Recent Advances in Carbohydrate Bioengineering*, H. J. Gilbert, G. J. Davies, B. Henrissat, B. Svensson, Eds. (The Royal Society of Chemistry, Cambridge, 1999).
119. Planas, A. (2000); Bacterial 1,3-1,4- β -glucanases: structure, function and protein engineering; *Biochim.Biophys.Acta*; **1543**, 361-382
120. E. Champion, thesis, Institut Quimic de Sarria (2004).
121. T. A. Addington, thesis, Institut Quimic de Sarria (2006).
122. Monegal, A.; Pinyol, R.; Planas, A. (2005); Capillary electrophoresis method for the enzymatic assay of galactosyltransferases with postreaction derivatization; *Analytical Biochemistry*; **346**, 115-123
123. Monegal, A.; Bulone, V.; Planas, A. (2005); Enzymatic characterization of bovine α -1,3-galactosyltransferase. Validation of a radiometric assay and kinetic mechanism; *Afinidad*; **62**, 505-512
124. A. Monegal, thesis, Institut Quimic de Sarria (2004).
125. Lee, K. B.; Desai, U. R.; Palcic, M. M.; Hindsgaul, O.; Linhardt, R. J. (1992); An electrophoresis-based assay for glycosyltransferase activity; *Anal.Biochem.*; **205**, 108-114
126. Le, X. C.; Zhang, Y.; Dovichi, N. J.; Compston, C. A.; Palcic, M. M.; Beever, R. J.; Hindsgaul, O. (1997); Study of the enzymic transformation of fluorescently labeled oligosaccharides in human epidermoid cells using capillary electrophoresis with laser-induced fluorescence detection; *Journal of Chromatography, A*; **781**, 515-522
127. Sujino, K.; Uchiyama, T.; Hindsgaul, O.; Seto, N. O.; Wakarchuk, W. W.; Palcic, M. M. (2000); Enzymatic synthesis of oligosaccharide analogues: evaluation of UDP-Gal analogues as donors for three retaining α -galactosyltransferases; *J Am Chem Soc*; **122**, 1261-1269
128. Grossman, P. and Nielsen, R. G. (1989); *Anal.Chem.*; **61**, 1186-1194
129. Kok, W. Y. (2000); Thermal management in capillary electrophoresis; *Chromatographia*; **Supplement**,
130. El Rassi, Z. (1997); Recent developments in capillary electrophoresis of carbohydrate species; *Electrophoresis*; **18**, 2400-2407
131. El Rassi, Z.; Postlewait, J.; Machref, Y.; Ostrander, G. (1997); Capillary electrophoresis of carboxylated carbohydrates; *Anal.Biochem.*; **244**, 283-290

132. Klockow, A. and Amadò, R. (1995); Separation of 8-aminonaphthalene-1,3,6-trisulfonic acid-labelled neutral and sialylated N-linked complex oligosaccharides by capillary electrophoresis.; *J Chromatogr.A*; **716**, 241-257
133. Saura-Valls, M.; Faure, R.; Ragas, S.; Piens, K.; Brumer, H.; Teeri, T. T.; Cottaz, S.; Driguez, H.; Planas, A. (2006); Kinetic analysis using low-molecular mass xyloglucan oligosaccharides defines the catalytic mechanism of a *Populus xyloglucan endotransglycosylase*; *Biochemical Journal*; **395**, 99-106
134. McDougall, G. J. and Fry, S. C. (1988); Inhibition of auxin-stimulated growth of pea stem segments by a specific nonasaccharide of xyloglucan; *Planta*; **175**, 412-416
135. McDougall, G. J. and Fry, S. C. (1989); Anti-Auxin Activity of Xyloglucan Oligosaccharides: the Role of Groups other than the Terminal α -L-Fucose Residue; *Journal of Experimental Botany*; **40**, 233-238
136. McDougall, G. J. and Fry, S. C. (1989); Structure-Activity Relationships for Xyloglucan Oligosaccharides with Antiauxin Activity; *Plant Physiol.*; **89**, 883-887
137. McDougall, G. J. and Fry, S. C. (1990); Xyloglucan Oligosaccharides Promote Growth and Activate Cellulase: Evidence for a Role of Cellulase in Cell Expansion; *Plant Physiol.*; **93**, 1042-1048
138. McDougall, G. J. and Fry, S. C. (1991); Purification and analysis of growth-regulating xyloglucan-derived oligosaccharides by high-pressure liquid chromatography; *Carbohydrate Research*; **219**, 123-132
139. Vincken, J. P.; de Keizer, A.; Beldman, G.; Voragen, A. G. (1995); Fractionation of xyloglucan fragments and their interaction with cellulose; *Plant Physiology*; **108**, 1579-85
140. Vincken, J. P.; Beldman, G.; Niessen, W. M. A.; Voragen, A. G. J. (1996); Degradation of apple fruit xyloglucan by endoglucanase; *Carbohydrate Polymers*; **29**, 75-85
141. Mitsuishi, Y. and Shoda, S. (2002); Construction of library of highly pure xyloglucan oligosaccharides; *Cellulose Communications*; **9**, 2-7
142. Chiesa, C. and Horvath, C. (1993); Capillary zone electrophoresis of malto-oligosaccharides derivatized with 8-aminonaphthalene-1,3,6-trisulfonic acid; *Journal of Chromatography*; **645**, 337-352
143. St.Claire, R. L. (1996); Capillary electrophoresis; *Anal.Chem.*; **68**, 569R-586R
144. Viladot, J. L.; Moreau, V.; Planas, A.; Driguez, H. (1997); Transglycosylation activity of *Bacillus* 1,3-1,4- β -D-glucan 4-glucanohydrolases. Enzymatic synthesis of alternate 1,3-1,4- β -D-glucooligosaccharides; *J.Chem.Soc.Perkin Trans. 1.*; 2383-2387
145. Viladot, J. L.; Stone, B. A.; Driguez, H.; Planas, A. (1998); Expeditious synthesis of a new hexasaccharide using transglycosylation reaction catalyzed by *Bacillus* 1,3-1,4- β -D-glucan 4-glucanohydrolase; *Carbohydr.Res.*; **311**, 95-99

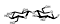
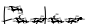

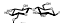
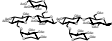

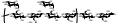



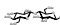
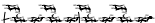

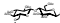








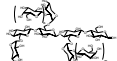

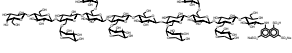
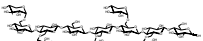




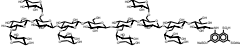
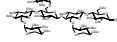

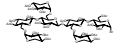
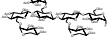
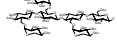
146. R. Fauré, thesis, Universite Joseph Fourier (2004).
147. Mackenzie, L. F.; Wang, Q.; Warren, R. A. J.; Withers, S. G. (1998); Glycosynthases: Mutant Glycosidases for Oligosaccharide Synthesis; *Journal of the American Chemical Society*; **120**, 5583-5584
148. Malet, C. and Planas, A. (1998); From β -glucanase to β -glucansynthase: glycosyl transfer to α -glycosyl fluorides catalyzed by a mutant endoglucanase lacking its catalytic nucleophile; *FEBS Letters*; **440**, 208-212
149. Fort, S.; Boyer, V.; Greffe, L.; Davies, G. J.; Moroz, O.; Christiansen, L.; Schuelein, M.; Cottaz, S.; Driguez, H. (2000); Highly Efficient Synthesis of β (1->4)-Oligo- and -Polysaccharides Using a Mutant Cellulase; *Journal of the American Chemical Society*; **122**, 5429-5437
150. Fort, S.; Christiansen, L.; Schulein, M.; Cottaz, S.; Driguez, H. (2000); Stepwise synthesis of celloextrins assisted by a mutant cellulase; *Israel Journal of Chemistry*; **40**, 217-221
151. Mayer, C.; Zechel, D. L.; Reid, S. P.; Warren, A. J.; Withers, S. G. (2000); The E358S mutant of *Agrobacterium* sp. β -glucosidase is a greatly improved glycosynthase; *FEBS Lett.*; **466**, 40-44
152. Trincone, A.; Perugino, G.; Rossi, M.; Moracci, M. (2000); A novel thermophilic glycosynthase that effects branching glycosylation; *Bioorg.Med.Chem.Lett.*; **10**, 365-368
153. Mayer, C.; Jakeman, D. L.; Mah, M.; Karjala, G.; Gal, L.; Warren, R. A. J.; Withers, S. G. (2001); Direct evolution of new glycosynthases from *Agrobacterium* β -glucosidase: a general screen to detect enzymes for oligosaccharide synthesis; *Chemistry & Biology*; **8**, 437-443
154. Nashiru, O.; Zechel, D. L.; Stoll, D.; Mohammadzadeh, T.; Warren, R. A. J.; Withers, S. G. (2001); β -mannosynthase: synthesis of β -mannosides with a mutant β -mannosidase; *Angewandte Chemie, International Edition*; **40**, 417-420
155. Tolborg, J. F.; Petersen, L.; Jensen, K. J.; Mayer, C.; Jakeman, D. L.; Warren, R. A. J.; Withers, S. G. (2002); Solid-phase oligosaccharide and glycopeptide synthesis using glycosynthases; *J.Org.Chem.*; **67**, 4143-4149
156. Jakeman, D. L. and Withers, S. G. (2002); On expanding the repertoire of glycosynthases: mutant β -galactosidases forming β -(1,6)-linkages; *Canadian Journal of Chemistry*; **80**, 866-870
157. Okuyama, M.; Mori, H.; Watanabe, K.; Kimura, A.; Chiba, S. (2002); α -Glucosidase mutant catalyzes " α -glycosynthase"-type reaction; *Bioscience, Biotechnology, and Biochemistry*; **66**, 928-933
158. Fairweather, J. K.; Faijes, M.; Driguez, H.; Planas, A. (2002); Specificity studies of *Bacillus* 1,3-1,4- β -glucanases and application to glycosynthase-catalyzed transglycosylation; *ChemBioChem*; **3**, 866-873

159. Fairweather, J. K.; Hrmova, M.; Rutten, S. J.; Fincher, G. B.; Driguez, H. (2003); Synthesis of complex oligosaccharides by using a mutated (1,3)- β -D-glucan endohydrolase from barley; *Chemistry--A European Journal*; **9**, 2603-2610
160. Jahn, M.; Stoll, D.; Warren, R. A. J.; Szabo, L.; Singh, P.; Gilbert, H. J.; Ducros, V. M. A.; Davies, G. J.; Withers, S. G. (2003); Expansion of the glycosynthase repertoire to produce defined manno-oligosaccharides; *Chemical Communications*; 1327-1329
161. Jahn, M.; Marles, J.; Warren, R. A. J.; Withers, S. G. (2003); Thioglycoligase: mutant glycosidases for thioglycoside synthesis; *Angewandte Chemie, International Edition*; **42**, 352-354
162. Jahn, M.; Chen, H.; Muellegger, J.; Marles, J.; Warren, R. A. J.; Withers, S. G. (2004); Thioglycosynthases: double mutant glycosidases that serve as scaffolds for thioglycoside synthesis; *Chemical Communications*; 274-275
163. Faijes, M.; Fairweather, J. K.; Driguez, H.; Planas, A. (2001); Oligosaccharide synthesis by coupled endo-glycosynthases of different specificity: a straightforward preparation of two mixed-linkage hexasaccharide substrates of 1,3/1,4- β -glucanases; *Chemistry--A European Journal*; **7**, 4651-4655
164. Faijes, M.; Perez, X.; Perez, O.; Planas, A. (2003); Glycosynthase Activity of *Bacillus licheniformis* 1,3-1,4- β -Glucanase Mutants: Specificity, Kinetics, and Mechanism; *Biochemistry*; **42**, 13304-13318
165. Faijes, M.; Saura-Valls, M.; Perez, X.; Conti, M.; Planas, A. (2006); Acceptor-dependent regioselectivity of glycosynthase reactions by *Streptomyces* E383A b-glucosidase; *Carbohydrate Research*; **341**, 2055-2065
166. Li, D. T. and Her, G. R. (1998); Structural analysis of chromophore-labeled disaccharides and oligosaccharides by electrospray ionization mass spectrometry and high-performance liquid chromatography/electrospray ionization mass spectrometry; *Journal of Mass Spectrometry*; **33**, 644-652
167. Pauly, M.; Andersen, L. N.; Kauppinen, S.; Kofod, L. V.; York, W. S.; Albersheim, P.; Darvill, A. (1999); A xyloglucan-specific endo- β -1,4-glucanase from *Aspergillus aculeatus*: expression cloning in yeast, purification and characterization of the recombinant enzyme; *Glycobiology*; **9**, 93-100
168. York, W. S.; Harvey, L. K.; Guillen, R.; Albersheim, P.; Darvill, A. G. (1993); The structure of plant cell walls. XXXVI. Structural analysis of tamarind seed xyloglucan oligosaccharides using β -galactosidase digestion and spectroscopic methods; *Carbohydrate Research*; **248**, 285-301
169. L. Aguirre et al., Validación de métodos analíticos, (2001).
170. G. Davies, M. L. Sinnott, S. G. Withers, in *Comprehensive Biological Catalysis*, M. L. Sinnott, Ed. (Academic Press Ltd., 1998) ,chap. 3.
171. I. H. Segel, Enzyme kinetics (John Wiley and Sons, Inc., New York, ed. 1993, 1975).

172. Faure, R.; Saura-Valls, M.; Brumer, H., III; Planas, A.; Cottaz, S.; Driguez, H. (2006); Synthesis of a Library of Xylogluco-Oligosaccharides for Active-Site Mapping of Xyloglucan endo-Transglycosylase; *Journal of Organic Chemistry*; **71**, 5151-5161
173. Shoda, S.; Kawasaki, T.; Obata, K.; Kobayashi, S. (1993); A facile enzymatic synthesis of cellooligosaccharide derivatives using β -lactosyl fluoride; *Carbohydrate Research*; **249**, 127-37
174. Boyer, V.; Fort, S.; Frandsen, T. P.; Schulein, M.; Cottaz, S.; Driguez, H. (2002); Glycosynthase-assisted synthesis of oligosaccharides, part III. Chemoenzymatic synthesis of a bifunctionalized cellohexaoside as a specific substrate for the sensitive assay of cellulase by fluorescence quenching; *Chemistry--A European Journal*; **8**, 1389-1394
175. Kempton, J. B. and Withers, S. G. (1992); Mechanism of *Agrobacterium* β -glucosidase: kinetic studies; *Biochemistry*; **31**, 9961-9
176. Armand, S.; Drouillard, S.; Schulein, M.; Henrissat, B.; Driguez, H. (1997); A bifunctionalized fluorogenic tetrasaccharide as a substrate to study cellulases; *J.Biol.Chem.*; **272**, 2709-2713
177. Cottaz, S.; Brasme, B.; Driguez, H. (2000); A fluorescence-quenched chitopentaose for the study of endo-chitinases and chitobiosidases; *European Journal of Biochemistry*; **267**, 5593-5600
178. Ludeman, J. P.; Pike, R. N.; Bromfield, K. M.; Duggan, P. J.; Cianci, J.; Le Bonniec, B.; Whisstock, J. C.; Bottomley, S. P. (2003); Determination of the P'1, P'2 and P'3 subsite-specificity of factor Xa; *International Journal of Biochemistry & Cell Biology*; **35**, 221-225
179. Marme, N.; Knemeyer, J. P.; Wolfrum, J.; Sauer, M. (2004); Highly sensitive protease assay using fluorescence quenching of peptide probes based on photoinduced electron transfer; *Angewandte Chemie, International Edition*; **43**, 3798-3801
180. Karvinen, J.; Laitala, V.; Maekinen, M. L.; Mulari, O.; Tamminen, J.; Hermonen, J.; Hurskainen, P.; Hemmilae, I. (2004); Fluorescence Quenching-Based Assays for Hydrolyzing Enzymes. Application of Time-Resolved Fluorometry in Assays for Caspase, Helicase, and Phosphatase; *Analytical Chemistry*; **76**, 1429-1436
181. Molinaro, G.; Carmona, A. K.; Juliano, M. A.; Juliano, L.; Malitskaya, E.; Yessine, M. A.; Chagnon, M.; Lepage, Y.; Simmons, W. H.; Boileau, G.; Adam, A. (2005); Human recombinant membrane-bound aminopeptidase P: production of a soluble form and characterization using novel, internally quenched fluorescent substrates; *Biochemical Journal*; **385**, 389-397
182. Takakusa, H.; Kikuchi, K.; Urano, Y.; Kojima, H.; Nagano, T. (2003); A novel design method of ratiometric fluorescent probes based on fluorescence resonance energy transfer switching by spectral overlap integral; *Chemistry--A European Journal*; **9**, 1479-1485

183. Selvin, P. R. (2000); The renaissance of fluorescence resonance energy transfer; *Nature structural biology*; **7**, 730-734
184. Bernard Valeur, Molecular Fluorescence. Principles and applications Weinheim (VCH), (2002), pp. 1-381.
185. Resonance energy transfer (John Wiley & sons Ltd, 1999), pp. 1-468.
186. Beythien, J. and White, P. D. (2005); A solid phase linker strategy for the direct synthesis of EDANS-labelled peptide substrates; *Tetrahedron letters*; **46**, 101-104
187. Baer, H. H. and Bell, A. J. (1979); The synthesis of 3-amino-3-deoxy- α -D-glucopyranosyl α -D-glucopyranoside (3-amino-3-deoxy- α , α -trehalose); *Carbohydrate Research*; **75**, 175-184
188. Kim, S.; Chang, H.; Kim, W. J. (1985); Selective benzylation of diols with 1-(benzyloxy)benzotriazole; *Journal of Organic Chemistry*; **50**, 1751-2
189. Soli, E. D.; Manoso, A. S.; Patterson, M. C.; DeShong, P.; Favor, D. A.; Hirschmann, R.; Smith, A. B., III (1999); Azide and Cyanide Displacements via Hypervalent Silicate Intermediates; *Journal of Organic Chemistry*; **64**, 3171-3177
190. Excoffier, G.; Gagnaire, D.; Utile, J. P. (1975); Synthesis of oligosaccharides on polymeric supports. V. Selective cleavage by hydrazine of the anomeric acetyl groups of acetylated glycosyl residues; *Carbohydrate Research*; **39**, 368-73
191. Card, P. J. (1983); Fluorinated carbohydrates. Use of DAST in the synthesis of fluorinated sugars; *Journal of Organic Chemistry*; **48**, 393-5
192. Lindhorst, T. K.; Braun, C.; Withers, S. G. (1995); Syntheses of 4'-deoxy- α -maltosyl fluoride and 4''-deoxy- α -maltotriosyl fluoride as probes of α -glucanotransferase mechanisms; *Carbohydrate Research*; **268**, 93-106
193. Ramsay, S. L.; Freeman, C.; Grace, P. B.; Redmon, J. W.; MacLeod, J. K. (2001); Mild tagging procedures for the structural analysis of glycans; *Carbohydr. Res.*; **333**, 59-71
194. Koshida, S.; Suda, Y.; Arano, A.; Sobel, M.; Kusumoto, S. (2001); An efficient method for the assembly of sulfated oligosaccharides using reductive amination; *Tetrahedron letters*; **42**, 1293-1296
195. Turnbull, W. B.; Kalovidouris, S. A.; Stoddart, J. F. (2002); Large Oligosaccharide-based glycodendrimers; *Chem. Eur. J.*; **8**, 2988-3000
196. Adachi, T.; Yamada, Y.; Inoue, I. (1977); An alternative method for the selective reduction of unsaturated nucleoside azides to the amines; *Synthesis*; 45-46
197. J. Sambrook, E. F. Fritsch, T. Maniatis, Molecular cloning: a laboratory manual (Cold Spring Harbor, New York, ed. 2nd edn, 1989).

198. J. F. Sambrook, D. W. Russell, Editors., *Molecular cloning: A laboratory manual*, third edition (Cold spring harbor laboratory press, New York, ed. 3rd edition, 2000).
199. Sanger, F.; Nicklen, S.; Coulson, A. R. (1977); DNA sequencing with chain-terminating inhibitors; *Proceedings of the National Academy of Sciences of the United States of America*; **74**, 5463-5467
200. W. L. F. Armarego and D. D. Perrin, *Purification of Laboratory Chemicals*, Fourth Edition Oxford, ed. 4th edition, 1997), pp. 1-529.
201. Greffe, L.; Jensen, M. T.; Chang-Pi-Hin, F.; Fruchard, S.; O'Donohue, M. J.; Svensson, B.; Driguez, H. (2002); Chemoenzymatic syntheses of linear and branched hemithiomaltodextrins as potential inhibitors for starch-debranching enzymes; *Chemistry--A European Journal*; **8**, 5447-5455
202. Ellis, K. J. and Morrison, J. F. (1982); Buffers of Constant Ionic Strength for Studying pH-Dependent Processes; *Methods Enzymol.*; **87**, 405-426

		
1 GGbF	18 n=1 XGGG	34 Ac(XXXG-OH)
	19 n=2 XGXGGG	
2 XGbF	19 n=2 XGXGGG	35 Ac(XXXG-ab-F)
		
3 Ac(GG)	20 n=3 XGXGXGGG	36 XXXG-a-F
	21 n=1 XXXGGG	
4 Ac(GG)□Br	21 n=1 XXXGGG	37 XXXGXXXGXXXG-ANTS
		
5 Ac(GG)□F	22 n=2 XXXGXXXGGG	38 GalGXXXGXXXG
	23 n=1 XXXGXXXG	
6 Ac(XG)□F	23 n=1 XXXGXXXG	39 GalGlc-a-F
	24 n=2 XXXGXXXGXXXG	
7 Bn(Xyl)SPh	24 n=2 XXXGXXXGXXXG	40 GalGXXXG
		
8 4,6-OH-Bn(GG)-OMP	25 n=m=0 XXXG-ANTS	41 Ac(LacXXXG-a-F)
	26 n=0 m=1 XXLG-ANTS	
9 4-OH-Bn(XG)-OMP	26 n=0 m=1 XXLG-ANTS	42 GalGXXXG-a-F
	27 n=1 m=0 XLXG-ANTS	
10 n=m=0 XXXG	27 n=1 m=0 XLXG-ANTS	43 GalGXXXG-ANTS
11 n=0 m=1 XXLG	28 n=1 m=1 XLLG-ANTS	
11 n=0 m=1 XXLG	28 n=1 m=1 XLLG-ANTS	44 GalGXXXGXXXG-ANTS
12 n=1 m=0 XLXG		
12 n=1 m=0 XLXG	29 XXGXXXG	45 XXXGXG
13 n=1 m=1 XLLG		
13 n=1 m=1 XLLG	30 XXG	46 XXXGXXG
		
14 XXXGbF	31 XXXGXXXG-ANTS	
		
15 Ac(XXXG)	32 Ac(XXG)	
		
16 Ac(XXXG)aBr	33 Ac(XXXG-a-F)	
		
17 Ac(XXXG)bF		

